

**THE CONDITIONAL NATURE OF THE MAMMALIAN HYPERCAPNIC
VENTILATORY RESPONSE: EFFECT OF AGE, STATE, AND TEMPERATURE**

by

Ryan Joseph Sprenger

B.Sc., University of Wisconsin-Oshkosh, 2014

M.Sc. University of Wisconsin-Oshkosh, 2016

A THESIS SUBMITTED IN PARTIAL FULFILLMENT OF
THE REQUIREMENTS FOR THE DEGREE OF

DOCTOR OF PHILOSOPHY

in

THE FACULTY OF GRADUATE AND POSTDOCTORAL STUDIES
(Zoology)

THE UNIVERSITY OF BRITISH COLUMBIA
(Vancouver)

September 2021

© Ryan Joseph Sprenger, 2021

The following individuals certify that they have read, and recommend to the Faculty of Graduate and Postdoctoral Studies for acceptance, the dissertation entitled:

The conditional nature of the mammalian hypercapnic ventilatory response: effect of age, state, and temperature

submitted by Ryan Sprenger in partial fulfillment of the requirements for

the degree of Doctor of Philosophy

in Zoology

Examining Committee:

Dr. William Milsom, Professor Emeritus, Zoology, UBC

Co-supervisor

Dr. Philip Matthews, Associate Professor, Zoology, UBC

Co-supervisor

Dr. Michael Koehle, Professor, Sport and Exercise Medicine, UBC

University Examiner

Dr. Dan Rurak, Professor Emeritus, Obstetrics and Gynaecology, UBC

University Examiner

Additional Supervisory Committee Members:

Dr. Colin Brauner, Zoology, UBC

Supervisory Committee Member

Dr. Doug Altshuler, Zoology, UBC

Supervisory Committee Member

Abstract

CO₂ is the primary respiratory stimulant under resting conditions in mammals and an elevation in internal or environmental CO₂ causes an increase in ventilation. My thesis focuses on two conditions in which the magnitude of the ventilatory response to excess CO₂ is altered within an animal: postnatal development and hibernation. I first examine the development of the hypercapnic ventilatory response (HCVR) in two fossorial species (golden-Syrian hamsters and 13-lined ground squirrels) to determine if the blunted adult fossorial HCVR is developed or inherited, then raised those species in burrow conditions to determine how peri- and postnatal exposure to burrow conditions affects the adult response. Both species developed their blunted adult HCVR over the first 15 days after birth, and peri- and postnatal exposure to the burrow environment sped up the development of the HCVR (5-10 days) without affecting the adult response. My data suggest that the HCVR is likely genetically determined and strongly influenced by neurochemical development which produces but not regulates the observed patterns in the development of the HCVR. I next examined the relatively elevated HCVR seen in adult hibernating mammals. I found that the HCVR diminishes during a period of CO₂ retention early in entrance into hibernation (where 7% CO₂ does not elicit a ventilatory response) that appears to contribute to metabolic suppression. After, it rises to the elevated HCVR in hibernation (~650% increase to 7% CO₂) tracking the reduction in metabolic rate. In steady state hibernation, the HCVR was elevated and plastic based on changes in metabolic rate, state, and body temperature. On arousal the HCVR is elevated further (~750% increase to 7% CO₂) when the animals are expelling excess CO₂ before falling as metabolic rate rises on arousal. These data suggest that chemoreceptor input, or changes to the integration of that input were altered but I confirm that the locus coeruleus is not involved in the changes in the HCVR during hibernation. Unlike development, CO₂ sensitivity appears to be tightly regulated to facilitate retention or expulsion of CO₂ in hibernation, thus the nature of the changes in CO₂ sensitivity are different between development and hibernation.

Lay Summary

CO₂ is the primary stimulant to breathe in mammals under resting conditions. Mammals primarily expel excess CO₂ by increasing ventilation to maintain a stable internal pH/CO₂, and the magnitude of this increase in ventilation varies among species. Development and hibernation state are two conditions that alter the magnitude of an animal's ventilatory response to excess CO₂. In developing mammals, there is a period of vulnerability where CO₂ does not elicit a ventilatory response as a consequence of neurochemical development. In hibernation, respiratory sensitivity to CO₂ is tightly regulated based on the current need of the animal for CO₂. I conclude that respiratory sensitivity to CO₂ is conditional consequential of changes to central CO₂ chemosensors (development) as well as subject to a tight regulation of chemoreceptor input, or integration of that input (hibernation). The nature of the shifts in CO₂ sensitivity appear to be different between these two conditions.

Preface

Chapter 2 has been published as Sprenger et al., 2019 entitled “Comparison of the CO₂ ventilatory response through development in three rodent species: Effect of fossoriality” in *Respiratory Physiology and Neurobiology* 246; 19-27, doi.org/10.1016/j.resp.2019.03.006. I performed all of the experiments with the help of Jessica Chiang, Grace Wong, and Anne Kim. I analyzed all the data and wrote the first draft of the manuscript which was edited by Dr. WK Milsom and Dr. Y Dzal.

Chapter 3 has been published as Sprenger and Milsom 2021 entitled “Respiratory development in burrowing rodents: Effect of perinatal hypercapnia” in *Respiratory Physiology and Neurobiology* 288; 1-11, doi.org/10.1016/j.resp.2021.103640. I performed all of the experiments with the help of Amanda Schuler, Sandy Hassoun, Chloe Lai, and Gurbinder Dhanda. I analyzed all of the data and wrote the first draft of the manuscript which was edited by Dr. Milsom.

Chapter 4 has been submitted for publication as Sprenger and Milsom 2021 entitled “Temperature effects on ventilatory sensitivity to hypercapnia in torpid 13-lined ground squirrels (*Ictidomys tridecemlineatus*)”. I performed the experiments with the help of Amanda Schuler and Chloe Lai, analyzed the data, and wrote the first draft of the manuscript which was edited by Dr. Milsom.

Chapter 5 has been submitted for publication as Sprenger and Milsom 2021 entitled “Changes in CO₂ sensitivity during entrance into, and arousal from hibernation in *Ictidomys tridecemlineatus*”. I performed the experiments and analyzed the data. I wrote the first draft of the manuscript which was edited by Dr. Milsom.

Chapter 6 is in preparation for publication as Sprenger and Milsom 2021 entitled “Locus coeruleus and the hypercapnic ventilatory response in euthermic and hibernating 13-lined ground squirrels (*Ictidomys tridecemlineatus*)”. I performed all of the experiments with the help of Jessica Li, analyzed the data and wrote the first draft of the manuscript which was edited by Dr. Milsom.

All experiments performed for this these follow the guidelines of the Canada Council for Animal Care under the approval of the animal care committees at the University of British Columbia (AUP#: A17-0018, A19-0250, A21-0013).

Table of Contents

Abstract.....	iii
Lay Summary	iv
Preface.....	v
Table of Contents	vii
List of Tables	xv
List of Figures.....	xvi
List of Abbreviations	xxiii
Acknowledgements	xxvii
Chapter 1: Introduction	1
1.1 Overview.....	1
1.2 Hypercapnic ventilatory response in mammals	1
1.3 Sites of chemoreception: peripheral and central.....	3
1.4 The conditional nature of the hypercapnic ventilatory response	6
1.4.1 <i>Development of the hypercapnic ventilatory response in mammals.....</i>	<i>6</i>
1.4.2 <i>Hibernation and hypercapnia</i>	<i>9</i>
1.5 Thesis objectives and chapter summaries	11
1.5.1 <i>Chapter 2: Development of the ventilatory response to CO₂ in fossorial rodents ...</i>	<i>11</i>
1.5.2 <i>Chapter 3: Effect of burrow conditions on the development of the hypercapnic ventilatory response in fossorial rodents.....</i>	<i>12</i>
1.5.3 <i>Chapter 4: Effect of temperature on the hypercapnic ventilatory response in steady state hibernation</i>	<i>12</i>

1.5.4	<i>Chapter 5: Changes in CO₂ sensitivity during entrance into and arousal from hibernation</i>	13
1.5.5	<i>Chapter 6: Does state and temperature alter the role of the locus coeruleus in the hypercapnic ventilatory response?</i>	13
Chapter 2: Comparison of the CO₂ Ventilatory Response Through Development in Three Rodent Species: Effect of Fossoriality		
		14
2.1	Summary	14
2.2	Introduction	14
2.3	Methods	16
2.3.1	<i>Animals</i>	16
2.3.2	<i>Measurement of Ventilation and Oxygen Consumption</i>	16
2.3.2.1	<i>Ventilatory Measurements</i>	16
2.3.2.2	<i>Metabolic Measurements</i>	18
2.3.3	<i>Measurement of Temperature</i>	18
2.3.4	<i>Experimental Protocol</i>	18
2.3.5	<i>Data Analysis</i>	19
2.3.6	<i>Statistical Analysis</i>	20
2.4	Results	21
2.4.1	<i>Sprague-Dawley rats</i>	21
2.4.2	<i>Golden-Syrian hamsters</i>	21
2.4.3	<i>13-lined ground squirrels</i>	22
2.5	Discussion	23
2.5.1	<i>Changes in the HCVR through development in non-fossorial neonates</i>	23

2.5.2	<i>Changes in the HCVR through postnatal development of semi-fossorial rodents....</i>	24
2.5.3	<i>Underlying basis of differences in developmental patterns of the HCVR</i>	25
2.6	Conclusions.....	27

Chapter 3: Respiratory Development in Burrowing Rodents: Effect of Perinatal

Hypercapnia35

3.1	Summary	35
3.2	Introduction.....	35
3.3	Methods.....	37
3.3.1	<i>Animals</i>	37
3.3.2	<i>The burrow environment.....</i>	38
3.3.3	<i>Measurement of oxygen consumption, ventilation, and temperature</i>	38
3.3.3.1	<i>Ventilation.....</i>	38
3.3.3.2	<i>Oxygen consumption.....</i>	39
3.3.3.3	<i>Temperature</i>	39
3.3.4	<i>Experimental protocol</i>	40
3.3.5	<i>Data analysis</i>	40
3.3.6	<i>Statistical analysis</i>	41
3.4	Results.....	42
3.4.1	<i>Sprague-Dawley Rats.....</i>	42
3.4.1.1	<i>Changes in O₂ Consumption Rate and Ventilation throughout Development in Chronic Hypercapnia.....</i>	42
3.4.1.2	<i>Changes in the Hypercapnic Ventilatory Responses throughout Development in Chronic Hypercapnia.....</i>	42

3.4.1.3	<i>Long Term Effects of Development In Chronic Hypercapnia on O₂ Consumption Rate, Ventilation and the Hypercapnic Ventilatory Response</i>	43
3.4.2	<i>Golden-Syrian hamsters</i>	44
3.4.2.1	<i>Changes in O₂ Consumption Rate and Ventilation throughout Development in Chronic Hypercapnia</i>	44
3.4.2.2	<i>Changes in the Hypercapnic Ventilatory Responses throughout Development in Chronic Hypercapnia</i>	45
3.4.2.3	<i>Long Term Effects of Development in Chronic Hypercapnia on O₂ Consumption Rate, Ventilation and the Hypercapnic Ventilatory Response</i>	45
3.4.3	<i>13-lined ground squirrels</i>	46
3.4.3.1	<i>Changes in O₂ Consumption Rate and Ventilation throughout Development in Chronic Hypercapnia</i>	46
3.4.3.2	<i>Changes in the Hypercapnic Ventilatory Responses throughout Development in Chronic Hypercapnia</i>	46
3.4.3.3	<i>Long Term Effects of Development In Chronic Hypercapnia on O₂ Consumption Rate, Ventilation and the Hypercapnic Ventilatory Response</i>	47
3.5	<i>Discussion</i>	47
3.5.1	<i>Changes in O₂ Consumption Rate and Ventilation throughout Development in Chronic Hypercapnia</i>	48
3.5.2	<i>Changes in the Hypercapnic Ventilatory Responses throughout Development in Chronic Hypercapnia</i>	50
3.5.3	<i>Long Term Effects of Development In Chronic Hypercapnia on O₂ Consumption Rate, Ventilation and the Hypercapnic Ventilatory Response</i>	51

3.6	Conclusions.....	52
Chapter 4: Temperature Effects on Ventilatory Sensitivity to Hypercapnia in Torpid 13-		
Lined Ground Squirrels (<i>Ictidomys Tridecemlineatus</i>).....62		
4.1	Summary.....	62
4.2	Introduction.....	62
4.3	Methods.....	64
4.3.1	<i>Animals</i>	64
4.3.2	<i>Measurement of Temperature</i>	65
4.3.3	<i>Measurement of Ventilation and Oxygen Consumption Rate</i>	65
4.3.4	<i>Experimental Protocol</i>	67
4.3.5	<i>Data Analysis</i>	67
4.3.6	<i>Statistical Analysis</i>	68
4.4	Results.....	68
4.4.1	<i>Normocapnic Ventilation and Oxygen Consumption Rate</i>	68
4.4.2	<i>Breathing Pattern</i>	69
4.4.3	<i>Hypercapnia and Breathing Pattern</i>	70
4.5	Discussion.....	71
4.5.1	<i>Normocapnic Ventilation and Oxygen Consumption Rate</i>	72
4.5.2	<i>Breathing Pattern</i>	73
4.5.3	<i>Hypercapnia and Breathing Pattern</i>	74
4.5.4	<i>Hypercapnic Ventilatory Response</i>	74
4.6	Conclusions.....	75

Chapter 5: Changes in CO₂ Sensitivity During Entrance Into, and Arousal from

Hibernation in <i>Ictidomys Tridecemlineatus</i>	83
5.1 Summary.....	83
5.2 Introduction.....	83
5.3 Methods.....	85
5.3.1 <i>Animals</i>	85
5.3.2 <i>Measurement of Temperature</i>	86
5.3.3 <i>Measurement of Ventilation and Oxygen Consumption</i>	86
5.3.4 <i>Experimental Protocol</i>	87
5.3.5 <i>Data Analysis</i>	87
5.3.6 <i>Statistical Analysis</i>	88
5.4 Results.....	89
5.4.1 <i>Normocapnia</i>	89
5.4.1.1 <i>Entrance</i>	89
5.4.1.2 <i>Arousal</i>	89
5.4.1.3 <i>RER and Gas Exchange</i>	90
5.4.1.4 <i>Correlations Between Changes in \dot{V}_E, \dot{V}_{O_2}, and T_b</i>	91
5.4.2 <i>Effects of Hypercapnia on the Rate of Entrance and Arousal</i>	91
5.4.2.1 <i>Entrance</i>	91
5.4.2.2 <i>Arousal</i>	92
5.4.3 <i>Progressive Changes in the Hypercapnic Ventilatory Response</i>	92
5.4.3.1 <i>The Change in the HCVR During Entrance and Arousal</i>	92
5.4.3.2 <i>Correlations Between Changes in \dot{V}_E, \dot{V}_{O_2}, and T_b</i>	93

5.5	Discussion.....	93
5.5.1	<i>Onset of Entrance and Arousal: Changes in the RER, ACR, and \dot{V}</i>	94
5.5.2	<i>Effects of Hypercapnia on the Rate of Entrance and Arousal</i>	97
5.5.3	<i>Progressive Changes in the Hypercapnic Ventilatory Response</i>	98
5.6	Conclusions.....	100

Chapter 6: Locus Coeruleus and the Hypercapnic Ventilatory Response in Euthermic and Hibernating 13-Lined Ground Squirrels (*Ictidomys tridecemlineatus*).....112

6.1	Summary.....	112
6.2	Introduction.....	112
6.3	Methods.....	114
6.3.1	<i>Animals</i>	114
6.3.2	<i>Surgery</i>	115
6.3.3	<i>Measurement of Temperature</i>	115
6.3.4	<i>Measurement of Oxygen Consumption Rate and Ventilation</i>	116
6.3.5	<i>Experimental Protocol</i>	116
6.3.6	<i>Assessment of 6-OHDA Chemical Lesions</i>	118
6.3.7	<i>Data Analysis</i>	118
6.3.8	<i>Statistical Analysis</i>	119
6.4	Results.....	120
6.4.1	<i>6-OHDA Lesion</i>	120
6.4.2	<i>Effects of Cannula Placement</i>	120
6.4.3	<i>Effects of LC Lesion</i>	121
6.5	Discussion.....	122

6.5.1	<i>6-OHDA Lesions</i>	123
6.5.2	<i>Effects of Cannula Placement</i>	124
6.5.3	<i>Effects of LC Lesion</i>	127
6.6	Conclusions	127
Chapter 7: General Discussion and Conclusions		142
7.1	CO ₂ and development	143
7.2	CO ₂ and Hibernation	146
Bibliography		155

List of Tables

Table 3.1 Daily values for ventilation and oxygen consumption in all three species under resting conditions.	54
Table 5.1 The effects of changing temperature (Q_{10}) over various temperature ranges on oxygen consumption rates (\dot{V}_{O_2}) and ventilation (\dot{V}_E) during entrance into, and arousal from hibernation.....	101
Table 5.2 Average time to completion of entrance and arousal in normocapnia (0% CO_2) and hypercapnia (5% and 7% CO_2) in minutes.	101

List of Figures

Figure 2.1 Breathing frequency, tidal volume, total ventilation, O ₂ consumption rate, and the air convection requirement in Sprague-Dawley rats through development (P0-30) in normocapnic conditions.	29
Figure 2.2 Percent change from normocapnia in breathing frequency, tidal volume, and ventilation in Sprague-Dawley rats through development (P0-30) when given hypercapnia.	30
Figure 2.3 Breathing frequency, tidal volume, total ventilation, O ₂ consumption rate, and the air convection requirement in golden-Syrian hamsters through development (P0-30) in normocapnic conditions..	31
Figure 2.4 Relative change from normocapnia in breathing frequency, tidal volume, and ventilation in golden-Syrian hamsters through development (P0-30) when given hypercapnia.	32
Figure 2.5 Breathing frequency, tidal volume, total ventilation, O ₂ consumption rate, and the air convection requirement in 13-lined ground squirrels through development (P0-30) in normocapnic conditions.	33
Figure 2.6 Relative change from normocapnia in breathing frequency, tidal volume, and ventilation in 13-lined ground squirrels through development (P0-30) when given hypercapnia.	34
Figure 2.7 Comparison of the developmental pattern of the hypercapnic ventilatory response of Sprague-Dawley rats, golden-Syrian hamsters, and 13-lined ground squirrels.	34

Figure 3.1 O ₂ consumption rate, ventilation, mass, air convection requirement, and lung oxygen extraction in Sprague-Dawley rats raised in chronic hypercapnia (CH) from P0-30 when given normocapnic air.	55
Figure 3.2 O ₂ consumption rate, ventilation, air convection requirement, % lung oxygen extraction, and the relative increase from AcN in ventilation in Sprague-Dawley rats raised in chronic hypercapnia when given hypercapnia.	56
Figure 3.3 O ₂ consumption rate, ventilation, mass, air convection requirement, and lung oxygen extraction in golden-Syrian hamsters raised in chronic hypercapnia (CH) from P0-30 given normocapnia.	57
Figure 3.4 O ₂ consumption rate, ventilation, air convection requirement, % lung oxygen extraction, and the relative increase in ventilation from AcN in golden-Syrian hamsters raised in chronic hypercapnia when given hypercapnia.	58
Figure 3.5 O ₂ consumption rate, ventilation, mass, air convection requirement, and lung oxygen extraction in 13-lined ground squirrels raised in chronic hypercapnia (CH) from P0-30 in normocapnia.	59
Figure 3.6 O ₂ consumption rate, ventilation, air convection requirement, % lung oxygen extraction, and the relative increase in ventilation from AcN in 13-lined ground squirrels raised in chronic hypercapnia when given hypercapnia.	60
Figure 3.7 Comparison of the HCVR in Sprague-Dawley rats, golden-Syrian hamsters, and 13-lined ground squirrels breathing hypercapnia while under CH conditions (P30) and 30 days after being removed from CH conditions (P60)..	61

Figure 4.1 Oxygen consumption rate in 13-lined ground squirrels at rest at 37°C and in steady state hibernation at various temperatures (20°-5°C).....	76
Figure 4.2 Representative breathing traces from an animal breathing normocapnia and 7% hypercapnia at temperatures ranging from 20-5°C in steady state hibernation.	77
Figure 4.3 Representative Poincaré plots from animals breathing normocapnia and hypercapnia at 37°C and in steady state hibernation at 20-5°C.	78
Figure 4.4 Breathing frequency components of episodes at 5, 7, and 10°C in normocapnia and hypercapnia.	79
Figure 4.5 Coefficient of variation for all individuals at each steady state temperature breathing normocapnia and hypercapnia.	79
Figure 4.6 Absolute ventilation, breathing frequency, and tidal volume in animals breathing normocapnic and hypercapnia air.	80
Figure 4.7 Relative changes in ventilation, breathing frequency, and tidal volume in animals breathing hypercapnic air.....	81
Figure 4.8 Oxygen consumption rate and the air convection requirement (over oxygen consumption rate and CO ₂ production rate) in animals breathing normocapnic and hypercapnic air.	82

Figure 5.1 Time course of changes in body temperature, ventilation, oxygen consumption rate, and air convection requirement during entrance into hibernation in 13-lined ground squirrels.....	102
Figure 5.2 Time course of changes in body temperature, ventilation, oxygen consumption rate, and air convection requirement during arousal from hibernation in 13-lined ground squirrels.....	103
Figure 5.3 Expanded time course of changes in the body temperature, ventilation, oxygen consumption rate, CO ₂ excretion rate, the air convection requirement, the RER, and the % pulmonary O ₂ extraction during entrance into hibernation in 13-lined ground squirrels.....	104
Figure 5.4 Expanded time course of changes in the body temperature, ventilation, oxygen consumption rate, CO ₂ excretion rate, the air convection requirement, the RER, and the % pulmonary O ₂ extraction during arousal from hibernation in 13-lined ground squirrels.....	105
Figure 5.5 Time course of the changes in oxygen consumption rate during 11 hours and the first 240 minutes of entrance into hibernation and all of arousal as well as the first 60 minutes of arousal from hibernation comparing animals given normocapnia and hypercapnia.....	106
Figure 5.6 Time course of the changes in oxygen consumption rate and body temperature during entrance into, and arousal from hibernation in animals breathing room air and hypercapnic air.....	107

Figure 5.7 Time course of the changes in the air convection requirement, oxygen consumption rate), body temperature, and the relative change in ventilation in animals breathing hypercapnic air during entrance and arousal.....	108
Figure 5.8 Time course of the changes in the HCVR (% change in ventilation) and the ACR during entrance into, and arousal from hibernation in animals breathing room air, and hypercapnic air.	109
Figure 5.9 Relationship between the HCVR, oxygen consumption rate, and body temperature in animals breathing hypercapnia during entrance into and arousal from hibernation. .	110
Figure 5.10 Time course of the changes in body temperature, the RER, breathing frequency, and tidal volume during entrance into hibernation in animals breathing room air.....	112
Figure 5.11 Time course of the changes in body temperature, the RER, breathing frequency, and tidal volume during arousal from hibernation in animals breathing room air	112
Figure 6.1 Representative diagrams from the rat atlas (for complete list of structures see; Paxinos, George, and Charles Watson. <i>The rat brain in stereotaxic coordinates: hard cover edition</i> . Access Online via Elsevier, 2006) of the cannula tract used for injections into the locus coeruleus in sagittal and transverse sections.....	129
Figure 6.2 Number of live cells in the derived outline of the tyrosine hydroxylase positive LC region determined by cresyl violet stains in 13-lined ground squirrels with various surgeries.	130

Figure 6.3 Representative breathing traces from euthermic squirrels and hibernating squirrels that had either no surgery (Control, top), or sham injection (bottom) in normocapnia. 131

Figure 6.4 Ventilation, tidal volume, and breathing frequency in euthermic and hibernating squirrels breathing normocapnia. 132

Figure 6.5 Oxygen consumption rate and the air convection requirement in Control, LC sham, LCnc, and PbC sham animals while breathing normocapnic air in euthermia and hibernation..... 133

Figure 6.6 Representative breathing traces from euthermic control, LC sham injection, or LC bilateral lesion squirrels in normocapnia and hypercapnia. 134

Figure 6.7 Ventilation, tidal volume, breathing frequency, oxygen consumption rate, and the air convection requirement in control, LC sham, LC unilateral lesion, and LC bilateral lesion euthermic animals breathing normocapnia and hypercapnia. 135

Figure 6.8 Relative increases in ventilation, tidal volume, and breathing frequency from normocapnia in control, LC sham, LC unilateral lesion, and LC bilateral lesion euthermic animals breathing hypercapnia..... 136

Figure 6.9 Representative breathing traces from hibernating control, LC sham, and LC bilateral lesion squirrels in normocapnia and hypercapnia. 137

Figure 6.10 Ventilation, tidal volume, breathing frequency, oxygen consumption rate, and the air convection requirement in control, LC sham, and bilateral LC lesion hibernating animals breathing normocapnia and hypercapnia. 138

Figure 6.11 Relative increases in ventilation, tidal volume, and breathing frequency from normocapnia in control, LC sham, and LC bilateral lesion hibernating animals breathing hypercapnia. 139

Figure 6.12 Representative staining of TH positive LC cells using TH and DAPI..... 141

Figure 6.13 Representative cresyl violet stains showing left and right slices from control, LC unilateral lesion, and LC bilateral lesion squirrels..... 142

List of Abbreviations

$\% \Delta \dot{V}_E$	percent change in ventilation rate
6-OHDA	6-hydroxydopamine
AcN	acute normocapnia
ACR	air convection requirement
ACR _c	air convection requirement-carbon dioxide
ACR _o	air convection requirement-oxygen
B	Burrow gas
BK channel	calcium activated potassium channels
CV	coefficient of variation
CA	Catecholaminergic
Ca ²⁺	calcium
CH	chronic hypercapnia
CO ₂	carbon dioxide
DAPI	4',6-diamidino-2-phenylindole
DCIC	dorsal cortex of the ipsilateral inferior colliculus
E	embryonic day
ECG	electrocardiogram
ECIC	external cortex of the ipsilateral inferior colliculus
EEG	electroencephalogram
Feco ₂	fractional expired carbon dioxide
Feo ₂	fractional expired oxygen
f _H	heart rate
Fico ₂	fractional inspired carbon dioxide
Fio ₂	fractional inspired oxygen
FLIR	forward looking infrared
FMS	field metabolic system
f _R	breathing frequency
FR	flow rate

GABA	γ -aminobutyric acid
GABA _a	γ -aminobutyric acid a receptor
GABA _b	γ -aminobutyric acid b receptor
Hb	hemoglobin
HCVR	hypercapnic ventilatory response
IBI	interbreath interval
K ⁺	potassium
KF	Kölliker-fuse
kg	kilogram
LC	locus coeruleus
LC sham	sham injection into the locus coeruleus
LCnc	insertion and withdrawal of cannula into the locus coeruleus
LPb	lateral parabrachial complex
LPbV	ventral part of the lateral parabrachial nucleus
MBF	midbrain reticular formation
$\dot{M}CO_2$	carbon dioxide metabolic rate
Me5	mesencephalic trigeminal neurons
min	minute
MK-801	(+)-5-methyl-10, 11-dihydroxy-5H-dibenzo (a, d) cyclohepten-5, 10-imine
ml	milliliters
$\dot{M}O_2$	Metabolic rate
MPbC	medial parabrachial complex
N	normocapnic gas
N ₂	nitrogen
NMDA	N-methyl-d-aspartate
NREM	non-rapid eye movement sleep
NTS	nucleus tractus solitarius
O ₂	oxygen
OCR	oxygen convection requirement
P	post-natal day

PaCO ₂	partial pressure of arterial carbon dioxide
PAH ₂ O	water vapor pressure at animal temperature
PaO ₂	partial pressure of arterial oxygen
PB	barometric pressure
PbC	parabrachial complex
PbC sham	sham injection into the parabrachial complex
PBS	phosphate buffered saline
PBW	parabrachial waist
PCal	pressure deflection at calibrating volume
PCH ₂ O	water vapor pressure at chamber temperature
PCO ₂	partial pressure of carbon dioxide
PFA	paraformaldahyde
PRG	pontine respiratory group
Q ₁₀	temperature effect on a variable
RAS	reticular activating system
REM	rapid eye movement sleep
RER	respiratory exchange ratio
RFID	radio-frequency identification
RTN/pFRG	retrotrapezoid nucleus/parafacial respiratory group
SEM	standard error of the mean
SIDS	sudden infant death syndrome
T _{am}	ambient temperature
T _b	body temperature
T _c	chamber temperature
TH	tyrosine-hydroxylase
TI	inspiratory time
T _n	nasal temperature
TTOT	total inspiratory and expiratory time
UBC	University of British Columbia
Vcal	calibrating volume

\dot{V}_{CO_2}	carbon dioxide production rate
VCOR	corrected volume
\dot{V}_E	ventilation rate
\dot{V}_{O_2}	oxygen consumption rate
V_T	tidal volume

Acknowledgements

Bill and Phil have given me opportunity and guidance in becoming a better scientist, and for that I am grateful. Numerous other mentors, colleagues, and friends provided invaluable support throughout my PhD; Agnes, Stella, Catie, Ken and Hanane, my other two committee members, Colin and Doug, both Jessicas, and Amanda, so I extend my gratitude to them. It is/was a privilege to work with them.

Friends and family have shaped me into the person I am, and without their support and presence I would not be where I am. My parents (all four of them), brothers, and closest friends have been nothing less than vital to me. Finally, my wife Nicha, who was by my side through it all; Thank you.

Chapter 1: Introduction

1.1 Overview

My thesis examines the conditional nature of the hypercapnic ventilatory response (HCVR) in 13-lined ground squirrels. In air breathing animals, hypercapnia (increased levels of CO_2) is considered the main ventilatory stimulant that drives breathing under resting conditions in order to maintain PCO_2/pH homeostasis. In a well described feedback loop (Cunningham *et al.*, 1986; Guyenet & Bayliss, 2015), CO_2 produced via metabolic activity is sensed at several chemoreceptive sites both peripherally at the carotid artery bifurcations as well as centrally in the brainstem. These sensors provide input to the central respiratory rhythm generators which acts to increase or decrease ventilation to maintain CO_2 homeostasis. The magnitude of the HCVR (which can be elicited by both internal and environmental hypercapnia) is known to vary, not only among different species, but also temporally within a single species. This thesis aimed to examine variation in the HCVR within a single species during postnatal development and during hibernation.

1.2 Hypercapnic ventilatory response in mammals

CO_2 is the primary respiratory stimulant in terrestrial vertebrates. Thus, most mammals increase ventilation when faced with elevated levels of arterial CO_2 (PaCO_2) whether from metabolic or environmental sources. This rise in ventilation during hypercapnia (elevated PaCO_2) is produced by changes in both tidal volume (volume of each breath; V_T) and the frequency of breaths (breaths per minute; f_R) (Jennings & Laupacis, 1982; Walker *et al.*, 1985; Saiki & Mortola, 1996) with the relative contributions of each being variable between species as well as between studies on the same species. For example, Mortola and Saiki, (1996) reported a greater contribution from increases in V_T in rats exposed to 5% CO_2 , while Walker *et al.*, (1985) reported a larger contribution from increases in f_R to the same stimulus in rats (Saiki & Mortola, 1996). The percent increase in total ventilation with inspired CO_2 also varies among mammalian species (Boggs & Birchard, 1989). Unlike hypoxia, which generally causes metabolic depression, hypercapnia at physiological levels tends to have little effect on metabolism in adult mammals (Saiki & Mortola, 1996). However, since the increase in ventilation may change

arterial O₂ levels, it is important to consider the change in ventilation relative to any changes in metabolism when measuring hypercapnic ventilatory responses in mammals

Part of the variability in the ventilatory responses seen in mammals lies in the hypercapnic threshold at which a response is elicited. This threshold can be defined as the concentration at which an appreciable ventilatory response is produced, but threshold levels vary substantially across a range of mammal species (Tenney & Boggs, 1986). While human subjects increase their ventilation starting around 2% inspired CO₂, in other species such as the pocket gopher and naked mole rat, ventilation does not increase until ~5.5% inspired CO₂ (Arieli & Ar, 1979; Tenney & Boggs, 1986). Other species, like the hamster and echidna, are in the middle of this range showing an increase in ventilation starting at ~3.5% inspired CO₂ (Parer & Hudson, 1974; Tenney & Boggs, 1986; Mortola, 1991).

In addition to the hypercapnic threshold, variability in the HCVR is also rooted in differences in sensitivity to hypercapnia (an increase in atmospheric PCO₂). Tenney and Boggs (1986) showed that while the inspired CO₂ threshold for humans, dogs and rats lies somewhere around 2% inspired CO₂, their sensitivities differ greatly. In dogs and humans, the percent increase in ventilation rate is much greater by 3% inspired CO₂ (~125% increase) than that of the rat (~50% increase). Boggs and Birchard (1989) compared the ventilatory responses to 5% inspired CO₂ in several adult mammalian species with differing lifestyles. Humans increase ventilation their rate by about 250% when breathing 5% CO₂, while Sprague-Dawley rats and albino mice increase ventilation rate by about 125% at the same level of CO₂ (Tenney & Boggs, 1986; Kuwaki *et al.*, 1996; Stunden *et al.*, 2001). Most notably, fossorial (burrowing) mammals (for example; mole rat, pocket gopher, ground squirrel, hamster) have a greatly attenuated sensitivity to levels of CO₂ that normally produce a strong response in non-fossorial species (dog, human, rat). Burrowing mammals tend to show a smaller increase, and in some cases a decrease, in their f_R response to elevated CO₂ (Boggs *et al.*, 1984b; Tenney & Boggs, 1986; Webb & Milsom, 1994). These differences in ventilatory responses between fossorial and non-fossorial species are hypothesized to be due to the chronic hypercapnic conditions faced in borrows (Tenney & Boggs, 1986; Šumbera *et al.*, 2004; Shams *et al.*, 2005; Roper *et al.*, 2019). Even under normoxic/normocapnic conditions the pocket gopher and naked mole rat have lower than expected breathing frequencies (Boggs *et al.*, 1984b). This leads to CO₂ retention and a higher

PaCO₂ in mole rats (48 torr) and other fossorial mammals (ground squirrel; 52.4 torr) compared to non-burrowing mammals (arboreal porcupine; 35 torr) (Boggs *et al.*, 1984b; Boggs & Birchard, 1989). The comparatively high arterial CO₂ suggests a higher threshold for ventilatory responses and a reduced sensitivity to hypercapnia, which is supported by the observation of an attenuated hypercapnic response in comparison to non-fossorial species. These attenuated responses to hypercapnia suggest that fossorial mammals may sense CO₂ differently at both peripheral and central sites of CO₂ chemosensing.

Thus, variability in the ventilatory response to high environmental CO₂ in mammals can be found in the threshold for the ventilatory response, the magnitude of the ventilatory response (sensitivity to CO₂) and in the relative contribution of changes in V_T and *f_R* to the ventilatory response. The root of these differences may be found in the sites in the mammalian body where CO₂ is sensed, the sites where this information is integrated, the transformation into efferent output or the generation of motor activity.

1.3 Sites of chemoreception: peripheral and central

The central pattern generators located in the medullary region of the brainstem are subject to modulation from several inputs. The modulation by these inputs is vital to the production of changes in ventilation to match metabolic demand. Two primary inputs that modulate respiration with regard to CO₂ originate peripherally from the carotid bodies and centrally from several key sites in the brainstem.

The peripheral chemoreceptors (carotid bodies) send afferent signals to the brainstem via the sinus nerve (a branch of the glossopharyngeal nerve), which modulate ventilation based on PaO₂, PCO₂, and pH amongst other stimuli (Milsom & Burlison, 2007; Nurse, 2014). This cluster of chemosensory cells are strategically located at the bifurcation of the common carotid artery (Heymans, C., 1930; González *et al.*, 1992; Milsom & Burlison, 2007), and denervation of this group causes hypoventilation with a range of animals showing a 30-35% reduction in ventilation under resting conditions (Webb & Milsom, 1990; Forster *et al.*, 2000). The carotid bodies are composed of glomus type-I cells responsible for chemoreception and glial-like type-II cells that likely participate and contribute to the chemo-response of the carotid bodies (Nurse, 2014). There is strong evidence that glomus type-I cells depolarize in response to hypoxia and

low pH resulting from hypercapnia as a result of K⁺ channel inhibition (Buckler *et al.*, 1991; Peers *et al.*, 2010; Kumar & Prabhakar, 2012; Nurse, 2014), and type-II cells modulate the response of the carotid bodies to hypoxia and hypercapnia via pannexin channels (Kumar & Prabhakar, 2012; Nurse, 2014).

Early investigations into the location of the central chemoreceptors suggested that superficial areas of the ventrolateral medulla in dogs and cats were sensitive to a low pH perfusate, which caused an increase in ventilation (Mitchell *et al.*, 1963; Mitchell, R.A., Loeschcke, H.H., Massion, W.H., Severinghaus, 1963; Loeschcke *et al.*, 1969). Electrical stimulation of these areas also produced an increase in ventilation, and, specifically, two distinct areas (3mm and 9mm caudal to the ponto-medullary boarder) produced the largest change in ventilation (Loeschcke *et al.*, 1969). These two areas coincided with areas that were shown to be sensitive to pH. Since then, several specific central sites have been shown to be sensitive to pH and PCO₂, but a definitive explanation of how pH and PCO₂ are sensed in the brainstem has not yet been produced. One site that has been shown to be highly involved in central CO₂ sensing is the retrotrapezoid nucleus (RTN) (Guyenet *et al.*, 2008; Marina *et al.*, 2009; Nattie & Li, 2009). This group of glutamatergic neurons is located on the ventral medullary surface (an area previously shown to be pH sensitive by Loeschcke and Mitchell) and selectively innervates rhythm-generating sites. When subject to lesion or blockade, a reduction of the response to CO₂ is seen (Guyenet *et al.*, 2008).

Serotonergic neurons in the medullary raphe (Wang *et al.*, 2001) have also been hypothesized to be a site of respiratory CO₂ sensing due to their chemosensitivity *in vitro* as well as their proximity to cerebral blood vessels (Wang *et al.*, 1998, 2001; Nattie & Li, 2009). *In vitro*, both an increase in PCO₂ and a decrease in pH cause an increase in the firing rate of medial medullary raphe neurons in cell culture (Wang *et al.*, 1998), although these same stimuli also produce an inhibition of some neurons in the same location (Wang *et al.*, 1998). *In vivo* support of the role of the medullary raphe in chemoreception is not well documented, but the proximity of the CO₂ sensitive neurons to cerebral blood vessels is highly suggestive of its involvement in chemoreception.

Noradrenergic neurons in the locus coeruleus (LC) have also been implicated as possible chemoreceptive sites similar to neurons of the medullary raphe, and to possibly provide excitatory input that stimulates breathing (Oyamada *et al.*, 1998; Hilaire *et al.*, 2004; Gargaglioni *et al.*, 2010). Located in the dorsal medial pons, this neuronal group has been shown to be pH/CO₂ sensitive (Elam *et al.*, 1981). The LC has limited afferent innervations from the rostral medulla which is an area containing chemosensitive regions (such as the retrotrapezoid nucleus/parafacial respiratory group (RTN/pFRG)), and the rhythm generating sites (pre-bötzinger complex (pre-BötC)) (Oyamada *et al.*, 1998). *In vivo*, single cell recordings from LC neurons show an increase in firing rate under hypercapnic conditions in rats (Elam *et al.*, 1981). Additionally, selective inhibition of noradrenergic neurons in the LC produces a blunted hypercapnic response in intact rats which is reduced by ~64% compared to a sham injection (Ballantyne & Scheid, 2001; Biancardi *et al.*, 2008), which is unsurprising considering the LC contains the highest percentage of CO₂-activated neurons (>80%) of all brainstem regions (Putnam *et al.*, 2004; Gargaglioni *et al.*, 2010).

The relative contributions to ventilation of inputs from the peripheral (carotid) and central chemoreceptors have received much attention (Comroe & Schmidt, 1937; Smith *et al.*, 2010). It is generally thought that central chemoreceptors play a larger role (60:40, central: peripheral), and that the two inputs contribute in an additive fashion (Adams & Severns, 1982). It has also been suggested that the two inputs are hyper-additive (Day & Wilson, 2009), or synergistic (Loeschcke *et al.*, 1963; Smith *et al.*, 2010). Additionally, peripheral inputs from the carotid body are received in the RTN (a central chemosensitive site) via the nucleus tractus solitarius (NTS) suggesting an interaction between the two. The change in PCO₂ is sensed by the carotid bodies before central chemoreceptors given the proximity to the gas exchange surfaces. Thus it has also been suggested that the carotid bodies provide an immediate response to changes in arterial PCO₂ and central CO₂ sensing takes on a stronger role in ventilatory control if hypercapnic conditions persist (Mitchell & Singer, 1965; O'Regan & Majcherczyk, 1982).

1.4 The conditional nature of the hypercapnic ventilatory response

1.4.1 *Development of the hypercapnic ventilatory response in mammals*

The mammalian HCVR changes through postnatal development and this change has been most thoroughly examined in Sprague-Dawley rats. A distinct developmental pattern, termed the triphasic hypercapnic response, has been consistently reported in this species (Serra *et al.*, 2001; Stunden *et al.*, 2001; Wickström *et al.*, 2002; Putnam *et al.*, 2005). The triphasic response is named for the temporal shift in the HCVR that starts as a robust increase in ventilation in response to CO₂ on the day of birth (phase I), but then severely blunts over the next 2-5 days of development reaching a nadir during this period (Stunden *et al.*, 2001; Putnam *et al.*, 2005)(phase II). This period of insensitivity to hypercapnia gives way to a return of the HCVR between postnatal days 10-14 (P10-14;phase III) that stabilizes at the adult response (Stunden *et al.*, 2001). In most reports the initial HCVR on the day of birth is slightly higher than that of the adult (>postnatal day 30 (P30)) response (Stunden *et al.*, 2001; Wickström *et al.*, 2002; Putnam *et al.*, 2005).

The triphasic response appears to be unique to Sprague-Dawley rats as examination into other rat species (brown Norway and salt-sensitive Dahl S rates) revealed a progressive rise to the adult response over early development (Davis *et al.*, 2006). Interestingly, the same study reported a progressive rise in the HCVR in Sprague-Dawley rats as well, and not a triphasic response (Davis *et al.*, 2006). The basis of this discrepancy between studies on Sprague-Dawley rats is unclear, but it does potentially highlight the variability in the development of the HCVR. A progressive rise in the HCVR over early development has also been commonly reported in other species such as mice, dogs, and humans (Nattie & Edwards, 1981; Bissonnette & Knopp, 2004; Sjøvik & Lossius, 2004). Thus, a developmental change in the HCVR is common among mammals, but the pattern by which it occurs is variable. It is also possible that the pattern of HCVR development is not variable, but rather the time during peri-and postnatal development in which it happens is. For example, phase I of the triphasic response may occur earlier or simply be absent in other species. In support of this, the most substantial rise in the HCVR of brown Norway and salt-sensitive Dahl S rats coincides with phase-III in Sprague-Dawley rats (Stunden

et al., 2001; Wickström *et al.*, 2002; Davis *et al.*, 2006). Examination of the mechanistic changes producing the shifts in the HCVR has shed some light on this.

It appears that changes in both peripheral and central chemoreceptors drive the global changes in the HCVR through development. Peripherally, the carotid bodies are not morphologically or functionally mature at birth (Bamford *et al.*, 1999; Wang & Bisgard, 2005; Wong-Riley *et al.*, 2013). Over postnatal maturation, significant changes in carotid body function and morphology occur at birth, and it is likely these changes are heavily influenced by the sudden increase in blood oxygen levels (~25 Torr *in utero* to ~100 Torr *post-partum*) at birth (Mortola, 2001a). Morphologically, there is a progressive enlargement of the carotid bodies. For example, in cats, carotid body volume (per unit of weight) is three times larger in adults compared to neonates (Clarke & de Burgh Daly, 1985; Wang & Bisgard, 2005). The increase in relative volume of the carotid bodies is mainly mediated by postnatal type-I cell proliferation, and to a lesser extent, type-II cell proliferation (Clarke & de Burgh Daly, 1985; Wang & Bisgard, 2005). The microvasculature of the carotid bodies also increase but in proportion to the carotid body size, and therefore does not differ between neonates and adults (Clarke & de Burgh Daly, 1985; Wang & Bisgard, 2005).

Along with morphological changes, the carotid bodies undergo significant functional changes in response to hypercapnia through development. While most reports focus on sensitivity to hypoxia, Bamford *et al.* (1999) reported that the increase in intracellular calcium in response to hypercapnia in type-I cells increased 5-fold over the first 8 days of postnatal development in rats (Bamford *et al.*, 1999). Few studies have investigated the role of changes in neurotransmitter distribution and abundance in relation to changes in carotid body sensitivity to hypercapnia, but it appears that acetylcholine, adenosine triphosphate (ATP), and dopamine content and receptor mRNA expression increase postnatally (Bairam & Carroll, 2005; Huxtable *et al.*, 2009; Kumar & Prabhakar, 2012; Bairam *et al.*, 2013). While progress has been made elucidating the various chemotransductive pathways and the associated neurotransmitters (reviewed in Bairam and Carroll 2005; Kumar and Prabhakar 2012; Nurse 2014), it is clear that the system is complex. Further, neurotransmitter abundance and type both vary with age, but this does not appear to be involved directly in the increase in carotid body sensitivity with maturation (Donnelly, 2005).

Maturation changes in central chemoreceptors have also been well examined, again most thoroughly in Sprague-Dawley rats. During the blunting (phase-I) period of the triphasic response, there is a precipitous drop in both excitatory networks as well as excitability of chemosensitive regions of the brainstem (Liu & Wong-Riley, 2008; Gao *et al.*, 2011; Wong-Riley *et al.*, 2019). This reduction is primarily in glutamatergic networks, but at the same time GABAergic networks increase in expression in the same regions (Wong-Riley & Liu, 2005). The net result is a transient preeminence of inhibitory over excitatory networks coinciding with the initial blunting of the HCVR. At the same time (~0-14 days post birth), Ca²⁺ and BK currents (L-type Ca²⁺ channels and large conductance Ca-activated K⁺ channels (BK)) in the locus coeruleus develop, and their role in the hypercapnia response of the LC may be to act as a “brake” (Imber *et al.*, 2018). Specifically, the increased activity of Ca⁺ channels should increase intracellular calcium and activate BK channels which would effectively serve as a negative feedback function in the hypercapnic response (Gargaglioni *et al.*, 2010; Imber *et al.*, 2018). Thus, excitatory and inhibitory imbalance in several central chemosensitive sites, as well as Ca²⁺ and BK current development potentially tempering the hypercapnia response of the LC, result in a period of greater relative inhibition that coincides with the period of hypercapnic insensitivity.

During the third phase of the triphasic response, where the HCVR is restored in Sprague-Dawley rats and rises in other mammalian species, the transient imbalance in the central chemoreceptors described above, reverses (Wong-Riley & Liu, 2005; Liu & Wong-Riley, 2008; Wong-Riley *et al.*, 2013, 2019). This period also coincides with the increase in carotid body responsiveness to hypercapnia (Bamford *et al.*, 1999; Wang and Bisgard, 2005). Additionally, it is possible that the maturation of the LC removes the relative braking of the LC hypercapnic response (Imber *et al.*, 2018) which may also contribute to the overall increase in the HCVR seen during phase-III. In adults this braking likely only has an effect on the total LC response to severe hypercapnia where the increase in LC neuron firing in response to hypercapnia plateaus, but maturation to this balance appears to occur at or after P10 in rats (Pineda & Aghajanian, 1997; Imber *et al.*, 2018).

It is unclear whether differences in the time course of these changes account for the differences seen in the development of the HCVR in different species, or if different species simply show different mechanistic changes. But the HCVR does shift with age, and in at least

one species there are clear central and peripheral chemoreceptor changes that coincide with the changes in the HCVR.

1.4.2 Hibernation and hypercapnia

During periods of resource scarcity or extreme environmental conditions, some mammals undergo torpor (either in a cyclic seasonal fashion, or facultatively at any point of the year). Mammals that hibernate (obligate seasonal torpor) display a suite of significant physiological changes during hibernation that include reductions of body temperature (T_b), metabolic rate, ventilation, and heart rate (Lyman & Chatfield, 1950; Lyman, 1958*b*). Most mammals that are in deep hibernation have a core body temperature that is at or near ambient temperature. In edible dormice (Wilz & Heldmaier, 2000; Elvert & Heldmaier, 2005), golden-mantled ground squirrels (Zimmer & Milsom, 2001), and the little-brown bat (Szewczak & Jackson, 1992) the fall in metabolism is linked to the fall in core body temperature, while arctic ground squirrels, bears (Barnes & Buck, 2000), marmots (Ortmann & Heldmaier, 2000), and echidnas (Nicol et al., 1992) drop metabolic rate rapidly at the onset of hibernation and it remains low despite further reductions in body temperature. Along with changes in metabolism and body temperature, total ventilation is reduced by as much as 98% from that of an active euthermic animal (Milsom & Jackson, 2011).

The relative responses to respiratory stimuli are greatly altered in hibernation. The ventilatory response to hypoxia is near absent in hibernation as even 3% inspired O_2 does not elicit a change in ventilation (McArthur & Milsom, 1991*a*; Barros *et al.*, 2001), which is likely due to the increase in Hb- O_2 affinity associated with lower temperatures. Hypercapnia, however, always produces a strong ventilatory response in hibernation (Endres & Taylor, 1930; Lyman, 1951; Tähti, 1975; McArthur & Milsom, 1991*a*; Harris & Milsom, 1993; Webb & Milsom, 2017). Further, the relative response to hypercapnia increases by as much as 10-fold in hibernating golden mantled ground squirrels and Columbian ground squirrels compared to their active counterparts (McArthur & Milsom, 1991*a*; Webb & Milsom, 2017). The increase in ventilation to hypercapnia in hibernation is mainly a product of increases in breathing frequency while increases in tidal volume occur only at more severe levels of hypercapnia (>5%) (McArthur & Milsom, 1991*a*; Webb & Milsom, 2017). Hypercapnia also induces arousal if the

level exceeds ~7-8% inspired CO₂ in golden-mantled ground squirrels (Harris & Milsom, 1993; Milsom & Jackson, 2011), and thus it is evident that levels of blood PCO₂ and pH have a greater role in determining breathing pattern and arousal state in hibernation than do levels of PO₂ (McArthur & Milsom, 1991a; Webb & Milsom, 2017).

The root of the enhanced hypercapnic ventilatory response in hibernation is unclear. In at least two species, (golden-mantled and Columbian ground squirrels), there appears to be no effect of season or ambient temperature on the HCVR of euthermic animals (McArthur & Milsom, 1991b). This suggests that the change in the HCVR in hibernation is not the result of changes associated with preparation for hibernation, but rather an effect associated with the physiological changes accompanying entrance into hibernation (Milsom & Jackson, 2011). A few studies have attempted to determine the basis of the change in the HCVR. In squirrels made artificially hypothermic, without the shift into a hibernating state, the HCVR in absolute and relative terms is almost identical to that of a euthermic animal (Zimmer & Milsom, 2002a). This suggests that the change in body temperature does not directly affect the HCVR in hibernation. However, cooling hibernating golden-mantled ground squirrels from 7°C to 5°C reduces the HCVR by 50%, suggesting that either a direct or indirect effect of temperature may contribute to the enhanced response (Webb & Milsom, 2017). But as the change in body temperature in these animals is also associated with changes in breathing pattern, total ventilation, and metabolic rate, the driving factors underlying the shift in the HCVR remain unclear (Webb & Milsom, 2017).

Data recorded during entrance into and arousal from hibernation support this notion in that CO₂ appears to contribute to metabolic suppression during the hibernation bout. Just prior to when the animal begins to enter into hibernation there is a precipitous drop in the respiratory exchange ratio (RER), calculated as the ratio of CO₂ production and O₂ consumption, minutes preceding the fall in metabolic rate (Snapp & Heller, 1981; Bickler, 1984; Malan, 1988; Nestler, 1990). This drop in RER is thought to be the consequence of a period of CO₂ retention that serves to suppress metabolism in a temperature independent manner (Snapp & Heller, 1981; Malan, 1988). This is supported by data showing that metabolic rate, as well as ventilation and heart rate, all drop before body temperature on entrance into hibernation (Endres & Taylor, 1930; Lyman, 1958b; Snapp & Heller, 1981). It is unclear if the associated respiratory acidosis is directly involved in reducing general body metabolism (Malan, 1988) or indirectly affects central

integrative processes (Snapp & Heller, 1981). But, for this to happen a drop in ventilation prior to the fall in metabolic rate signaling a hypoventilation that must occur to retain CO₂. And furthermore, hypoventilation during this period would mean that changes in ventilation would have to supersede homeostatic regulation of blood gases and pH (Milsom & Jackson, 2011). Similarly, on arousal a transient spike in the RER signals a large CO₂ “dump” that would effectively remove the brake on metabolic rate (Snapp & Heller, 1981; Bickler, 1984; Nestler, 1990). Thus, the sensitivity to hypercapnia must shift during these periods to facilitate the retention and expulsion of CO₂, as well as present a period of tighter CO₂/pH regulation given the importance to metabolic regulation during hibernation.

The change in sensitivity to hypercapnia through a hibernation bout further exemplifies the conditional nature of the ventilatory response to CO₂. The driving force underlying the change in the response to hypercapnia remains unclear but may lie in changes in state and temperature.

1.5 Thesis objectives and chapter summaries

The objective of this thesis was to examine and compare the conditional nature of the HCVR in mammals under two major conditions where it is known to change: during postnatal development and during transition into and out of the hibernating state.

1.5.1 Chapter 2: Development of the ventilatory response to CO₂ in fossorial rodents

The goal of this chapter was to examine the development of the HCVR in fossorial mammals. Adult fossorial rodents have a greatly attenuated HCVR similar both to the second phase of the Sprague-Dawley rat’s triphasic response, and to the initial blunted response of other newborn mammals. This prompted me to examine if burrowing rodents (13-lined ground squirrels, an obligate hibernator, and golden-Syrian hamsters, a facultative hibernator) are born with their blunted adult response or if it is a retention of the secondary blunted period seen in non-burrowing mammals (Sprague-Dawley rats) in an attempt to shed light on the development of the HCVR in mammals. I hypothesized that fossorial rodents were born with their adult response given previous evidence for a strong genetic component to the adult HCVR seen in other species.

1.5.2 Chapter 3: Effect of burrow conditions on the development of the hypercapnic ventilatory response in fossorial rodents

The results of Chapter 2 showed that the blunted HCVR in adult fossorial mammals is genetically determined. The goal of chapter 3 was to expand on this observation by examining whether it is also plastic and modified by environmental effects. The fossorial animals in chapter 2 were raised in non-burrow conditions yet still developed the blunted adult response. By raising the same species in burrow-like conditions, I aimed to examine to what degree the burrow environment affects the development of the adult fossorial HCVR. Previous studies showed that raising non-fossorial rodents in a hypercapnic environment only transiently affected the HCVR, and that removal from the burrow conditions reset the HCVR back to what it would have been had the animals been raised in room conditions. This study was designed to determine whether this is the case in fossorial species also. Considering both groups (fossorial and non-fossorial) develop their adult response, I hypothesized that the fossorial HCVR would be strongly determined by genetic influences and neurochemical development, and thus would be plastic through development but that the adult response would be unaffected.

1.5.3 Chapter 4: Effect of temperature on the hypercapnic ventilatory response in steady state hibernation

The main purpose of this study was to examine temperature effects on the HCVR in adult 13-lined ground squirrels in steady state hibernation. It has been consistently observed that the HCVR is enhanced in hibernation in several species. These studies compared responses in animals at one hibernation temperature with those of euthermic animals. Studies on hypothermic animals suggested that the change in the HCVR was not due to the decrease in temperature implicating change in hibernation state. There is also evidence in some species that core body temperature in steady state hibernation may reflect changes in hibernation state. I hypothesized then that the HCVR in 13-lined ground squirrels would be dependent only on state, thus the HCVR would be uniformly elevated in hibernation and only fall when the animals arouse from a deep hibernation state at their lower critical temperature. Thus, I measured the HCVR of hibernating ground squirrels at varying core body temperatures determined by varying ambient temperature.

1.5.4 Chapter 5: Changes in CO₂ sensitivity during entrance into and arousal from hibernation

This study examines the shift in respiratory sensitivity to CO₂ first, at the onset of entrance into hibernation, and second, as animals progressively cool in hibernation (an extension of chapter 4). Just prior to the entrance into hibernation, a period of CO₂ retention has been reported in many species, but for this to occur there must be a period of hypoventilation and reduced CO₂ sensitivity. The first part of this study was to confirm that there is a transient reduction in CO₂ sensitivity that precedes entrance into hibernation. The second part of this study examined the change in the HCVR as entrance and arousal progressed. During these transitional periods, there is a hysteresis between the correlation between body temperature and metabolic rate. Metabolic rate drops before body temperature on entrance and rises before body temperature on arousal. This allowed me to separate temperature and state effects (as indicated by the change in metabolic rate) on the HCVR observed in chapter 4. I hypothesized that the HCVR would become elevated as the animals entered hibernation as state shifted (indicated by metabolic rate) and that there would be a period of hypercapnia insensitivity just prior to this. On arousal, the HCVR would fall with state, but remain elevated until the retained CO₂ was blown off.

1.5.5 Chapter 6: Does state and temperature alter the role of the locus coeruleus in the hypercapnic ventilatory response?

Data from chapters 4 and 5 suggested that the shift in CO₂ sensitivity was adjusted according to the current need of the animal and was affected by state and not temperature. The HCVR likely was altered either by changes in chemoreceptor input, or central integration of these inputs. The locus coeruleus (LC) serves as a major central chemosensor as well as an integral part of the reticular activating system in charge of determining state. I chemically lesioned the LC to determine first, its contribution to the HCVR in euthermic 13-lined ground squirrels and second, its contribution to the HCVR in steady state hibernation. I hypothesized that the LC would contribute to the HCVR in euthermia via increasing tidal volume, but in hibernation its role would shift to elevating breathing frequency, but it would still contribute to the HCVR.

Chapter 2: Comparison of the CO₂ Ventilatory Response Through Development in Three Rodent Species: Effect of Fossoriality

2.1 Summary

Burrowing rodents have a blunted ventilatory response to CO₂ in comparison to non-burrowing rodents. Non-burrowing rats display a period during development where ventilatory responses to hypercapnia become transiently blunted. This study examined the ventilatory responses to CO₂ of rats, hamsters and ground squirrels through neonatal development to determine whether the blunted adult response of burrowing species is a retention of the blunting period seen in rats or present from birth. All three species increased ventilation in response to hypercapnia on the day of birth (70-170% in response to 5% CO₂; 100 to 250% in response to 7% CO₂). Rats in our study exhibited the triphasic ventilatory response (when expressed as %Δ) to CO₂ previously described. In golden-Syrian hamsters, the ventilatory response slowly and progressively waned to a blunted adult response while in the 13-lined ground squirrels, the early ventilatory response to CO₂ decreased within days and remained attenuated through development. Our study shows three distinct developmental patterns in the hypercapnic ventilatory response.

2.2 Introduction

Elevated environmental CO₂ (hypercapnia) is a strong respiratory stimulant in mammals (Walker *et al.*, 1985; Feldman, 1986; Tenney & Boggs, 1986; Nattie & Li, 2009). Typically, when given hypercapnic air, mammals respond with an increase in ventilation (\dot{V}_E) due to increases in both tidal volume (V_T) and breathing frequency (f_R) (Walker *et al.*, 1985). In contrast, adult fossorial rodents (rodents that live in underground burrows) are known to have a high tolerance for hypercapnia compared to non-fossorial rodents like rats, presumably due to their burrowing nature (Boggs *et al.*, 1984b; Boggs & Birchard, 1989). Though burrow structures are variable, depending on species, (Tenney & Boggs, 1986), burrows can be hypercapnic and hypoxic because gas diffusion through soil is inadequate for the amount of CO₂ produced and O₂

consumed by their occupants (Wilson & Kilgore, 1978). The level of CO₂ in burrows can rise to between 1-8% (Tenney & Boggs, 1986), and since developing neonates of burrowing rodents are born and remain in these conditions until weaning, this may contribute to their tolerance and reduced sensitivity. For example, the threshold for eliciting a ventilatory response in the fully-fossorial (lives permanently underground) naked mole rat is ~5% CO₂, (Arieli & Ar, 1979; Boggs *et al.*, 1984b) while that for the semi-fossorial (spends time both above and below ground) echidna is ~3% CO₂ (Parer & Hudson, 1974). Humans and dogs, on the other hand, begin to hyperventilate at ~0.5% inspired CO₂ (Tenney & Boggs, 1986) and adult rats at about 2% inspired CO₂ (Arieli & Ar, 1979). In addition to higher thresholds, fully and semi-fossorial rodents also have an attenuated ventilatory response after their threshold is surpassed. For example, in hypercapnia (5% CO₂) golden-Syrian hamsters increase \dot{V}_E by about 40% of their normocapnic ventilation compared to the 120% increase under the same conditions reported in rats (Boggs & Birchard, 1989).

Non-fossorial rodents do have a developmental window during which their hypercapnic ventilatory response (HCVR) is also blunted, however (Stunden *et al.*, 2001; Wickström *et al.*, 2002). In rats for example, a distinct triphasic response pattern has been consistently observed where an early postnatal (P0-2) response becomes blunted (P7-9), but subsequently rises again to adult response levels (P14-adult) (Stunden *et al.*, 2001; Wickström *et al.*, 2002; Putnam *et al.*, 2005). This raises the question of whether neonates of semi-fossorial species are born with an attenuated response to hypercapnia, or develop an attenuated response, as do rats, but one that is then retained. We used Sprague-Dawley rats (*Rattus norvegicus*), golden-Syrian hamsters (*Mesocricetus auratus*, facultative hibernators that are semi-fossorial), and 13-lined ground squirrels (*Ictidomys tridecemlineatus*; seasonal hibernators that are fully-fossorial during the hibernating season) to address this question in more detail. Thus, these species range in degree of fossoriality and heterothermy.

We hypothesized that the developmental pattern in the HCVR of semi-fossorial mammals would differ from the triphasic rat response, and that the attenuated adult fossorial response would be present at birth. Furthermore, we hypothesized that the two semi-fossorial mammals would have the same pattern of development of the HCVR. Thus, the HCVR of these three species was examined over the developmental period from birth (postnatal day zero (P0)) to

adulthood (P29-30) in animals raised under normocapnic conditions to separate out genetic factors from developmental plasticity.

2.3 Methods

2.3.1 Animals

All procedures were conducted under a protocol approved by the UBC Animal Care Committee (A17-0018) and were in compliance with the policies of the Canadian Council on Animal Care. Gravid Sprague-Dawley rats and golden-Syrian hamsters were acquired commercially from Charles River (Wilmington, Massachusetts). Gravid 13-lined ground squirrels were acquired by trapping in Carman, MB, Canada (49°30' N, 98°01' W) and transferred to an animal care housing facility at the University of British Columbia in Vancouver, BC, Canada. 13-lined ground squirrels were trapped with the approval of Manitoba Conservation and Water Stewardship, under wildlife scientific permit WB15027. Wild female 13-lined ground squirrels were treated with Ivermectin and Droncit for endoparasites (0.4 mg/kg, subcutaneous), and flea spray for ectoparasites. Any pup born before the mother was treated, was dosed with Ivermectin and Droncit once a minimum body mass was met (50g). All animals were kept in a temperature-controlled chamber ($20\pm 2^{\circ}\text{C}$) on a photoperiod that matched the daily outdoor photoperiod in Vancouver. Sprague-Dawley rats and golden-Syrian hamsters were fed a rodent chow diet (Lab Chow) supplemented with assorted cereals and nuts *ad libitum*. 13-lined ground squirrels were fed IAMS large chunk dog chow supplemented with apples, assorted cereals, peanuts, and sunflower seeds *ad libitum*. All species were allowed access to water *ad libitum*.

2.3.2 Measurement of Ventilation and Oxygen Consumption

2.3.2.1 Ventilatory Measurements

During the ages when pups could not maintain a large enough body temperature/ambient temperature (T_b/T_{am}) difference for whole body plethysmography (~P0-P20) (Ivy & Scott, 2017) ventilation was measured using pneumotachography. A small facemask was made from the barrel of a 5, 10, or 30ml syringe tube depending on the size of the animal to reduce dead space.

The mask was sealed tightly around the head (caudal to the ears) of the animal with a rubber cuff. A rubber stopper was used to seal the open end of the mask. Inflow and outflow ports were inserted into the rubber cork. A pneumotachograph was attached on the outflow side of the facemask. Pressure changes across the pneumotachograph were measured with a differential pressure transducer (Validyne model DP103-18; Validyne Engineering Northridge, California) and amplified with a Gould DC amplifier (Gould; Valley View, Ohio). Inflow gases were metered with a rotameter (Matheson 4334; Whitby, Ontario) and a flow rate of 20-120ml/min was used based on the oxygen consumption of the animal. The system was calibrated for tidal volume by injecting known volumes (0.1, 0.2 and 0.3 mL) across the pneumotachograph on top of the constant gas flow (at a frequency similar to the respiratory frequency of each respective species).

Whole body plethysmography (otherwise known as the barometric method) was used to measure ventilation during the ages when pups were able to maintain a large enough T_b/T_{am} difference ($>4^{\circ}\text{C}$) for accurate measurement (~P20-29, 30) (Drorbaugh & Fenn, 1955a; Malan, 1973; Jacky, 1980). For this study, the minimum T_b/T_{am} difference seen was 7°C with most T_b/T_{am} differentials ranging from 10°C to 15°C . Pups were placed in one of two identical plexiglass chambers (large set: 10cm x 10cm x 10cm, medium set: 9cm x 6cm x 7cm, small set: 7cm x 5cm x 7cm (length x width x height)) that allowed them to move freely. These experimental chambers were housed in a temperature-controlled chamber to allow for a consistent known ambient temperature. A constant flow (100-120ml/min) was maintained through both chambers that were each connected to a pressure transducer (Validyne model DP103-18). Ports on two sides of the chamber allowed for gas movement into and out of the chamber, and a port on the top allowed for connection to the pressure transducer. Pressure changes from the warmed and humidified expired air in the animal chamber were detected by the pressure transducer (Validyne model DP103-18) and amplified with a Gould DC amplifier (Gould; Valley View, Ohio). The system was calibrated for tidal volume, and gas concentrations as described above but by injecting known volumes directly into the chamber. The plethysmograph remained closed for the duration of breathing pattern measurement and calibration.

2.3.2.2 *Metabolic Measurements*

Flow-through respirometry was used to measure O₂ consumption and CO₂ production ($\dot{V}O_2$ and $\dot{V}CO_2$) as indicators of metabolic rate. For the younger animals (P0-P20), the facemask also served as a respirometer. Gas flow rate through the mask was 20-120ml/min set such that the fractional composition of the O₂ in the outflow gas did not fall by more than 1%. For older animals (P20-P29, P30) the whole body plethysmograph served as a respirometer and a constant flow (100-120ml/min) was maintained through the animal chamber again set such that the fractional composition of the O₂ in the outflow gas did not fall by more than 1%. In both cases, outflow gas was connected to a desiccant (silica beads) and then to a field metabolic system (FMS; Sable Systems International; North Las Vegas, Nevada) or to Beckman gas analyzers (OM-11 and LB-2; Beckman Coulter Indianapolis, Indiana) for analysis of O₂ and CO₂ composition. Inflow gases were analyzed for gas composition at the start of each trial at each respective flow rate. O₂ and CO₂ analyzers were calibrated to correct for drift with pre-mixed gases of known concentrations (0, 5, and 7% CO₂ with 21% O₂, balanced with N₂) daily.

2.3.3 *Measurement of Temperature*

Chamber temperature was monitored with a T- type thermal probe connected to a physitemp (Bat-12, Physitemp, Clifton NJ) analyzer and maintained between 21-30°C, adjusted to ensure animals remained at normal body temperatures (~38°C). Animal T_b and nasal temperature (T_n) were monitored with a FLIR (forward looking infrared) thermal monitoring system (FLIR; Wilsonville, Oregon, United States) throughout the experimental trials in order to make adjustments to ambient temperature to allow for a normal T_b (~38°C). FLIR thermal imaging provided a non-invasive method to monitor temperature in neonatal rodents that are imperfect thermal regulators (Tattersall, 2016). Animal chambers were housed in a temperature-controlled unit to help maintain temperature.

2.3.4 *Experimental Protocol*

For pneumotachography, pups were taken from the litter and placed on a heating pad. A mask was custom fit to each pup (as previously described in section 2.2.1) and the body of the animal was placed in a plastic syringe open on both sides. This body chamber was clipped to the facemask chamber, limiting the animal from excessive movement. Animals were allowed to

acclimate while breathing normocapnic air (21% O₂ balanced with N₂) for 1h prior to the administration of the hypercapnic gas mixtures.

For whole body plethysmography, pups were taken from the litter and placed in a plexiglass chamber with bedding and allowed a 1h acclimation period breathing normoxic air prior to the administration of the hypercapnic gas mixtures. Bedding was changed before the start of each trial.

In all cases, pups were exposed to pre-mixed gasses (Praxiar Canada, Vancouver B.C.) containing 0%, 5%, and 7% CO₂ combined with 21% O₂ (balanced with N₂) in random order. Each gas combination was administered for 15 minutes with normoxic air supplied for 15 minutes in between each CO₂ trial. Total run time for each experiment was about 120 minutes. Pups from multiple litters (golden-Syrian hamsters: 3 litters, Sprague-Dawley rats: 2 litters, 13-lined ground squirrels: 5 litters) were required to obtain a sample size of 5-6 for each day of development (P0-P29 or 30) for each species. Given litter size, the minimum time between testing of the same pup was ~4 days and this time increased with litter size. All data, except body and nasal temperature, were acquired using a PowerLab 16/32 data acquisition system (ADInstruments; Colorado Springs, Colorado).

2.3.5 *Data Analysis*

Data analysis was done on Labchart v8.1.9 (ADInstruments; Colorado Springs, Colorado). Two 1-2 minute windows from the middle and end of each trial (during ~6-8th and 13-15th minutes) were analyzed. The respiratory variables tidal volume (V_T; ml/kg) and breathing frequency (f_R; breaths/min) were averaged for each gas trial on each animal. The oxygen and CO₂ fractional concentration values for calculating O₂ consumption and CO₂ production (ml/min/kg) were taken from the minute before the trial (inflow) and the same time intervals over which the respiratory variables were measured (outflow). Ventilation ($\dot{V}E = V_T \times f_R$; ml/min/kg) and the air convection requirement (ACR = $\dot{V}E / \dot{V}O_2$) were calculated from the measured variables. $\dot{V}O_2$ was calculated using the following equation;

$$\dot{V}O_2 = FR \left\{ F_{iO_2} - \frac{(1 - F_{iO_2} - F_{iCO_2})}{(1 - F_{eO_2} - F_{eCO_2})} (F_{eO_2}) \right\}$$

where FR is the flow rate of the inflow gas; Fio₂ is the fraction of inspired oxygen; Feo₂ is the fraction of expired oxygen; Fico₂ is the fraction of inspired carbon dioxide; and Feco₂ is the fraction of expired carbon dioxide (Lighton, 2008). For pneumotachography, V_T was determined by integrating the differential pressure signal produced by the change in flow due to each breath. For whole body plethysmography, V_T was calculated using the following equation;

$$Tidal\ Volume = \frac{P_m \times \dot{V}_{cal} \times T_A(PB - P_{CH_2O})}{P_{Cal}(T_A(PB - P_{CH_2O}) - T_C(PB - P_{AH_2O}))}$$

where P_m is the measured pressure deflection; V_{cal} the calibration volume; T_A the body temperature; PB the barometric pressure; P_{CH₂O} the water vapor pressure at chamber temperature; P_{Cal} the measured pressure deflection of the calibration volume; P_{AH₂O} the water vapor pressure at animal body temperature. These tidal volumes were then corrected for the difference in whole body versus nasal temperature with the following equation;

$$\frac{\dot{V}}{VCOR} = 1 - \left(\frac{TI}{TTOT} \right) \left(1 - \frac{T_b}{T_n} \right)$$

where VCOR is the corrected volume; TI the inspiratory time; TTOT the total time for inspiration and expiration; T_b the body temperature and T_n the nasal temperature (Drorbaugh & Fenn, 1955a; Jacky, 1980).

2.3.6 Statistical Analysis

A two-way ANOVA was used to determine the effect of age (within treatment group compared to the starting value (P₀)) and treatment (between CO₂ treatments on the same day) on respiratory and metabolic variables. A separate two-way ANOVA was used to determine the effect of age and species on the percent increase in ventilation to 5 and 7% inspired CO₂. A Shapiro-Wilks test was used to test for normality, and a Levene test was used to test for equal variance in all two- way ANOVAs. Tukey's post-hoc tests were used for comparisons and a significance level of p<0.05 was used throughout. All statistics were run with R Studio statistical software (RStudio Version 1.1.447) with the exception of the species comparison, and all comparisons made on percent change data, which were run with GraphPad Prism 7 statistical software. All values are reported as mean ± S.E.M.

2.4 Results

2.4.1 Sprague-Dawley rats

Normocapnia

Breathing frequency increased significantly with age in Sprague-Dawley rats as did V_T (Fig. 2.1). Thus \dot{V}_E (ml/kg/min) also increased significantly with age (Fig. 2.1). Mass specific oxygen consumption (\dot{V}_{O_2} ; ml/min/kg) initially increased with age; P13-17 animals had a significantly larger \dot{V}_{O_2} compared to P0 animals ($p < 0.05$) (Fig. 2.1). Shortly after, \dot{V}_{O_2} fell to adult levels, which were still elevated but not significantly different from values for P0 animals (Fig. 2.1). The air convection requirement (ACR; $\dot{V}_E / \dot{V}_{O_2}$) did not change with age with the exception of the oldest (P29-P30) animals, which had a significantly larger ACR in comparison to animals of all other ages ($p < 0.05$) (Fig. 2.1).

Hypercapnia

Hypercapnia (5 and 7% CO_2) significantly increased f_R , V_T , and \dot{V}_E early in development (roughly P1-7) ($p < 0.05$) and again later in development (roughly P12-29) ($p < 0.05$) (Fig. 2.1 and 2.2) but did not have any significant effect on ventilation between ~P8-12. Hypercapnia had no effect on oxygen consumption at any time during development (Fig. 2.1). Thus, the ACR also significantly increased in hypercapnia early in development (P0-6) and again later in development (P12-29) (Fig. 2.1). The \dot{V}_E responses to 5 and 7% inspired CO_2 were not significantly different with the exception of two days (P3 and P5) where \dot{V}_E increased significantly more in 7% CO_2 .

2.4.2 Golden-Syrian hamsters

Normocapnia

In golden-Syrian hamsters f_R increased significantly throughout development until roughly day 20 ($p < 0.05$) (Fig. 2.3), while V_T remained relatively constant (Fig. 2.3). \dot{V}_E increased significantly until age P15, largely due to the increases in f_R (Fig. 2.3). Mass-specific \dot{V}_{O_2} (ml/min/kg) increased significantly with age and reached a maximum at P21 before decreasing again to adult levels (Fig. 2.3). The ACR did not change significantly with age (Fig. 2.3).

Hypercapnia

In golden-Syrian hamsters, hypercapnia (5 and 7% CO₂) only increased f_R and V_T significantly early in development (Fig. 2.3). However, when the net effects of the changes in both were combined, \dot{V}_E increased significantly under hypercapnic conditions from P0-P20 (Fig. 2.3 and 2.4). There was no effect of hypercapnia on oxygen consumption (Fig. 2.3). The ACR increased significantly in hypercapnia early in development but this effect slowly tapered off (Fig. 2.3). When expressed as % change, the increase in all ventilatory variables due to hypercapnia progressively decreased throughout development (Fig. 2.4). The \dot{V}_E responses to 5 and 7% inspired CO₂ were not significantly different with the exception of two days (P1 and P2) where \dot{V}_E increased significantly more in 7% CO₂.

2.4.3 13-lined ground squirrels

Normocapnia

During early postnatal development (P0-P7) f_R increased significantly but then leveled off and declined to levels that were not significantly different from values recorded for P0 animals (Fig. 2.5). V_T , on the other hand, did not increase with age early on, but did increase significantly starting at age P16 (Fig. 2.5). As a result, \dot{V}_E increased reaching a peak in animals between the ages of P16-P26 ($p < 0.05$) but then declined to values similar to those of P0 animals (Fig. 2.5). Mass-specific \dot{V}_{O_2} increased significantly with age (Fig. 2.5) leveling off after P17 but remained elevated in comparison to P0 animals (Fig. 2.5). The ACR did not change with age (Fig. 2.5).

Hypercapnia

Hypercapnia did not significantly alter f in the 13-lined ground squirrels (Fig 2.5 and 2.6). V_T and \dot{V}_E , however, increased significantly during the first half of development (Fig. 2.5 and 2.6) but these responses were reduced throughout the second half. Hypercapnia did not have an effect on oxygen consumption in 13-lined ground squirrels (Fig. 2.5). Thus, the ACR also increased significantly during the first half of development (Fig. 2.5). When expressed as % change, the initial increase in breathing frequency due to hypercapnia on P0 decreased rapidly but then rose again in late development (Fig. 2.6). The initial increase in V_T decreased progressively. The net effect was that the initial increase in \dot{V}_E due to hypercapnia was rapidly reduced and the net response remained low throughout the rest of development. The \dot{V}_E

responses to 5 and 7% inspired CO₂ were not significantly different with the exception of one day (P18) where \dot{V}_E increased significantly more in 7% CO₂.

2.5 Discussion

The pattern of development of the HCVR in semi-fossorial golden-Syrian hamsters and 13-lined ground squirrels differs from that of the non-fossorial rat. Our results also show that the pattern of development of the HCVR in the two semi-fossorial species differ from each other (Fig. 2.7) (Putnam *et al.*, 2005). In both cases, the attenuated HCVR seen in the adults of the semi-fossorial species was not present at birth (Fig. 2.7). Indeed, the newborns of the semi-fossorial species in the present study were more responsive to hypercapnia than newborns of the non-fossorial rat (Fig. 2.7).

2.5.1 Changes in the HCVR through development in non-fossorial neonates

In Sprague-Dawley rats we saw a triphasic pattern in the HCVR through development (an initial robust increase in ventilation at birth that became attenuated and reached a nadir around P15 before rising again into adulthood) as has been reported by others (Stunden *et al.*, 2001; Putnam *et al.*, 2005). The initial HCVR present at birth (P0-1) in Sprague-Dawley rats appears to have been due to increases in V_T only (Fig. 2.2) with contributions from breathing frequency developing over the next few days. The subsequent nadir in the HCVR was due to reductions in both V_T and f_R , both of which increase again during late development (P11-29). However, the nadir was mostly due to reductions in tidal volume. Previous studies show a similar trend, where tidal volume contributes more to the changes in ventilation early in development, with breathing frequency making larger contributions later in development (Stunden *et al.*, 2001; Putnam *et al.*, 2005). A lower HCVR in neonates compared to adults has also been reported in other non-fossorial mammals including neonates of humans, dogs, and pigs (Nattie & Edwards, 1981; Wolsink *et al.*, 1992; Sjøvik & Lossius, 2004; Putnam *et al.*, 2005). In pigs, as in the Sprague-Dawley rats, the ventilatory response reached a nadir around postnatal day 15 before rising again (Wolsink *et al.*, 1992) while in humans and dogs, the secondary rise to adult response levels occurred over the first few (~ 2-3) postnatal weeks with no reported drop in sensitivity (Nattie & Edwards, 1981; Sjøvik & Lossius, 2004; Putnam *et al.*, 2005). Because hypercapnia (5 and 7%

CO₂) did not affect oxygen consumption, but did increase ventilation, early (~P0-5) and late (~P12-29) animals hyperventilated in hypercapnia and the magnitude of the hyperventilation, as reflected in the increases in the air convection requirement, increased significantly through development (ACR, Fig. 2.1).

2.5.2 Changes in the HCVR through postnatal development of semi-fossorial rodents

The initial response to hypercapnia seen in animals immediately after birth (P0-2) was largest in golden-Syrian hamsters (represented as percent change from normocapnia to 5% and 7% CO₂) compared to the other species examined in this study (Fig. 2.7). Shortly after, the ventilatory response fell transiently (P3), rose again (P5), and then gradually fell to the attenuated adult response (Fig. 2.4, 2.7). Like golden-Syrian hamsters, 13-lined ground squirrels are semi-fossorial. Examination of their HCVR through development reveals another pattern when expressed as percent change from normocapnia. In this species, there was an early ventilatory response to CO₂ (P0-1) like the Sprague-Dawley rats and golden-Syrian hamsters, however, this response fell almost immediately and remained attenuated through development (Fig. 2.7). There was a small increase in the HCVR in 13-lined squirrels at the same age at which the HCVR in Sprague-Dawley rats began to increase to adult levels (P8, Fig. 2.7). However, this trend was not significant and not sustained.

Because of the large HCVR at birth and the low metabolic rate, the effect of hypercapnia on the ACR was initially very large. Unlike the Sprague-Dawley rats, the relative increase in ventilation was reduced while metabolic rate increased in golden-Syrian hamsters. The ACR, and hence the magnitude of the hyperventilation, was reduced in golden-Syrian hamsters (Fig. 2.3). In the 13-lined ground squirrels, ventilation tracked metabolism and hence the ACR, and increases in the ACR in hypercapnia, remained relatively constant through much of development (until roughly P20). The ACR and hence the relative hyperventilation in hypercapnia, declined as they reached adulthood (Fig 2.5).

The response to CO₂ seen in golden-Syrian hamsters was produced by equal increases in both V_T , and f_R (Fig. 2.4) (Stunden *et al.*, 2001; Wickström *et al.*, 2002) throughout development (Fig. 2.4). Interestingly, the age at which the HCVR in golden-Syrian hamsters began to asymptote (~P9-12) coincided with the time at which the hypercapnic sensitivity began

to increase again in the Sprague-Dawley rats (Fig. 2.4 and 2.7). The initial increase in ventilation in hypercapnia in the 13-lined ground squirrels was due to equal contributions from increases in V_T and f_R when given 5% CO_2 , but when given 7% CO_2 , f_R did not increase beyond the 5% value while V_T did (Fig. 2.6). This change will result in an increase in effective ventilation and a reduction in dead space ventilation more inspired air will reach the alveoli.

2.5.3 Underlying basis of differences in developmental patterns of the HCVR

The specific underlying changes that produce the different developmental patterns in the HCVR remain unknown. In rats, there are changes in both peripheral and central chemosensory regions that coincide with the blunting phase (Wang & Richerson, 1999; Nottingham *et al.*, 2001; Vincent *et al.*, 2004; Liu & Wong-Riley, 2005; Wong-Riley & Liu, 2005; Gao *et al.*, 2011). Centrally, there is a precipitous fall in glutamate (excitatory neurotransmitter) and its NMDA receptors in chemosensitive brainstem regions (Vincent *et al.*, 2004; Wong-Riley & Liu, 2005). During this drop, increases in $GABA_A$, $GABA_B$, and glycine receptors (all involved in inhibitory pathways), are seen in the same areas (Wong-Riley & Liu, 2005). This transient pre-eminence of inhibitory over excitatory neurotransmission has been reported to occur around postnatal days 3-5 in rats (Wong-Riley & Liu, 2005; Gao *et al.*, 2011), which could contribute to the fall in responsiveness of the central chemoreceptors in this study (Putnam *et al.*, 2005) (Parisian *et al.*, 2004). Peripherally, the carotid body also undergoes postnatal changes (Hertzberg *et al.*, 1990; Pepper *et al.*, 1995; Ling *et al.*, 1997; Bamford *et al.*, 1999). At birth, the carotid body goes from a hypoxic environment to a hyperoxic environment, which could contribute to the immediate fall in responsiveness to respiratory stimuli after birth (Hertzberg *et al.*, 1990). This fall coincides with both the blunting phase seen in rats, as well as the period (P3) in which the carotid body is least responsive to hypoxic and hypercapnic stimuli (Pepper *et al.*, 1995; Bamford *et al.*, 1999).

With age, $GABA_A$, and $GABA_B$ receptor density begins to fall, starting at postnatal day 5 and reaches a nadir at postnatal day 11 (Liu & Wong-Riley, 2005; Wong-Riley & Liu, 2005). During this period, glutamate begins to increase in the nucleus tractus solitarius (NTS) and nucleus ambiguus (Liu & Wong-Riley, 2005; Wong-Riley & Liu, 2005). The postnatal development of the carotid body could also contribute to the secondary rise in rats. The size of

the carotid body has been shown to increase early in development in mammals (Wang & Bisgard, 2005). This is mostly due to type I cell hyperplasia, and an increase in type II cell proliferation and synapse formation between type I and II cells (Wang and Bisgard, 2005; Bamford et al., 1999; Pepper et al., 1995). Following this, both hypoxic and hypercapnic responses increase and reach adult responsiveness at ~P8 (CO₂) and ~P16 (O₂) (Bamford *et al.*, 1999). Though carotid body input to the HCVR has been shown to be non-essential in neonates (Forster *et al.*, 2000), it may still contribute to the patterns we report in this study.

Postnatal development of the lung and related respiratory musculature may also contribute to the differences we report in the development of the HCVR. Rodents are typically altricial unlike some other mammalian species., so their lungs are immature at birth and develop with age. In rats, growth of the lung is slow in newborns and starts to increase in volume faster relative to body weight between ~P5 and P14 (Thurlbeck, 1975) before slowing again. Additionally, respiratory musculature including the diaphragm and intercostal muscles, as well as the shape of the thorax all change with age (Mortola, 2001*b*). Differences in respiratory mechanics could affect the ability of the neonates to produce chest wall, and diaphragmatic movement in hypercapnia.

The differences seen in the developmental response patterns in the golden-Syrian hamsters and 13-lined ground squirrels could arise from differences in underlying mechanisms or simply from differences in the developmental time course of the same underlying mechanisms.

We did not distinguish between the responses of males versus females in our study. It has been shown that P10–15 includes a critical developmental period in male but not female rats. Compared to age-matched females, P12–13 male rats had lower ventilation in normoxia and hypercapnia, which correlated with increased levels of circulating estradiol (Holley et al., 2012). This effect will be in part offset in our study by the use of pups of both genders and should not have had an effect on the pattern of change that we observed.

2.6 Conclusions

The present study shows three distinct patterns in the development of the HCVR in three different species. While the present study cannot attribute these differences to lifestyle directly, differences in lifestyle most likely play a partial role. Both golden-Syrian hamsters and 13-lined ground squirrels are semi-fossorial, and the mothers of each species raise their litters in the burrow. Litter sizes are slightly different between the two species. 13-lined ground squirrels have smaller litters (6-12 pups) (Vaughan *et al.*, 2006), with litters as small as 4 (personal observation). Golden-Syrian hamsters have less variable, but larger litters (8-14) (Schneider & Wade, 1990). Being contained in the burrow, larger litters likely produce greater perturbations in ambient gas concentrations particularly as the animals' age. Both semi-fossorial species are solitary in the burrows as adults. Soil type may vary between the two species which would contribute to the gas diffusion rate (Wilson & Kilgore, 1978; Burda *et al.*, 2007). Golden-Syrian hamsters naturally reside in sand or clay-like soils and have a mean burrow depth of 65cm. Details on the structure of 13-lined ground squirrel burrows are not well known, but the soils this species burrow in are a moist top soil found in grassy fields (personal observation).

The triphasic developmental pattern in the HCVR seen in the rat has been reported in other non-fossorial species (Wolsink *et al.*, 1992; Stunden *et al.*, 2001). While the time course and pattern of the blunting phase of the HCVR differs between the two semi-fossorial species, the absence of the secondary increase in sensitivity is consistent. The differences seen between the two semi-fossorial species could lie either in the level of fossoriality, which differs between the two, or in the hibernation lifestyle seen in the 13-lined ground squirrel. The second of the two proposed possibilities seems less likely given that golden-Syrian hamsters have been shown to enter multi-day torpor bouts (Ibuka & Fukumura, 1997). However, the characteristics of torpor differ between the two (Ibuka & Fukumura, 1997; Carey *et al.*, 2003), and this study cannot attribute the differences seen to the use of torpor directly. Whether any differences seen arise from similar or different underlying causes is not clear but either way it suggests there has been selection for sustaining a blunted response in semi-fossorial species.

It is also apparent that both fossorial species are not born with attenuated responses but rather they develop, even when the neonates are raised in normocapnic/normoxic conditions. It

remains unknown how raising the neonates in a “burrow-like” hypoxic/hypercapnic environment would alter the developmental pattern. In rats, it has been shown that chronic perinatal hypercapnia transiently reduces the HCVR but it then returns to a normal adult response after removal from hypercapnia (Saiki & Mortola, 1996; Bavis & Kilgore Jr, 2001). This is also true for mice (Birchard *et al.*, 1984). The effect of perinatal hypercapnia in semi-fossorial species remains to be explored.

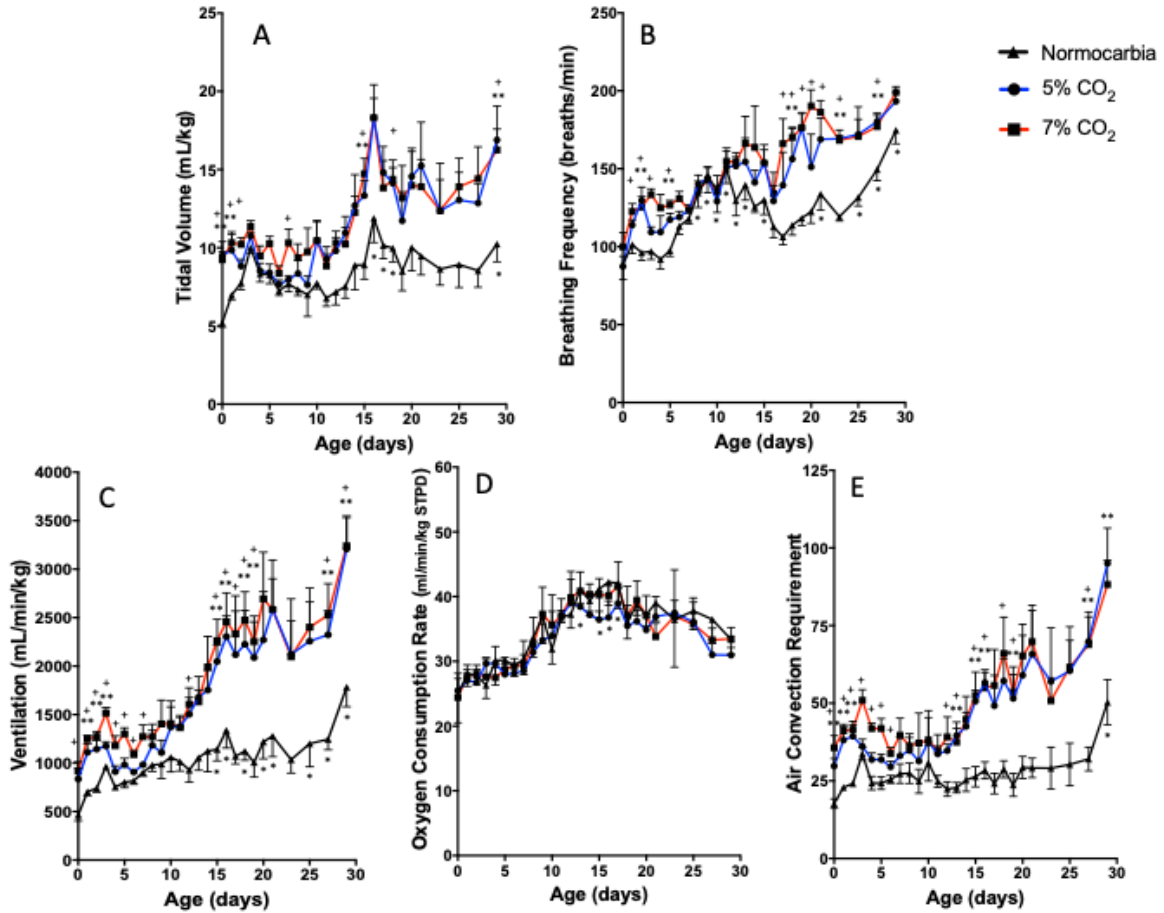


Figure 2.1 Breathing frequency (breaths/minute)(A), tidal volume (mL/kg) (B), and total ventilation (mL/min/kg) (C), O₂ consumption rate (mL/min/kg) (D), and the air convection requirement (E) in Sprague-Dawley rats through development (P0-30). Rats were given normocarbic (open triangles), and hypercapnic (5% CO₂, (open circles) and 7% CO₂ (closed circles)) gas mixtures. (n = 3-6 for each day). Error bars show SEM. * denotes a significant differences (P<0.05) from day 0 within the normocarbic treatment, and ** (5% CO₂) and + (7% CO₂) denote differences (p<0.05) between hypercapnic and normocarbic gas on that day (ANOVA with Tukey's post hoc test).

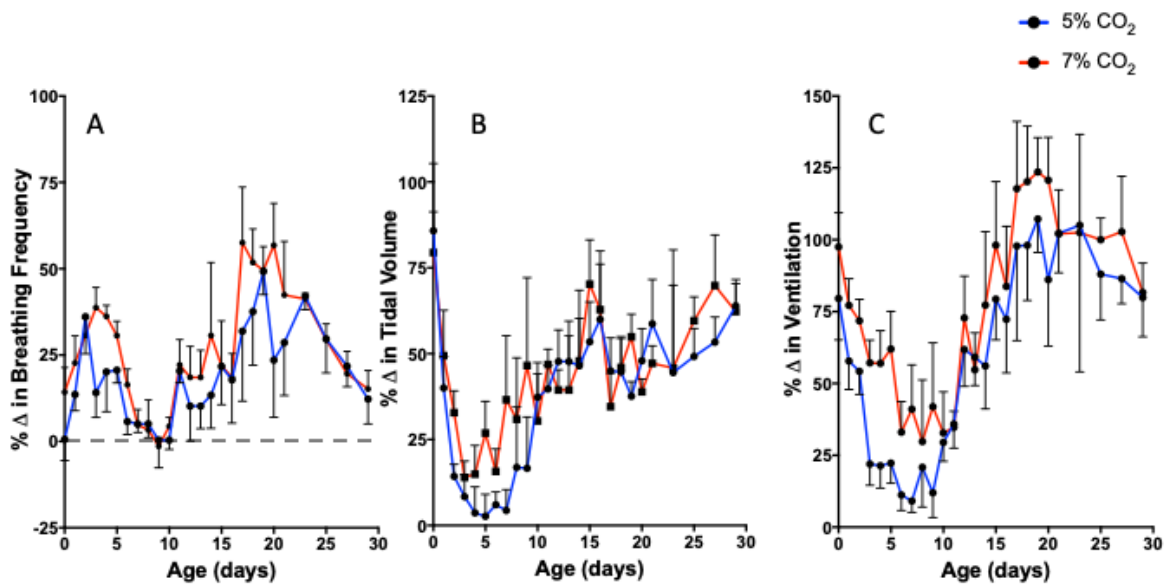


Figure 2.2. Percent change from normocapnia in breathing frequency (A), tidal volume (B), and ventilation (C) in Sprague-Dawley rats through development (P0-30) when administered 5% CO₂ (open circles), and 7% CO₂ (closed circles). (n = 3-6 for each day). Error bars show SEM.

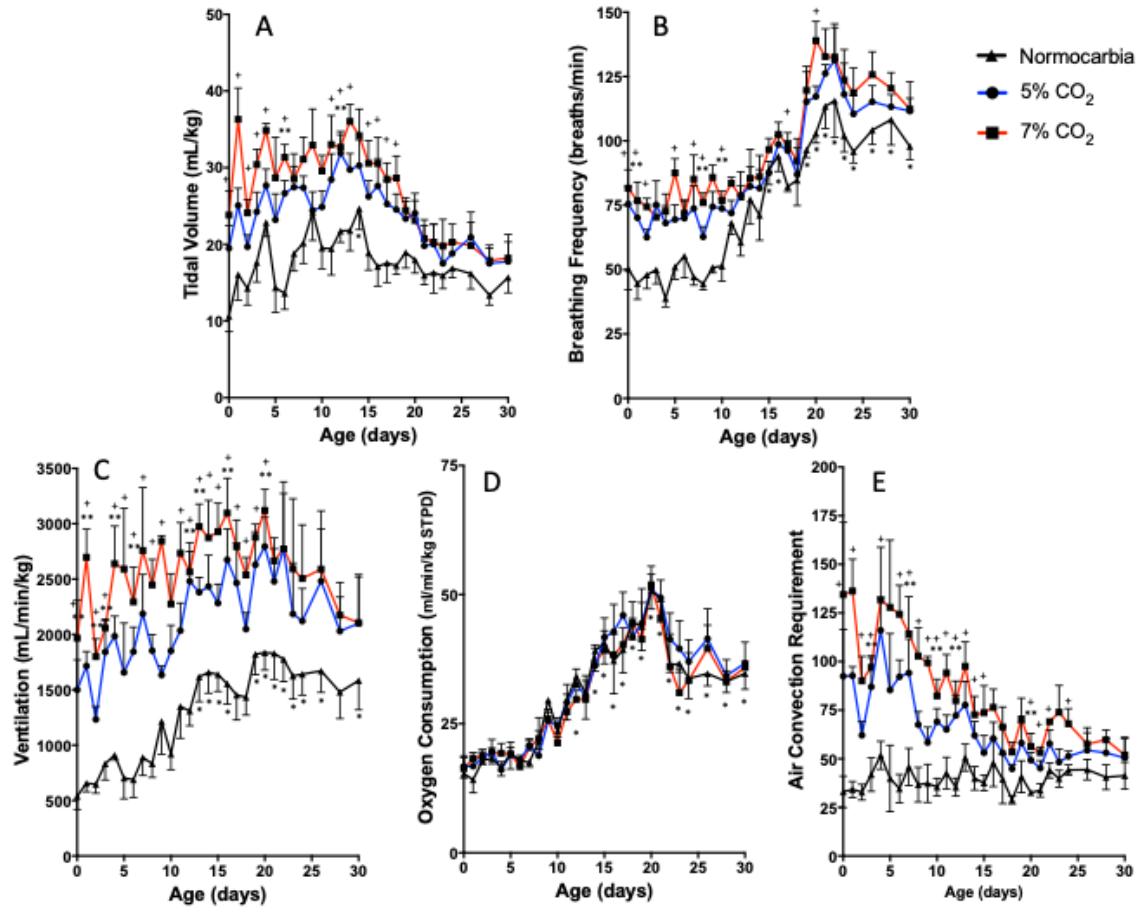


Figure 2.3 Breathing frequency (breaths/minute)(A), tidal volume (mL/kg) (B), and total ventilation (mL/min/kg) (C), O₂ consumption rate (mL/min/kg) (D), and the air convection requirement (E) in golden-Syrian hamsters through development (P0-30). Hamsters were given normocapnic (open triangles), and hypercapnic (5% CO₂, (open circles) and 7% CO₂ (closed circles)) gas mixtures. (n = 3-6 for each day). Error bars show SEM. * denotes significant differences (P<0.05) from day 0 within the normocapnic treatment, and ** (5% CO₂) and + (7% CO₂) denote differences (p<0.05) between hypercapnic and normocapnic gas on that day (ANOVA with Tukey’s post hoc test).

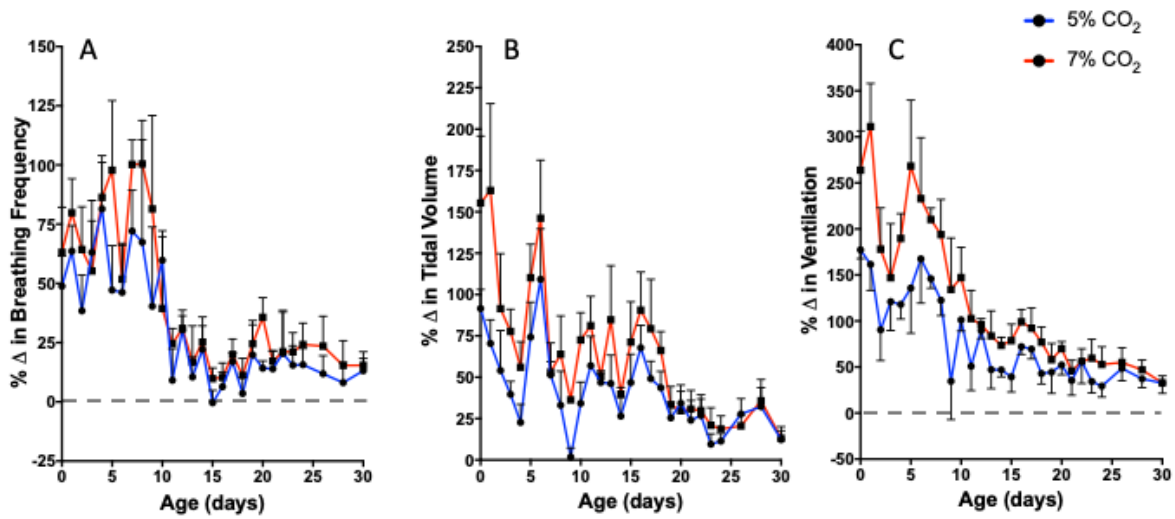


Figure 2.4 Percent change from normocapnia in breathing frequency (A), tidal volume (B), and ventilation (C) in golden-Syrian hamsters through development (P0-30) when administered 5% CO₂ (open circles), and 7% CO₂ (closed circles). (n = 3-6 for each day). Error bars show SEM.

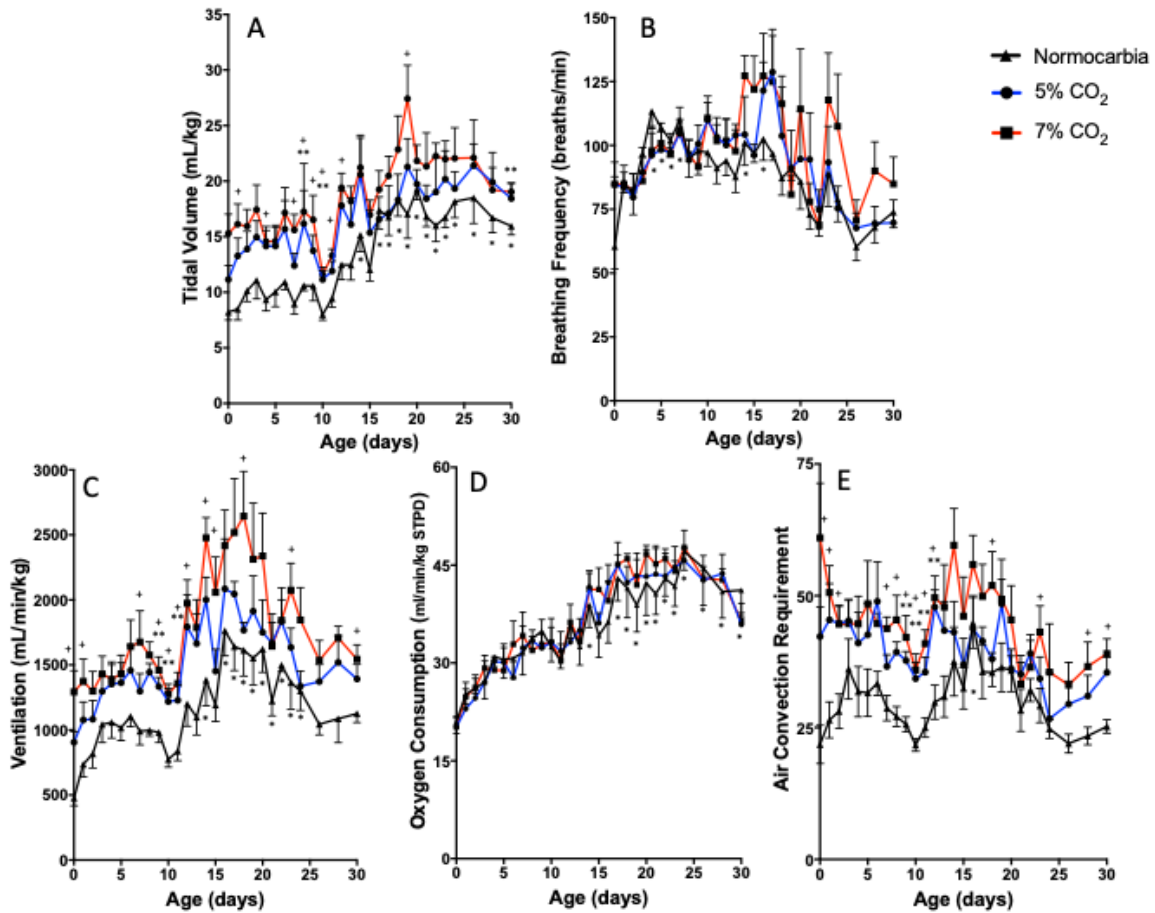


Figure 2.5 . Breathing frequency (breaths/minute) (A), tidal volume (mL/kg) (B), and total ventilation (mL/min/kg) (C), O₂ consumption rate (mL/min/kg) (D), and the air convection requirement (E) in 13-lined ground squirrels through development (P0-30). Squirrels were given normocapnic (open triangles), and hypercapnic (5% CO₂, (open circles) and 7% CO₂ (closed circles)) gas mixtures. (n = 3-6 for each day). Error bars show SEM. * denotes significant differences (P<0.05) from day 0 within the normocapnic treatment, and ** (5% CO₂) and + (7% CO₂) denote differences (p<0.05) between hypercapnic and normocapnic gas on that day (ANOVA with Tukey's post hoc test).

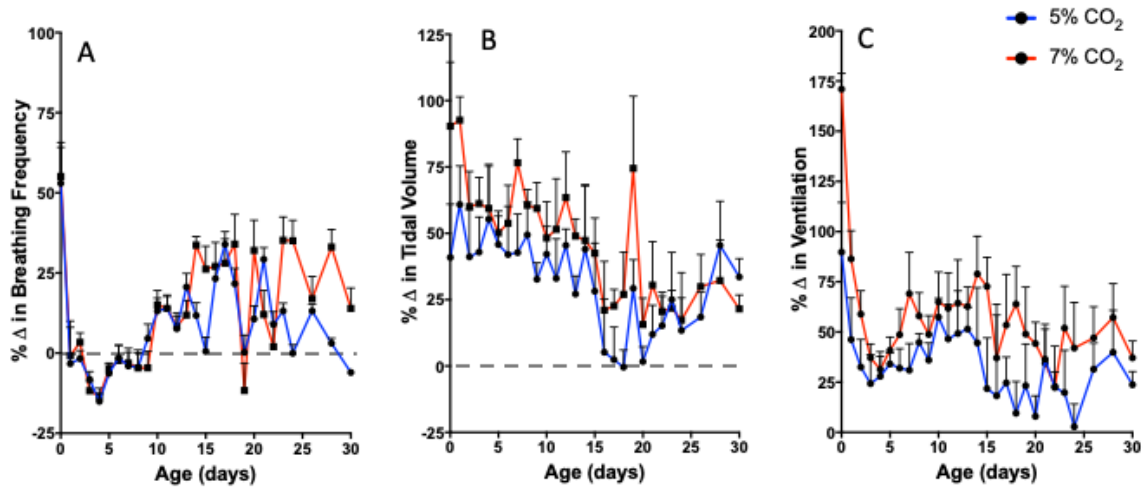


Figure 2.6 Percent change from normocapnia in breathing frequency (A), tidal volume (B), and ventilation (C) in 13-lined ground squirrels through development (P0-30) when administered 5% CO₂ (open circles), and 7% CO₂ (closed circles). (n = 3-6 for each day). Error bars show SEM.

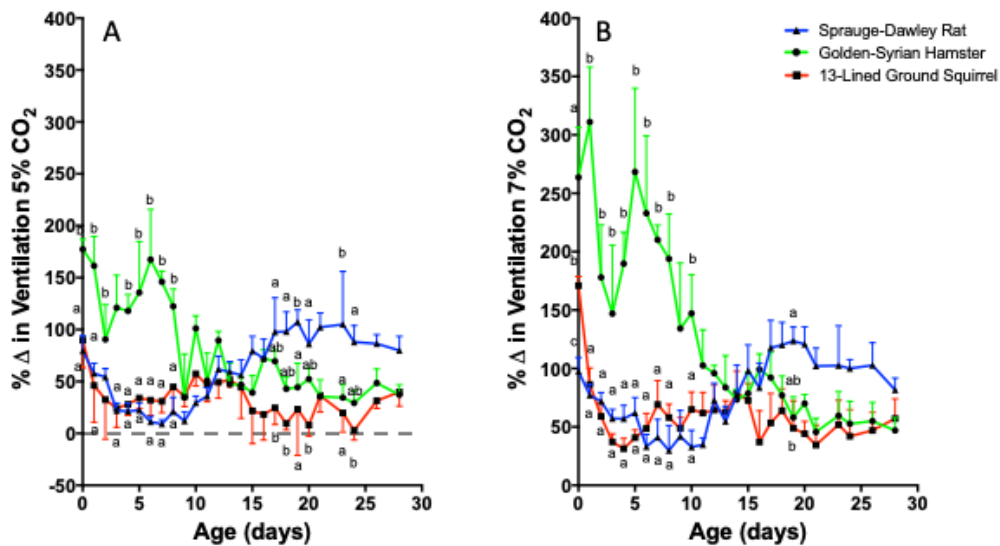


Figure 2.7 Comparison of the developmental pattern of the hypercapnic ventilatory response of Sprague-Dawley rats (blue), golden-Syrian hamsters (green), and 13-lined ground squirrels (red). Figure shows the percent change in ventilation from breathing 0% to 5% CO₂ (A) and from 0% to 7% CO₂ (B) (n = 3-6 for each day). Letter differences denote significant differences (p < 0.05) between the species on each day (ANOVA with Tukey's post hoc test).

Chapter 3: Respiratory Development in Burrowing Rodents: Effect of Perinatal Hypercapnia

3.1 Summary

Burrowing rodents have a blunted hypercapnic ventilatory response compared to non-burrowing rodents, but semi-fossorial ground squirrels and hamsters are not born with this blunted response when raised in room conditions. This study examined the hypercapnic ventilatory response of rats, hamsters, and ground squirrels raised in burrow-like hypercapnia (~3% CO₂) through development (embryonic day 16-18 to postnatal day 30) to determine if chronic hypercapnia exerts any effect on the developing and adult semi-fossorial response. Chronic hypercapnia attenuated the ventilatory response to 5% CO₂ by 60% (rats), 150% (hamsters), and 70% (squirrels) in newborns when compared to newborns raised in normal conditions. When raised in burrow conditions, squirrels and hamsters reached the blunted adult response ~8-12 days sooner in development than their room air counterparts, while burrow-reared rats maintained a consistently blunted response until removal from chronic hypercapnia. Our study revealed no lasting effect of chronic hypercapnia on the ventilatory responses to CO₂ in burrowing rodents, but rather a change in the developmental profile such that the blunted adult response was reached earlier in development.

3.2 Introduction

Burrowing mammals exhibit a low resting ventilation, CO₂ retention, and an elevated arterial CO₂ partial pressure (PaCO₂), an elevated CO₂ threshold for eliciting a ventilatory response and a reduced ventilatory response to CO₂ once the threshold is reached (Parer and Hudson, 1974; Arieli and Ar, 1979; Boggs et al., 1984; Walker *et al.*, 1985; Birchard et al., 1984; Tenney and Boggs, 1986). Several studies in the past have examined how plastic CO₂ responsiveness is and the extent to which it is altered by persistent hypercapnia in adults as well as during development. Rats that were exposed to chronic hypercapnia as neonates exhibited a moderate reduction in the hypercapnic ventilatory response that persisted for only a short period after return to normocapnia later in development (Bavis et al., 2006; Lai et al., 1981; Kondo et al., 2000). In adult golden-mantled ground squirrels, chronic exposure to a hypoxic-hypercapnic

mix had no effect on the overall sensitivity to hypercapnia. While chronic hypoxic-hypercapnia (CHH) did cause an overall elevation in the CO₂ ventilatory response curve, neither the hypercapnic response threshold nor the pattern of ventilatory response was altered by CHH exposure. On return to breathing room air, ventilation remained elevated (~ 35 %) compared to control animals suggesting that reacclimation to normoxic normocapnia takes time (Webb and Milsom, 1994). In rats, mice and opossums, chronic perinatal CO₂ exposure also did not alter the adult hypercapnic ventilatory response (Farber *et al.*, 1972; Birchard *et al.*, 1984; Boggs *et al.*, 1984; Bavis *et al.*, 2006). Based on these studies, collectively, it has been suggested that the reduced CO₂ response seen in burrowing mammals is genetically determined (Birchard *et al.*, 1984; Webb and Milsom, 1994; Bavis *et al.*, 2006).

These latter studies, however, focused on the effects of chronic hypercapnia in adults following the perinatal period. It has now been shown that in rats, there is a developmental window during the first two weeks of life during which the respiratory control system undergoes significant change as it completes development (Davis *et al.*, 2006; Liu and Wong-Riley, 2008; Bavis and MacFarlane, 2017; Wong-Riley *et al.*, 2019). During this period, the hypercapnic ventilatory response in rats changes markedly. In Sprague-Dawley rats, the strong HCVR seen on the day of birth becomes severely attenuated by postnatal days (P) 7-9 but subsequently rises again to adult response levels (by roughly P14) (Putnam *et al.*, 2005; Stunden *et al.*, 2001; Wickström *et al.*, 2002). In brown Norway and salt-sensitive Dahl S rats there is no initial attenuation but the subsequent rise to the adult levels in the HCVR occurs at the same age (Davis *et al.*, 2006).

We recently examined the hypercapnic ventilatory response in two semi-fossorial species through development and found that 13-lined ground squirrels responded to 7% CO₂ with an increase in ventilation (\dot{V}_E) of about 150% at birth, and golden-Syrian hamsters by 250% (Sprenger *et al.*, 2019 (chapter 2)). These responses were not only not blunted, they were greater than those seen in the non-fossorial rat (~100%). By P30, however, the ventilatory responses to CO₂ of both species had been reduced to the blunted responses typical of adults of these species (~40% increase in \dot{V}_E to 7% CO₂). Thus, pups of these species were not born with a blunted response, rather it developed over the first three weeks of life. In this study however, the animals were raised in normoxic and normocapnic conditions. Since the attenuation occurs over the now

well-described developmental window for respiratory control it raises the questions of how peri- and neonatal exposure to CO₂ would alter these developmental profiles, and whether such exposure in a semi-fossorial species during this period would further blunt the adult hypercapnic ventilatory response. Accordingly, we raised 13-lined ground squirrels, golden-Syrian hamsters, and Sprague-Dawley rats in simulated burrow conditions (3% CO₂ and 18% O₂) from 5-6 days before birth to postnatal day 30 (P30) and recorded the hypercapnic ventilatory response every day through development (P0-P30). We also recorded the hypercapnic ventilatory response again at P60, 30 days after removal from the burrow conditions. We hypothesized that, considering both fossorial and non-fossorial species develop their adult HCVR, the fossorial HCVR is strongly genetically determined, but plastic through development.

3.3 Methods

3.3.1 Animals

All procedures were conducted under a protocol approved by the UBC Animal Care Committee (A17-0018) and complied with the policies of the Canadian Council on Animal Care. Gravid 13-lined ground squirrels (*Ictidomys tridecemlineatus*) were trapped in Carman, MB, Canada (49°30'N, 98°01'W) and transferred to an animal care facility at the University of British Columbia. 13-lined ground squirrels were trapped with the approval of Manitoba Conservation and Water Stewardship, under wildlife scientific permit WB15027. Wild caught females were treated with Ivermectin and Droncit for endoparasites (0.4 mg/kg, subcutaneous), and flea spray for ectoparasites immediately after capture. Gravid Sprague-Dawley rats and golden-Syrian hamsters were acquired commercially from Charles River (Wilmington, Massachusetts). 13-lined ground squirrels were provided water and IAMS small chunk dog chow supplemented with apples and peanuts *ad libitum*. Sprague-Dawley rats and golden-Syrian hamsters were provided water and rodent chow (Lab Chow) supplemented with assorted cereals *ad libitum*. All animals were kept in a temperature-controlled chamber (20 ± 2 °C) on a photoperiod that matched the daily photoperiod in Vancouver, British Columbia, Canada. Housing conditions of animals in the present study were identical to those of animals in the study of Sprenger et al., 2019 (chapter 2) with the exception of being raised in an artificial burrow

environment (see below). Data were collected at the same time of year and during the same time of day. All animal husbandry and handling were the same between the two studies.

3.3.2 *The burrow environment*

To raise animals in a simulated burrow environment, large, sealed plexiglass chambers were outfitted with three sealable holes. One hole was connected to an air pump with a one-way valve, one hole on the opposite side of the chamber was sealed with a one-way valve allowing air to exit the chamber. The final hole was plugged with a rubber cork with a CO₂ sensor attached for measurement of the chamber CO₂ levels. An O₂ sensor was attached in place of the CO₂ sensor periodically to measure chamber oxygen. The CO₂ sensor was connected to an alternating switch that controlled the air pump. The switch was set to turn on the air pump when chamber CO₂ reached 3%, and off when the chamber CO₂ reached 2%, establishing the chronic hypercapnic conditions. The CO₂ was thus produced by the respiration of the animals inside the chamber with the servo-controlled pump maintaining the level relatively constant. Oxygen ranged from 17-18% O₂ which is not a sufficient drop to stimulate a hypoxic ventilatory response in these species (Cragg & Drysdale, 1983; McArthur & Milsom, 1991*b*). A fan inside the chamber mixed the chamber gas. The chamber floor was filled with biofresh bedding, woodchips, and tekfresh soft bedding for nests. A plastic PVC tube was provided for enrichment. The bedding was changed every 5-7 days based on need with the exception of the nests the animals constructed, which were left undisturbed. During this time, a brief reversion to normoxia/normocapnia would occur lasting ~10-15 minutes. Temperature inside the chamber was equal to that of the room. Gravid females were placed in the chamber with embryos back calculated from the day of parturition to be at E16-18, and all animals remained in the chamber until P30, after which all animals were removed from the chamber.

3.3.3 *Measurement of oxygen consumption, ventilation, and temperature*

3.3.3.1 *Ventilation*

Ventilation was measured using whole body plethysmography (barometric method) as described in Sprenger et al., 2019 (chapter 2). Briefly, pups were placed in one of two identical plexiglass chambers that allowed them to move freely. A constant regulated flow was either pushed through both of the chambers (Jacky, 1978) or through only the animal chamber with the

other chamber referencing ambient conditions. Because neonatal pups are imperfect thermoregulators, the chambers were housed in a temperature-controlled unit, allowing for precise regulation of ambient temperature (Jacky, 1978). A minimum differential (body temperature to ambient temperature) of 4°C was required for ventilatory measurements (Malan, 1973). Measurements made at any differential lower than this were excluded from final analysis. The plethysmograph was calibrated for tidal volume (V_T) by injecting known volumes of air into the empty animal chamber at a rate similar to that of the animal prior to placing the animal into the chamber.

3.3.3.2 *Oxygen consumption*

Oxygen consumption was measured using a similar method to the one used in Sprenger et al. 2019 (chapter 2) (Lighton, 2008). Briefly, the plethysmograph served as a metabolic chamber for measurement of oxygen consumption. Incurrent gas compositions (O_2 , and CO_2) were measured prior to each trial using a field metabolic system (FMS; Sable Systems International; North Las Vegas, Nevada) or Beckman gas analyzers (OM-11 and LB-2; Beckman Coulter Indianapolis, Indiana). Incurrent flow rate was adjusted so that excurrent O_2 and CO_2 concentrations would not change by more than 1%. O_2 and CO_2 analyzers were calibrated to correct for drift with pre-mixed gases of known concentrations (0, 3, 5, and 7% CO_2 with 21% O_2 , bal. N_2) daily. Excurrent air was dried before analysis using silica beads. Oxygen consumption and CO_2 production were measured continuously through all trials.

3.3.3.3 *Temperature*

Chamber temperature was monitored continuously using a thermal probe set between the animal and reference chambers. The thermal probe was connected to a physitemp (BAT-12, Physitemp, Clifton NJ). Animal body temperatures were maintained at ~37°C-38°C by altering chamber temperatures between 21°C and 33°C. Animal body temperature and nasal temperature were measured using a FLIR (forward looking infrared) thermal monitoring system (FLIR; Wilsonville, Oregon, United States) throughout the experimental trials. The FLIR system allowed for a non-invasive measure of temperature in neonatal rodents (Tattersall, 2016). The most accurate measurement of body temperature was acquired by analyzing the inside corner of

the eye. Temperatures were checked against rectal temperatures to ensure accuracy (Sprenger et al., 2019 (chapter 2)).

3.3.4 *Experimental protocol*

Pups were taken from the litter contained in the burrow chambers, weighed, and placed in the animal plexiglass chamber with bedding flushed with normocapnic air (21% O₂, 0% CO₂, N₂ balance). Pups were allowed 30 minutes acclimation in these conditions before administration of the hypercapnic gases. Pups were then given premixed gases (Praxiar Canada, Vancouver B.C.) containing 3%, 5%, and 7% CO₂ in 21% O₂ balanced with N₂. The 3% CO₂, which was the level in which the animals were raised under simulated burrow conditions, was given after the acclimation period then the hypercapnic gases were given in random order with no return to 0% or 3% CO₂. Each gas was given for 15 minutes unless a steady state was not achieved, in which case the treatment was extended until a combined 5 minutes of uninterrupted breathing was present. Total run time was about 120 minutes. To obtain a sample size of 4-6 for each age point, pups from 2 litters (hamsters and rats) and 4 litters (squirrels) were used. All data except body, nasal, and chamber temperature were recorded using a PowerLab 16/32 data acquisition system (ADInstruments; Colorado Springs, Colorado). No individual pup was used more than once in any given 3-day period. Thus, data were collected for every day during development in each species until P20, after which, data were collected every other day until P30, then once more on P60.

3.3.5 *Data analysis*

Data analysis was performed as described in Sprenger et al. 2019 (chapter 2). Briefly, the last 15 minutes of the 30-minute acclimation period where animals were given normocapnic air (N), (0% CO₂, 21% O₂, N₂ bal.) was analyzed. During this period two 1-2 minute windows from the middle and end of the trial were analyzed for ventilation and oxygen consumption. If no clean ventilatory measurement was found in these windows, the data were taken from the closest possible time point. Data collected from animals breathing simulated burrow gas (B) (3% CO₂, 21% O₂, N₂ bal.) and hypercapnic gas mixtures (5% and 7% CO₂, 21% O₂, N₂, balance) were analyzed the same way. No data were obtained for P0-P3 rat pups breathing simulated burrow gas. All respiratory and ventilatory calculations were made as described in Sprenger et al. (2019)

(chapter 2), with the exception of percent lung oxygen extraction. This was calculated with the following equation:

$$OCR = ACR \times FiO_2 \qquad \% \text{ Lung oxygen extraction} = \frac{100}{OCR}$$

where OCR is the oxygen convection requirement, ACR is the air convection requirement ($\dot{V}_E / \dot{V}O_2$), and FiO_2 is the fractional inspired O_2 .

3.3.6 *Statistical analysis*

Linear mixed-effects models were used to determine the effect of age on all respiratory and metabolic variables. Since each animal was not repeatedly measured each day, with a minimum 3 days between exposures to test gases, we tested for the random effects of litter and animal. The effect of animal was not statistically significant ($P > 0.10$) and was therefore removed from the final models.

A separate mixed linear model with litter (random effect) and animal (repeated measure) was used to determine the effect of inspired gas within an age group on all metabolic and ventilatory variables

A third mixed linear model with litter (random effect) was used to determine the effect of environment (CH and AcN vs. N) on all metabolic and ventilatory variables within an age group.

Sex was not considered in our analysis as we were mainly interested in the effect on the group as a whole. Additionally, the control group of animals not raised in a burrow are the animals from Sprenger et al., 2019 (chapter 2).

Tukey post-hoc tests were run as appropriate; within each treatment to determine significant differences in ages (compared to postnatal day 0; day 4 for CH rats) for the first model, among inspired gases within each day for the second model, and among the three environmental conditions within each day for the third. T-tests were used to determine significance of the HCVR after removal from the burrow environment. All statistics were run on Rstudio using the lme4 package (Bates et al., 2015) with a significance level of $P < 0.05$ throughout. Error bars represent S.E.M. throughout.

3.4 Results

3.4.1 Sprague-Dawley Rats

3.4.1.1 Changes in O₂ Consumption Rate and Ventilation throughout Development in Chronic Hypercapnia

The Sprague-Dawley rat pups raised under burrow conditions (CH rats) gained weight more slowly than rat pups raised in room air ($p < 0.05$) (Fig. 3.1C)

\dot{V}_{O_2} (ml/min), and \dot{V}_E (ml/min) all increased with age (Table 3.1). When expressed as mass specific values, \dot{V}_{O_2} remained relatively constant (Fig. 3.1A) while mass specific \dot{V}_E rose through development (Fig. 3.1B). The ACR remained relatively constant early in development but rose progressively after ~P15 (Fig. 3.1D). Correspondingly, the amount of O₂ extracted from each breath, the % lung O₂ extraction, remained between 20 and 30% early in development, but then fell progressively as the ACR increased. It was reduced to ~13% by the end of development (Fig. 3.1E).

Exposing CH rats acutely to normocapnic air (0% CO₂) (AcN) had no significant effect on \dot{V}_{O_2} or \dot{V}_E , at any age (Fig. 3.1).

When compared to data reported previously for rats raised in room air (N in Figure 3.1), both \dot{V}_E and \dot{V}_{O_2} were reduced in the CH rat pups (Table 3.1). When expressed as mass specific values, beyond ~P15 CH animals consistently had a lower mass specific \dot{V}_{O_2} (Fig. 3.1A). Mass specific \dot{V}_E , in CH rat pups, however, was slightly lower in CH animals early in development with several days being significantly lower (~P11-18, and 29) ($p < 0.05$) (Fig. 3.1B). Thus, the ACR and lung O₂ extraction were not consistently different between the two groups (Fig. 3.1D, E).

3.4.1.2 Changes in the Hypercapnic Ventilatory Responses throughout Development in Chronic Hypercapnia

Breathing both 5% and 7% CO₂ had no effect on \dot{V}_{O_2} at any stage of development (Fig. 3.2A). Breathing 5% CO₂ stimulated \dot{V}_E starting at P10 with the increases becoming significant after P12 (Fig. 3.2B) ($p < 0.05$). Breathing 7% CO₂ significantly increased mass specific \dot{V}_E

starting at P0-4 ($p < 0.05$) after which ventilation fell and then rose again significantly from P12-60 ($p < 0.05$) (Fig. 3.2B). When expressed as percent change (Fig. 3.2E), breathing 5% CO₂ minimally increased ventilation prior to P10. After P10, the ventilatory response to 5% CO₂ increased gradually to about a 60% increase in ventilation at P17 and then slowly dropped to the adult response of about a 50% increase. Breathing 7% CO₂ increased ventilation by about 75% on the day of birth (Fig. 3.2F). Shortly after this the response fell to about a 15% increase at P7, then after P10 it rose to the level seen in adults (~70% increase). The net result of these changes was that the ACR increased significantly after P15 in 5% CO₂ ($p < 0.05$) and after P10 in 7% CO₂ ($p < 0.05$). There was a clear decrease in lung O₂ extraction later in development for animals breathing both 5% and 7% hypercapnia (Fig. 3.2D).

When expressed as percent change, the HCVR was only significantly lower in CH rats compared to rats raised in room air on P0-1 and P18, 22, and 24 ($p < 0.05$) in 5% CO₂ (Fig. 3.2E). The HCVR of CH and N rats breathing 7% CO₂ were not significantly different (Fig. 3.2F), although CH rats tended to have a reduced response particularly after P16 ($P = 0.24$), a pattern similar to that of rats breathing 5% CO₂. While the CH rats were insensitive to 5% CO₂ on the day of birth, in general, the CH rats expressed the same three phase response during development as N rats (an initial brisk response on the day of birth followed by a decrease and secondary increase to adult levels).

3.4.1.3 Long Term Effects of Development In Chronic Hypercapnia on O₂ Consumption Rate, Ventilation and the Hypercapnic Ventilatory Response

Thirty days after removal from the burrow environment (at P60), the mass specific metabolic rate of the rats in normocapnia had fallen to levels below those seen in newborns exposed to normocapnia acutely (Fig. 3.2A). Total ventilation, however, was unchanged compared to AcN animals and thus the ACR increased and lung O₂ extraction was reduced. The HCVR of the rats noticeably but non-significantly increased when breathing both 5% ($p = 0.09$) (~25% increased) and 7% CO₂ ($p = 0.12$) (~25% increased) from P30 to P60 (Fig. 3.7). This led to further increases in the ACR (Fig. 3.2C) and decreases in lung extraction (Fig. 3.2D) in P60 rats.

3.4.2 Golden-Syrian hamsters

3.4.2.1 Changes in O₂ Consumption Rate and Ventilation throughout Development in Chronic Hypercapnia

Compared to hamsters raised in room air, CH hamsters on average gained mass at the same rate as hamsters raised in room air (Fig. 3.3C). However, when nearing adulthood (P25 - P30) the mean rate of growth of CH hamsters slowed (Fig. 3.3C). There was tremendous individual variability in the rate of growth of the CH hamsters, however, with some growing at the same rate as animals raised in room air and some growing at a much slower rate. For example, at P30 two CH hamsters weighed 63g and 68g (similar to the 71g average of the room air raised hamsters) while other P30 CH hamsters were only 39-40g. The greatest variability in CH hamster mass appeared after P20 (Fig. 3.3C) and this variability persisted for the rest of development.

\dot{V}_{O_2} (ml/min), and \dot{V}_E (ml/min) all progressively increased with age in CH hamsters (Fig. S1). Mass specific \dot{V}_{O_2} was stable early in development (P0-P10), rose from P10-P20 (albeit not significantly) and then progressively fell to starting values. Mass specific \dot{V}_E rose sharply on the days after birth (P1) and remained stable through development (Fig. 3.3D). As a result of the initial rise in \dot{V}_E , there was also a sharp rise in the ACR the day after birth (Fig. 3.3D) and a significant fall in lung extraction (Fig. 3.3E) ($p < 0.05$). From this point on both the ACR and lung O₂ extraction remained stable through development with the exception of a stark dip in the ACR at ~P16-17 (Fig. 3.3D, E).

There was no significant difference between hamsters breathing CH gas and hamsters breathing AcN gas through development (Fig. 3.3).

Early in development (P0-10), mass specific \dot{V}_{O_2} was significantly greater in CH hamsters, compared to N hamsters (Fig. 3.3A). The difference in mass specific \dot{V}_{O_2} disappeared later in development (~P12). \dot{V}_E remained constant throughout development in the CH hamsters while increasing progressively in hamsters raised in normocapnia ($P < 0.05$) (Fig. 3.3B). The net result of this was the ACR in CH hamsters tended to be lower (Fig. 3.3D) and the lung O₂ extraction higher throughout development (P0-30) (Fig. 3.3E).

3.4.2.2 *Changes in the Hypercapnic Ventilatory Responses throughout Development in Chronic Hypercapnia*

Neither breathing 5% or 7% CO₂ affected mass specific $\dot{V}O_2$ at any point in development in CH hamsters (Fig. 3.4A). The effects of breathing 5% CO₂ on mass specific \dot{V}_E were modest but still significant for much of development ($p < 0.05$) (Fig. 3.4B). Breathing 7% CO₂, however, significantly increased mass specific \dot{V}_E to a greater degree throughout development ($P < 0.05$) (Fig. 3.4B). When expressed as percent change, the increases in \dot{V}_E due to breathing both 5% and 7% CO₂ were greatest on the day of birth (~25% and 110% respectively) (Fig. 3.4E,F). Shortly thereafter the ventilatory responses to 5% and 7% hypercapnia progressively fell, and by P7 in both cases, stabilized and remained constant into adulthood (Fig. 3.4E,F). The ACR only increased significantly in P2-4 and P22 hamsters breathing 5% CO₂ ($P < 0.05$) (Fig. 3.4C) and in most hamsters breathing 7% CO₂ ($p < 0.05$) (Fig. 3.4C). Lung O₂ extraction was little affected by breathing 5% CO₂ but more so breathing 7% CO₂ ($p < 0.05$). It was never reduced by more than 14%, and for most days, it was only reduced by 5% (Fig. 3.4D), although it was significantly lower in P0-6 hamsters breathing 7% CO₂ ($p < 0.05$).

Hamsters raised under burrow conditions had a substantially reduced response to both 5% and 7% CO₂ compared to hamsters raised in room air ($p < 0.05$) (Fig. 3.2E,F). The greatest difference was seen early in development (P0-12). On the day of birth (P0) CH hamsters had an increase in \dot{V}_E of about 100% while hamsters raised in room air increased \dot{V}_E by about 275% in response to breathing 7% CO₂ (Fig. 3.2E,F). The HCVR in CH hamsters was progressively reduced throughout development just as it was in hamsters raised in room air. By ~P15-30 the relative magnitude of the HCVR to 5% and 7% CO₂ were more alike in the CH and N animals, however in both cases CH hamsters tended to have a slightly lower and less variable HCVR.

3.4.2.3 *Long Term Effects of Development in Chronic Hypercapnia on O₂ Consumption Rate, Ventilation and the Hypercapnic Ventilatory Response*

Thirty days after removal from the burrow environment (at P60), the mass specific metabolic rate of the hamsters had fallen to levels below those seen in newborns acutely exposed to normocapnia (Fig. 3.4A). Total ventilation was unchanged compared to AcN animals and thus the ACR increased and lung O₂ extraction was reduced. The HCVR of the hamsters, however,

increased only modestly and not significantly when breathing 5% and 7% CO₂ from P30 to P60 (Fig. 3.7). At P60 this led to further increases in the ACR (Fig. 3.4C) and decreases in lung O₂ extraction (Fig. 3.4D), but the latter changes were not significant.

3.4.3 13-lined ground squirrels

3.4.3.1 Changes in O₂ Consumption Rate and Ventilation throughout Development in Chronic Hypercapnia

Squirrels raised in burrow conditions grew more slowly through most of development ($p < 0.05$) (Fig. 3.5C) catching up to their cohort raised in normoxia by P30 (Fig. 3.5C). \dot{V}_{O_2} (ml/min), and \dot{V}_E (ml/min) in CH squirrels increased gradually with age (Table 3.1). When expressed as mass specific values, \dot{V}_{O_2} (insignificantly) and mass specific \dot{V}_E (significantly) progressively increased with age ($p < 0.05$) (Fig. 3.5A) until roughly P20 at which point they stabilized (Fig. 3.5A,B). Early in development the ACR was low and the lung extraction was high (Fig. 3.5D and E) with the ACR rising and the lung extraction falling progressively through development (Fig. 3.5D and E).

Exposing CH squirrels acutely to normocapnia (0% CO₂) did not affect any measured variable except in P1 squirrels where lung extraction significantly increased ($p < 0.05$) (Fig. 3.5).

\dot{V}_E and mass specific \dot{V}_E tended to be smaller throughout development ($p < 0.05$) in CH squirrels compared to squirrels raised in room air (Fig. 3.5B, Table 3.1). \dot{V}_{O_2} and mass specific \dot{V}_{O_2} were much lower in CH squirrels for most of development ($P < 0.05$) (Fig. 3.5A, Fig S1). The net result was, later in development, CH squirrels tended to have a higher ACR and lower lung O₂ extraction than N squirrels ($p < 0.05$) (Fig. 3.5D and E).

3.4.3.2 Changes in the Hypercapnic Ventilatory Responses throughout Development in Chronic Hypercapnia

Breathing 5% and 7% CO₂ did not significantly affect mass specific \dot{V}_{O_2} in CH squirrels at any time in development (Fig. 3.6A). Mass specific \dot{V}_E was significantly elevated in 5% CO₂ late in development (P24 and 28) and in 7% CO₂ throughout development ($p < 0.05$) (Fig. 3.6B). When expressed as percent change, the HCVR to breathing 5% and 7% CO₂ in squirrels was

modest but greatest at P0-1 (Fig. 3.6E,F). Shortly after this, the response fell to a relatively stable level (Fig. 3.6E,F). ACR was not consistently altered in animals breathing the different CO₂ gas mixtures but lung extraction was significantly reduced early in development ($p < 0.05$).

Raising squirrels under burrow conditions had little effect on the HCVR when compared to squirrels raised in room air. Squirrels raised in room air had a significantly larger HCVR on both 5% and 7% CO₂ on the day of birth ($p < 0.05$) (Fig. 3.6E,F). On this day the HCVR was reduced by about 75% in 5% CO₂, and 100% in 7% CO₂ in CH squirrels. From this age on, however, the HCVR was significantly blunted in both cohorts (Fig. 3.6E,F). However, of the two cohorts, CH raised squirrels tended to have a smaller and less variable HCVR.

3.4.3.3 Long Term Effects of Development In Chronic Hypercapnia on O₂ Consumption Rate, Ventilation and the Hypercapnic Ventilatory Response

Thirty days after removal from the burrow environment (at P60), the mass specific metabolic rate of the squirrels in normocapnia had fallen to levels below those seen in newborns exposed to acute normoxia (Fig. 3.6A). Total ventilation was also lower and there were modest increases (not significant) in the ACR and decreases in lung extraction. The HCVR of the squirrels was largely unchanged (Fig. 3.7) when comparing P30 squirrels still in chronic hypercapnia to P60 squirrels. The ACR was only significantly elevated in squirrels breathing 7% CO₂ at P60 ($p < 0.05$) (Fig. 3.6C).

3.5 Discussion

It is well known that rodents with a burrowing (fossorial) lifestyle exhibit a reduced hypercapnic ventilatory response as adults (HCVR) (Boggs et al., 1984; Walker *et al.*, 1985; Birchard et al., 1984; Tenney and Boggs, 1986). We recently reported that pups of two semi-fossorial species (hamsters and 13-lined ground squirrels) were not born with a blunted response, rather the blunted response developed over the first three weeks of life in animals raised in normoxic and normocapnic conditions. Since the attenuation of the HCVR occurred during a developmental window for respiratory control documented in rats (Wong-Riley and Liu, 2008; Bavis and MacFarlane, 2017; Wong-Riley et al., 2019), we asked whether peri and neonatal exposure to burrow conditions would alter these developmental profiles, and whether such

exposure would further blunt the adult hypercapnic ventilatory response in burrowing species. Our results show that the developmental profiles were altered in the semi-fossorial hamsters and ground squirrels but not the rats. The hypercapnic ventilatory responses of the adults, however, were not further blunted; they simply became blunted earlier in development. Thus it appears that the fossorial HCVR is 1) plastic during postnatal development, and 2) strongly genetically determined such that the adult HCVR develops regardless of environment.

3.5.1 Changes in O₂ Consumption Rate and Ventilation throughout Development in Chronic Hypercapnia

In the present study, development in chronic hypercapnia significantly slowed growth in all species. Slowed growth in rats reared in hypercapnia has been reported previously (Rezzonico and Mortola, 1989; Bavis et al., 2006) although the differences in mass disappeared by adulthood (before removal from chronic hypercapnia (Rezzonico and Mortola, 1989) and 2 weeks after removal from chronic hypercapnia (Bavis et al., 2006)). Our rats (~250 grams at P60) were similar in size to age matched (8 weeks) Sprague-Dawley rats (~260 grams, males and females averaged) after removal from hypercapnia (DeMoss and Wright, 1998). In golden-Syrian hamsters, the reduction in growth was highly variable. At P30 some hamsters were significantly smaller than pups raised in room air while others were of a similar weight. Unlike hamsters, although 13-lined ground squirrels raised in hypercapnia were as much as 32% smaller than age matched controls, by P30 they had caught up in weight to animals raised in room air as well as to age matched squirrels from previous reports (Sprenger et al., 2018).

In all three species, a brief reversion back to acute normoxia/normocapnia, which in relative terms would be hyperoxia/hypocapnia, did not result in any noteworthy changes in any of the ventilatory or metabolic variables. This is consistent with the results of Rezzonico and Mortola (1989) who found that 2 days after removal from 7% chronic hypercapnia, ventilation in P9 rats was also still elevated .

In general, in rats the changes in O₂ consumption rates and ventilation, and hence in the air convection requirement and in pulmonary O₂ extraction through development, were very little different to those seen in rats raised in normocapnia. Oxygen consumption rates tended to be lower in CH rats later in development, but the reductions were not always significant. As with

rats raised in normocapnia, as development progressed O₂ delivery became more dependent on ventilation and less on pulmonary O₂ extraction. Previous studies have also reported that total ventilation was similar in the adults of animals that were raised in normocapnia and hypercapnia after being removed from chronic hypercapnia (Birchard *et al.*, 1984; Rezzonico & Mortola, 1989; Bavis *et al.*, 2006).

The effects of rearing in chronic hypercapnia in the 13-lined ground squirrels were not dissimilar to those seen in the rats. In the case of the ground squirrels, however, the reduction in O₂ consumption rates were significant through development. The balance between O₂ consumption rates and ventilation was such that as development progressed O₂ delivery became more dependent on ventilation and less on pulmonary O₂ extraction, more so in the CH squirrels than in those raised in normocapnia.

The switch in relative roles of increasing ventilation versus pulmonary O₂ extraction through development in the rats and ground squirrels is intriguing. In rats and mice, the diffusing capacity of the lung increases dramatically over this time frame indicating that it is not due to a developmental reduction in morphological diffusing capacity (Kaufman *et al.*, 1974; Kawakami *et al.*, 1984; Bolle *et al.*, 2008). The extent to which the change reflects morphological changes in lung wall stiffness and ventilatory capacity remains an open question. In newborn mammals the chest wall is much more compliant than the lungs leading to chest wall distortion during inspiration and increased respiratory work (Frappell and Mortola, 1989; Mortola, 2001). The changes seen here may more likely reflect maturation of the respiratory pump rather than of the lungs themselves.

The CH hamster pups, on the other hand, maintained relatively constant but high rates of mass specific O₂ consumption and low levels of ventilation through development. This was different than the developmental profile reported for hamster pups raised in normocapnia where both O₂ consumption rates and ventilation increased progressively over the first 20 days of life (Sprenger *et al.*, 2019 (chapter 2)). As a result, the air convection requirement tended to be lower and pulmonary O₂ extraction higher in the CH pups throughout development compared to hamster pups raised in normocapnia. The underlying causes of these changes is also unknown but suggests that lung and/or chest wall development differ in the hamsters.

3.5.2 *Changes in the Hypercapnic Ventilatory Responses throughout Development in Chronic Hypercapnia*

Acute hypercapnia (5% and 7% CO₂) did not affect metabolic rate in any of the species at any point in development as has been shown by others (Mortola and Lanthier, 1996; Saiki and Mortola, 1996; Sprenger et al., 2019 (chapter 2); Dzal et al., 2020).

Rats raised in normocapnia express a triphasic hypercapnic ventilatory response through development (Stunden et al., 2001; Putnam et al., 2005; Sprenger et al., 2019 (chapter 2)). At birth there is a strong increase in ventilation in response to 5% and 7% CO₂ (phase I). Over the first week of birth the HCVR is dramatically reduced, reaching a nadir at ~P7-9 (phase II). At P10 the ventilatory response begins to recover (phase III) reaching adult response levels around P20. There were two notable differences in CH rats. The first was the near absence of any ventilatory response to 5% CO₂ in newborn rats (i.e. no phase I). The other was that the progressive increase in the HCVR in phase III stabilized at maximum values that were lower, and hence reached earlier in development (Fig. 3.2).

The blunting of the HCVR from chronic hypercapnia in adult birds and mammals has been attributed to changes in H⁺ buffering via changes in bicarbonate concentration (Dempsey & Forster, 1982; Bebout & Hempleman, 1999). This could also be the case in newborn rats raised in chronic hypercapnia. Additionally, in rats, it could be due to changes in central CO₂ chemosensitivity. Specifically, chemoreceptors in the medullary raphé (Wang & Richerson, 1999) and the locus coeruleus (LC) (Stunden *et al.*, 2001) are less responsive to chemical stimuli prior to P8-10. Chemoreceptors in the LC are more chemosensitive early in development (P1) but show a significant reduction in sensitivity, reaching their basal responsiveness around P8 before rising again; a similar trend to the whole animal HCVR (Stunden *et al.*, 2001). In addition, around phase II, there is a precipitous drop in excitatory receptors in chemosensitive brainstem regions (glutamate and NMDA-type glutamate receptors) and a sharp increase in GABA_A and GABA_B receptors (Liu & Wong-Riley, 2005; Gao *et al.*, 2011; Wong-Riley *et al.*, 2013, 2019).

We have previously shown that both golden-Syrian hamsters and 13-lined ground squirrels have a brisk hypercapnic ventilatory response on the day of birth. In the golden-Syrian

hamster the hypercapnic ventilatory response slowly and progressively wanes to the blunted adult response while in the 13-lined ground squirrels, it is reduced within days and remains attenuated through development (Sprenger et al., 2019 (chapter 2)). When raised in chronic hypercapnia, the HCVR in both species was greatly reduced on the day of birth and was reduced to adult levels at a much earlier time point. Clearly this was largely, if not exclusively the result of the perinatal CO₂ exposure.

As noted for these species raised under normocapnic conditions, all species have a strong hypercapnic ventilatory response on the day of birth and all show an initial and dramatic attenuation of this response (Sprenger et al., 2019 (chapter 2)). While the rate of decline varies, what distinguishes the non-fossorial rat from the two semi-fossorial species is the secondary increase in hypercapnic responsiveness in the rat. This remains the case for animals raised in chronic hypercapnia. Again, the mechanisms underlying the differences in the developmental profiles of the HCVR in fossorial and semi-fossorial newborns are unknown, but are likely due to differences in the timing and degree of the changes outlined above with respect to the triphasic response seen in the rats (Bebout and Hempleman, 1999; Dempsey and Forster, 1982; Liu and Wong-Riley, 2005; Nottingham et al., 2001; Stunden et al., 2001; Wang and Richerson, 1999; Wong-Riley et al., 2019).

3.5.3 Long Term Effects of Development In Chronic Hypercapnia on O₂ Consumption Rate, Ventilation and the Hypercapnic Ventilatory Response

Consistent with other studies, thirty days after removal from chronic hypercapnia, rats had normal levels of resting O₂ consumption (Mortola, 1991) and ventilation (Mortola, 1991), The same was true for the hamsters (Mortola, 1991). Unfortunately, there are no data available for age-matched squirrels (P60) for comparison. Note that in all cases, mass specific metabolic rate had fallen as would be expected for growing animals, but levels of total ventilation in normocapnia remain relatively constant leading to slight increases in the air convection requirement and falls in pulmonary O₂ extraction.

The attenuated HCVR of the rats had also returned to normal levels by 60 days after birth as has been reported by others (Birchard *et al.*, 1984; Rezzonico & Mortola, 1989; Bavis *et al.*, 2006, 2018). Rats increased ventilation by ~80% in response to breathing 5% CO₂ and by 100%

in response to breathing 7% CO₂ similar to the increases recorded in animals raised in normocapnia at P30 (Fig. 3.7) and at ~P35-42, but slightly lower than that of rats older than 13 weeks (~100% increase in ventilation to 5% CO₂ vs. 80% in the present study) (Bavis *et al.*, 2006). After 30 days of chronic exposure to hypercapnia the HCVR of the hamsters and ground squirrels were not significantly different from those of animals raised in normocapnia and after removal from the chronic conditions there was little change in the HCVR in either species. There was a slight trend for an increase in the HCVR of both species when exposed to 7% CO₂, but this increase was non-significant and thus these data are consistent with previous observation of adult golden-mantled ground squirrels indicating that exposure to chronic hypercapnia has no lasting effects in burrowing mammals (Webb & Milsom, 1994).

3.6 Conclusions

Fossorial and semi-fossorial rodents gestate, are born into, and develop in a hypoxic/hypercapnic environment (Baudinette, 1974; Boggs *et al.*, 1984b; Roper *et al.*, 2001). Several factors such as litter size (Schneider & Wade, 1990; Vaughan *et al.*, 2006) and soil type (Wilson & Kilgore, 1978; Burda *et al.*, 2007) likely affect gas composition during development. Unsurprisingly, adult fossorial and semi-fossorial rodents tend to have a smaller HCVR compared to non-fossorial rodents (Boggs *et al.*, 1984b; Boggs & Birchard, 1989). Recent data from our lab showed that semi-fossorial hamsters and 13-lined ground squirrels are not born with the attenuated adult response, but that it develops over the first 30 days of life (Sprenger *et al.*, 2019 (chapter 2)). We asked whether development under burrow conditions affects the development of the HCVR. Data from the present study indicates that development in chronic hypercapnia speeds the developmental attenuation of the HCVR.

In non-fossorial rats, chronic hypercapnia eliminated the HCVR to 5% CO₂ early in development and attenuated the HCVR to 5% and 7% CO₂ later in development. The attenuation of the HCVR was not sustained on return to normocapnic conditions as has been reported by others (Birchard *et al.*, 1984; Rezzonico & Mortola, 1989; Bavis *et al.*, 2006)

With such a limited comparison, this study cannot directly attribute lifestyle differences to the differences seen in how these species responded to chronic hypercapnia. There also exists

the possibility that the two sexes may be differentially affected (Holley et al., 2012) as our analysis excluded this comparison. However, given the similarities in the developmental profile of changes in the HCVR in the two semi-fossorial species and the stark difference in the profile of the non-fossorial rat, it is likely that lifestyle does play a significant role. This remains to be adequately examined by more species comparisons. The data do, however, lend strong support to the suggestion that the attenuated HCVR seen in fossorial and semi-fossorial rodents is genetically derived (Birchard *et al.*, 1984; Bavis *et al.*, 2006) and further suggest there is significant plasticity in the time course of its expression.

Table 3.1 : Daily values for oxygen consumption (ml/min) and ventilation (ml/min) in all species

Age (days)	Ventilation (ml/min±SEM)						Oxygen Consumption (ml/min±SEM)					
	Rats		Hamsters		Squirrels		Rats		Hamsters		Squirrels	
	CH	N	CH	N	Ch	N	CH	N	CH	N	Ch	N
0	2.563±0.425	2.959±0.455	1.647±0.150	1.730±0.364	2.247±0.163	2.409±0.309	0.160±0.011	0.159±0.031	0.090±0.005	0.047±0.004	0.133±0.009	0.117±0.010
1	3.068±0.678	5.852±0.366	3.024±0.048	2.194±0.245	2.568±0.302	4.525±0.608	0.179±0.021	0.233±0.016	0.113±0.006	0.048±0.009	0.134±0.013	0.171±0.008
2	7.025±0.405	6.821±0.646	3.518±0.156	2.625±0.317	4.065±0.758	5.877±0.825	0.254±0.028	0.254±0.016	0.131±0.009	0.073±0.004	0.149±0.016	0.206±0.006
3	6.579±0.379	10.13±0.946	4.922±0.113	4.219±0.793	5.142±0.705	8.643±1.200	0.274±0.027	0.274±0.024	0.170±0.010	0.092±0.009	0.170±0.028	0.247±0.021
4	7.217±0.930	9.297±0.738	5.510±0.188	4.993±0.280	5.454±0.371	10.47±1.236	0.367±0.027	0.363±0.035	0.199±0.013	0.090±0.007	0.193±0.034	0.337±0.013
5	9.242±0.932	11.11±0.711	6.501±0.449	4.800±1.455	6.604±0.831	11.52±1.277	0.382±0.028	0.419±0.020	0.240±0.017	0.124±0.016	0.240±0.023	0.380±0.033
6	8.795±0.811	13.53±1.097	7.370±0.253	5.174±1.596	8.401±0.623	14.16±1.106	0.465±0.054	0.482±0.039	0.271±0.008	0.128±0.014	0.292±0.013	0.434±0.039
7	10.66±1.346	14.36±0.447	8.210±0.366	7.726±1.609	8.274±0.303	14.60±1.443	0.591±0.090	0.485±0.046	0.297±0.009	0.140±0.015	0.306±0.012	0.517±0.048
8	12.12±0.466	20.10±1.934	9.640±0.462	8.634±1.511	10.18±0.783	14.83±1.219	0.662±0.056	0.691±0.074	0.357±0.012	0.221±0.017	0.341±0.046	0.548±0.028
9	14.55±0.564	22.48±1.806	10.79±0.706	11.97±1.383	11.62±0.565	17.31±1.680	0.739±0.077	0.855±0.120	0.355±0.021	0.302±0.046	0.325±0.037	0.679±0.054
10	15.78±2.118	21.86±1.046	11.91±0.425	10.91±2.085	11.16±1.086	15.42±1.155	0.843±0.052	0.799±0.090	0.448±0.060	0.270±0.024	0.384±0.102	0.720±0.055
11	18.12±1.178	32.12±3.048	13.80±0.531	17.57±5.113	13.01±1.356	18.28±2.187	0.941±0.061	1.109±0.074	0.478±0.035	0.374±0.079	0.388±0.027	0.718±0.037
12	19.08±1.169	28.60±3.967	14.05±1.022	17.03±1.941	13.66±0.797	25.96±3.630	1.053±0.057	1.196±0.090	0.474±0.022	0.449±0.049	0.399±0.012	0.860±0.036
13	21.10±1.804	37.70±2.136	16.94±1.908	22.82±4.007	16.02±0.752	26.78±3.195	1.060±0.083	1.489±0.064	0.575±0.082	0.444±0.093	0.435±0.015	0.876±0.060
14	24.49±1.707	42.51±7.564	20.06±1.425	24.89±3.772	17.30±0.775	36.29±4.759	1.169±0.097	1.554±0.077	0.675±0.028	0.586±0.087	0.449±0.020	1.115±0.099
15	27.38±2.633	45.46±2.770	22.39±1.182	25.32±2.989	20.18±1.124	33.51±3.537	1.242±0.045	1.716±0.161	0.780±0.055	0.663±0.118	0.456±0.031	1.067±0.094
16	28.80±3.368	49.01±5.575	23.24±2.153	26.81±3.488	21.77±0.458	47.81±6.450	1.219±0.097	1.797±0.130	0.962±0.094	0.694±0.168	0.520±0.030	1.080±0.125
17	34.41±2.372	50.02±5.746	25.85±3.425	30.13±4.315	25.48±0.909	52.45±5.679	1.342±0.079	1.765±0.101	1.026±0.075	0.859±0.157	0.569±0.009	1.509±0.074
18	39.72±2.700	54.43±4.203	27.70±3.233	28.73±6.143	27.02±1.636	52.28±5.437	1.321±0.073	1.653±0.088	1.058±0.103	0.904±0.190	0.626±0.014	1.482±0.108
19	45.54±2.885	49.49±7.167	35.42±5.270	51.50±4.866	32.39±1.060	53.60±7.121	1.489±0.090	1.976±0.187	1.255±0.156	1.319±0.226	0.690±0.013	1.478±0.123
20	51.18±3.876	63.63±10.266	35.61±7.437	50.73±3.190	37.80±1.078	51.26±4.182	1.546±0.144	2.024±0.147	1.267±0.146	1.417±0.103	0.772±0.076	1.469±0.099
21		60.69±4.681		64.62±12.395		43.22±3.759		2.081±0.080		1.706±0.181		1.588±0.103
22			36.31±4.332	70.21±3.744	40.40±4.769	54.53±3.610			1.395±0.120	1.467±0.066	0.864±0.052	1.717±0.101
23	62.47±2.971	72.27±4.184		71.69±4.462		52.92±8.158	1.926±0.095	2.622±0.609		1.683±0.125		1.796±0.139
24			38.70±5.775	83.57±7.218	46.10±3.550	50.14±6.940			1.509±0.141	1.726±0.161	0.935±0.028	2.012±0.161
25	69.29±3.842	91.64±11.078					1.949±0.109	3.135±0.266				
26			47.17±6.870	92.22±6.456	46.38±2.933	41.30±2.563			1.564±0.132	1.968±0.164	1.019±0.047	1.929±0.150
27	80.86±5.575	128.9±24.765					2.372±0.114	3.692±0.378				
28			49.44±4.663	92.12±12.666	52.38±3.550	46.00±5.625			1.627±0.105	2.118±0.145	1.094±0.056	1.993±0.134
29	101.84±9.026	191.1±27.878					2.805±0.224	3.822±0.325				
30			47.86±4.449	109.20±14.071	56.50±6.957	56.27±2.348			1.632±0.088	2.471±0.193	1.501±0.039	2.269±0.162
60	250.3±14.496		84.88±14.205		143.96±8.185		5.061±0.107		2.201±0.087		2.862±0.144	

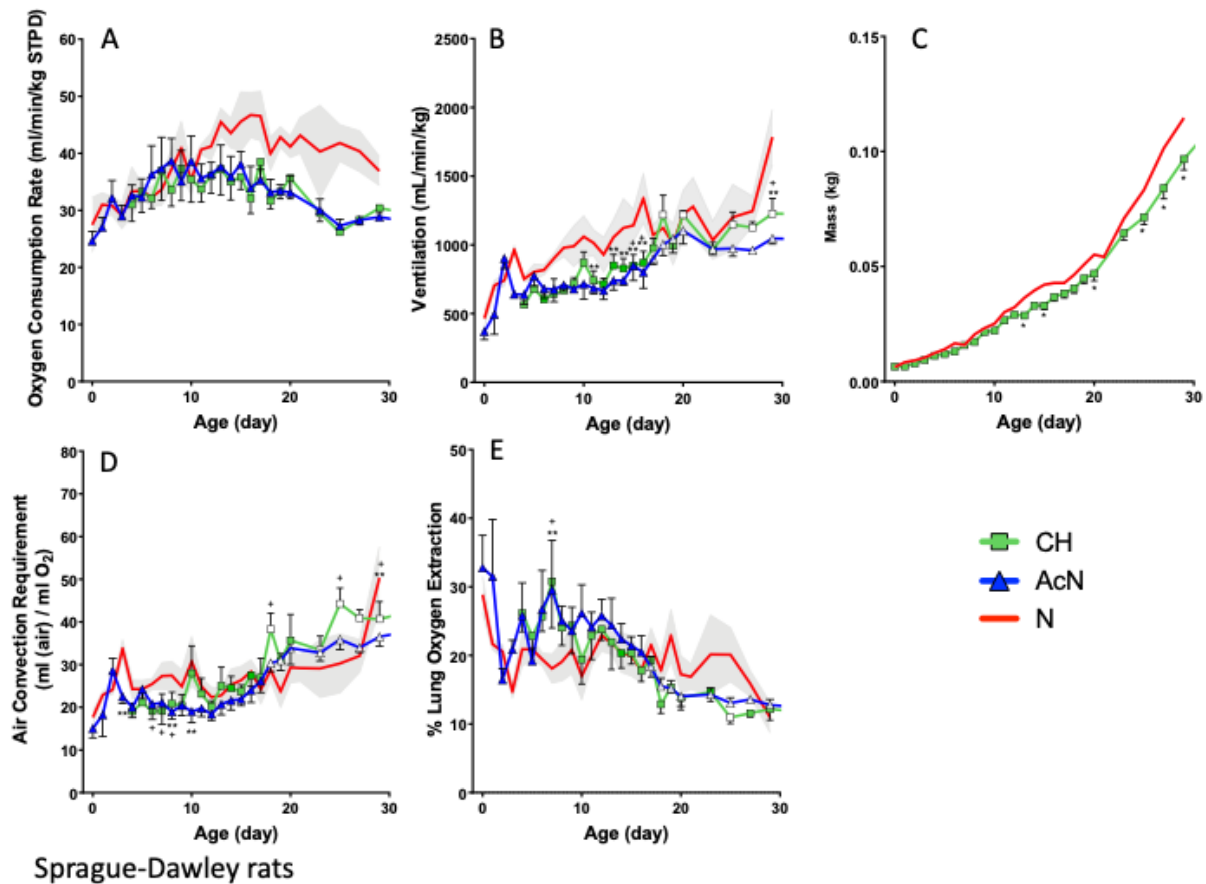


Figure 3.1 O₂ consumption rate (ml/min/kg) (A), ventilation (ml/min/kg) (B), mass (kg) (C), air convection requirement (ml (air)/ml O₂) (D), and lung oxygen extraction (E) in Sprague-Dawley rats raised in chronic hypercapnia (CH) from P0-30. Scatter plots are shown for rats breathing the CH mix (3% CO₂ in air; green line, squares) and rats acutely exposed to normocapnic air (AcN) (0% CO₂; blue line, triangles). n=4-6 for each day. Error bars show S.E.M. Summary traces are also shown for rats raised in room air (N) (0% CO₂; red line). Open symbols denote significant differences from P0 within each treatment (P<0.05) (Linear mixed model with Tukeys post hoc test). ** (AcN) and + (CH) denote significant differences between each of the experimental conditions compared to the room air treatment (N) within each day (p<0.05) (Linear mixed model with Tukeys post hoc test). Data for animals raised in normocapnia adapted from Sprenger et al., 2019 (chapter 2).

Sprague-Dawley rats

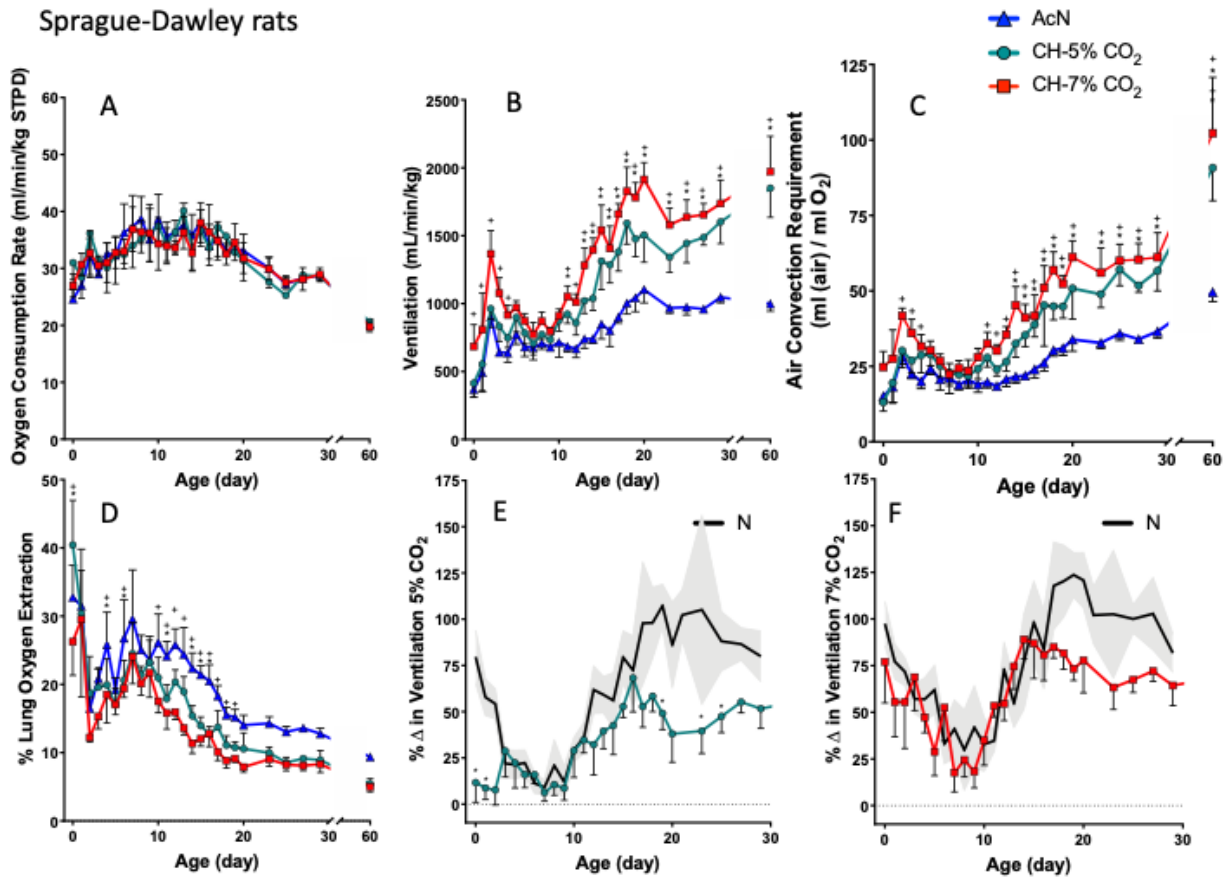
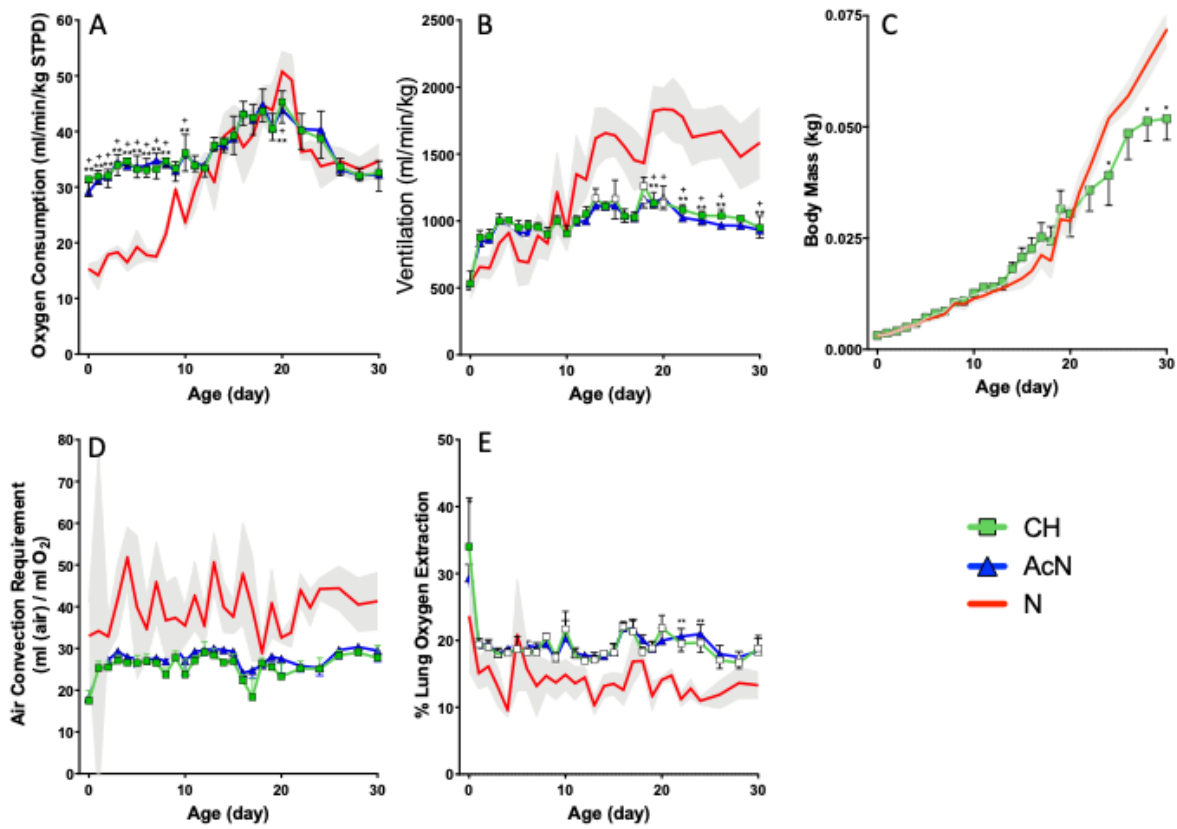


Figure 3.2 O₂ consumption rate (ml/min/kg)(A), ventilation (ml/min/kg) (B), air convection requirement (ml (air)/ml O₂) (C), % lung oxygen extraction (D), and the relative increase from AcN in ventilation in Sprague-Dawley rats raised in chronic hypercapnia breathing either 5% CO₂ (E) or 7% CO₂ (F). Scatter plots are presented for rats given normocapnia (AcN) (0% CO₂; blue line, triangles) or hypercapnia (5% CO₂; cyan line, circles (CH-5%) and 7% CO₂; red line, squares (CH-7%)) to breathe. n=4-6 for each day. Error bars show S.E.M. * (5% hypercapnia) and +(7% hypercapnia) denote significant differences between each hypercapnia treatment compared with the AcN treatment within each day (p<0.05) (Linear mixed model with Tukeys post hoc test). In panels E and F solid lines are data from pups raised in normocapnia breathing 5 and 7% CO₂ respectively. * denotes a significant difference between CH raised pups, and pups raised in normocapnia within each day for each treatment (p<0.05) (Linear mixed model with Tukeys post hoc test). Data for animals raised in normocapnia adapted from Sprenger et al., 2019 (chapter 2).



Golden-Syrian hamsters

Figure 3.3 O₂ consumption rate (ml/min/kg) (A), ventilation (ml/min/kg) (B), mass (kg) (C), air convection requirement (ml (air)/ml O₂) (D), and lung oxygen extraction (E) in golden-Syrian hamsters raised in chronic hypercapnia (CH) from P0-30. Scatter plots are shown for hamsters breathing the CH mix (3% CO₂ in air; green line, squares) and hamsters acutely exposed to normocapnic air (AcN) (0% CO₂; blue line, triangles). n=4-6 for each day. Error bars show S.E.M. Summary traces are also shown for hamsters raised in room air (N) (0% CO₂; red line). Open symbols denote significant differences from P0 within each treatment (P<0.05) (Linear mixed model with Tukeys post hoc test). ** (AcN) and +(CH) denote significant differences between each of the experimental conditions compared to the room air treatment (N) within each day (p<0.05) (Linear mixed model with Tukeys post hoc test). Data for animals raised in normocapnia adapted from Sprenger et al., 2019 (chapter 2).

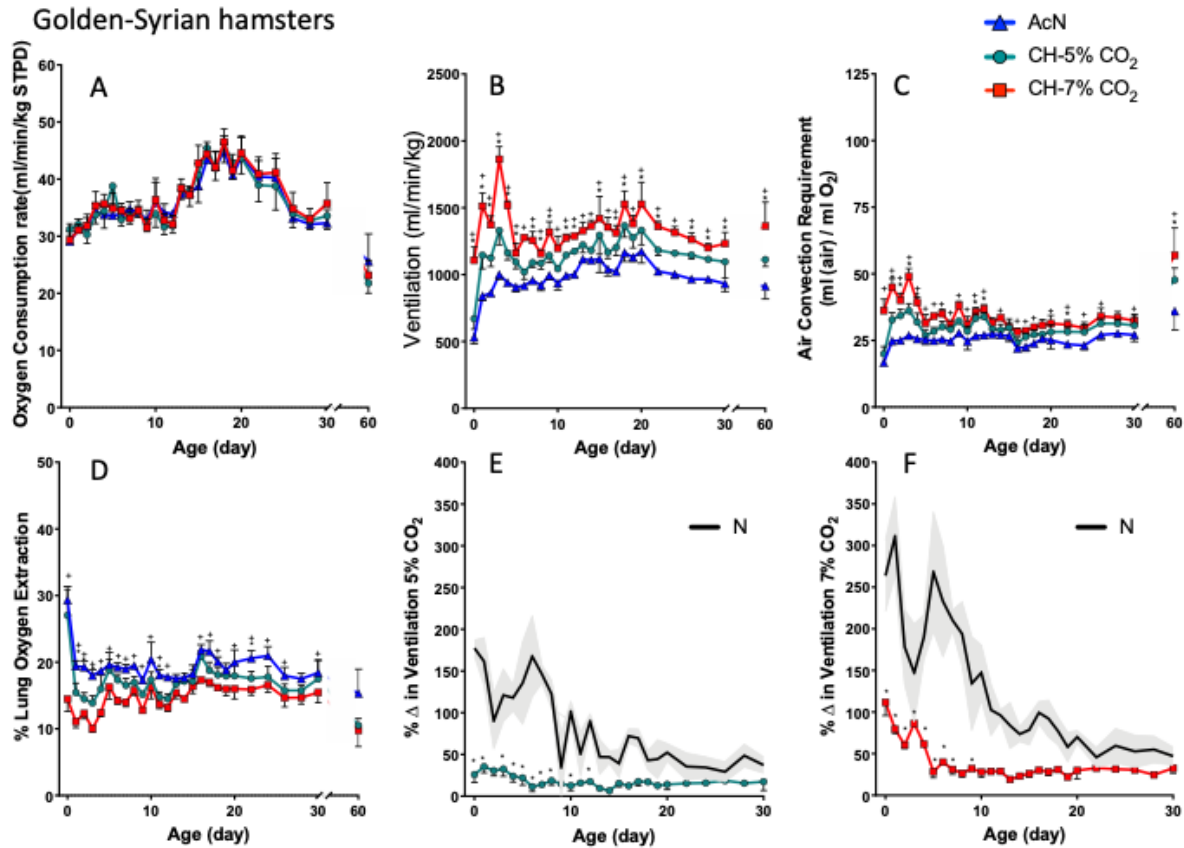


Figure 3.4 O₂ consumption rate (ml/min/kg)(A), ventilation (ml/min/kg) (B), air convection requirement (ml (air)/ml O₂) (C), % lung oxygen extraction (D), and the relative increase in ventilation from AcN in golden-Syrian hamsters raised in chronic hypercapnia breathing either 5% CO₂ (E) or 7% CO₂ (F). Scatter plots are presented for hamsters given normocapnia (AcN) (0% CO₂; blue line, triangles) or hypercapnia (5% CO₂; cyan line, circles (CH-5%) and 7% CO₂; red line, squares (CH-7%)) to breathe. n=4-6 for each day. Error bars show S.E.M. * (5% hypercapnia) and +(7% hypercapnia) denote significant differences between each hypercapnia treatment compared with the AcN treatment within each day (p<0.05) (Linear mixed model with Tukeys post hoc test). In panels E and F solid lines are data from pups raised in normocapnia breathing 5 and 7% CO₂ respectively. * denotes a significant difference between CH raised pups, and pups raised in normocapnia within each day for each treatment (p<0.05) (Linear mixed model with Tukeys post hoc test). Data for animals raised in normocapnia adapted from Sprenger et al., 2019 (chapter 2).

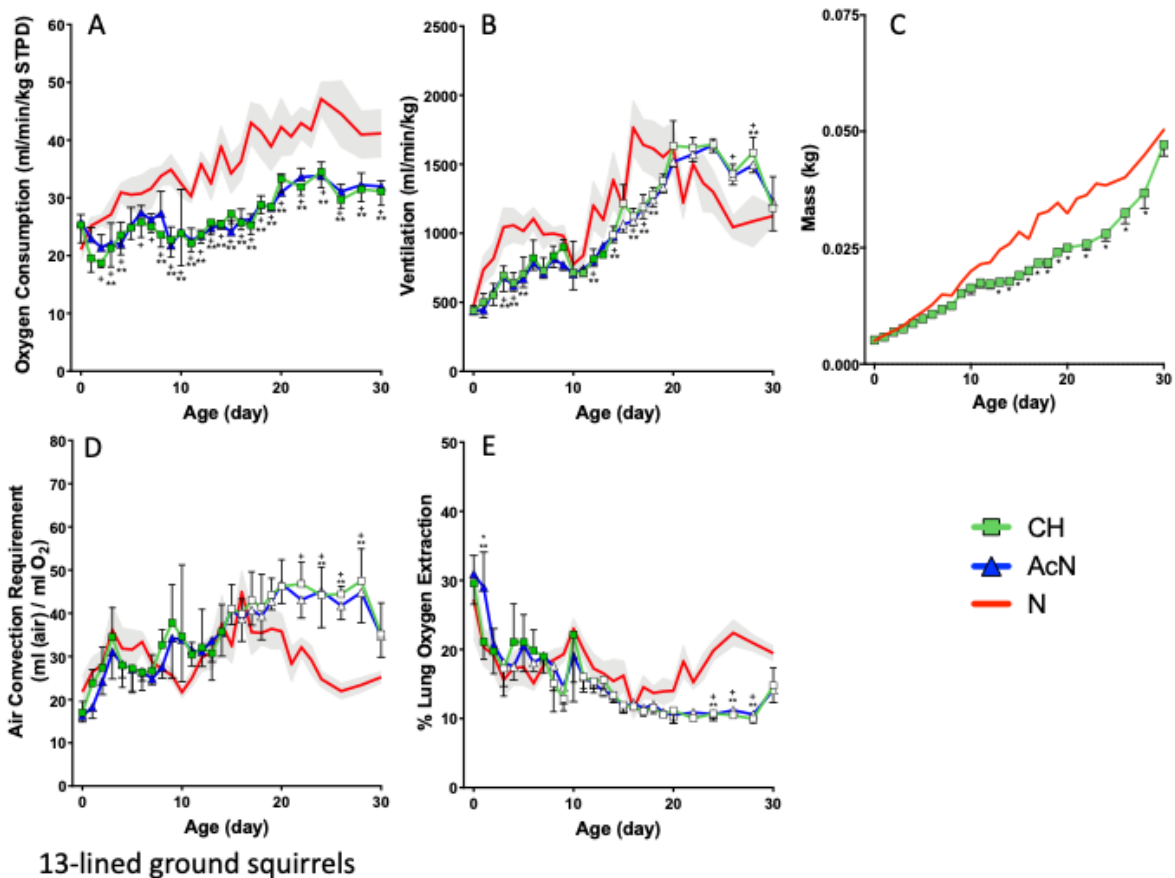


Figure 3.5 O₂ consumption rate (ml/min/kg) (A), ventilation (ml/min/kg) (B), mass (kg) (C), air convection requirement (ml (air)/ml O₂) (D), and lung oxygen extraction (E) in 13-lined ground squirrels raised in chronic hypercapnia (CH) from P0-30. Scatter plots are shown for squirrels breathing the CH mix (3% CO₂ in air; green line, squares) and squirrels acutely exposed to normocapnic air (AcN) (0% CO₂; blue line, triangles). n=4-6 for each day. Error bars show S.E.M. Summary traces are also shown for squirrels raised in room air (N) (0% CO₂; red line). Open symbols denote significant differences from P0 within each treatment (P<0.05) (Linear mixed model with Tukeys post hoc test). ** (AcN) and +(CH) denote significant differences between each of the experimental conditions compared to the room air treatment (N) within each day (p<0.05) (Linear mixed model with Tukeys post hoc test). Data for animals raised in normocapnia adapted from Sprenger et al., 2019 (chapter 2).

13-lined ground squirrels

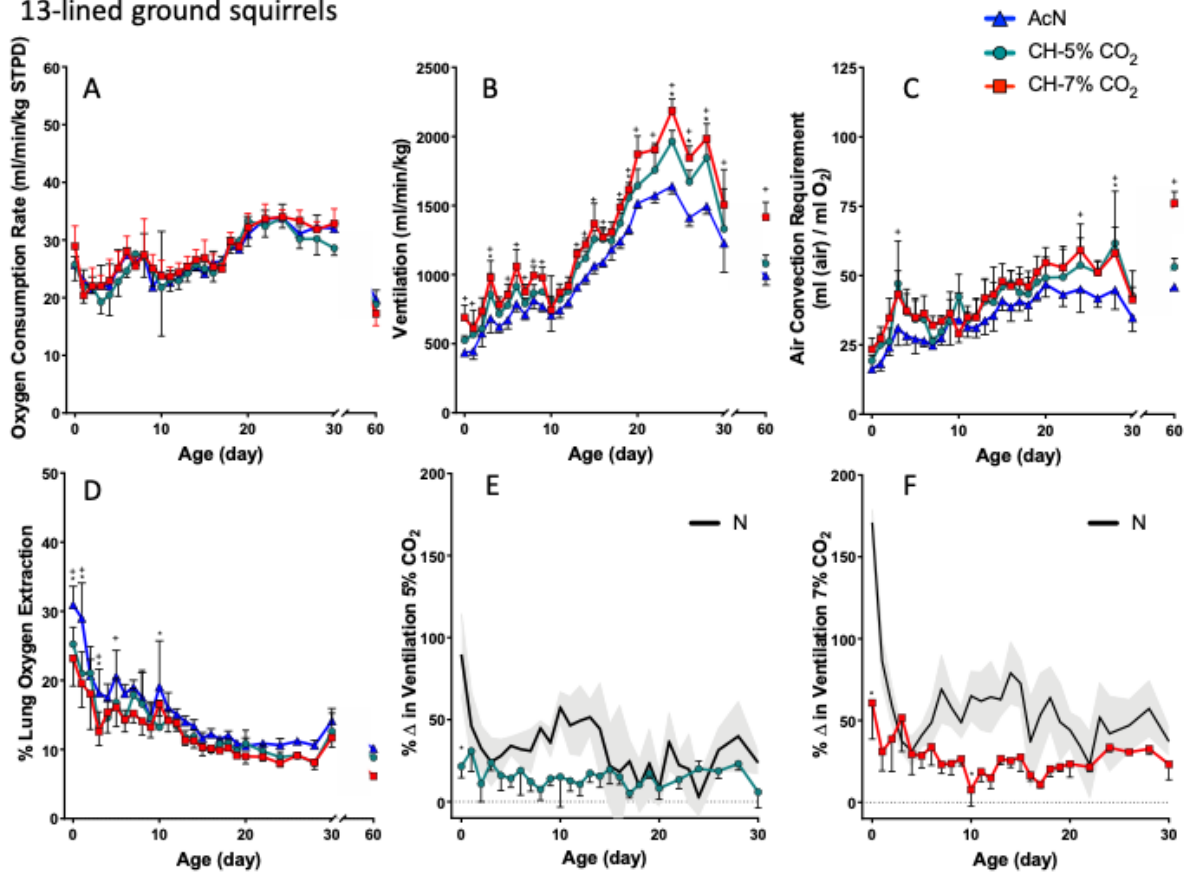


Figure 3.6 O₂ consumption rate (ml/min/kg)(A), ventilation (ml/min/kg) (B), air convection requirement (ml (air)/ml O₂) (C), % lung oxygen extraction (D), and the relative increase in ventilation from AcN in 13-lined ground squirrels raised in chronic hypercapnia breathing either 5% CO₂ (E) or 7% CO₂ (F). Scatter plots are presented for ground squirrels given normocapnia (AcN) (0% CO₂; blue line, triangles) or hypercapnia (5% CO₂; cyan line, circles (CH-5%) and 7% CO₂; red line, squares (CH-7%)) to breathe. n=4-6 for each day. Error bars show S.E.M. * (5% hypercapnia) and +(7% hypercapnia) denote significant differences between each hypercapnia treatment compared with the AcN treatment within each day (p<0.05) (Linear mixed model with Tukeys post hoc test). In panels E and F solid lines are data from pups raised in normocapnia breathing 5 and 7% CO₂ respectively. * denotes a significant difference between CH raised pups, and pups raised in normocapnia within each day for each treatment (p<0.05) (Linear mixed model with Tukeys post hoc test). Data for animals raised in normocapnia adapted from Sprenger et al., 2019 (chapter 2).

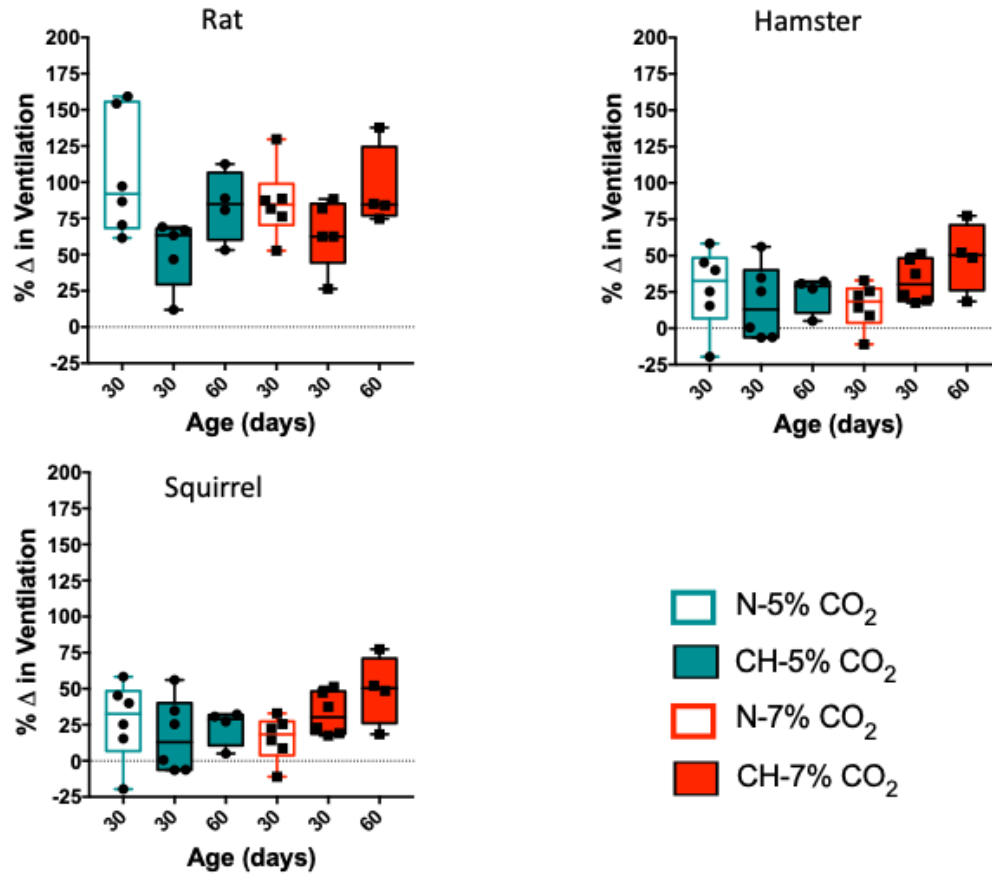


Figure 3.7 Comparison of the HCVR in Sprague-Dawley rats (top left panel), golden-Syrian hamsters (top right panel), and 13-lined ground squirrels (bottom left panel) breathing 5% (cyan) and 7% (red) CO₂ while under CH conditions (P30) and 30 days after being housed in room air (P60). Error bars denote S.E.M. n = 4-6 each day. Dotted lines indicate the HCVR of each respective species raised in normocapnia at P30. Data for animals raised in normocapnia adapted from Sprenger et al., 2019 (chapter 2).

Chapter 4: Temperature Effects on Ventilatory Sensitivity to Hypercapnia in Torpid 13-Lined Ground Squirrels (*Ictidomys Tridecemlineatus*)

4.1 Summary

Seasonal mammalian hibernators display extraordinary physiological changes in response to resource deprivation. Among these changes are drastic reductions in metabolic rate (~2% of active rates) and body temperature (T_b) (as low as -2°C). Although ventilation (\dot{V}_E) is greatly reduced in torpid ground squirrels, their relative ventilatory response ($\% \Delta \dot{V}_E$) to 7% CO_2 (~400% increase) dwarfs that of a euthermic squirrel (~60% increase). Based on earlier studies, we hypothesized that this switch in apparent ventilatory sensitivity was the result of the change in state (from active to torpid) and not due to the change in core T_b and would thus be present at all steady state hibernation temperatures. We used whole body plethysmography to assess the hypercapnic ventilatory response (HCVR) in 13-lined ground squirrels in steady state torpor at 20°C , 15°C , 10°C , 7°C , and 5°C . The transition into torpor resulted in a change in breathing pattern that became more clustered (episodic) as T_b fell. Total \dot{V}_E and the oxygen consumption rate (\dot{V}_{O_2}) decreased progressively as T_b fell in torpor until $T_b \sim 5^\circ\text{C}$ where both increased marginally. The HCVR increased substantially as core T_b decreased in torpor both in absolute and relative terms. Torpid squirrels at a core T_b of 20°C increase ventilation by 150% from normocapnia when given 7% CO_2 , while squirrels at a T_b of 7°C increase ventilation by 650% when given the same inspired CO_2 . When T_b was cooled from 7°C to 5°C however, the increase in the HCVR fell to 450% associated with the rises in \dot{V}_E and \dot{V}_{O_2} . These results reveal progressive changes in breathing pattern and the HCVR with decreasing T_b , in torpor that suggest that state may be T_b dependent.

4.2 Introduction

The physiological characteristics of hibernation in small mammals include reductions of body temperature (T_b), metabolic rate, ventilation, and heart rate (Lyman and Chatfield, 1955; Lyman et al., 1982). In deep hibernation, the T_b of most small mammals approaches ambient

temperature (T_{am}). Metabolism also falls with T_{am} in some species (golden-mantled ground squirrels (Hammel et al., 1963; Zimmer and Milsom, 2001), edible dormice (Elvert and Heldmaier 2005; Wilz and Heldmaier 2000), and the little brown bat (Szewezak and Jackson, 1992)), but not all (bears, arctic ground squirrels (Barnes and Buck, 2000;), alpine marmots (Ortmann and Heldmaier, 2000), and the echidna (Nicol et al., 1992)). In the latter group, metabolic rate appears to fall rapidly to some minimum by the time T_{am} has fallen to 18-20°C and is sustained at that level throughout the bout of hibernation, regardless of further falls in T_a (Barnes and Buck, 2000; Nicol et al., 1992; Ortmann and Heldmaier, 2000). Thus, the extent to which metabolic rate is affected by changes in state versus temperature appears to vary between species.

In golden-mantled and Columbian ground squirrels, ventilation falls by as much as 98% with breathing frequency falling to as low as one breath every minute during hibernation at $T_{am} \sim 5^\circ\text{C}$ (McArthur and Milsom 1991b; Zimmer and Milsom 2001; Webb and Milsom 2017). Along with reductions in ventilation, significant changes also occur in breathing pattern (McArthur and Milsom 1991b; Harris and Milsom 1993; Zimmer and Milsom 2002a; Milsom and Jackson 2011a). At low body temperatures, Columbian ground squirrels and marmots exhibit a pattern of single breaths spaced 30 sec – to 1min apart, while golden-mantled ground squirrels and dormice exhibit a pattern characterized by long apneas (up to 50 minutes) flanked by episodes of continuous breathing (Endres and Taylor 1930; McArthur and Milsom 1991b; Wilz and Heldmaier 2000; Zimmer and Milsom 2002a; Webb and Milsom 2017). At extremely low T_a ($< 5^\circ\text{C}$), the episodic breathing pattern in golden-mantled ground squirrels converts to one of slow uniform breathing. From these studies it is difficult to assess the effects of changes in temperature versus metabolism or state on breathing pattern as all three change together. From studies employing experimentally induced hypothermia, however, it has been concluded that reductions in temperature alone will produce episodic breathing in golden-mantled ground squirrels but that decreases in metabolism, and/or changes in state contribute to the shaping of the breathing episodes (Milsom et al. 1993; Zimmer and Milsom, 2001; Osborne and Milsom, 1993).

Sensitivity to respiratory stimuli is also altered during steady state torpor (McArthur and Milsom 1991b). The ventilatory response to hypoxia is almost entirely eliminated due to

temperature effects on oxygen-hemoglobin binding affinity, and even 3% inspired O₂ fails to elicit a ventilatory response from Columbian ground squirrels (McArthur and Milsom 1991b; Barros et al. 2001). The ventilatory response to hypercapnia, however, is enhanced in both hibernating Columbian and golden-mantled ground squirrels, suggesting that levels of blood PCO₂ and pH have a greater role in determining breathing pattern in torpor than do levels of PO₂ (McArthur and Milsom 1991b; Webb and Milsom 2017). In some species the relative response to hypercapnia increases by almost 10-fold from active to torpid conditions (McArthur and Milsom 1991b; Webb and Milsom 2017). This increase is seen in hibernating golden-mantled ground squirrels but not hypothermic ones suggesting that it is due to entrance into hibernation rather than to a fall in body temperature (Osborne & Milsom, 1993). But while this increase in relative CO₂ sensitivity has been recorded in Columbian ground squirrels as well as golden-mantled ground squirrels employing both episodic and slow uniform breathing patterns, all recordings were made at low T_{am} ($\leq 5^{\circ}\text{C}$). Furthermore, when cooled from 6°C to 2.5°C T_{am}, the HCVR of hibernating golden-mantled ground squirrels was reduced by half in association with the switch from an episodic to a slow uniform breathing pattern (Webb & Milsom, 2017).

In the present study we use the 13-lined ground squirrel to examine the effects of changing ambient temperature of animals in steady state torpor over the range of 5 to 20°C on ventilation, breathing pattern and the HCVR. From preliminary observations we know that this species does breathe episodically at low temperatures. Based on the previous studies from other species just described, we hypothesized that ventilation would correlate with metabolic rate, that the appearance of episodic breathing would be primarily temperature dependent and that the HCVR would be uniformly elevated throughout torpor until body temperature approached the animal's lower critical limit where metabolic rate begins to rise again to support thermogenesis to prevent freezing. At this point, ventilation and O₂ consumption rate would increase and sensitivity to hypercapnia would fall.

4.3 Methods

4.3.1 Animals

All procedures were conducted under a protocol approved by the UBC Animal Care Committee (UBC A17-0018) and complied with the policies of the Canadian Council on Animal

Care. 13-lined ground squirrels (*Ictidomys tridecemlineatus*) were trapped in Carman, MB, Canada (49°30'N, 98°01'W) and transferred to an animal care facility at the University of British Columbia. Squirrels were trapped with the approval of the Manitoba Conservation and Water Stewardship, under wildlife scientific permit WB15027. Wild caught squirrels were treated with Ivermectin and Droncit for endoparasites (0.4 mg/kg, subcutaneous), and flea spray for ectoparasites immediately after capture. Squirrels were provided water and IAMS small chunk dog chow supplemented with apples and peanuts *ad libitum* during the active period. No food or water was provided during the hibernation period. All animals were kept in a temperature-controlled chamber (20 ± 2 °C) on a photoperiod that matched the daily photoperiod in Vancouver, British Columbia, Canada during the active period and at (5 ± 2 °C) in the dark during the hibernation period.

4.3.2 Measurement of Temperature

Chamber temperature was monitored continuously with two complimentary systems. The first system used a thermal probe connected to a physitemp (BAT-12, Physitemp, Clifton, NJ). The second used a scannable RFID temperature chip (ITPP-300 extended calibration) that was read with a DAS-8017 programable reader (Biomedic data systems, Seaford, DE). The thermal probe was situated just over the experimental animal box, and the scannable chip was secured on the experimental animal box. The two systems gave comparable readings.

Intraperitoneal body temperature was measured with one of two systems. The first system used implantable RFID temperature chips (ITPP-300 extended calibration) read with a DAS-8017 reader (Biomedic data systems). The second system used wireless real-time telemeters (CTA-F40 (recording ECG as well) and TA-F40; Data Sciences international, St. Paul, MN). The telemeters were read with an MX2 and physiotel connect system continuously during measurement. To ensure comparable measurement, some animals were co-implanted with both systems.

4.3.3 Measurement of Ventilation and Oxygen Consumption Rate

Ventilatory and metabolic variables were continuously measured with flow through whole-body plethysmography (Drorbaugh & Fenn, 1955*b*; Malan, 1973; Jacky, 1978; Sprenger *et al.*, 2019 (chapter 2)). Two identical plexiglass boxes were placed in a small temperature-

controlled cooling chamber. The temperature-controlled chamber was situated on a sturdy table with padding underneath to reduce vibration. The set temperature was maintained within ± 1 °C. An equal flow of air was maintained constantly through the chambers. The pressure differential between the two chambers was monitored with a differential pressure transducer (Validyne model DP103-18 amplified with a Gould DC amplifier (Gould; Valley View, Ohio)). As animals entered torpor body temperature fell. A minimum body temperature to ambient temperature differential ($T_b - T_{am}$) of 2°C was required to obtain accurate tidal volume measurements. Any differential lower than 2°C was excluded from the final analysis. Oxygen consumption rate, CO₂ production rate, and water vapor pressure were measured using the excurrent gas concentrations from the system (FMS; Sable systems). Gases were calibrated before the start of each trial from pre-mixed tanks (Praxair; 0%, 5%, 7% CO₂ with 21% O₂ balanced in N₂). Volume was calibrated before each measurement using volumes comparable to the animal's tidal volume. This was done by injection at a comparable rate to the animal's breathing frequency (~1 breath/min in torpor and ~60 when active).

To check for accurate tidal volume measurement, some animals were run using pneumotachography as a benchmark. Animals were fitted with a facemask made from the barrel of a 50ml syringe sealed with cotton and high vacuum grease. Animals were trained for ~4-6 weeks to not respond to the placement of the mask during torpor. Once trained, the mask was sealed around the mouth and nose of the torpid animal and incurrent and excurrent air flowed via tubes running into and out of the mask. For the validation experiments, torpid animals were placed in the temperature-controlled system described above and allowed to remain in torpor with the mask on for at least 12 hours before recording. A pneumotachograph was attached to the outflow tube for measuring pressure changes using a pressure transducer (Validyne model DP103-18 amplified with a Gould DC amplifier (Gould; Valley View, Ohio)). The system was calibrated by injecting several known volumes at a rate similar to that of the animal's breathing superimposed on the constant flow through rate. The calibrating volumes used were also similar to those of the animal's tidal volume.

4.3.4 *Experimental Protocol*

Experimental animals were placed in the recording box while active, and moved into the temperature-controlled chamber at $\sim 5 \pm 1^\circ\text{C}$. Animals were left overnight in the chamber with an incurrent flow rate of 800 ml/min. Once an animal had entered torpor and exhibited a steady body temperature, flow rate was reduced to $\sim 50\text{-}80$ ml/min. The chamber temperature was then adjusted until the animal's body temperature was at the desired temperature ($\sim 5, 7, 10, 15$ or 20°C). Measurements at each temperature were from separate runs. Animals were then maintained at the desired temperature for at least 6 hours. Resting torpid normocapnic ventilation and metabolism were then recorded for at least 1 hour before hypercapnic (5% and 7% CO_2 , 21% O_2 , balanced in N_2) gases were administered in random order for a minimum of 1 hour each or until a steady ventilatory response was reached. Body temperature was scanned approximately once every 5 minutes during recording periods unless the animal had a real-time telemeter, in which case temperature was monitored continuously. Measurements were again made after animals had aroused and were at 37°C T_b .

4.3.5 *Data Analysis*

Breathing traces were analyzed over the last 30 minutes (hypercapnia) and 1 hour (normocapnia) of the exposures. Only periods of steady ventilation were taken for analysis. Tidal volume (V_T), breathing frequency (f_R), T_b , oxygen consumption rate (\dot{V}_{O_2}), CO_2 production rate (\dot{V}_{CO_2}), and inter-breath intervals (IBI) were extracted from the breathing traces. The frequency components (breaths/episode, IBIs within an episode, and duration of apneas between episodes) were extracted from traces where episodic breathing was present. Ventilation (\dot{V}_E) was calculated via the multiplication of V_T and f_R . V_T was calculated as described in Sprenger et al., 2019 (chapter 2) with the exception that nasal temperature was not corrected for as it was assumed to be similar to ambient temperature. \dot{V}_{O_2} was calculated as described in Sprenger et al 2019 (chapter 2), and \dot{V}_{CO_2} was calculate using the following equation (Lighton, 2008):

$$\dot{V}_{\text{CO}_2} = \text{FR} \frac{(1 - \text{Fio}_2 - \text{Fico}_2)}{(1 - \text{Feo}_2 - \text{Feco}_2)} \{\text{Feco}_2 - \text{Fico}_2\}$$

where FR is flow rate, Fio_2 is fractional inspired oxygen, Feo_2 is fractional expired oxygen, Fico_2 is fractional inspired CO_2 , and Feco_2 is the fractional expired CO_2 .

Poincaré plots were generated by plotting all the IBIs (in seconds) of the analysis period against the next corresponding IBI (IBI-1). Coefficient of variation (CV) was calculated by dividing the standard deviation of the IBIs over a period by the mean of the IBIs over the same period. ACR (O₂ and CO₂; ACR_o and ACR_c) were calculated by dividing \dot{V}_E by either \dot{V}_{O_2} or \dot{V}_{CO_2} . Body mass was taken at the end of the experiment.

4.3.6 Statistical Analysis

A two-way repeated measures ANOVA was used to determine the effect of inspired gas on all absolute metabolic and ventilatory variables. A separate two-way ANOVA was generated to determine the effect of temperature within a treatment group on absolute ventilation and oxygen consumption rate as well as all percent change metabolic and ventilatory variables. If a significant effect was found in either test, a Tukey's post-hoc test was performed for multiple comparisons with an alpha of 0.05. A one-way ANOVA was used to determine if there were differences among the CVs for each temperature. All statistical tests were performed using Graphpad Prism 9.0.0.

4.4 Results

4.4.1 Normocapnic Ventilation and Oxygen Consumption Rate

All metabolic and ventilatory variables were greatly reduced with the transition into torpor, except V_T and the ACR (table 1). V_T rose from 0.73ml/100g while active to ~1.2ml/100g (table 1) during torpor. The ACR_o also rose in torpor, going from 26.3 ± 0.85 during the active state to values of ~33-39 depending on the steady state temperature (Table 1.) Breathing frequency, \dot{V}_E , and \dot{V}_{O_2} were all reduced by about 98% even at the warmest torpid temperature (Table 1 and fig. 4.1). The Q₁₀ for the initial drop in \dot{V}_{O_2} from active to 20°C was 9.03 while the Q₁₀ for the whole range (37-5°C) was 3.83 (Table 2).

While \dot{V}_{O_2} at the warmest torpid temperature was already nearing the minimum \dot{V}_{O_2} seen in torpor (fig. 4.1), \dot{V}_{O_2} did continue to fall progressively as T_b fell during torpor, until 5°C where \dot{V}_{O_2} doubled from 1.0ml/hr/100g to 2.0ml/hr/100g when transitioning from 7°C to 5°C T_b (Table 1 and fig. 4.1). The Q₁₀ for the range of torpid temperatures (20-5°C) was 1.45, with the increase

in \dot{V}_{O_2} from 7°C to 5°C lowering this value substantially (Table 2). If the 5°C group is excluded from the Q_{10} calculation in the torpor groups, then the value becomes 2.29.

In steady state torpor, T_b tracked ambient temperature and the average T_b-T_{am} differential across temperature groups was $\sim 3^\circ\text{C}$ (Table 1) with the 5°C group having the lowest differential ($\sim 2^\circ\text{C}$). V_T was unaffected by the change in T_b in torpor (Table 1). Breathing frequency progressively fell from about 1.4 breaths per minute (b/min) at 20°C torpor to 0.56 b/min at 7°C torpor before rising again to 0.8 b/min at 5°C torpor (Table 1). The net result of the changes in f and V_T were a gradual reduction in \dot{V}_E with the reduction in T_b with the lowest \dot{V}_E being 0.67 ± 0.1 ml/min/100g at 7°C torpor (Table 1 and fig. 4.1). Because the changes in \dot{V}_E paralleled the changes in \dot{V}_{O_2} with the change in temperature in torpor, the ACR_o and ACR_c were largely unaffected by temperature in torpor (Table 1).

4.4.2 Breathing Pattern

In the transition from active to torpid at 20°C the breathing pattern remained one of relatively evenly spaced breaths with a lengthening of the IBI (figs. 4.2 and 4.3). In torpor at 15°C however, breathing became erratic, and at lower torpor temperatures breathing occurred in distinct episodes (figs. 4.2 and 4.3). At the lower temperatures (5, 7, 10°C), very few single breaths were observed although the breathing episodes were never larger than 8 breaths/episode at any temperature in normocapnia. The largest clusters (mean ~ 3.7 breaths/cluster) were found at 7°C (fig. 4.4). The frequency of breaths within an episode didn't change dramatically with temperature but were slightly (but insignificantly) higher at 5 and 7°C ($p < 0.05$) (fig. 4.4). Perhaps the largest change in the shape of the clusters was the length of the apneas between clusters which peaked at 7°C (fig. 4.4) and were on average ~ 4 minutes in length.

At 37°C, the CV was small (~ 0.3) and this value rose with the transition to torpor (~ 1 at 20°C) (fig. 5). Similarly, as T_b fell during torpor, the CV rose significantly compared to 37°C starting at 10°C ($p < 0.05$) (fig. 5). The CV peaked at 7°C with a value of ~ 2.4 (fig. 4.5). Despite the change in breathing pattern from evenly spaced breaths (20°C) to episodes (15°C), total ventilation did not change substantially (Table 1 and fig. 4.1). Ventilation did fall as T_b fell beyond 15°C and 20°C, during which the CV was rising (fig. 4.5).

4.4.3 *Hypercapnia and Breathing Pattern*

The addition of hypercapnia altered breathing pattern particularly at colder torpor temperatures (fig. 4.2 and 4.3). At warmer temperatures (37 and 20°C) breathing simply became faster in hypercapnia (fig. 4.2 and 4.4) with no change in the regularity of breathing (fig. 4.3). At the lower temperatures, when episodic breathing was common, the addition of 5% and 7% hypercapnia significantly changed the length of the apnea between the breathing episodes ($p < 0.05$) (fig. 4.4). In both cases the frequency of breaths within the episodes fell slightly but insignificantly ($p > 0.05$) (fig. 4.4) and the number of breaths in each episode rose slightly but also insignificantly ($p > 0.05$) (fig. 4.4). The net result of these changes at the colder temperatures (10, 7, and 5°C) was that hypercapnia induced more regular breathing (fig. 4.3 and 4.4) and the CV fell significantly in 7% hypercapnia ($p < 0.05$) compared to normocapnia, as the length between the apneas became more consistent in hypercapnia (fig. 4.4 and 4.5).

The Hypercapnic Ventilatory Response

Both 5% and 7% hypercapnia significantly increased \dot{V}_E at all temperatures ($p < 0.05$) (fig. 4.6). During the active state, the increase in absolute \dot{V}_E was primarily mediated by a significant increase in V_T ($p < 0.05$) along with smaller, insignificant increases in f (fig. 4.6B and 4.C). In torpor, however, all increases in \dot{V}_E were produced by increases in f_R ; V_T was unaffected by hypercapnia in torpor (fig 4.6B and C). Interestingly, the absolute increase in breathing frequency when breathing 7% CO_2 was almost identical ($\sim 4\text{b/min}$) at all temperatures (active and torpid) (fig. 4.6B).

The relative increases in \dot{V}_E changed significantly from the active to torpid state, as well as among differing torpid temperatures ($p < 0.05$) (fig. 4.7A). When active, the percent increase in \dot{V}_E was about 30% and 70% when breathing 5% and 7% CO_2 respectively, but at 20°C torpor the respective hypercapnic responses were $\sim 75\%$ and 150% (fig. 4.7A). By 15°C torpor the increase in ventilation was significantly higher than what was seen in active animals ($p < 0.05$), and this trend continued with torpor at lower temperatures, where the hypercapnic response peaked at 275% and 650% when breathing 5 and 7% CO_2 at a T_b of 7°C ($p < 0.05$) (fig. 4.7A). The 7% hypercapnic response in torpor at 7°C was significantly higher than any other response, and the

response to 5% hypercapnia was significantly higher than any response at T_b 's warmer than 10°C ($p < 0.05$) (fig. 4.7A).

Hypercapnia had no significant effect on $\dot{V}O_2$ at any temperature (fig. 4.8A). With no effect on $\dot{V}O_2$ and a large effect on \dot{V}_E , both the ACR_o and ACR_c increased significantly at lower temperatures in hypercapnia ($p < 0.05$) (fig. 4.8B and C). The absolute increases in both the ACR_o and ACR_c were significantly higher in torpor compared to the active state ($p < 0.05$) (fig. 4.8B and C). At 7°C the ACR_o was about 150 and 275 ml(air)/ml(O_2) for 5% and 7% respectively, while at 37°C the ACR_o was about 50 and 60 ml(air)/ml(O_2) for 5% and 7% respectively (fig. 4.8B, C). Among torpid temperatures, the ACR_o increased gradually from 75 to 275 ml(air)/ml(O_2) in 7% hypercapnia as T_b fell from 20-7°C (fig. 4.8B). A similar trend was seen in 5% hypercapnia (fig. 4.8). When body temperature was maintained at 5°C, the ACR_o and ACR_c were significantly lower in comparison to the values recorded at 7°C ($p < 0.05$) (fig. 4.8B and C).

4.5 Discussion

Based on the previous studies from other species conducted primarily on Columbian and golden-mantled ground squirrels (McArthur and Milsom 1991b; Zimmer and Milsom 2001; Webb and Milsom 2017), we hypothesized that 13-lined ground squirrels in steady state torpor at decreasing ambient temperatures would 1) show a progressive decrease in oxygen consumption rate, 2) that ventilation would correlate with changes in the oxygen consumption rate, 3) that episodic breathing would appear at lower temperatures and 4) that the HCVR would be uniformly elevated throughout torpor until body temperature approached the animal's lower critical limit where metabolic rate begins to rise again to support thermogenesis to prevent freezing. We found that 1) changes in oxygen consumption rate were largely state dependent and only partially temperature dependent, 2) that ventilation was tightly correlated with oxygen consumption rate, 3) that while episodic breathing does arise at lower temperatures its initial appearance is erratic and 4) that the increase in the HCVR appeared to be temperature dependent down to 7°C.

4.5.1 Normocapnic Ventilation and Oxygen Consumption Rate

The transition to torpor under normocapnic conditions was accompanied by the expected dramatic changes in ventilation and metabolic rate. \dot{V}_E , f_R , V_T , and \dot{V}_{O_2} were all comparable to previous reports for 13-lined ground squirrels (Lyman, 1951) and other related ground squirrel species (McArthur and Milsom 1991b; Zimmer and Milsom 2001; Webb and Milsom 2017) at similar body temperatures in torpor. However, squirrels in the present study tended to take deeper breaths less frequently compared to previous reports on golden-mantled and Columbian ground squirrels, while levels of total \dot{V}_E were similar (McArthur and Milsom 1991b; Zimmer and Milsom 2001; Webb and Milsom 2017). While the decreases in \dot{V}_E and \dot{V}_{O_2} were tightly correlated during torpor at different T_{am} , they did not fall equally, and thus their ACR was elevated in torpor (from ~20-35) suggesting a relative hyperventilation. This is consistent with previous reports for other ground squirrel species (McArthur and Milsom 1991a, 1991b; Webb and Milsom 2017). The basis of the relative hyperventilation among these species during torpor remains an intriguing question, but is supported by blood gas data where PaO_2 is elevated in torpor and $PaCO_2$ is reduced (Twente and Twente 1968).

Normocapnic ventilation and oxygen consumption rate both decreased with decreasing T_b under steady state conditions down to 7°C (Table 1 and fig. 4.1). Once T_b was reduced to 5°C however, both \dot{V}_{O_2} and \dot{V}_E rose, presumably as a result of increased thermogenesis to defend a lower critical T_b limit that lies between 5°C and 7°C. Golden-mantled ground squirrels have a similar critical limit (~5°C) (Webb & Milsom, 2017) while arctic ground squirrels and pygmy possums have lower limits (~0°C and 4°C respectively) (Geiser, 1987; Buck & Barnes, 2000).

Species such as the Arctic ground squirrel (Buck & Barnes, 2000), echidna (Nicol et al., 1992), pygmy possum (Song *et al.*, 1997), and alpine marmot (Arnold *et al.*, 1991) have all been reported to maintain a relatively constant metabolic rate over a T_b range of 0° to 18°C suggesting that O_2 consumption rates are reduced to their lowest level at the onset of torpor. Other species like golden-mantled ground squirrels (Zimmer & Milsom, 2001), bats (Szewczak & Jackson, 1992), and the edible dormouse (Wilz & Heldmaier, 2000) display a temperature dependent reduction in O_2 consumption rate in torpor. Our data suggest that the 13-lined ground squirrel lies somewhere in between these two strategies. \dot{V}_{O_2} was reduced dramatically in squirrels in

torpor at the highest steady state temperature employed in the present study (20°C) resulting in a Q_{10} for O_2 consumption rate of 9.03. However, it still fell further in squirrels in steady state torpor at lower temperatures yielding a Q_{10} for \dot{V}_{O_2} of 2.29 between 20 and 7°C, a decrease that could be explained by the decrease in temperature *per se*. Thus, in 13-lined ground squirrels, the O_2 consumption rate in steady-state torpor appears to be determined by both temperature-dependent and -independent factors.

4.5.2 Breathing Pattern

As body temperature fell, \dot{V}_E also fell with the reduction being mediated exclusively by changes in f_R as V_T either remained constant or increased. At the warmest steady state temperature, breaths were relatively evenly spaced. As T_b was reduced further, small episodes of 2-4 breaths began to form and were most common at 7°C and 5°C. At steady state T_b down to 7°C, once episodes appeared, further falls in \dot{V}_E were due to a lengthening of the apneas between episodes rather than to any change in the number of breaths within an episode. The Poincaré plots suggest that the episodes were quantal in nature resulting from a common underlying rhythm. The transition to the episodic breathing pattern did not appear to have any effect on the overall level of ventilation, just the breathing pattern. Between 20 and 10°C, overall breathing frequency fell from 1.4 to 0.9 b/min while the inter-breath interval went from roughly 40 seconds between breaths to 260 seconds between episodes with roughly 5 seconds between breaths within the episode.

A similar slow, and sometimes erratic transition from uniform single breaths to episodic breathing has also been recorded in the echidna (Nicol et al., 1992) although in the golden-mantled ground squirrel and the edible dormouse, episodic breathing arises from a waxing and waning of ventilation during entrance into torpor that gives rise to episodic breathing across the entire range from 5-20°C (Zimmer and Milsom 2001; Wilz et al., 2000; Wilz and Heldmaier, 2000). The mechanistic basis of episodic breathing remains enigmatic. It has been suggested that reductions in temperature alone will produce episodic breathing but that decreases in metabolism, and/or changes in state contribute to the shaping of the breathing episodes (Milsom et al. 1993; Zimmer and Milsom, 2001; Osborne and Milsom, 1993). If this is the case, our data would suggest that this balance is somewhat different in the 13-lined ground squirrel.

4.5.3 *Hypercapnia and Breathing Pattern*

The effects of hypercapnia on the breathing pattern were most evident in the colder, episodically breathing animals. While both the number of breaths per episode, and the frequency of breaths in each episode increased, these changes were not significant. The apneic length between episodes, however, became significantly shorter. Similar results have been reported in golden-mantled ground squirrels where apneic periods became less frequent in hypercapnia until breathing became continuous at inhaled levels of CO₂ above 4% (Webb and Milsom 2017). The net result of the changes in breathing pattern in the present study was a more regular breathing pattern, and this is evident by the fall in the CV in animals breathing 5% and 7% CO₂ compared to animals breathing normocapnia. This increase in regularity was a result of an increase in the consistency of the apneic lengths in hypercapnia. Consistent with other studies, it appears the apneas/episodes become the regulated variable, and not the individual breath (Milsom and Jackson 2011).

4.5.4 *Hypercapnic Ventilatory Response*

Hypercapnia produced an increase in ventilation at all temperatures in both states (active and torpid at all steady state temperatures) in the present study. The increase in \dot{V}_E in absolute terms was substantially smaller in torpid squirrels compared to active squirrels (~4-6mL/min/100g vs. ~35mL/min/100g in response to breathing 7% CO₂). When expressed as % change from baseline \dot{V}_E , the HCVR was much greater in torpid animals compared to active animals. This is consistent with previous reports in golden-mantled ground squirrels (Harris & Milsom, 1993; Webb & Milsom, 2017) and Columbian ground squirrels (McArthur and Milsom 1991b). The relative increase in the HCVR increases dramatically at lower steady state body temperatures, which is novel. At 20°C torpor the % change to 7% CO₂ was ~150%, but by 15°C it was 250% and by 7°C it was 650%. Like the golden-mantled ground squirrel, the fall from 7°C to 5°C caused a significant reduction in the HCVR and this overlaps with the lower critical limit of T_b at which thermogenesis is recruited in both species (Webb & Milsom, 2017). Given that hypercapnia had no effect on O₂ consumption rates, not surprisingly, changes in the ACR closely mirrored the changes in the relative HCVR. This is consistent with previous reports (McArthur and Milsom 1991b; Webb and Milsom 2017).

Based on previous studies performed on hypothermic golden-mantled ground squirrels that found no effect of reducing temperature on the HCVR (Osborne and Milsom, 1993), we hypothesized that the increase in the HCVR in torpid animals was due to entrance into hibernation rather than to a fall in body temperature per se. Our data, however, suggest the opposite. Our data also suggest that active animals rely almost entirely on increases in V_T to increase ventilation in response to hypercapnia while torpid animals rely on increases in f_R . Active burrowing mammals tend to use increases in V_T rather than f_R to produce increases in ventilation in response to hypercapnic challenges (Boggs *et al.*, 1984a), and torpid mammals have been reported to increase f_R to a greater degree in hypercapnia (Lyman 1951; Tähti 1975; McArthur and Milsom 1991a, 1991b; Webb and Milsom 2017). Thus, while these results are consistent with previous reports on other species, they do indicate that there is a change in the primary regulated variable with the change in state. As noted above, with decreasing temperature it appears the apneas/episodes become the regulated variable, and not the individual breath (Milsom and Jackson 2011) but this transition does not appear to influence the pattern of change in the HCVR.

4.6 Conclusions

Our data suggest that in 13-lined ground squirrels, the O_2 consumption rate in steady-state torpor is determined primarily by temperature-independent factors. \dot{V}_{O_2} was reduced dramatically in squirrels in torpor at the highest steady state temperature employed in the present study. However, it fell further in squirrels in steady state torpor at lower temperatures suggesting that there was a temperature-dependent component to the fall as well. Ventilation was also reduced becoming episodic in squirrels in steady state torpor but only at lower temperatures. This supports the suggestions that the appearance of episodic breathing is primarily temperature dependent (Milsom *et al.* 1993; Zimmer and Milsom, 2001; Osborne and Milsom, 1993). Previous studies have shown that there is a relative increase in the hypercapnic ventilatory response in animals in deep torpor and based on studies performed on hypothermic golden-mantled ground squirrels that found no effect of reducing temperature on the HCVR (Osborne and Milsom, 1993), it was suggested that the increase was due to the change in state and not the

change in body temperature or metabolic rate. Our data for the 13-lined ground squirrel, however, demonstrated the opposite. We show that there is a progressive increase in the relative HCVR as body temperature lowers. The basis of this increase remains unclear. As temperature decreases, so too does metabolic rate and there is also possibly a ‘deepening’ of the hibernation state (Reviewed in van Breukelen and Martin 2015). Sorting out the relative contributions of temperature, metabolism, and state on ventilation, breathing pattern and the HCVR is not straightforward. However, given that the changes in these components become dissociated during entrance and arousal from hibernation, future studies during these transition phases of the torpor cycle rather than during steady state torpor may be revealing.

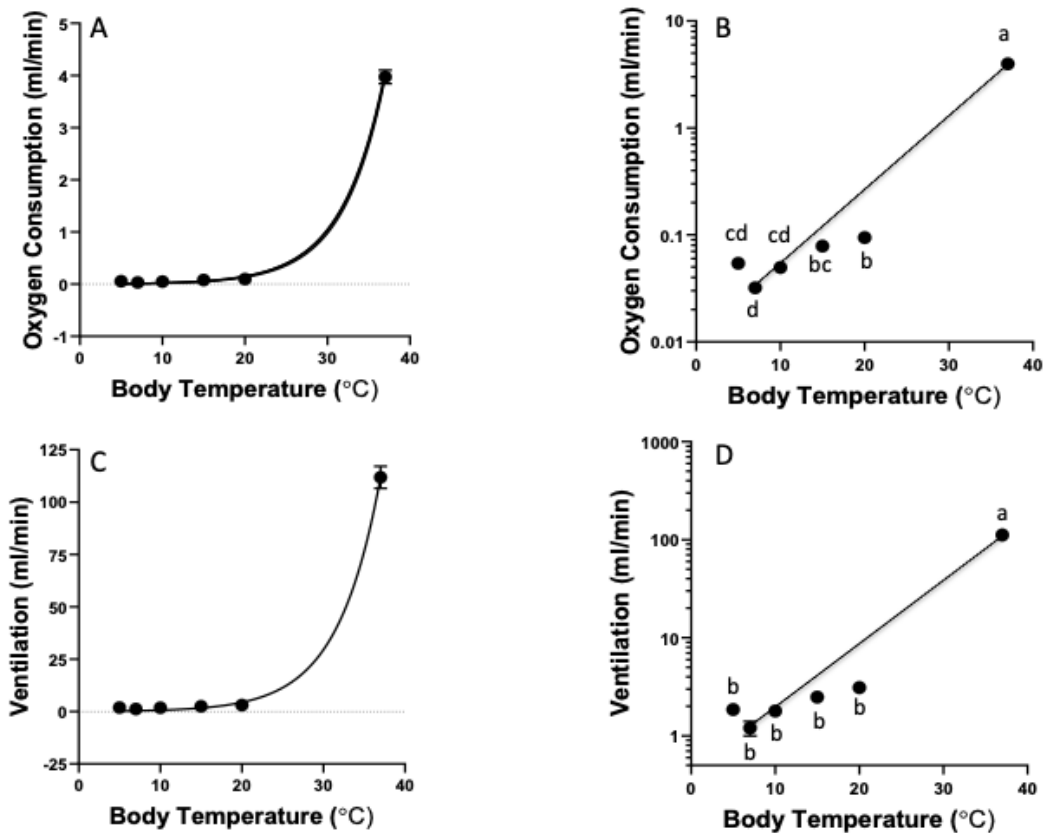


Figure 4.1 Oxygen consumption rate (mL/min) in 13-lined ground squirrels at rest at 37°C and in steady state torpor at various temperatures (20°-5°C). Oxygen consumption rate appears to follow an exponential decay but on a semi-logarithmic scale (B) the oxygen consumption rate falls close to minimum at 20°C. Dotted line in (A) is the minimum metabolic rate seen in torpor.

C. Ventilation (ml/min) at the same body temperatures as in (A) and also plotted on a semi-logarithmic scale in D. Lines in B and D are drawn between the highest and lowest oxygen consumption rates to show that the changes in O₂ consumption rate and ventilation do not follow a simple exponential decay. Error bars denote S.E.M, letters indicate significant differences among the various temperature groups (two-way ANOVA with Tukey's post hoc test; p<0.05). Lines in all graphs bear no statistical significance, but rather used merely to highlight the reduction in oxygen consumption in relation to body temperature.

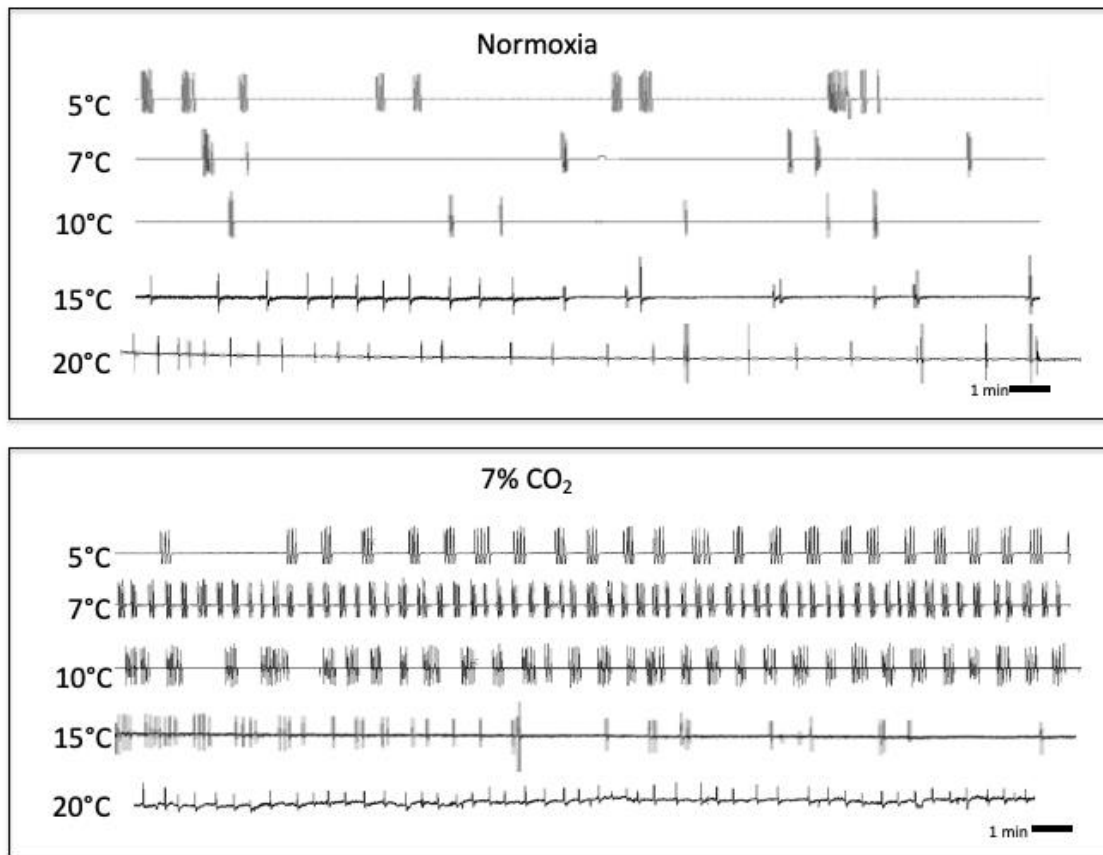


Figure 4.2 Representative breathing traces from an animal breathing normocapnia (top) and 7% hypercapnia (bottom) at temperatures ranging from 20-5°C in steady state torpor.

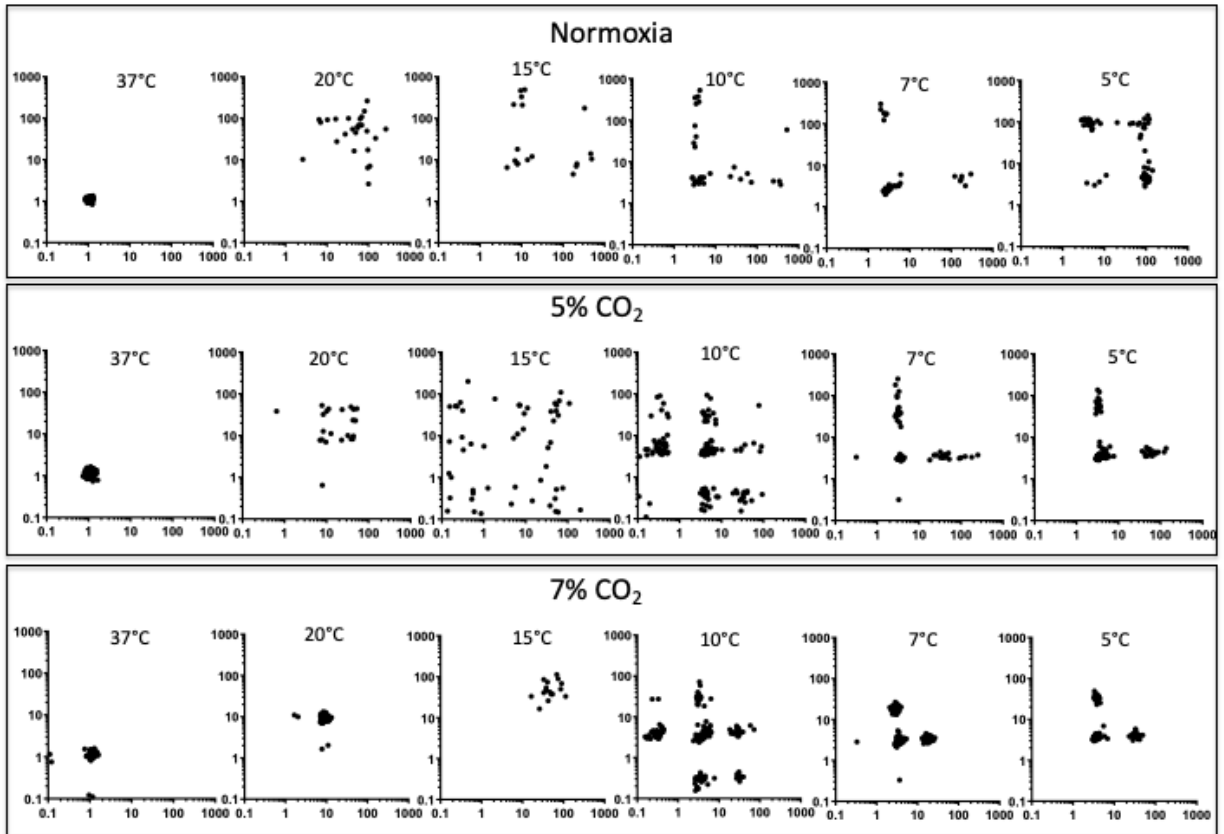


Figure 4.3 Representative Poincaré plots from animals breathing normocapnia (top) and 5% (middle) and 7% (bottom) CO₂ at 37°C and in steady state torpor at 20-5°C. Plots were generated by plotting inter-breath intervals (IBI) against the following inter-breath interval (IBI-1).

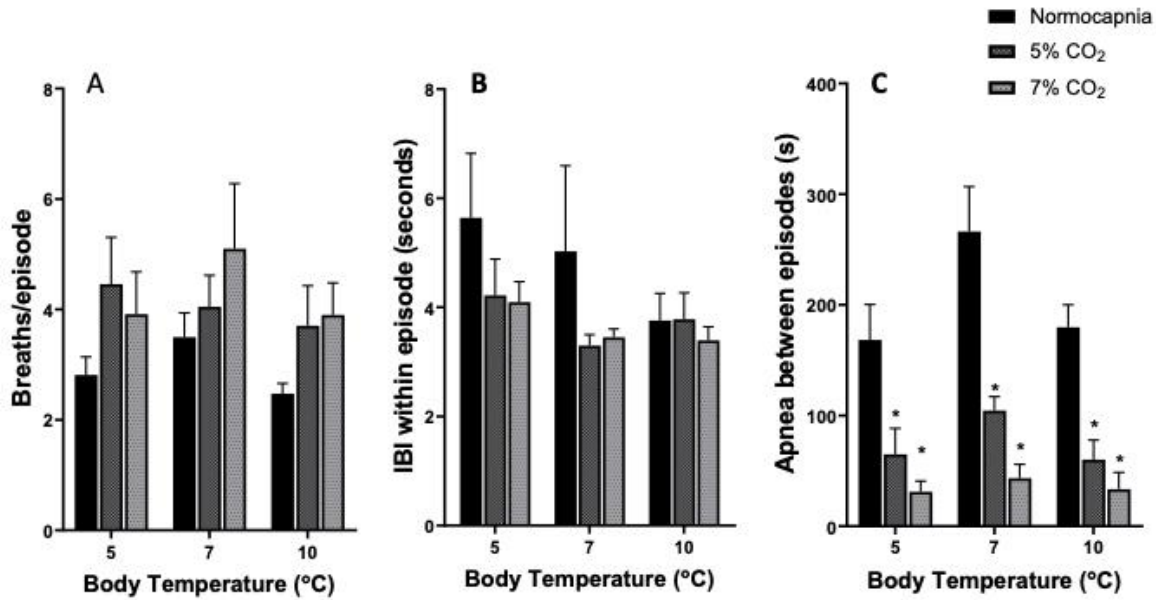


Figure 4.4 Breathing frequency components of episodes at 5, 7, and 10°C in normocapnia (black bars), 5% CO₂ (orange bars), and 7% CO₂ (blue bars). A; breaths/episode, B; inter-breath intervals within episodes, and C; the apneic length between episodes. * denotes significant differences from normocapnia within the same temperature group (two-way ANOVA with Tukey’s post-hoc test; $p < 0.05$). Error bars represent S.E.M.

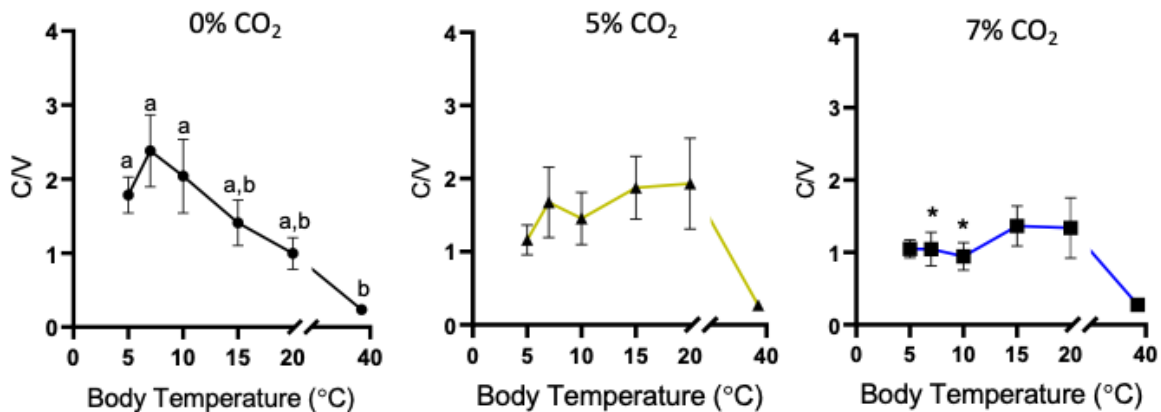


Figure 4.5 Coefficient of variation for all individuals at each steady state temperature breathing air (left), 5% CO₂ (middle), and 7% CO₂ (right). Error bars represent S.E.M and letters indicated significant difference within normocapnia (one-way ANOVA with Tukey’s post-hoc test; $p < 0.05$) and * denotes a significant difference from normocapnia within a temperature group (2-way ANOVA with Tukey’s post-hoc test; $p < 0.05$).

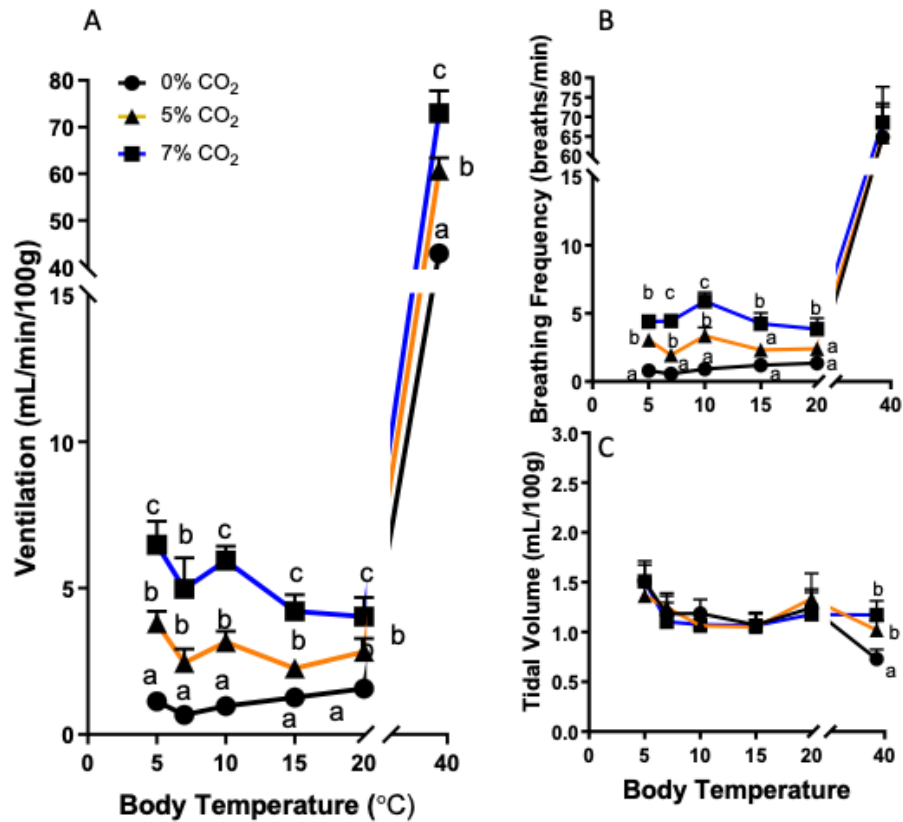


Figure 4.6 Absolute ventilation (mL/min/100g) (A), breathing frequency (breaths/min) (B), and tidal volume (mL/100g) (C) in animals breathing normocapnic gas (black lines) and 5% (orange lines) and 7% (blue lines) CO₂. Error bars represent S.E.M and letters indicate significant differences within each temperature group (two-way ANOVA with Tukey's post hoc test; $p < 0.05$).

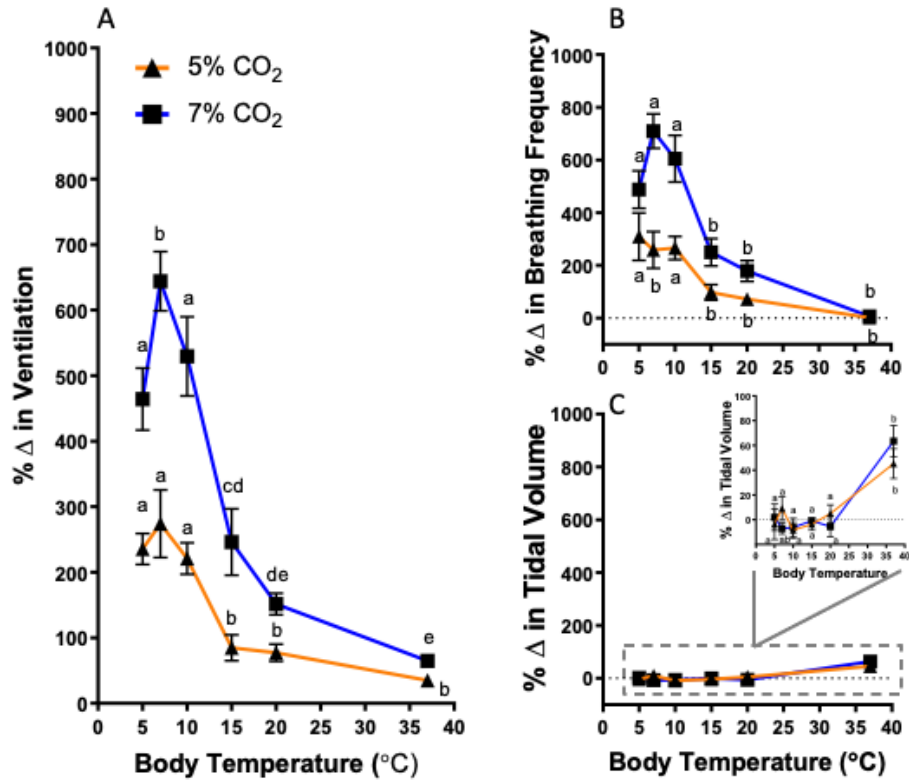


Figure 4.7 Relative changes in ventilation (A), breathing frequency (B) and tidal volume (C) in animals breathing 5% (orange lines) and 7% (blue lines) CO₂. Relative changes were calculated as % change from normocapnia. Error bars represent S.E.M and letters indicate significant differences among temperature groups within each treatment (two-way ANOVA with Tukey's post hoc test; $p < 0.05$).

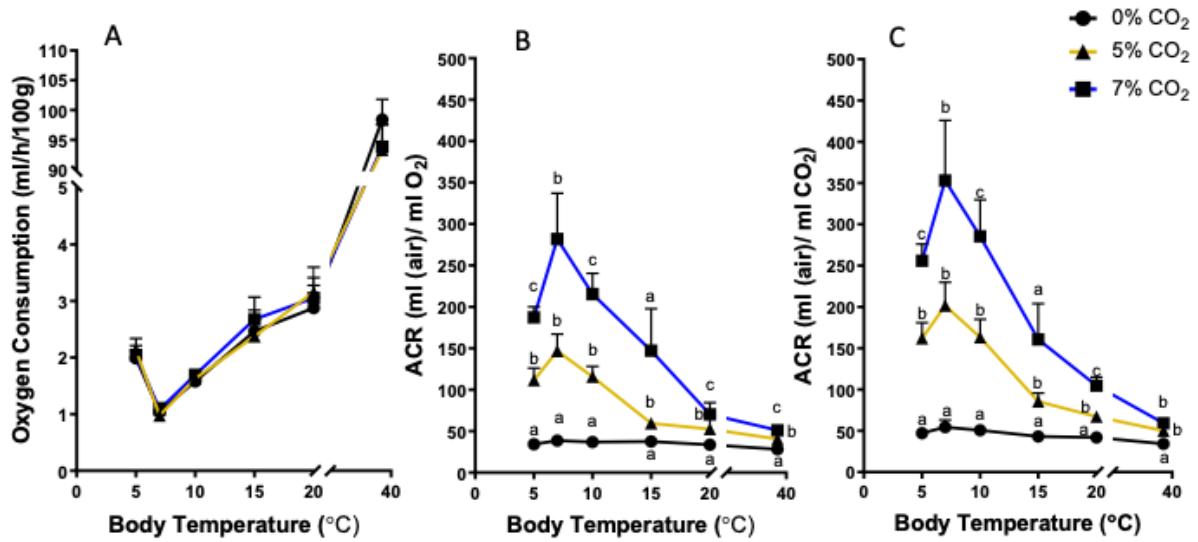


Figure 4.8 Oxygen consumption rate (ml/h/100g (A)) and the air convection requirement (over oxygen consumption rate (B) and CO₂ production rate (C)) in animals breathing air (black lines), 5% (orange lines) and 7% (blue lines) CO₂. Error bars represent S.E.M and letters indicate significant differences within each temperature group (two-way ANOVA with Tukey's post hoc test; p<0.05).

Chapter 5: Changes in CO₂ Sensitivity During Entrance Into, and Arousal from Hibernation in *Ictidomys Tridecemlineatus*

5.1 Summary

Just prior to entrance into hibernation in many mammals, there is a reduction in the respiratory exchange ratio (RER) thought to result in a retention of CO₂ that contributes to the ensuing metabolic suppression. In steady state hibernation the relative hypercapnic ventilatory response (HCVR; the % change in ventilation to CO₂) is elevated. Paradoxically, this suggests a transient decrease in CO₂ sensitivity at the onset of entrance into hibernation, allowing the retention of CO₂, then a subsequent increase in CO₂ sensitivity giving rise to the elevated HCVR in steady state hibernation. We examined the time course of the changes in ventilation, O₂ consumption rates (\dot{V}_{O_2}), CO₂ excretion rates (\dot{V}_{CO_2}), body temperature, and the RER and ACR (air convection ratio, ventilation/ \dot{V}_{O_2}) and the HCVR throughout entrance and arousal into and out of hibernation in 13-lined ground squirrels to confirm this. We observed a significant drop (entrance) and rise (arousal) in the RER produced by hypo- and hyperventilation respectively. CO₂ chemosensitivity was also blunted on entrance into torpor, associated with the reduced RER, and rose at the end of entrance. On arousal CO₂ chemosensitivity was elevated when the RER was elevated and fell immediately after RER returned to normal values. At any given T_b the HCVR was lower during entrance compared to arousal producing a significant hysteresis. The HCVR, however, was the same at any given \dot{V}_{O_2} during entrance and arousal. These data suggest that both the changes in \dot{V}_{O_2} and in the HCVR are associated with changes in central regulation of the effector limbs that establish steady state hibernation.

5.2 Introduction

The present study was designed to investigate two intriguing aspects of respiratory sensitivity to CO₂ in hibernating mammals: an apparent brief transient decrease in CO₂ sensitivity at the onset of entrance into hibernation (Snapp & Heller, 1981; Bickler, 1984; Nestler, 1990) and a subsequent progressive increase in CO₂ sensitivity with decreasing body

temperature in steady state hibernation (Mcarthur and Milsom 1991b; Webb and Milsom 2017; Sprenger and Milsom 2021(submitted)(chapter 4)).

Several studies have documented decreases in the respiratory exchange ratio (RER) at the very onset of entrance into hibernation and increases in the RER at the initiation of arousal (Snapp and Heller 1981; Bickler 1984; Malan 1988; Nestler 1990). The decrease in the RER during entrance is thought to result in CO₂ retention, and this has been hypothesized to produce a respiratory acidosis that contributes to the initial decrease in metabolic rate (Snapp & Heller, 1981; Bickler, 1984; Malan, 1988; Nestler, 1990). The transient rise in the RER at the onset of arousal is hypothesized to produce a respiratory alkalosis that removes this metabolic inhibition. These transient changes in RER suggest that there are transient changes in respiratory sensitivity to CO₂ altering the regulated arterial CO₂ partial pressure (PaCO₂) and allowing the retention/excretion of CO₂ at the onset of entrance/arousal leading to hypoventilation at the onset of entrance and hyperventilation at the onset of arousal. These changes occur at a constant body temperature (T_b) and metabolic rate (as reflected by the oxygen consumption rate, \dot{V}_{O_2}) and thus appear to be associated with the initiation of the change in state (euthermic versus hibernation) and not a reduction in T_b. The first goal of the present study was to confirm that these changes in the RER were due to hypo and hyperventilation by examining the relationship between changes in ventilation and changes in the RER at the onset of entrance into and arousal from hibernation in the 13-lined ground squirrel.

During entrance into hibernation, body temperature (T_b), oxygen consumption rate (\dot{V}_{O_2}), and ventilation (\dot{V}_E) fall dramatically (Lyman, 1958*b*; Barnes, 1989; Buck & Barnes, 2000; Carey *et al.*, 2003). In steady state hibernation at body temperatures of ~5°C, these variables fall by about 98% from euthermic values. Although ventilation (\dot{V}_E) is greatly reduced in torpid ground squirrels, paradoxically, their relative ventilatory response ($\% \Delta \dot{V}_E$) to CO₂ increases. Recently, based on results from hypothermic ground squirrels where CO₂ sensitivity was not reduced (Zimmer and Milsom, 2002a) we hypothesized that this switch in apparent ventilatory sensitivity to CO₂ in hibernation was the result of the change in state (from active to torpid) and not due to the change in core T_b, and would thus be present at all steady state hibernation temperatures. However, we found progressive increases in the hypercapnic ventilatory response (HCVR) with decreasing T_b in hibernation. We also obtained data to suggest that state may be T_b

dependent making it difficult to discern between the underlying roles of changes in T_b versus state (Sprenger and Milsom 2021(submitted)(chapter 4)).

This previous study was performed on animals in steady state hibernation at different ambient temperatures. The reductions in T_b , \dot{V}_{O_2} , and \dot{V}_E during entrance into hibernation occur over a period of ~10-20 hours and reverse on arousal from hibernation in as little as 1-2 hours (Lyman & Chatfield, 1950). The fall in T_b lags behind the fall in \dot{V}_{O_2} and \dot{V}_E during entrance and the rise in T_b also lags behind the rise in \dot{V}_{O_2} and \dot{V}_E during arousal (Lyman, 1958b; Nestler, 1990; Milsom & Jackson, 2011). This results in a notable hysteresis in the relationship between T_b , and metabolic rate and \dot{V}_E . The second goal of the present study was to exploit this hysteresis to examine the extent to which changes in the HCVR are associated with changes in T_b , versus \dot{V}_{O_2} during entrance and arousal. Assuming that the changes in \dot{V}_{O_2} and \dot{V}_E (which are the first signs of entrance) reflect the initiation of the change in state this would allow us to discriminate between the effects of changes in T_b versus changes in state in producing the change in the HCVR. We hypothesized a period of CO_2 insensitivity just prior to entrance into hibernation that would give way to an elevated HCVR at the end of entrance, and the elevated HCVR would rise as metabolic rate fell (and thus state shifts to hibernation).

5.3 Methods

5.3.1 Animals

All procedures were conducted under a protocol approved by the UBC Animal Care Committee and complied with the policies of the Canadian Council on Animal Care. 13-lined ground squirrels (*Ictidomys tridecemlineatus*) were trapped in Carman, MB, Canada (49°30'N, 98°01'W) and transferred to an animal care facility at the University of British Columbia. Squirrels were trapped with the approval of Manitoba Conservation and Water Stewardship, under wildlife scientific permit WB15027. Wild caught squirrels were treated with Ivermectin and Droncit for endoparasites (0.4 mg/kg, subcutaneous), and flea spray for ectoparasites immediately after capture. Squirrels were provided water and IAMS small chunk dog chow supplemented with apples and peanuts *ad libitum* during the active period. No food or water were provided during the hibernation period. All active animals were kept in a temperature-

controlled chamber ($20 \pm 2^\circ\text{C}$) on a photoperiod that matched the daily photoperiod in Vancouver, British Columbia, Canada and all hibernating animals were kept at ($5 \pm 2^\circ\text{C}$) in the dark.

5.3.2 *Measurement of Temperature*

Two complimentary systems were used to continuously measure chamber temperature. A thermal probe connected to a physitemp (BAT-12, Physitemp, Clifton, NJ) was used in conjunction with a scannable RFID temperature chip (ITPP-300 extended calibration) that was read with a DAS-8017 programable reader (Biomedic data systems, Seaford, DE). The thermal probe was situated just over the experimental animal box, and the scannable chip was secured on the experimental animal box. The two systems read comparably.

Intraperitoneal body temperature was measured with one of two systems. The first system used implantable RFID temperature chips (ITPP-300 extended calibration) read with a DAS-8017 reader (Biomedic data systems). The second system used wireless real-time telemeters ((CTA-F40) and (TA-F40); Data sciences international, St. Paul, MN). The telemeters were read with an MX2 and physiotel connect system continuously during measurement. To ensure comparable measurement, some animals were co-implanted with both systems.

5.3.3 *Measurement of Ventilation and Oxygen Consumption*

Ventilatory and metabolic variables were continuously measured using flow through whole-body plethysmography (Drorbaugh & Fenn, 1955*b*; Malan, 1973; Jacky, 1978; Sprenger *et al.*, 2019 (chapter 2)). Two identical plexiglass boxes (one recording and one reference) were placed in a small temperature-controlled cooling chamber ($\pm 1^\circ\text{C}$) and fitted with temperature measurement systems (see measurement of temperature). Animals were placed in the recording chamber with bedding and allowed to move freely. Excess volume in the recording chamber was kept to a minimum while allowing the animal enough space to build a small nest for hibernation. Dried air was flushed through the chambers equally (at a flow rate large enough to maintain $\text{CO}_2 < 1\%$), which allowed for pressure changes from the recording chamber due to the addition of heat and water vapor during inhalation measured with a pressure transducer (Validyne model DP103-18 amplified with a Gould DC amplifier (Gould; Valley View, Ohio)). Accurate recordings were obtained as long as there was a minimum body temperature to ambient

temperature differential ($T_b - T_{am}$) of 4°C. Incurrent and excurrent gas composition was measured with a field metabolic system (FMS; Sable systems). The system was calibrated before the start of each measurement from pre-mixed tanks (Praxair; 0%, 5%, 7% CO₂ with 21% O₂ balanced in N₂). Volume was calibrated before each measurement using volumes comparable to the animal's tidal volume injected at a rate comparable to the animal's breathing frequency (~1 breath/min in hibernation and ~60 breaths/min when active).

5.3.4 Experimental Protocol

Active animals were moved to the recording chamber that was then placed in the temperature-controlled unit at $5 \pm 1^\circ\text{C}$. Animals were allowed to move freely and usually entered hibernation within 48 hours. Flow rate through the chamber was maintained at 800ml/min. Body temperature, \dot{V}_{O_2} , and \dot{V}_E were monitored continually. One group of animals (control) breathed room air (21% O₂ balanced in N₂) for the duration of entrance. In two other groups, the gas flow through the chamber was switched to either 5 or 7% CO₂ at a flow rate of 150ml/min once there was an indication that the animals were about to enter hibernation (a slowing of ventilation accompanied by a fall in oxygen consumption (\dot{V}_{O_2}) of greater than 1ml/min below resting values.). This was maintained throughout entrance which was determined to be complete once T_b had stabilized at close to ambient levels. Animals weren't aroused until at least 24 hours after entrance was completed. During this period normocapnic air (21% O₂ balanced in N₂) was administered to all animals. Given that natural arousals are difficult to predict with hibernation bouts lasting 3-21 days, animals in the present study were artificially aroused (recording chamber shaken) and hypercapnia (5% or 7% CO₂ in 21% O₂ balanced with N₂) was administered for the duration of the arousal. The same variables were continuously measured as in entrance.

5.3.5 Data Analysis

Normocapnic traces were analyzed in 5-minute increments (entrance) and 2-minute increments (arousal) for oxygen consumption (\dot{V}_{O_2}), CO₂ production (\dot{V}_{CO_2}), breathing frequency (f_R), tidal volume (V_T) and body temperature (T_b) for the duration of the entrance or arousal. Hypercapnic traces were analyzed when T_b was 35, 30, 25, 20, 15, 10, and 7°C during entrance and arousal. The time at which each of these temperatures occurred was recorded as well. \dot{V}_E was calculated by multiplying V_T and f_R . V_T was calculated as described in Sprenger et al., 2019

(chapter 2). The air convection requirement (ACR) was calculated by dividing \dot{V}_E by \dot{V}_{O_2} . The respiratory exchange ratio was calculated by dividing \dot{V}_{CO_2} by \dot{V}_{O_2} . \dot{V}_{O_2} was calculated as described in Sprenger et al., 2019 (chapter 2). \dot{V}_{CO_2} was calculated using the following equation (Lighton, 2008):

$$\dot{V}_{CO_2} = FR \frac{(1 - F_{iO_2} - F_{iCO_2})}{(1 - F_{eO_2} - F_{eCO_2})} \{F_{eCO_2} - F_{iCO_2}\}$$

where FR is flow rate, F_{iO_2} is fractional inspired oxygen, F_{eO_2} is fractional expired oxygen, F_{iCO_2} is fractional inspired CO₂, and F_{eCO_2} is the fractional expired CO₂. Q_{10} values were calculated for each 5°C increment on entrance and arousal with the addition of the 7-10°C increment. The Q_{10} for entire range of temperatures was also taken for entrance and arousal. % O₂ extraction was calculated by dividing 100 by the product of the ACR multiplied by the fractional inspired O₂. Body mass was taken at the end of the arousal exposure.

5.3.6 Statistical Analysis

One-way repeated measures ANOVAs were used to determine whether \dot{V}_E , \dot{V}_{O_2} , RER, and ACR had changed from the initial point during entrance and arousal in normocapnia air (compared to the first point within measurement). If significance was found, a Dunnett's post-hoc test was used to determine which time points were significantly different ($0 < 0.05$). T-tests were used to determine when the percent change in ventilation became significantly different over time during entrance and arousal. The initial time point (baseline) was compared to all subsequent time points ($p < 0.05$). Adjusted p-values were used to account for multiple comparisons for the t-tests. Two-way ANOVAs were used to determine if the percent change in ventilation and the ACR differed at any given T_b or oxygen consumption between entering and arousing animals. Only T_b or oxygen consumption points that overlapped between entrance and arousal were used for this analysis. A separate two-way ANOVA was used to determine if oxygen consumption was affected at any timepoint by the addition of CO₂. If significance was found in any two-way ANOVA, a tukey's post-hoc test was used ($P < 0.05$) for multiple comparisons. All statistics were run using Graphpad Prism (9.0.0121) statistical program.

5.4 Results

5.4.1 Normocapnia

5.4.1.1 Entrance

Entrance into hibernation was accompanied by large reductions in \dot{V}_E , \dot{V}_{O_2} and T_b , (fig. 5.1). On average it took 10-12 hours for T_b to reach its minimum value of $\sim 10^\circ\text{C}$ from a starting value of 35°C (a drop of 25°C). \dot{V}_E and \dot{V}_{O_2} fell quickly reaching their minimum values after ~ 8 hours (fig. 5.1). Both reached half of their total drop within the first 1.5 hours of entrance (fig. 5.1). The first significant drop in \dot{V}_E occurred at the 80-minute mark falling to 112.2 ± 10 ml/min from a starting value of 155.19 ± 7.42 ml/min ($p < 0.05$) (fig. 5.1). The first significant drop in \dot{V}_{O_2} was from a starting value of 6.06 ± 0.21 ml/min to 4.42 ± 0.13 ml/min ($p < 0.05$) which occurred at the 130-minute mark (fig. 5.1). T_b initially started to drop at the ~ 140 -minute mark (fig. 5.1) and took 30 minutes to fall 1 degree and another 3 hours after this to reach half of the total 25°C fall (fig. 5.1).

The net result of the disconnect between \dot{V}_E and \dot{V}_{O_2} was a significant reduction in the ACR between 80-140 minutes where the ACR fell as low as 15.31 from a starting ACR of 25.94 ($p < 0.05$) (fig. 5.1). This appears to be due to a reduction in breathing frequency while tidal volume remained unchanged (fig. 5.10). After this, the fall in \dot{V}_{O_2} was quicker than the fall in \dot{V}_E and the ACR began to slowly rise above the starting value and becoming increasingly more variable (fig. 5.1). By the end of entrance, the ACR ranged between 35-45 (fig. 5.1).

5.4.1.2 Arousal

Arousal from hibernation was associated with rapid increases in \dot{V}_E , \dot{V}_{O_2} and T_b (fig. 5.2). On average it took ~ 90 minutes for animals to reach their euthermic active T_b (fig. 5.2). The T_b prior to arousal initiation was on average 8.5°C and animals reached 10°C within 10 minutes after being aroused (arousal initiation was at 10 minutes in fig. 5.2). Both \dot{V}_E and \dot{V}_{O_2} peaked between 55-60 minutes after the onset of arousal before falling to their euthermic active values at approximately the same time that T_b reached its maximum ($\sim 36^\circ\text{C}$) (fig. 5.2). The peak of this overshoot in \dot{V}_E and \dot{V}_{O_2} occurred when T_b was between 25 and 30°C (fig. 5.2).

\dot{V}_E and \dot{V}_{O_2} rose significantly from their starting values in hibernation within 2 minutes of the onset of arousal ($p < 0.05$) (fig. 5.2). \dot{V}_{O_2} tripled from 0.11 ± 0.01 ml/min to 0.36 ± 0.01 within the first 4 minutes of arousal ($p < 0.05$) (fig. 5.2). \dot{V}_E also rose dramatically over the first few minutes of arousal, starting at 3.57 ± 0.4 ml/min and rising to 19.34 ± 2.95 ml/min within 4 minutes. During this period T_b increased by 1°C .

\dot{V}_E rose more rapidly than \dot{V}_{O_2} during the start of arousal (fig. 5.2) and, thus, the ACR spiked at this time (fig. 5.2). The ACR rose significantly to 71.59 ± 3.86 within minutes after the onset of arousal ($p < 0.05$) (fig. 5.2). The rise in ACR was due to an initial spike in tidal volume with breathing frequency rising shortly thereafter (fig. 5.11). After this the ACR slowly fell reaching its minimum values between 50-75 minutes after the onset of arousal. This was significantly lower than the starting ACR value ($p < 0.05$) (fig. 5.2). By the end of arousal, the ACR had risen to ~ 25 (fig. 5.2).

5.4.1.3 RER and Gas Exchange

During entrance into hibernation, the RER also fell significantly to a minimum value of 0.64 at ~ 100 minutes from a starting value of 0.75 ($p < 0.05$) (fig. 5.3). The RER quickly stabilized and thus the drop in RER lasted only about 40 minutes just prior to \dot{V}_{O_2} falling significantly ($p < 0.05$) (fig. 5.3a). After this, the RER fluctuated around 0.8 for the remainder of the entrance period (fig. 5.3). Conversely, at the onset of arousal, the RER rose significantly to a maximum value of 1.16 ± 0.02 from a starting value of 0.78 ± 0.026 and remained elevated for ~ 10 minutes ($p < 0.05$) (fig. 5.4). After this the RER stabilized at a value of ~ 0.75 for the rest of the arousal period (fig. 5.4). While the changes in the RER accompany the changes in the ACR, during entrance they began later, and in both entrance and arousal, were of shorter duration.

The time course of the changes in \dot{V}_{O_2} , \dot{V}_{CO_2} , and hence the RER along with the changes in the ACR are complex. Elvert and Heldmaier (2005) divided entrance into hibernation in dormice into four phases and we use their classification system here (fig. 5.3). Phase I is the period preceding entrance (Phase I in fig. 5.3) At the onset of entrance into hibernation, there is a brief rise in both \dot{V}_{O_2} and \dot{V}_{CO_2} during which the RER is relatively constant but the ACR has begun to fall due to the fall in \dot{V}_E (Phase II, fig. 5.3). Then \dot{V}_{CO_2} falls more rapidly than \dot{V}_{O_2} leading to the fall in the RER (Phase IIIa, fig. 5.3). This differential reflects a rise in pulmonary

O₂ extraction (% O₂ extraction doubled from ~19% to ~37% (fig. 5.3)) maintaining \dot{V}_{O_2} while \dot{V}_{CO_2} falls. Following this \dot{V}_{O_2} falls more rapidly than \dot{V}_{CO_2} leading to the secondary rise in the RER and then subsequent reductions in both mirror each other maintaining an RER of ~0.8 for the remainder of entrance (Phase 3b, fig. 5.3).

The reverse occurs on arousal (fig. 5.4). When the animal begins to arouse, the ACR increases due to the rise in \dot{V}_E while the \dot{V}_{O_2} is relatively constant. The RER also begins to rise as \dot{V}_{CO_2} rises more rapidly than \dot{V}_{O_2} (not visible in fig. 5.4 due to scaling). This differential is a result of the rise in \dot{V}_E . This is accompanied by a fall in pulmonary O₂ extraction (% O₂ extraction fell from ~17% to 7-8% (fig. 5.4)). Following this pulmonary O₂ extraction returned to normal levels (~19% (fig. 5.4)) and \dot{V}_{O_2} rose more rapidly than \dot{V}_{CO_2} leading to the return of the RER to a value of ~0.75 where it remained for the rest of the arousal period (fig. 5.4).

5.4.1.4 Correlations Between Changes in \dot{V}_E , \dot{V}_{O_2} , and T_b

Over the entire entrance the Q₁₀ for \dot{V}_{O_2} was 5.03 (Table 5.1). The Q₁₀ for \dot{V}_{O_2} was as high as 7.7 during the initial phase of entrance (35-30°C) and decreased as temperature fell further throughout entrance (Table 5.1). For \dot{V}_E , the Q₁₀ remained between 2-3 until entrance was close to complete (35-15°C), but then rose substantially at the end of entrance (Table 5.1). The Q₁₀ value for \dot{V}_{O_2} over the entire arousal was 4.6 with the value for the first half of the arousal (7-15°C) being significantly greater (Table 5.1). \dot{V}_E followed a very similar trend to \dot{V}_{O_2} where at the initiation of arousal, the Q₁₀ was high but fell as the arousal progressed and was below 1 after T_b had risen to 25°C (Table 5.1). The overall Q₁₀ for \dot{V}_E on arousal was 4.4 (Table 5.1).

5.4.2 Effects of Hypercapnia on the Rate of Entrance and Arousal

5.4.2.1 Entrance

The addition of CO₂ to the respiratory gas flow during entrance resulted in a quicker initial reduction \dot{V}_{O_2} (fig. 5.5a and c, fig. 5.6). The \dot{V}_{O_2} was significantly lower in hypercapnia (p<0.05) for the first 80 minutes while breathing 5% CO₂ and from 20 minutes to 170 minutes while breathing 7% CO₂ (fig. 5.5a and c, fig. 5.6). While hypercapnic animals reached their minimum \dot{V}_{O_2} on average 40 minutes before normocapnic animals (Table 5.2), in all cases \dot{V}_{O_2} ultimately fell to the same level (fig. 5.5a, fig. 5.6). The rate of fall in body temperature was slightly, but not significantly faster in hypercapnia.

5.4.2.2 *Arousal*

At the onset of arousal, \dot{V}_{O_2} rose only slightly slower in hypercapnic animals than in normocapnic animals ($p>0.05$). However, the peak \dot{V}_{O_2} at the end of arousal was significantly lower in hypercapnic animals ($p<0.05$) (fig. 5.5b and d, fig. 5.6). Peak values were ~ 11 ml/min in hypercapnic animals while normocapnic animals averaged ~ 14 ml/min during this period (fig. 5.5b). At the end of arousal \dot{V}_{O_2} did not differ between groups (figs. 5.5, 5.6). Animals in normocapnia aroused on average in ~ 86 minutes where hypercapnic animals aroused in ~ 87 and 83 minutes (5% and 7% respectively) (fig. 5.5, Table 5.2). The rate of rise in body temperature was unaffected by hypercapnia.

5.4.3 *Progressive Changes in the Hypercapnic Ventilatory Response*

5.4.3.1 *The Change in the HCVR During Entrance and Arousal*

The magnitude of the HCVR ($\% \Delta \dot{V}_E$) to 5% and 7% hypercapnia changed progressively during both entrance and arousal (figs. 5.7, 5.8). The HCVR to both 5% and 7% fell initially during entrance (first 60 and 110 minutes in fig 5.6, 5.7) and then progressively increased becoming significantly larger than the starting responses after the 6- and 5-hour mark during entrance while breathing 5 and 7% CO_2 respectively at which time T_b was $\sim 16^\circ C$ in each case ($p<0.05$) (fig. 5.7a and c). The ACR in normocapnic animals initially fell and then slowly increased as described earlier (figs. 5.1 and 5.8). Due to both the initial reduction in \dot{V}_{O_2} and increase in \dot{V}_E in animals breathing CO_2 , the ACR was elevated under hypercapnic conditions leading into hibernation. As the animals entered hibernation, however, the effect of CO_2 on all variables (\dot{V}_{O_2} , \dot{V}_E and ACR) initially dissipated (50–230 min in fig. 5.8). As hibernation progressed, however, the HCVR progressively increased as did the ACR (>290 min in fig. 5.8). The ventilatory response to 5% CO_2 peaked at an increase of 328% from baseline while the ventilatory response to 7% CO_2 peaked at an increase of 579% (fig. 5.7 a, c). Both peaks occurred towards the end of entrance at which time \dot{V}_{O_2} had already reached its minimum (fig. 5.7a, and c; fig. 5.6).

At the initiation of arousal, the $\% \Delta$ in \dot{V}_E rose initially in animals breathing 5% CO_2 but not 7% CO_2 (fig. 5.7b and d). As arousal progressed the HCVR to both 5% and 7% hypercapnia fell progressively ($p<0.05$) (fig. 5.6b and d; fig. 5.8). The HCVR fell below euthermic levels 50 -

70 minutes after the start of arousal at which point T_b had risen to $\sim 25^\circ\text{C}$ ($P < 0.05$) (fig. 5.7b and d, fig. 5.8). It then rose to euthermic values again at the end of arousal. The \dot{V}_{O_2} was initially reduced in the animals breathing CO_2 and \dot{V}_E was elevated and hence the ACR was also initially elevated. Again, the effect of CO_2 on all variables (\dot{V}_{O_2} , \dot{V}_E and ACR) dissipated throughout arousal.

5.4.3.2 Correlations Between Changes in \dot{V}_E , \dot{V}_{O_2} , and T_b

The correlation between the $\% \Delta$ in \dot{V}_E and the \dot{V}_{O_2} in animals breathing both 5% and 7% CO_2 was not significantly different between animals entering or arousing from hibernation ($p > 0.05$) (fig. 5.9a and b). The $\% \Delta$ in \dot{V}_E increased progressively with decreasing \dot{V}_{O_2} on entrance and decreased with increasing \dot{V}_{O_2} on arousal (fig. 5.9). At any given body temperature, however, the HCVR was significantly greater during entrance than arousal ($p < 0.05$) (fig. 5.9c and d).

5.5 Discussion

The present study was designed to determine whether the brief transient decrease in the RER in animals entering hibernation was associated with hypoventilation leading to CO_2 retention (Snapp & Heller, 1981; Bickler, 1984; Nestler, 1990) and whether the subsequent progressive increase in CO_2 sensitivity with decreasing body temperature in steady state hibernation was a result of changes in body temperature or in activity state (i.e. euthermia versus hibernation). Our results confirm that in the 13-lined ground squirrel 1) at the onset of entrance there is a clear drop in the RER as CO_2 excretion falls while O_2 consumption is maintained. This is associated with hypoventilation producing a drop in the ACR as \dot{V}_E falls before \dot{V}_{O_2} and is combined with an increase in pulmonary O_2 extraction. The reverse happens on arousal. 2) Exposure to hypercapnia speeds the drop in \dot{V}_{O_2} during entrance but has no significant effect on the timing of arousal. 3) The relative change in the HCVR is reduced early in entrance, enhanced late in entrance, and dissipates early in arousal. The changes in the HCVR appear to coincide with 1) a period of CO_2 retention at the start of entrance into hibernation (reduced), and 2) a period of CO_2 expulsion just prior to the start of arousal (enhanced). During these state changes,

the HCVR appears to be more closely tied to changes in metabolic rate (and thus state) than to changes in body temperature. The implications of these findings are discussed below.

5.5.1 *Onset of Entrance and Arousal: Changes in the RER, ACR, and \dot{V}*

Elvert and Heldmaier (2005) divided entrance into torpor in dormice into four phases. Phase I was the period of slow wave sleep prior to entrance into torpor (Heller 1979). Phase II was described as a phase of pre-torpor adjustments during which \dot{V}_{O_2} , fH and fV all suddenly increased in the dormice. Similar increases in metabolic rate prior to entrance into hibernation have also been observed in other hibernating mammals (pocket mice (*Perognathus longimembris*, Withers, 1977), Djungarian hamster (*Phodopus sungorus*, Heldmaier *et al.*, 1999) and alpine marmots (*Marmota marmota*, Ortmann and Heldmaier, 2000)). It was postulated that these increases were associated with the molecular or endocrinological changes that initiate entrance (Elvert and Heldmaier, 2005). In the present study we see similar increases in \dot{V}_{O_2} and \dot{V}_{CO_2} in this phase but not in ventilation (fig. 5.1 and 5.3).

Phase III was when the animals actually entered torpor. Dormice entering this phase rapidly depressed their metabolic rate, heart rate and ventilation rate. While these fell simultaneously in dormice, in other species \dot{V}_E has been reported to fall before \dot{V}_{O_2} resulting in a fall in the ACR (Musacchia & Volkert, 1971; Malan *et al.*, 1973; Snapp & Heller, 1981; Bickler, 1984; Geiser, 1988; Elvert & Heldmaier, 2000). Body temperature was also depressed but this occurred at a much slower rate. Transient decreases in the RER have also been reported to occur during this phase in several other species (Snapp and Heller, 1981; Bickler, 1984; Malan, 1986; Nestler, 1990). It has been hypothesized that the fall in the RER reflects CO_2 retention in body fluids and contributes to the initial inhibition of thermoregulation, glycolysis, neural activity, and brown fat thermogenesis (Malan *et al.*, 1973; Malan 1982, 1986, 1988, Bharna and Milsom 1993).

It has also been suggested that the transient fall in the RER is due to the fall in the ACR reflecting a transient period of hypoventilation. As noted above, ventilation does fall before metabolic rate in many species on entrance and this will reduce CO_2 excretion if a constant metabolic rate is maintained (both CO_2 production and O_2 consumption). This, however, requires that \dot{V}_E/\dot{V}_{O_2} must fall while \dot{V}_E/\dot{V}_{CO_2} does not; i.e. CO_2 excretion must be reduced while O_2

consumption is not. This cannot be explained by hypoventilation alone. There should also be simultaneous and transient falls in both the ACR and the RER (the ratio of $\dot{V}_{CO_2}/\dot{V}_{O_2}$). This was not the case in the studies of the dormice by Elvert and Heldmaier (2000,2004), while Nestler (1990) did not measure ventilation in the deer mice, and Bickler reported decreases in \dot{V}_E/\dot{M}_{CO_2} in round tailed ground squirrels (1984). While the latter would lead to CO_2 retention, Bickler's measures were of \dot{V}_{CO_2} and not \dot{M}_{CO_2} . Given these discrepancies, one of the goals of the present study was to closely examine the temporal relations between the changes in \dot{V}_{O_2} , \dot{V}_{CO_2} , \dot{V}_E , and hence the ACR and RER, as well as in pulmonary O_2 extraction and T_b in phase III as 13-lined ground squirrels entered hibernation.

At the onset of entrance into hibernation (the start of phase III), 13-lined ground squirrels in the present study reduced their \dot{V}_E prior to any noticeable reduction in \dot{V}_{O_2} . This resulted in a significant drop in the ACR. This was due exclusively to a reduction in breathing frequency. Respiratory tidal volume was unchanged as has also been reported in other species during hibernation (McArthur & Milsom, 1991a; Webb & Milsom, 2017). While there was a fall in \dot{V}_{CO_2} associated with the reduction in \dot{V}_E indicative of hypoventilation, \dot{V}_{O_2} remained constant producing a fall in the RER (0.64 minimum). Given the close association of these changes in the RER, and the fall in ventilation and the ACR, it seems safe to assume that they led to CO_2 retention although blood gases would be needed to confirm this. That \dot{V}_{O_2} was not affected by the hypoventilation is explained by an increase in calculated pulmonary oxygen extraction. What underlies the increase in pulmonary O_2 extraction, at the same time that CO_2 is being retained, is not clear but one possible explanation is an increase in blood O_2 carrying capacity.

The reductions in \dot{V}_E and \dot{V}_{CO_2} are followed by the rapid reduction in \dot{V}_{O_2} and slow fall in T_b , that are the hallmark of entrance into hibernation (Lyman 1958; Elvert and Heldmaier 2000). The Q_{10} value from the present study for the initial fall in \dot{V}_{O_2} early in entrance (35°C-30°C) was 7.76 consistent with a temperature-independent suppression of metabolism (Snapp & Heller, 1981; Bickler, 1984; Geiser, 1988; Nestler, 1990; Ortmann & Heldmaier, 2000; Elvert & Heldmaier, 2005).

As the 13-lined ground squirrels progressed into steady-state hibernation the RER returned to normal as did the ACR before slowly increasing and becoming highly variable as \dot{V}_{O_2}

now fell faster than \dot{V}_E . The Q_{10} was reduced to 3.3-3.2 suggesting a switch to a more temperature-dependent depression of metabolic rate. This is consistent with the observations of others (Lyman 1958; Heldmaier et al., 1993; Ortmann and Heldmaier 2000; Heldmaier and Elvert 2004; Heldmaier et al. 2004; Milsom and Jackson 2011) who have suggested that as T_b falls, the Q_{10} effects of temperature becomes predominant and the final depression of metabolic rate is due to a synergistic action of temperature effects and metabolic inhibition.

At the onset of arousal, we saw the reverse sequence of events in the 13-lined ground squirrels. They increased their \dot{V}_E prior to any noticeable increase in \dot{V}_{O_2} resulting in a significant transient increase in the ACR. This hyperventilation was initially due to increases in respiratory tidal volume followed shortly by increases in breathing frequency. During the spike in the ACR, there was also a large transient increase in the RER (to 1.16 maximum) indicating that CO_2 excretion rose faster than O_2 consumption. Several large deep breaths were observed initially in the present study, as well as previous studies (Malan *et al.*, 1973; Snapp & Heller, 1981) and it is likely that the deep breaths serve as a method of enhanced CO_2 expulsion. It is thought that this expulsion is needed to correct the depressive effect of acidosis on metabolism, (Nestler, 1990). The Q_{10} data from the present study are consistent with data from previous studies indicating that the initial metabolic increase is temperature independent (Lyman 1958; Heldmaier et al., 1993; Ortmann and Heldmaier 2000; Heldmaier and Elvert 2004; Heldmaier et al. 2004) From $7^\circ C$ - $15^\circ C$ the Q_{10} for \dot{V}_{O_2} was extremely high. As arousal progressed there was a period of seemingly temperature dependent rises in metabolic rate (15 - $25^\circ C$), but after this \dot{V}_{O_2} peaked and fell prior to T_b reaching its active, euthermic level. The initial increase in ventilation was not accompanied by any significant increase in oxygen consumption rate resulting in a transient decrease in pulmonary O_2 extraction. Shortly after this, \dot{V}_{O_2} increased as did T_b .

Whether the initial CO_2 retention on entrance directly inhibits general metabolism, (Malan *et al.*, 1985) or indirectly inhibits metabolism by altering central integrative processes that contribute to metabolic suppression (Snapp & Heller, 1981), and whether CO_2 expulsion at the onset of arousal removes inhibition, is still debated (Snapp and Heller 1981; Bickler 1984; Nestler 1990; Elvert and Heldmaier 2000, 2005; Milsom and Jackson, 2011). The data from the present study are consistent with a definitive period of CO_2 retention just prior to entrance into hibernation that coincides with the initiation of the temperature-independent metabolic

inhibition, and of CO₂ release at the onset of arousal coincident with the initiation of the temperature-independent metabolic increase.

Regardless, these transient changes in the RER, the transient hypoventilation and the sustained CO₂ retention also suggest that there has been an increase in the regulated level of arterial PCO₂. Whether this occurs as a result of changes in CO₂ chemosensing, or in the central integration of chemoreceptor input remains to be determined. The reverse of this at the onset of arousal suggests that this process is rapid. These shifts in the regulated level of PCO₂ are also temperature independent as both changes occur before there are changes in body temperature. For \dot{V}_{CO_2} to fall so that internal CO₂ can accumulate also suggests there has been a decrease in CO₂ sensitivity (see below).

5.5.2 Effects of Hypercapnia on the Rate of Entrance and Arousal

Giving animals CO₂ to breathe during entrance significantly sped the rate at which \dot{V}_{O_2} fell. Additionally, animals breathing hypercapnic gases (5% and 7%) reached their minimum metabolic rates on average 40 minutes faster than animals breathing air. These results are similar to those from previous studies in which hypercapnia and hypoxia also facilitated entry into hibernation by appearing to suppress metabolism (Studier & Baca, 1968; Williams & Rausch, 1973; Schaefer & Wünnenberg, 1976; Kuhnen *et al.*, 1983). However, there are studies in pocket mice and golden-mantled ground squirrels where hypercapnia neither induced nor facilitated entrance into hibernation (Withers, 1977; Webb & Milsom, 1994). While the protocol from the current study did not permit observation of whether hypercapnia induced hibernation, hypercapnia did appear to facilitate the reduction in metabolic rate. The largest effect of hypercapnia on \dot{V}_{O_2} was early during entrance during the period when the ACR, CO₂ excretion, and the HCVR were reduced.

Unlike entrance, the addition of hypercapnia during arousal, had little effect on the rate of increase in \dot{V}_{O_2} . Hypercapnic animals did exhibit a significantly lower peak in \dot{V}_{O_2} compared to normocapnic animals. Thus, hypercapnia did not prolong arousal nor hibernation in the present study and has even been reported to induce arousal in golden-mantled ground squirrels (McArthur & Milsom, 1991a; Harris & Milsom, 1993). Overall, a role of CO₂ accumulation in metabolic suppression appears to be most prevalent during early entrance.

5.5.3 *Progressive Changes in the Hypercapnic Ventilatory Response*

The relative HCVR (% increase in \dot{V}_E) during the early stages of entrance (50-230 min in figs. 5.7, 5.8) was reduced compared to animals prior to entrance. Ventilation during the first 50 minutes was only changed by ~0% and 40% in animals breathing 5% and 7% CO₂, compared to ~33% and 60% respectively in animals prior to hibernation (Sprenger and Milsom 2021(submitted) (chapter 4)). The relative HCVR remained depressed for the first 4 hours coinciding with the period during which the ACR and the RER were transiently reduced. The magnitude of the HCVR then slowly increased with the largest increase occurring between four and eight hours into entrance at a time when \dot{V}_{O_2} had fallen to near minimum values. By eight hours the relative HCVR had risen to ~350% and 600% in animals breathing 5% and 7% CO₂, (500 min time point in fig. 5.8). These values are similar to the changes reported for 13-lined ground squirrels at different levels of steady state hibernation in an earlier study (Sprenger and Milsom 2021(submitted)(chapter 4)). On arousal, this elevation in the HCVR faded and by 60 minutes into the arousal, the ventilatory responses to both 5% and 7% CO₂ were virtually gone (fig. 5.8). This decrease in the HCVR occurred in parallel with increases in T_b and \dot{V}_{O_2} . By the end of arousal, the HCVR had recovered to the normal levels seen in active animals (fig. 5.7, 5.8).

This raises an interesting paradox. The reduction in CO₂ sensitivity at the onset of entrance into hibernation is consistent with the hypoventilation and falls in the RER and ACR seen in normocapnic animals that we believe are associated with a temperature-independent increase in the regulated level of arterial PCO₂. The data indicate that this is followed, however, by a progressive increase in CO₂ sensitivity. During arousal, this elevation in CO₂ sensitivity decreases progressively and late in arousal the ventilatory response to CO₂ disappears, returning to euthermic levels at the end of arousal. Thus, entrance is associated with an initial decrease followed by a progressive increase in CO₂ sensitivity and arousal is associated with a progressive decrease followed by a final increase in CO₂ sensitivity.

The significance of the elevation in the relative HCVR in steady state hibernation is not clear but given the left shift in the hemoglobin-O₂ equilibrium curve at low body temperatures and the dramatic reduction in sensitivity to hypoxia seen in hibernating mammals (Milsom and

Jackson, 2011), it is not surprising that changes in PaCO_2 take on a more important role in regulating ventilation.

The second goal of the present study was to exploit the time lag between changes in \dot{V}_{O_2} and T_b to examine the extent to which the progressive changes in the HCVR during hibernation are temperature or state dependent during entrance and arousal. When the relative HCVR was plotted against each of these variables (fig. 5.8) there was a considerable hysteresis in the correlation between the HCVR and T_b of entering and arousing animals. In contrast, when plotted against \dot{V}_{O_2} , the correlation was the same whether the animal was entering or arousing from hibernation. This suggests that the changes in the HCVR were related to the changes in metabolic rate rather than temperature.

In an earlier study on hypothermic animals, there was no change in the HCVR despite falls in both O_2 consumption rate and body temperature, suggesting that the increase in the HCVR seen in animals in hibernation was due to a state change that was unique to hibernation (Zimmer & Milsom, 2002a). The current data suggest a more complex picture in which the initial change in state at the onset of entrance has very different effects on the HCVR than further changes in state as entrance into hibernation progresses. They suggest that state must change progressively and that the HCVR subsequently increases as \dot{V}_{O_2} and \dot{V}_E fall further.

This raises the possibility that the changes in the HCVR may differ in different species. In some species including bears, arctic ground squirrels (Barnes and Buck, 2000), alpine marmots (Ortman and Heldmaier, 2000), and the echidnas (Nicol et al., 1992) \dot{V}_{O_2} falls rapidly to low levels and is temperature independent over a wide range of steady state temperatures. In other species including golden-mantled ground squirrels (Hammel et al., 1968; Zimmer and Milsom, 2001), edible dormice (Elvert and Heldmaier, 2005; Wilz and Heldmaier, 2000), and the little brown bat (Szewczak & Jackson, 1992), \dot{V}_{O_2} falls proportionately with T_b during steady state hibernation as it does in the 13-lined ground squirrels. Based on the data from the current study we would expect that in the former group, the HCVR would also increase rapidly and remain temperature-independent over a wide range of steady state temperatures.

5.6 Conclusions

It has long been established that in many species of hibernating mammals there is a decrease in the RER and ACR at the start of entrance into hibernation (Snapp and Heller, 1981; Bickler, 1984; Malan et al., 1973; Malan 1982, 1986, 1988; Geiser et al., 1988; Nestler, 1990; Elvert and Heldmaier, 2000, 2005). In the present study on 13-lined ground squirrels we have confirmed that this is due exclusively to hypoventilation resulting from a decrease in breathing frequency. Further, we have shown that this is also associated with a decrease in the hypercapnic ventilatory response, indicating a decrease in CO₂ sensitivity. This leads to CO₂ retention and a rise in arterial PCO₂, suggesting that these changes are also associated with a change in the homeostatic levels at which PaCO₂/pHa are maintained. We have shown that a rise in PaCO₂ at this time decreases $\dot{V}O_2$, more so than at any other time during the hibernation cycle. Subsequent to this, CO₂ sensitivity increases progressively as the squirrels enter deep hibernation. The rise in the HCVR is tightly correlated with the decrease in $\dot{V}O_2$ and not with changes in T_b. While there is an increase in the RER and ACR at the onset of arousal, associated with increases in both respiratory tidal volume and breathing frequency, exposure to hypercapnia at this time has no effect on the rate of rise in $\dot{V}O_2$. The increase in CO₂ sensitivity that has been maintained throughout hibernation dissipates as $\dot{V}O_2$ and T_b rise. Late in arousal the squirrels were totally insensitive to hypercapnia but CO₂ sensitivity and the HCVR returned to euthermic values in the final stages of arousal. Thus, entrance is associated with an initial decrease followed by a progressive increase in CO₂ sensitivity and arousal is associated with a progressive decrease followed by a final increase in CO₂ sensitivity. The significance of the elevation in the relative HCVR in steady state hibernation is not clear but may reflect a change in the relative roles of hypercapnia and hypoxia in the control of resting breathing associated with the increase in hemoglobin-O₂ binding affinity at low body temperatures and the dramatic reduction in sensitivity to hypoxia seen in hibernating mammals (Milsom and Jackson, 2011).

The studies of Heller and colleagues (see Heller 1979 for review) suggest the entrance into hibernation is due to a resetting of the T_b setpoint and that the suppression of $\dot{V}O_2$ is an active component of the process (Heldmaier et al., 1993; Ortman and Heldmaier, 2000; Elvert and Heldmaier, 2005). Our data suggest that changes in the HCVR are also a component of this process. The initial fall in $\dot{V}O_2$ is rapid and temperature-independent. As animals approach

steady-state hibernation, active metabolic suppression appears to be slowly replaced by a passive suppression due to the direct (Q_{10}) effects of low temperature; the final depression of metabolic rate is due to a synergistic action of temperature effects and metabolic inhibition (Heldmaier and Elvert, 2004). The initial decrease in the HCVR on entrance is associated with the rapid temperature-independent fall in \dot{V}_{O_2} (applying the brake) while the subsequent progressive increase in the HCVR is associated with the slower fall in \dot{V}_{O_2} associated with release of the active brake and transfer to the passive effects of temperature. This suggests that both the changes in \dot{V}_{O_2} and in the HCVR are associated with changes in central regulation of the effector limbs establishing steady state hibernation.

Table 5.1 The effects of changing temperature (Q_{10}) over various body temperature ranges on oxygen consumption rates (\dot{V}_{O_2}) and ventilation (\dot{V}_E) during entrance into, and arousal from hibernation.

Temperature range °C	Q_{10} : normocapnia			
	\dot{V}_{O_2} entrance	\dot{V}_{O_2} arousal	\dot{V}_E entrance	\dot{V}_E arousal
35-30	7.7629	0.2104	2.1813	0.1223
30-25	6.2895	0.8915	2.6503	0.8913
25-20	6.2438	1.8542	3.1270	1.2767
20-15	3.2651	2.5575	3.9635	1.6149
15-10	3.3942	15.880	4.8960	3.3884
10 -7	6.9242	2850.5	12.019	12925
<i>start to end</i>	<i>5.0318</i>	<i>4.5899</i>	<i>3.5743</i>	<i>4.4090</i>

Table 5.2 Average time to completion of entrance and arousal in normocapnia (0% CO_2) and hypercapnia (5% and 7% CO_2) in minutes.

Percent inspired CO_2	Entrance			Arousal		
	0% CO_2	5% CO_2	7% CO_2	0% CO_2	5% CO_2	7% CO_2
Time (min)	<i>621±5.1</i>	<i>581±18</i>	<i>586±13</i>	<i>86.8±1.0</i>	<i>87.3±0.5</i>	<i>83.2±2.4</i>

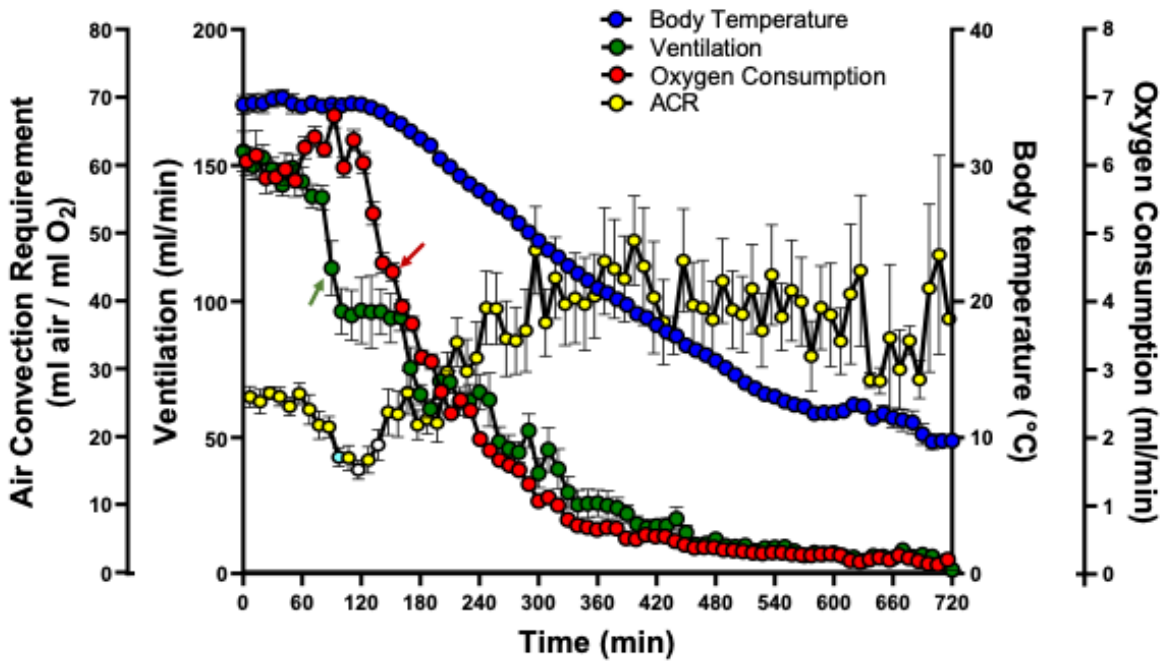


Figure 5.1 Time course of changes in body temperature (°C) (blue), ventilation (ml/min) (green), oxygen consumption rate (ml/min) (red) and air convection requirement (yellow) during entrance into hibernation in 13-lined ground squirrels. Error bars are S.E.M. All points after the arrows (red; oxygen consumption rate, green; ventilation) are significantly different from the starting value (time point 0) ($p < 0.05$). Open circles denote significant differences for air convection requirement compared to the starting value (time point 0) ($p < 0.05$) (one-way ANOVA; Tukeys post hoc test).

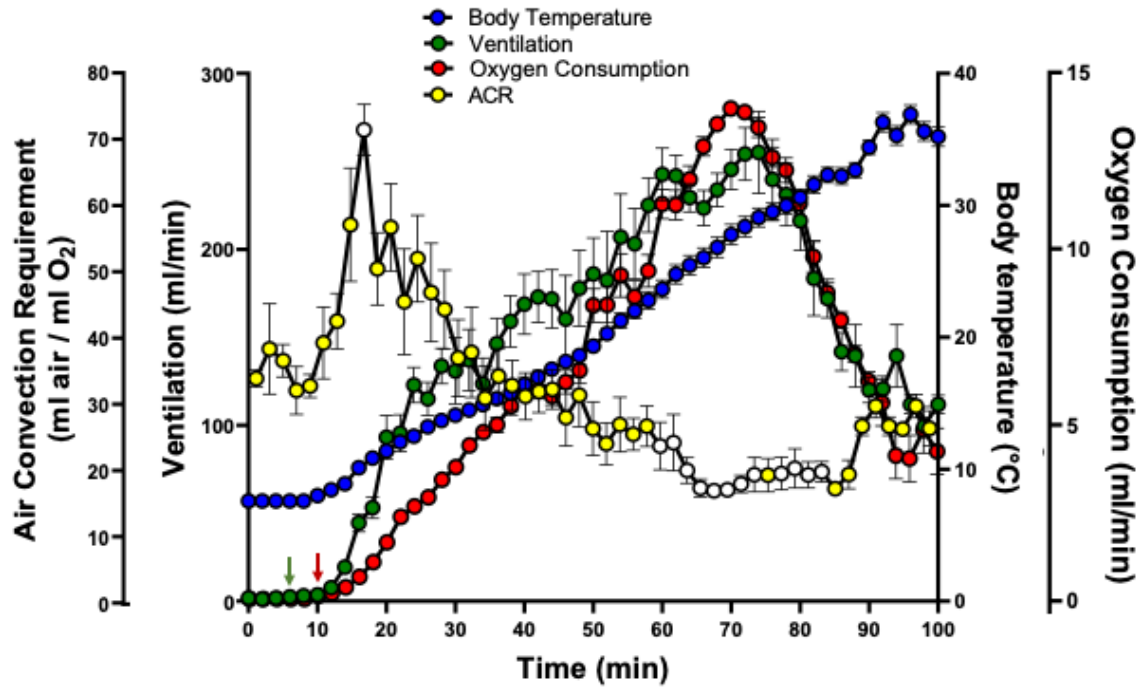


Figure 5.2 Time course of changes in body temperature (°C) (blue), ventilation (ml/min) (green), oxygen consumption rate (ml/min) (red) and air convection requirement (yellow) during arousal from hibernation in 13-lined ground squirrels. Error bars are S.E.M. All points after the arrows (red; oxygen consumption rate, green; ventilation) are significantly different from the starting value (time point 0) ($p < 0.05$). * denotes significant differences for air convection requirement compared to the starting value (time point 0) ($p < 0.05$) (one-way ANOVA; Tukeys post hoc test).

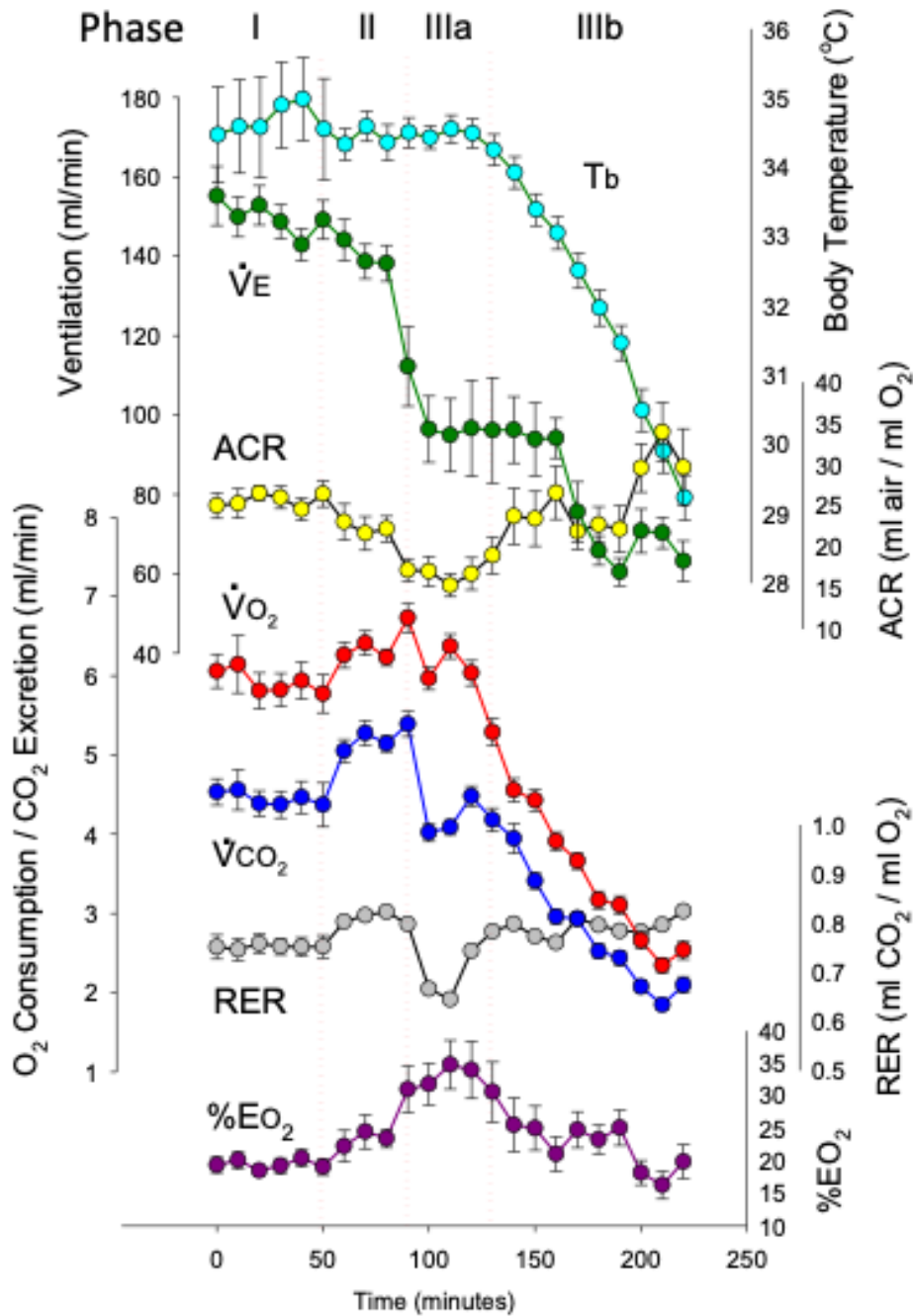


Figure 5.3 Expanded time course of changes in the body temperature (°C) (cyan), ventilation (ml/min) (green), oxygen consumption rate (ml/min) (red), CO₂ excretion rate (blue) the air convection requirement (yellow), the RER (grey) and the % pulmonary O₂ extraction (purple) during entrance into hibernation in 13-lined ground squirrels. Phases (dotted lines; I, II, IIIa, IIIb) were identified according to Elvert and Heldmier (2005). Error bars denote S.E.M.

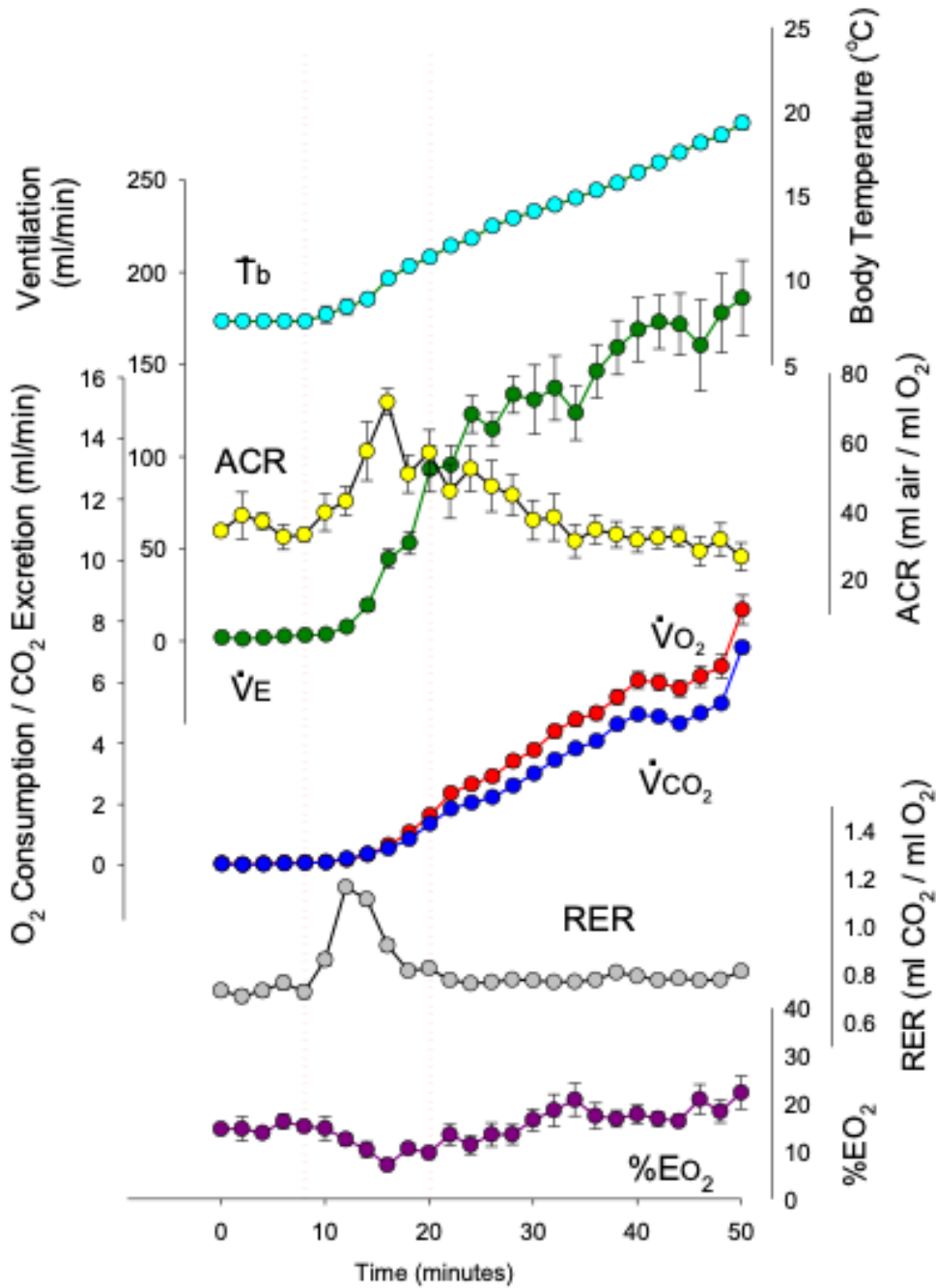


Figure 5.4 Expanded time course of changes in the body temperature (°C) (cyan), ventilation (ml/min) (green), oxygen consumption rate (ml/min) (red), CO₂ excretion rate (blue) the air convection requirement (yellow), the RER (grey) and the % pulmonary O₂ extraction (purple) during arousal from hibernation in 13-lined ground squirrels. Red dotted lines indicate the start of arousal (left) and the return of the RER to starting values (right). Error bars denote S.E.M.

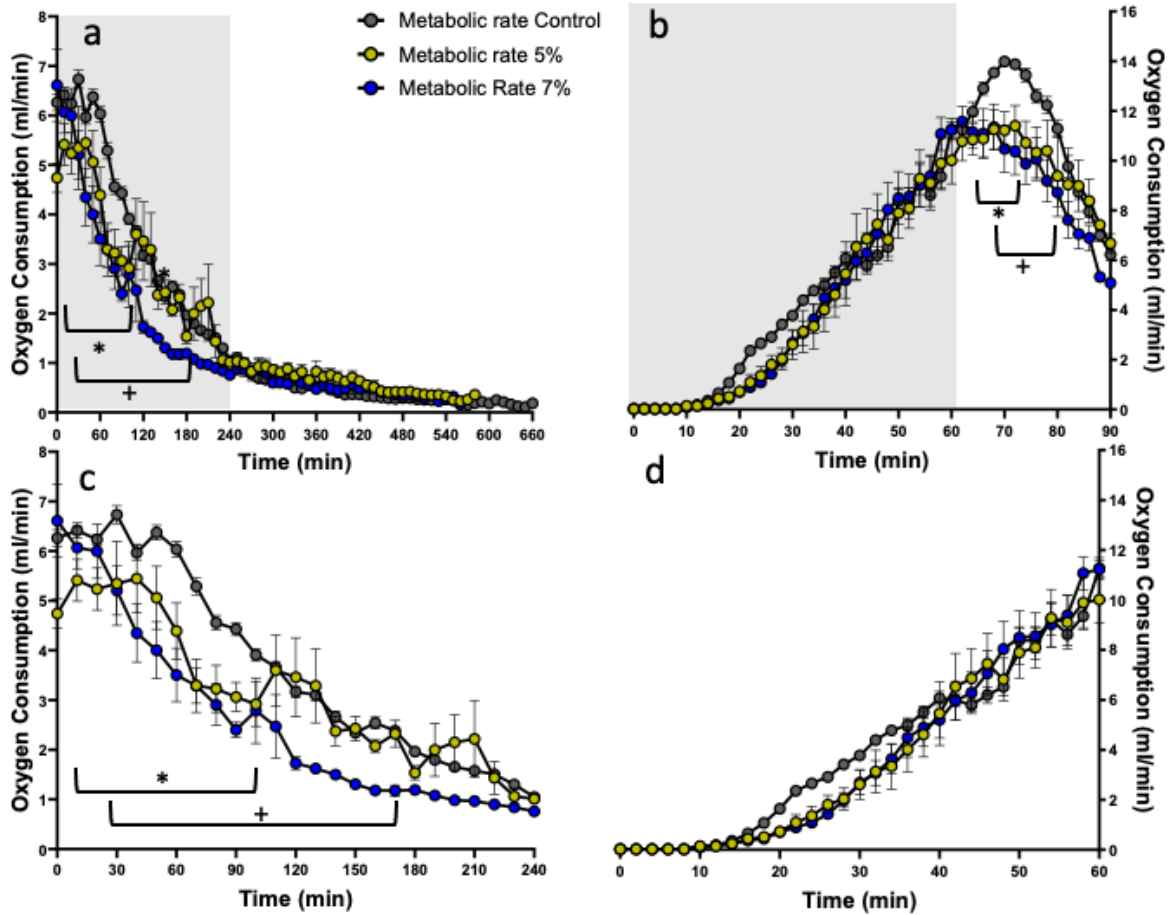


Figure 5.5 Time course of the changes in oxygen consumption rate (ml/min) during 11 hours (a) and the first 240 minutes (c) of entrance into hibernation and all of arousal (b) as well as the first 60 minutes (d) of arousal from hibernation. Data points are for animals breathing normocapnic air (grey), 5% CO₂ (orange), and 7% CO₂ (blue). Error bars denote S.E.M. * (5% hypercapnia) and + (7% hypercapnia) denote significant differences at the same time point from normocapnia ($p < 0.05$) (two-way ANOVA; tukeys post hoc test). Areas in gray in panels a and c indicate the areas shown in b and d.

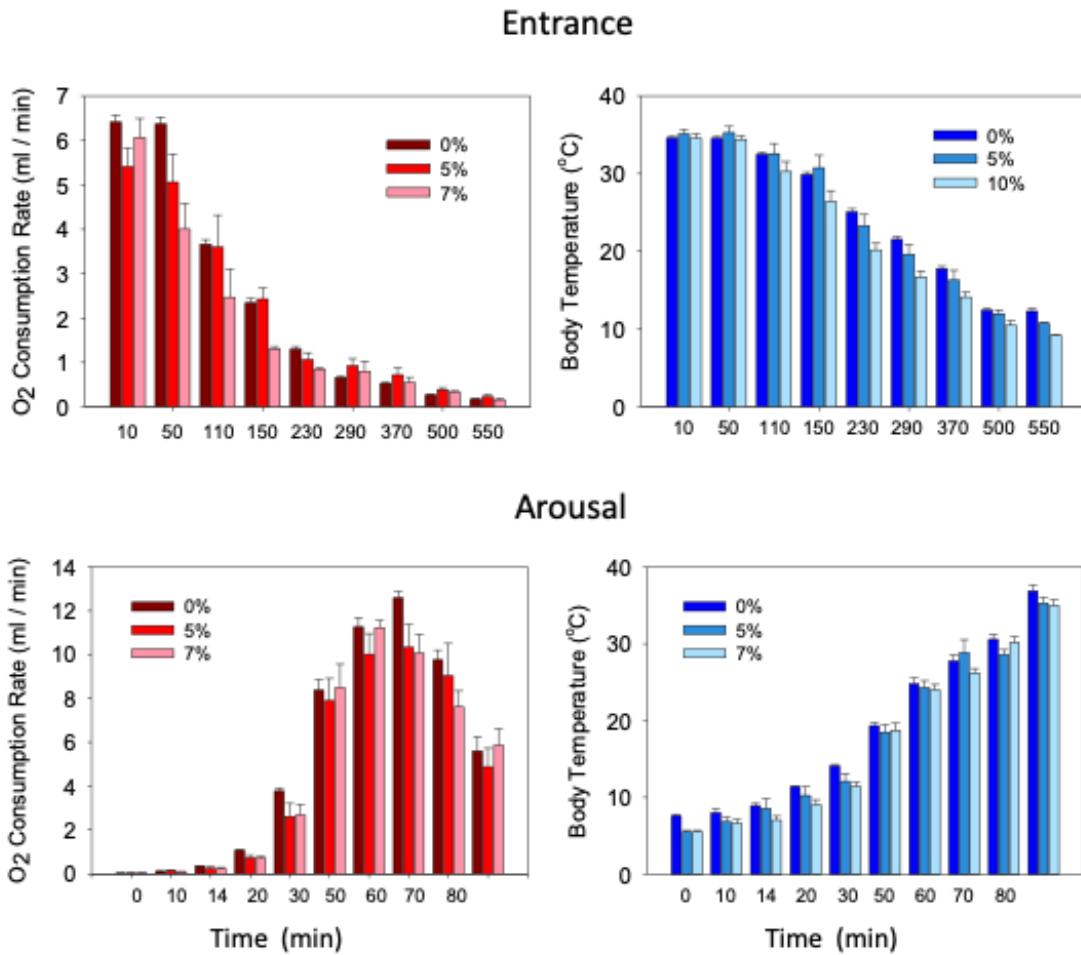
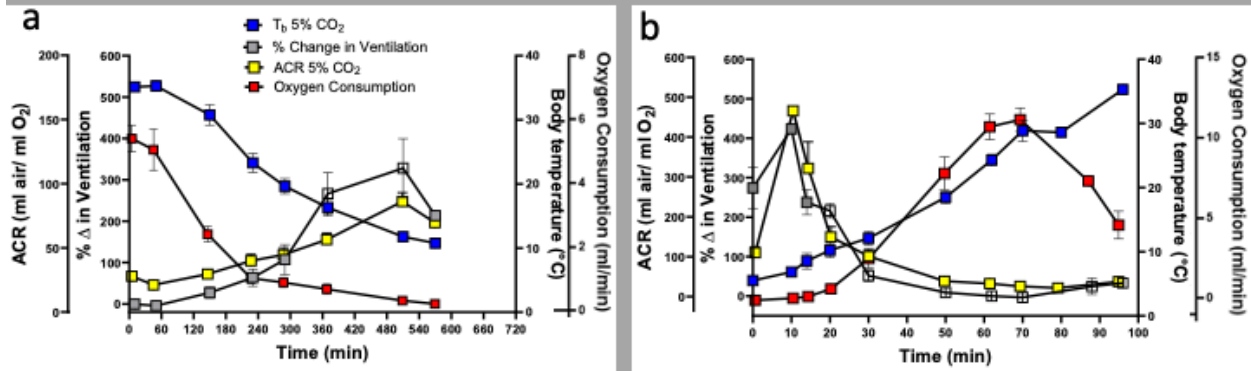


Figure 5.6 Time course of the changes in oxygen consumption rate (ml/min) and body temperature (°C) during entrance into, and arousal from hibernation in animals breathing room air, 5% CO₂ or 7% CO₂. Error bars denote S.E.M.

5% CO₂



7% CO₂

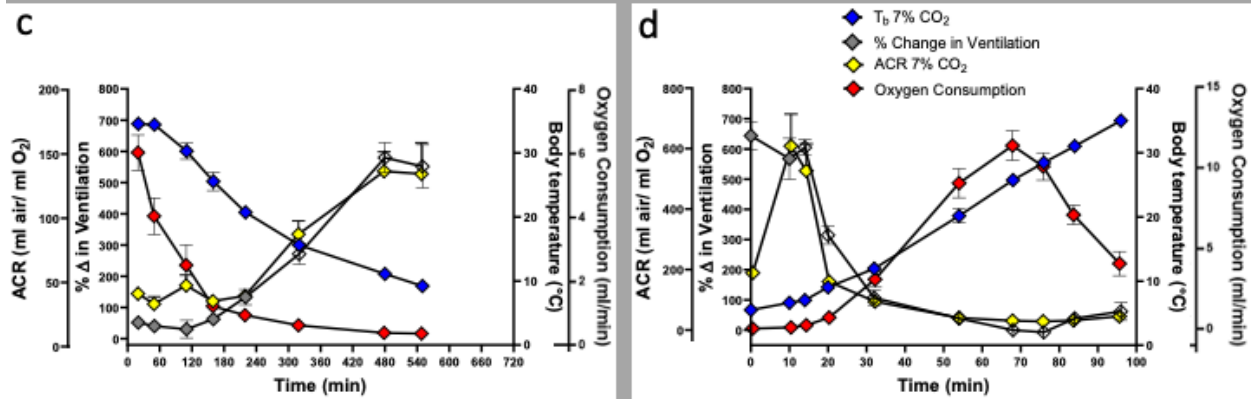


Figure 5.7 Time course of the changes in the air convection requirement (yellow), oxygen consumption rate (ml/min) (red), body temperature (blue), and the relative change in ventilation (grey) in animals breathing 5% CO₂ (top panels, squares) and 7% CO₂ (bottom panels, diamonds) during entrance (a and c) and arousal (b and d). Error bars denote S.E.M. Open data points denote a significant difference from the starting value for the relative change in ventilation (two-way ANOVA; tukeys post-hoc test (p<0.05)).

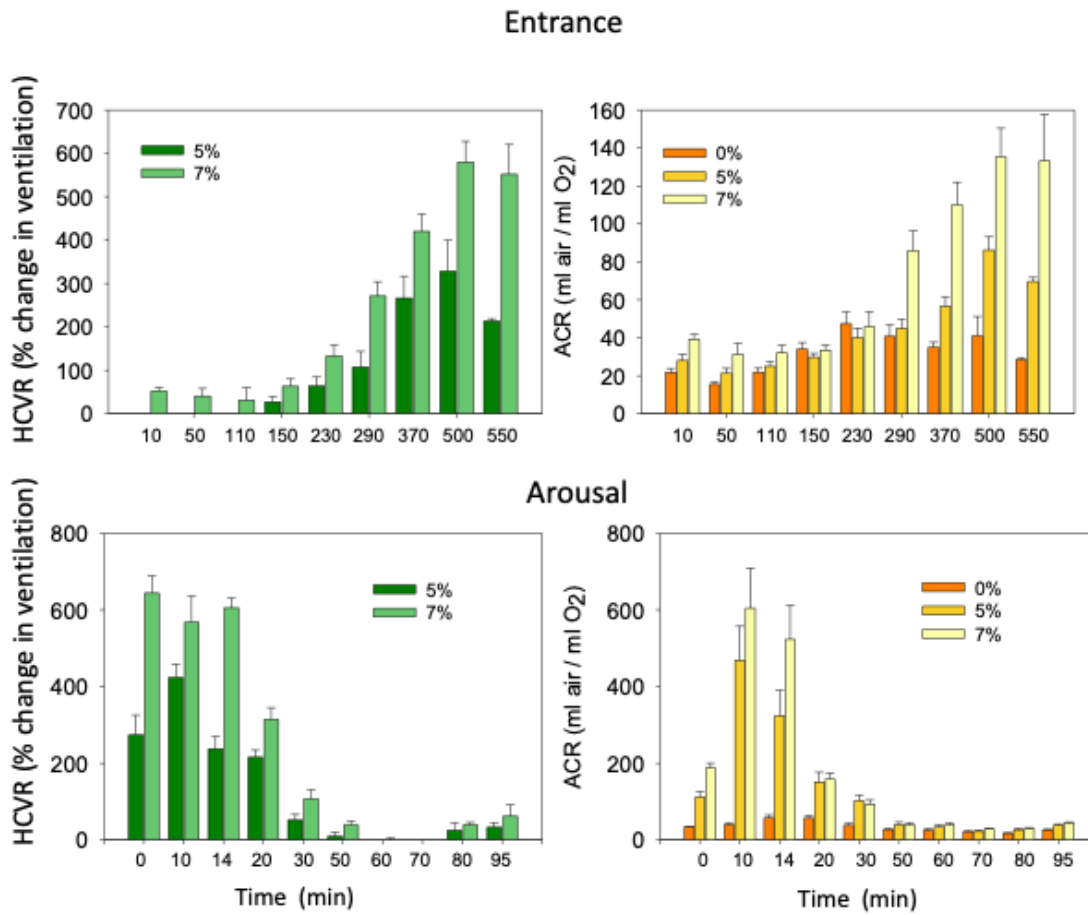


Figure 5.8 Time course of the changes in the HCVR (% change in ventilation) and the ACR (ml air/ml O₂) during entrance into, and arousal from hibernation in animals breathing room air, 5% CO₂ or 7% CO₂. Error bars denote S.E.M.

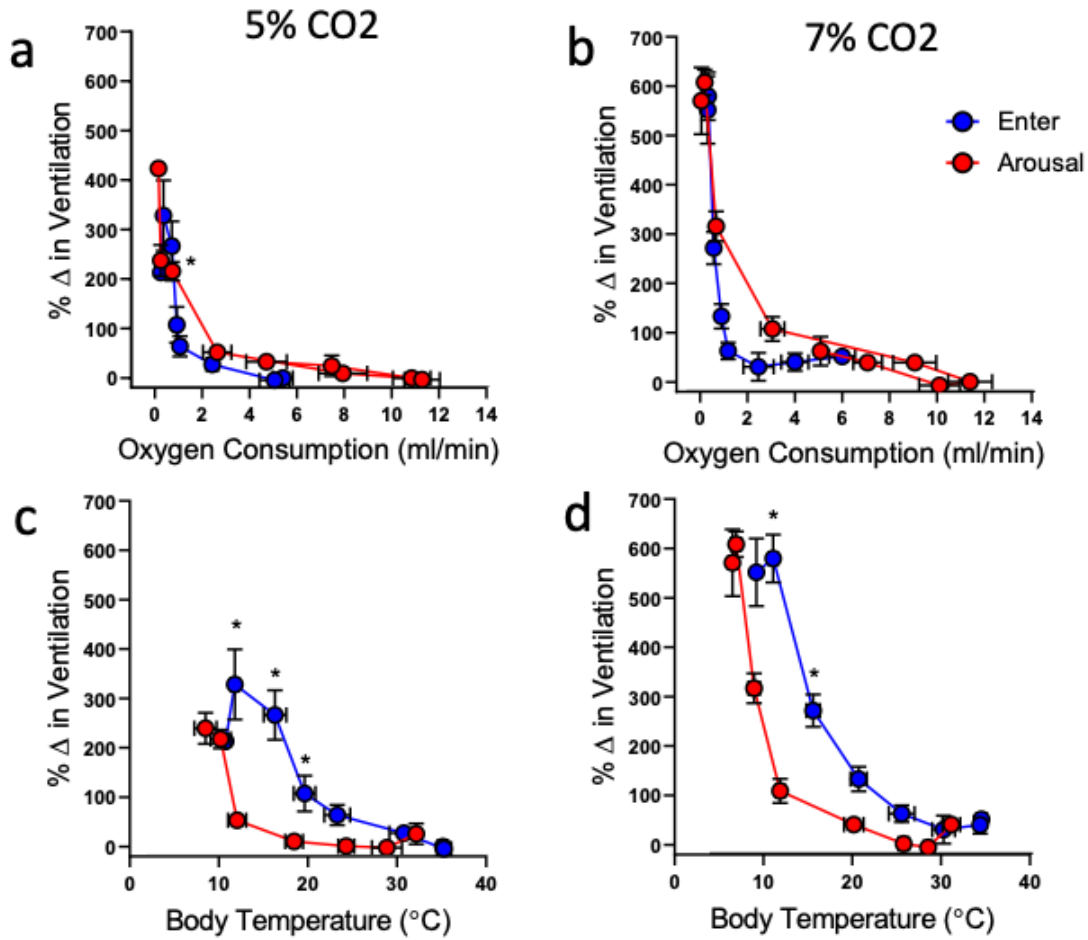


Figure 5.9 Relationship between the HCVR (relative change in ventilation (ml/min)) and oxygen consumption rate (ml/min) (a and b) and body temperature (c and d) in animals breathing 5% (a and c) and 7% CO₂ (b and d) during entrance into (blue) and arousal from hibernation (red). Error bars indicate S.E.M. * denote significant differences between overlapping points in entrance and arousal (two-way ANOVA; tukeys post-hoc (p<0.05)).

Supplemental figure 1

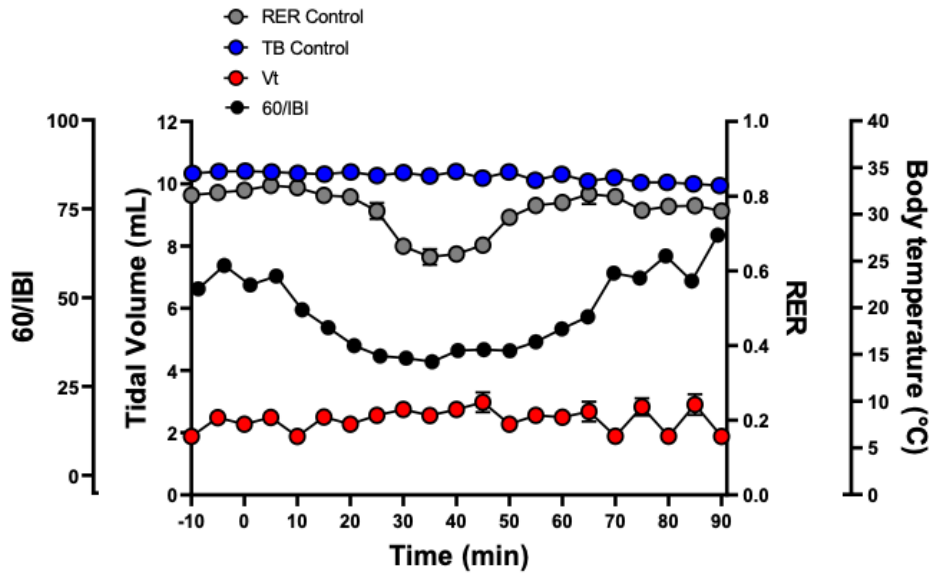


Figure 5.10 Time course of the changes in body temperature (blue), the RER (grey,) breathing frequency (black) and tidal volume (red) during entrance into hibernation in animals breathing room air. Error bars denote S.E.M.

Supplemental figure 2

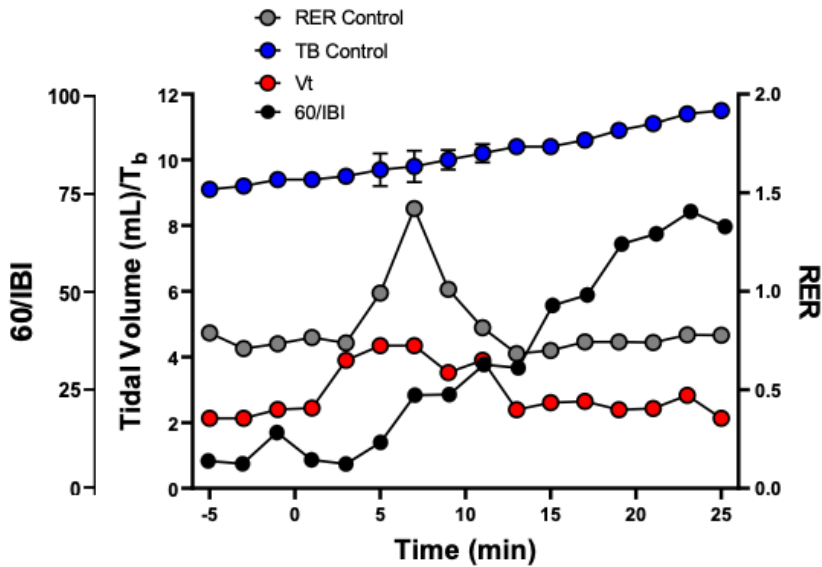


Figure 5.11 Time course of the changes in body temperature (blue), the RER (grey,) breathing frequency (black) and tidal volume (red) during arousal from hibernation in animals breathing room air. Error bars denote S.E.M.

Chapter 6: Locus Coeruleus and the Hypercapnic Ventilatory Response in Euthermic and Hibernating 13-Lined Ground Squirrels (*Ictidomys Tridecemlineatus*)

6.1 Summary

In this study we examined the extent to which input from the locus coeruleus plays a role in the increase in the relative hypoxic ventilatory response (HCVR) seen in hibernating 13-lined ground squirrels. The locus coeruleus (LC), located bilaterally in the pons, is a major noradrenergic site that contributes to both activity state and the HCVR in rats. We hypothesized that the output of the LC was altered by the change into the hibernating state in 13-lined ground squirrels contributing to the enhanced hibernating HCVR. We chemically lesioned the LC unilaterally and bilaterally using 6-hydroxydopamine (6-OHDA) and examined the HCVR in euthermic and hibernating 13-lined ground squirrels using whole-body plethysmography. Our data indicate that in euthermic animals, the LC provides a modest inhibitory input under normocapnic conditions by decreasing breathing frequency and ventilation but provides a significant excitatory input to the HCVR that is primarily due to increases in tidal volume. In hibernating animals, on the other hand, the LC provides a modest excitatory input to ventilation under normocapnic conditions, as well as during the HCVR, by increasing breathing frequency. The data do not support a significant role for the LC in the increase in the relative hypercapnic ventilatory response seen in hibernating 13-lined ground squirrels.

6.2 Introduction

Hibernation in small mammals is marked by dramatic changes in metabolic rate, body temperature (T_b), heart rate, and ventilation (\dot{V}_E) (Lyman, 1958*b*). The initial drop in metabolic rate in most hibernators appears to be independent of temperature (Snapp & Heller, 1981; Geiser, 1988; Malan, 1988). A brief, precipitous drop in the respiratory exchange ratio (RER) just prior to reductions in metabolic rate early in the hibernation bout has been reported in several species (Snapp & Heller, 1981; Bickler, 1984; Nestler, 1990). The drop in RER is thought to be a

consequence of hypoventilation leading to CO₂ retention that contributes to metabolic suppression early during entrance into hibernation (Snapp & Heller, 1981; Malan, 1988). Consistent with this, \dot{V}_E falls prior to changes in metabolism early in entrance suggesting that 1) changes in \dot{V}_E must supersede central and peripheral chemoreceptor drive to maintain pH/PCO₂ homeostasis (Milsom & Jackson, 2011) and 2) ventilatory sensitivity to hypercapnia must be transiently reduced during the period of reduced RER and CO₂ retention.

We recently confirmed that there is indeed a period of reduced CO₂ sensitivity at the onset of entrance into hibernation in 13-lined ground squirrels. We also found that the sensitivity to hypercapnia was elevated in steady state hibernation and there was a period of hypersensitivity at the onset of arousal (Sprenger and Milsom 2021 (submitted)(chapters 4 and 5)). The ventilatory response to CO₂ in steady state hibernation was also enhanced by as much as 10-fold in hibernating golden-mantled ground squirrels (McArthur & Milsom, 1991c, 1991a; Webb & Milsom, 2017). However, this enhanced response was not elicited by hypothermia in golden-mantled ground squirrels (Zimmer & Milsom, 2004), suggesting that it is entrance into the hibernating state and not the reduction in body temperature that is key to the changes in CO₂ sensitivity, although the change in state appeared to be temperature dependent (Sprenger and Milsom 2021a (submitted)(chapter 4); Webb and Milsom 2017). But, which parts of the chemosensory pathway are affected by the change in state and/or temperature is unknown. In hibernation, carotid body denervation marginally affects the hypercapnic ventilatory response (HCVR) (Webb & Milsom, 2017), suggesting that any changes in CO₂ sensitivity in hibernation are more likely derived from modification of the sensitivity of central chemoreceptors. Several central sites are known to intrinsically sense changes in pH/Pco₂ and contribute to the hypercapnic ventilatory response (HCVR) including the medullary raphé (Wang *et al.*, 1998; Li *et al.*, 2006), retrotrapezoid nucleus/parafacial respiratory group (RTN/pFRG) (Guyenet *et al.*, 2008), nucleus tractus solitarius (NTS) (Parisian *et al.*, 2004), and locus coeruleus (LC) (Biancardi *et al.*, 2008). The LC is of particular interest because of its role in sympathetic activation as well as its hypercapnic sensitivity. The autonomic nervous system is instrumental in directly and indirectly regulating metabolic rate (Drew *et al.*, 2007; Shibao *et al.*, 2007). Entrance into hibernation is accompanied by increased parasympathetic tone and decreased sympathetic tone. In deep steady state hibernation, both sympathetic and parasympathetic tone

appear to be absent, and on arousal, sympathetic tone is increased (Harris & Milsom, 1995; Milsom *et al.*, 1999). The LC, located bilaterally in the pons, is part of the reticular activating system (RAS). It is a major site of noradrenergic influence (Samuels & Szabadi, 2008; Gargaglioni *et al.*, 2010) and exhibits arousal-state dependent activity. It is considered a major wakefulness promoting nucleus (Samuels & Szabadi, 2008) and is hypothesized to contribute to changes in arousal state during hibernation (Heller, 1979; Drew *et al.*, 2007). More than 80% of LC neurons respond to hypercapnia with an increased firing rate (Oyamada *et al.*, 1998; Filosa *et al.*, 2002). In adult rats, LC function is primarily mediated by gap-junctions (Gargaglioni *et al.*, 2010), and chemical inhibition of the LC in awake animals reduces the HCVR *in vivo* without altering basal ventilation (Biancardi *et al.*, 2008). Non-selective catecholaminergic neuron (CA) depletion in the LC was found to reduce the HCVR in sleep and in wakefulness as well, but also to decrease breathing frequency under resting conditions (Li & Nattie, 2006).

In the present study we selectively lesioned the LC (6-hydroxydopamine (6-OHDA)) and sought to determine 1) the role of LC noradrenergic neurons in basal ventilation and in the HCVR of euthermic 13-line ground squirrels, and 2) if that role changes when 13-lined ground squirrels enter a hibernating state signaling modification of LC input into the HCVR. Based on previous data we hypothesized the LC would not contribute to basal ventilation but would contribute to the HCVR in euthermic squirrels, as well as to the enhanced HCVR in steady state hibernation.

6.3 Methods

6.3.1 Animals

All procedures were conducted under a protocol approved by the UBC Animal Care Committee (UBC A17-0018) and complied with the policies of the Canadian Council on Animal Care. 13-lined ground squirrels (*Ictidomys tridecemlineatus*) were trapped in Carman, MB, Canada (49°30'N, 98°01'W) and transferred to an animal care facility at the University of British Columbia. Squirrels were trapped with the approval of Manitoba Conservation and Water Stewardship, under wildlife scientific permit WB15027. Wild caught squirrels were treated with Ivermectin and Droncit for endoparasites (0.4 mg/kg, subcutaneous), and flea spray for

ectoparasites immediately after capture. Squirrels were provided water and IAMS small chunk dog chow supplemented with apples and peanuts *ad libitum* during the euthermic period. No food or water was provided during the hibernation period. All animals were kept in a temperature-controlled chamber (20 ± 2 °C) on a photoperiod that matched the daily photoperiod in Vancouver, British Columbia, Canada during the euthermic period and at (5 ± 2 °C) in the dark during the hibernation period.

6.3.2 Surgery

All surgical procedures were performed under inhaled isoflurane anesthesia (4%) in conjunction with ketamine (25mg/kg) and xylazine (1mg/kg). Squirrels were anesthetized and fixed in a stereotaxic frame. A cannula (23-gauge needle barrel) containing a microinjection needle was advanced into the LC for unilateral or bilateral injection of 6-hydroxydopamine (6-OHDA; Sigma) (8µg in 1µL of vehicle over 2 minutes). The coordinates (-7.2mm from lambda; ± 1.2 mm from midline; -7.6mm from skull surface; bite bar at 5mm; 13° angle) were used to locate the LC. One group of squirrels (LC sham) were injected unilaterally with vehicle only (1µg of ascorbic acid in 1µL of saline over 2 minutes). Because the sham injections altered the breathing pattern, in a subset of animals, the cannula was only inserted -7.0mm from the skull surface terminating in the parabrachial complex (PbC situated immediately above the LC for sham (vehicle only) injections (PbC sham)). After injection, the injection needle was withdrawn, and the cannula was sealed and secured with dental glass ionomer (GC Fuji Plus (GC America, US) (from Sinclair dental supply, Vancouver, B.C.)). In a final group of animals, the cannula was inserted into the LC and then withdrawn with no injections (LCnc). All injections (sham or 6-OHDA) were made during the surgery.

RFID chips (ITPP-300 extended calibration) were implanted intraperitoneally at the end of the surgery (Biomedic data systems). Animals were allowed to recover for 7 days after the surgery and given Metacam (oral meloxicam; 1.5mg/mL) for the first 5 days. Any animal showing signs of pain, infection, or inflammation were removed from the study.

6.3.3 Measurement of Temperature

Chamber temperature was monitored continuously with two complimentary systems. The first system used a thermal probe connected to a Physitemp monitor (BAT-12, Physitemp,

Clifton, NJ). The second used a scannable RFID temperature chip (ITPP-300 extended calibration) that was read with a DAS-8017 programable reader (Biomedic data systems). The thermal probe was situated just over the experimental animal chamber, and the scannable chip was secured on the inside of the experimental animal chamber. The two systems read comparably. Intraperitoneal body temperature was also measured from the surgically implanted RFID temperature chips with a DAS-8017 reader (Biomedic data systems).

6.3.4 Measurement of Oxygen Consumption Rate and Ventilation

Ventilatory and metabolic variables were continuously measured with flow through whole-body plethysmography and respirometry (Drorbaugh & Fenn, 1955*b*; Malan, 1973; Jacky, 1978; Sprenger *et al.*, 2019(chapter 2)). Two identical plexiglass boxes were placed in a temperature-controlled cooling chamber. One served as the experimental animal chamber and the other as a reference chamber. The temperature-controlled chamber was situated on a sturdy table with padding underneath to reduce vibration. Temperature was maintained within ± 1 °C. An equal flow of air was maintained constantly through the experimental animal and reference chambers. The pressure differential between the two chambers was monitored with a differential pressure transducer (Validyne model DP103-18 amplified with a Gould DC amplifier (Gould; Valley View, Ohio)). As animals entered hibernation body temperature fell. A minimum body temperature to ambient temperature differential ($T_b - T_{am}$) of 3°C was required to obtain accurate tidal volume measurements with this set-up. Any differential lower than 3°C was excluded from the final analysis. The fractional composition of oxygen and CO₂, and the water vapor pressure, were measured from the excurrent gas from the system (FMS; Sable systems). The FMS was calibrated before the start of each trial using gases from pre-mixed tanks (Praxair; 0%, 3%, 5%, 7% CO₂ with 21% O₂ balanced in N₂). Tidal volume was calibrated before each measurement by injecting volumes comparable to the animal's tidal volume at a rate similar to the animals breathing frequency (~1 breath/min in hibernation and ~60 when euthermic) into the chamber.

6.3.5 Experimental Protocol

Euthermic

One day prior to surgery, “pre-surgery” or control squirrels were placed into the animal chamber of the plethysmography setup and allowed to acclimate for 30 minutes breathing room

air (21% O₂; 0 % CO₂; balanced in N₂). Next the animals were given hypercapnic gases (3%, 5%, and 7% CO₂; 21% O₂; balanced in N₂) in random order for 30 minutes each. Animals breathed room air (0% CO₂) between hypercapnic gases. A flow rate of 800ml/min was used for each measurement to ensure CO₂ did not change by more than 0.8%. Body temperature was measured 3 times during each treatment. Seven days after surgery, the same squirrels were measured using the same protocol. These squirrels fell into three groups: animals with a single LC cannula placed unilaterally having received the sham injection on the day of surgery (LC sham, n=5); animals with a unilateral lesion (LC – unilateral lesion, n=8); and animals with a bilateral lesion (LC – bilateral lesion, n=7).

Hibernating

In another group of squirrels, seven days after surgery animals were placed in the recording box while euthermic, and moved into the temperature-controlled chamber at $\sim 5 \pm 1^\circ\text{C}$. Animals were left overnight in the chamber with an incurrent flow rate of 800 ml/min. Once an animal had entered hibernation and exhibited a steady body temperature, flow rate was reduced to $\sim 50\text{-}80$ ml/min. The chamber temperature was then adjusted until the animal's body temperature was at the desired temperature ($\sim 7^\circ\text{C}$). Animals were then maintained at the desired temperature for at least 2 hours. Resting hibernating normocapnic ventilation and oxygen consumption rate were then recorded for at least 1 hour before hypercapnic gases (3%, 5% and 7% CO₂, 21% O₂, balanced in N₂) were administered in random order for a minimum of 1 hour each or until a steady ventilatory response was reached. Body temperature was scanned 4 times during the recording periods. These squirrels fell into 5 groups. Three groups were the same as for the study of euthermic animals; Control (n=13), LC sham (n=5), and LC-bilateral lesion (n=6). Because insertion of the cannula and sham injection in the LC group altered the breathing pattern of hibernating squirrels but not euthermic squirrels (see results) we also ran one group in which the cannula was only inserted as far as the PbC (PbC sham, which also received vehicle injections on the day of surgery) (n=2), and a group in which only the injection cannula was inserted into the LV and then withdrawn with no injections (LCnc) (n=4). For the hibernation component of the study, the control group were a separate group of squirrels that did not undergo any surgery.

6.3.6 Assessment of 6-OHDA Chemical Lesions

At the end of experiments animals were deeply anesthetized with inhaled isoflurane and rapidly perfused with 0.1M phosphate buffered saline (~1-2 minutes). Brains were then removed and frozen in supercooled (-20C) 2-methylbutane, before being fixed in cryomatrix for sectioning. Serial sections (20 μ m) were taken over the expected LC location (using the rat atlas as a guide). Slices were placed on slides, rehydrated with 0.1M PBS and then post-fixed (4% PFA in 0.1M PBS at pH 7.4) for 10 minutes.

In a pilot study to determine the coordinates of CA neurons of the LC, tyrosine hydroxylase (TH) immunofluorescence was used to examine the brains of animals that had had no surgery. Following post-fix, slices were incubated in rabbit polyclonal anti-TH antibody (1:2000) for 48 hours, followed by 2h in secondary anti-body ALEXA-fluorophore 594 (1:400) in the dark. Slices were then serially dehydrated through graded concentrations of ethanol, cleared with xylene, and sealed with a cover slip with a mounting medium (vectashield containing DAPI). TH and DAPI staining were imaged with fluorescence microscopy (Fig. 12). Transverse, coronal, and sagittal locations of the LC were noted from this staining. Then, prior to making any lesions, accurate cannula placement using these coordinates was verified in 6 animals by examining brains in which Evans blue dye had been injected into the re-entrant cannula.

To verify efficacy of 6-OHDA lesion, cresyl violet staining was used in all the experimental animals to determine the number of live cells in the region of the LC that was determined by TH staining in the group of animals of the pilot study. After post-fix, slices were incubated in cresyl violet (5% w.v.) for 20 minutes before being serially dehydrated in ethanol and cleared with xylene. Slides were sealed with a cover slip with mounting medium (vectashield containing DAPI). Cresyl violet stains were imaged with light microscopy.

6.3.7 Data Analysis

Oxygen Consumption Rate and Ventilation

Recordings were analyzed over the last 30 minutes (hibernation) and over the last 10 minutes (euthermic) of the exposures. Only periods of steady ventilation were taken for analysis. Tidal volume (V_T), breathing frequency (f_R), T_b , oxygen consumption rate (\dot{V}_{O_2}), CO_2 production

rate (\dot{V}_{CO_2}), and inter-breath intervals (IBI) were extracted from the recorded traces. Ventilation (\dot{V}_E) was calculated via the multiplication of V_T and f_R . V_T was calculated as described in Sprengr et al., 2019(chapter 2) with the exception that nasal temperature was not corrected for in torpid animals as it was assumed to be similar to ambient temperature. \dot{V}_{O_2} was calculated as described in Spenger et al. 2019 (chapter 2), and \dot{V}_{CO_2} was calculate using the following equation (Lighton, 2008):

$$\dot{V}_{CO_2} = FR \frac{(1 - F_{iO_2} - F_{iCO_2})}{(1 - F_{eO_2} - F_{eCO_2})} \{F_{eCO_2} - F_{iCO_2}\}$$

where FR is flow rate, F_{iO_2} is fractional inspired oxygen, F_{eO_2} is fractional expired oxygen, F_{iCO_2} is fractional inspired CO_2 , and F_{eCO_2} is the fractional expired CO_2 .

ACRs (O_2 and CO_2 ; ACR_{O_2} and ACR_{CO_2}) were calculated by dividing \dot{V}_E by either \dot{V}_{O_2} or \dot{V}_{CO_2} . Body mass was taken at the end of the experiment.

Chemical Lesion of LC

TH immunofluorescence slices were analyzed for location of CA neurons. The location of the LC was determined by TH positive staining (~-1.0 to -0.8mm from lambda, -7.2mm from skull surface, ~1.1 to 1.2 on either side of midline). TH and cresyl violet images were matched for magnification and adjusted to match size. The TH positive area was then used to create a guide for the area in which cells were counted in the cresyl violet stains. Cresyl violet stains were analyzed for total live cells in the guide area over the entire length of the LC group (-1.0 to -0.8mm transverse). Cells were determined by setting a cell size range (in pixels²) and threshold level for cresyl stain intensity. The counting was repeated twice to ensure accuracy. Squirrels where less than 50% of the LC was lesioned were excluded from analysis.

6.3.8 Statistical Analysis

Two-way repeated measures ANOVA were used to determine the effect of lesion on all ventilatory and metabolic variables for euthermic animals (Dunnet's post-hoc test; $p < 0.05$). Two-way ANOVAs were used to determine the effect of lesion on all ventilatory and metabolic variables for torpid animals (Tukey's post-hoc test; $p < 0.05$). T-tests with multiple comparisons corrections were used to determine the effect of the sham operation on all metabolic and

ventilatory variables ($p < 0.05$). Separate t-tests were used to test if the lesions significantly reduced the number of cells in the LC region ($p < 0.05$). All statistics were run using Graphpad Prism (9.0.0121) statistical program.

6.4 Results

6.4.1 6-OHDA Lesion

Figure 6.1 shows the geographical location of the cannula tract for lesion of the LC in 13-lined ground squirrels, and other regions that the cannula passed through in the sagittal (A), and transverse planes (B). Panels C and D show a closer field of view of the location of the cannula tip of injections producing LC lesion on the right side only in sagittal (C) and transverse (D) view. The location of TH positive cells in this location are shown in serial transverse sections in figure 6.12 (fig. 6.12). TH positive cells were densely packed bilaterally in the LC with the greatest concentration being at -0.9mm from the interaural line (fig. 6.12). Figure 6.13 (fig. 6.13) shows cresyl violet staining of intact (top), unilaterally lesioned (middle), and bilaterally lesioned (bottom) LC at the same locations as the TH stains. Bilateral LC lesions resulted in an average 71% decrease in cells in this region compared to sham injected animals (fig. 6.2A) and unilateral LC lesion resulted in an on average 63% decrease on the side with the lesion (fig. 6.2B).

6.4.2 Effects of Cannula Placement

Euthermic Animals

The \dot{V}_E and \dot{V}_{O_2} of sham injected animals breathing room air were not significantly different from those of control animals ($p > 0.05$) (fig. 6.3A, 6.4A and 6.5A). Thus, the ACR was unchanged by the sham injections (fig. 6.5A). However, in normocapnia, breathing frequency was significantly lower in sham animals (39 breaths/min) compared to control animals (58 breaths/min) ($p < 0.05$) (fig. 6.3A, 6.4A) while tidal volume was slightly, but insignificantly higher ($p > 0.05$) (fig. 6.4A).

Hibernating Animals

In hibernation, \dot{V}_E was significantly elevated in sham animals breathing room air (~13ml/min) compared to control animals (~1.8ml/min) ($p < 0.05$) due to a large increase in f_R

with no change in V_T ($p < 0.05$) (fig. 6.3B, 6.4B). \dot{V}_{O_2} was also significantly greater in sham operated animals (~ 0.125 mL/min) compared to control animals (~ 0.02 mL/min) (fig. 6.5B). The net result was a similar ACR in normocapnia in the two groups (fig. 6.5B). Insertion and withdrawal of the cannula into the LC without vehicle injection had a similar effect on f_R and also increased V_T significantly, while sham injections into the PbC above the LC had a similar, but reduced effect; while the increase in breathing frequency was still significant, the increase in \dot{V}_E was not (fig. 6.5B)

6.4.3 Effects of LC Lesion

Euthermic Animals

Both unilateral and bilateral lesions had modest but insignificant effects on the recorded variables in euthermic animals breathing room air. \dot{V}_E was modestly, but not significantly elevated ($p > 0.05$) in lesioned animals compared to the LC sham animals when breathing normocapnia (fig. 6.7A). This was primarily due an increase in f_R that was offset by a reduction in V_T (fig. 6.7B and C). \dot{V}_{O_2} was unaffected by LC lesion, and thus the ACR was slightly (but not significantly) elevated in lesioned animals (fig. 6.7D,E). Body temperature was significantly higher in bilaterally lesioned animals (37.9°C) compared to sham (36.1°C) operated animals ($p < 0.05$) (fig. 6.7F).

Hypercapnia increased \dot{V}_E in both sham operated and control animals primarily via increases in tidal volume with little contribution from increases in breathing frequency (fig. 6.6 and 6.7A,B,C). \dot{V}_{O_2} was unaffected by hypercapnia in both sham and control animals ($p > 0.05$) (fig. 6.7D). The net result was an increase in the ACR in hypercapnia that mirrored the change in \dot{V}_E (fig. 6.7E).

Hypercapnia also elicited an increased in \dot{V}_E in the lesioned animals. This increase was significantly reduced in bilaterally lesioned animals compared to control animals when breathing a 7% hypercapnic mixture ($\sim 25\%$ increase compared to a $\sim 60-75\%$ increase in LC sham animals) ($p < 0.05$) ($p < 0.05$) (fig. 6.8A). As with LC sham animals, the increase in \dot{V}_E in LC lesioned animals was mostly due to increases in V_T with smaller changes in f_R (fig. 6.7B, C and 6.8B, C). The reduction in V_T seen in normocapnic animals became significant in bilaterally lesioned animals when breathing 5% and 7% hypercapnia ($p < 0.05$) (fig. 6.7B, 6.8B). \dot{V}_{O_2} was

unaffected by hypercapnia in LC lesioned animals, thus the ACR increased in hypercapnia (fig. 6.7D and E). The increase in the ACR was slightly smaller in LC lesioned animals in 5% and 7% hypercapnia compared to LC sham animals, but this was not significant ($p>0.05$) (fig. 6.7E).

Hibernating Animals

In hibernating ground squirrels, \dot{V}_E increased significantly in both control and LC sham animals breathing 5% and 7% CO_2 by an increase in f_R with no change in V_T (fig. 6.9, 6.10A, B, and C). \dot{V}_{O_2} was unaffected by hypercapnia (fig. 6.10D), thus the ACR increased significantly with increasing levels of hypercapnia in both control and LC sham animals (fig. 6.10E).

\dot{V}_E was slightly, but insignificantly reduced in bilaterally lesioned animals compared to sham animals breathing normocapnic air ($p>0.05$) (fig. 6.10A). V_T and f_R were similar in lesioned and sham animals (fig. 6.10B and C). \dot{V}_{O_2} in LC lesioned animals breathing normocapnia was $\sim 0.05\text{mL}/\text{min}$ which was lower than that in sham animals ($\sim 0.125\text{mL}/\text{min}$) (fig. 6.10D). The net result was that ACR was unaffected by the LC lesion (fig. 6.10E). Body temperature was not significantly different between any group in hibernation (fig. 6.10F).

Hypercapnia (5% and 7%) increased \dot{V}_E significantly in both LC sham and LC lesioned animals in hibernation ($p<0.05$) (fig. 6.10A). The increase in \dot{V}_E was due to increases in f_R with little contribution from changes in V_T in both groups (fig. 6.10B and C). Hypercapnia did not affect \dot{V}_{O_2} in LC sham or LC lesioned animals (fig. 6.10D), thus the ACR increased with hypercapnia in both groups (fig. 6.10E).

When expressed as $\% \Delta$, the increase in \dot{V}_E in LC lesioned and sham animals breathing 3% and 5% CO_2 was identical to the increase in control animals when breathing 3 and 5% CO_2 (fig. 6.11A). However, the relative increase in \dot{V}_E when breathing 7% CO_2 was significantly smaller in LC sham and LC lesioned animals ($\sim 400\%$ increase) compared to control animals ($\sim 650\%$ increase) ($p<0.05$) due to a reduction in the increase in breathing frequency (fig. 6.11C).

6.5 Discussion

Ventilatory sensitivity to hypercapnia is greatly altered during the transition into and out of hibernation, as well as in steady state hibernation (Snapp and Heller 1981; Bickler 1984;

Nestler 1990; McArthur and Milsom 1991b; Webb and Milsom 2017; Sprenger and Milsom 2021a (submitted)(chapter 4); Sprenger and Milsom 2021b (submitted)(chapter 5)). The enhanced HCVR in steady state hibernation appears to be affected by changes in body temperature associated with changes in state (Webb and Milsom 2017; Sprenger and Milsom 2021 (submitted)(chapter 4)). In the present study we sought to determine whether the LC (a central chemoreceptor site) plays a role in the changes to the HCVR associated with hibernation. We hypothesized that the LC would not contribute to basal ventilation but would contribute to the HCVR promoting increases in tidal volume in euthermic squirrels and contribute to the enhanced HCVR in hibernating squirrels by enhancing the increase in breathing frequency. Our data show that the LC has modest effects on breathing pattern but does not contribute significantly to establishing levels of basal ventilation or the HCVR in hibernating animals and only contributes to the HCVR in euthermic animals. Our data also show that the LC lesion significantly reduced the increase in \dot{V}_E in unilaterally and bilaterally lesioned euthermic animals when breathing 5% CO₂ (~10% increase compared to a 45% increase in LC sham animals and 7% CO₂ (~25% increase compared to a ~60-75% increase in LC sham animals) gas mixtures. Thus, the elevated HCVR seen in hibernation is not due to temperature or state dependent changes in LC input.

Placement of the sham injection cannula had significant effects on normocapnic \dot{V}_E and \dot{V}_{O_2} in hibernating animals implicating a role of the PbC in the regulation of metabolic depression and the control of hibernation state.

6.5.1 6-OHDA Lesions

In the present study, 6-OHDA injection substantially reduced the number of cells in the LC region in both unilateral and bilateral lesioned animals. We first determined the region of the LC via TH staining in a pilot study, then used this pre-determined region to count cresyl violet stained cells. In unilaterally lesioned animals, 6-OHDA significantly reduced the number of cells on the lesion side by ~62% compared to the side that was left intact (fig. 6.5). Bilateral LC lesion resulted in a reduction of ~71% of cells in the region of the LC compared to control animals. Biancardi et al. 2008 also used 6-OHDA to bilaterally lesion the LC in vivo in rats and reported a loss of 88% of TH positive cells in the LC. 6-OHDA may also have affected other neurons

(Nattie & Li, 2009) in the region of the LC. Interestingly, unilateral and bilateral lesions of the LC produced similar changes in both pattern and magnitude (see following sections). This is consistent with other studies where unilateral and bilateral lesions produced similar results (Biancardi *et al.*, 2008, 2010) (de Moreno *et al.*, 2010; Silva *et al.*, 2017).

6.5.2 *Effects of Cannula Placement*

In the present study, insertion of the re-entrant cannula and sham injection of vehicle during surgery (sham injection) produced only minor changes in breathing in 13-lined ground squirrels. Total \dot{V}_E in sham squirrels in normocapnia (~ 100 ml/min) was similar to that of control animals as well as with previous reports for this species (Sprenger and Milsom 2021a (submitted)(chapter 4)) (~ 108 ml/min). However, the respiratory pattern was altered. Specifically, sham animals had a significantly lower f_R and slightly (but insignificantly) higher V_T in normocapnia. Total \dot{V}_E was also unaffected by a sham injection into the LC in rats in normocapnia although in rats the breathing pattern was also unaffected (Biancardi *et al.* 2008; Gargaglioni *et al.* 2010).

Sham injection of vehicle into the LC or the PbC, as well as insertion and withdrawal of the cannula with no injection, however, all had significant effects on both the O_2 consumption rate and ventilation of animals in hibernation. Basal \dot{V}_E in sham animals was ~ 13 ml/min while in control animals \dot{V}_E was ~ 1.8 ml/min. The difference in \dot{V}_E was produced by significant increases in f while V_T was unchanged. Interestingly, this is opposite to the effect of the sham injection surgery in euthermic squirrels where breathing frequency was reduced.

The data suggest that these changes were due to damage to cells along the insertion track. Similar results from the PbC sham injection indicates that the changes were not due to damage to cells of the LC but to cells somewhere above the LC. That the cannula insertion with no injection had similar effects suggests that the changes were due to the insertion of the cannula itself and not the vehicle injections. The increase in total ventilation matched the increase in \dot{V}_{O_2} . As a result, there was no net effect on the ACR. The increase in \dot{V}_{O_2} raises the possibility that the damage due to the placement of the cannula reduced the ability of the animals to suppress metabolism to the same extent suggesting that they entered a lighter plane of hibernation resulting in an elevated \dot{V}_{O_2} and \dot{V}_E .

One key site along the cannula tract of the present study that has direct effects on wake-sleep state in other mammals is the pontine respiratory group (PRG; parabrachial complex (PbC) and Kölliker-Fuse nucleus (KF)). Specifically, the cannula passed through the medial region of the PbC (MPbC). The PbC has been implicated in the regulation of sleep and arousal state in rats via the ascending arousal system. The connectivity of the PbC to the ascending arousal system is well established (Saper & Loewy, 1980; Fulwiler & Saper, 1984; Krukoff *et al.*, 1993), and it has been shown that rats enter a comatose state and fail to arouse after parabrachial lesion (Fuller *et al.*, 2011; Martelli *et al.*, 2013). Further, systemic injection of MK-801 (NMDA-type glutamate receptor antagonist) into the fourth ventricle aroused golden mantled ground squirrels implicating NMDA-type glutamate receptors of the PRG in setting arousal thresholds (Lyman 1982; Harris and Milsom 2000; Martelli et al. 2013). The extent to which the PRG contributes to hibernation depth remains an intriguing question.

While the increases in \dot{V}_{O_2} and \dot{V}_E seem large, they are relatively small in the context of euthermic to hibernating values. \dot{V}_{O_2} was reduced by 98.9% in control animals and was still reduced by 93.1% in the LC sham animals. \dot{V}_E was reduced by 98.6 % in the control animals and 87% in the LC sham animals. These were the levels to which \dot{V}_{O_2} and \dot{V}_E fell once the animals were in steady state hibernation. Cannula placement and vehicle injections were done during the surgery and the animals subsequently entered hibernation. This suggests that they entered a lighter state of hibernation, which is consistent with observations that the depth of hibernation is not ‘all or none’ but is regulated in this species (Sprenger and Milsom 2021a,b (chapter 4 and 5)). MK-801 injection into the PbC does arouse animals fully from hibernation (Harris and Milsom, 1993), thus partial damage to the PbC would fit this scenario. The increase in ventilation was exclusively due to changes in frequency and not tidal volume. This is also consistent with the increases seen in ventilation due to CO₂ in this species in steady state hibernation (chapter 4; Sprenger and Milsom, 2021a (submitted)).

It is clear that the effect of the re-entrant cannula was far greater in hibernating squirrels compared to euthermic squirrels. Several studies show that PbC activity is state dependent, and that during sleep PbC activity decreases in NREM and becomes variable in REM (Harper & Sieck, 1980) (reviewed in Martelli et al. 2013). Thus, not only does the PbC contribute to arousal

state, but also the activity of the PbC is dependent on the state of the animal. It is possible that the differences reported here are partly derived from state dependent activity of the PbC.

In euthermia, both LC sham and control animals responded similarly to hypercapnia in both the magnitude and pattern of the response. This suggests the insertion of the re-entrant cannula had no effect on the HCVR. Similar results have been obtained in rats (Biancardi et al. 2008; Gargaglioni et al. 2010). In the present study, total \dot{V}_E increased with increasing levels of hypercapnia while \dot{V}_{O_2} was unaffected. The net result was a hyperventilation in hypercapnia, produced mainly by increases in V_T with marginal changes in f_R , a pattern of change in response to CO_2 that is commonly reported in fossorial species as well as in 13-lined ground squirrels (Boggs et al. 1984; Boggs and Birchard 1989; Sprenger and Milsom 2021(submitted)(chapter 4)).

In hibernation, possibly due to the increased basal level of f_R and \dot{V}_E in normocapnic LC sham animals, hypercapnia elicited less of a relative increase in \dot{V}_E . However, it is equally possible that the reduced HCVR was due to the animals being in a lighter plane of hibernation (Boon *et al.*, 2004; Boon & Milsom, 2008). We have shown previously that the relative increase in the HCVR in hibernation is state and temperature dependent (Sprenger and Milsom 2021a,b (chapters 4 and 5)). The pattern by which \dot{V}_E increased during hypercapnia in sham animals was similar to that of control animals; it was entirely mediated by increases in f_R . Hypercapnia did not affect \dot{V}_{O_2} in either the sham or control animals. This pattern of hyperventilation produced by increases in f_R is consistent with previous reports in 13-lined ground squirrels (Sprenger and Milsom 2021a (submitted)(chapter 4)), as well as golden-mantled ground squirrels (McArthur and Milsom 1991a; Webb and Milsom 2017). It would seem then, that the re-entrant cannula had little effect on the HCVR itself.

Thus, it appears that the insertion of the cannula damaged sites somewhere along the insertion track that regulate the depth of hibernation and metabolism in hibernation. The fall in \dot{V}_{O_2} was reduced as was the corresponding level of \dot{V}_E . Our interpretation of the effects of lesions to the LC are superimposed on this new pattern.

6.5.3 Effects of LC Lesion

In euthermic squirrels, there was no difference between unilaterally and bilaterally lesioned animals for all ventilatory and metabolic measurements in normocapnia. In both cases \dot{V}_E was slightly elevated (~125ml/min) compared to sham animals (~105ml/min). LC lesion resulted in a non-significant increase in f_R , while V_T was slightly (and also non-significantly) lowered. Likewise, rats with LC lesions show no change in their breathing pattern under resting conditions either (Biancardi *et al.*, 2010; de Carvalho *et al.*, 2010; de Moreno *et al.*, 2010).

Lesion of the LC in the present study significantly reduced the HCVR equally in both unilaterally and bilaterally lesioned euthermic animals. When expressed as % Δ from baseline, the HCVR of lesioned animals was substantially lower (~20 and 25% increase) than sham and control animals (~35 and 75% increase) in animals breathing 5 and 7% CO₂ respectively. In both cases the V_T response was greatly reduced, as has also been shown in rats (Biancardi *et al.* 2008). \dot{V}_{O_2} was unaffected by hypercapnia. Thus, a 70% decrease in neurons in the bilateral LC regions resulted in a 66% reduction in the HCVR in squirrels indicating a substantial contribution of the LC to the HCVR in euthermia (Biancardi *et al.* 2008).

In hibernation, animals with bilateral lesion of the LC had a slightly, but insignificantly, reduced f , \dot{V}_E and \dot{V}_{O_2} in normocapnia compared to sham injected animals indicating that input from the LC does not contribute significantly to basal ventilation in hibernation. It is also clear from the present study that the LC plays no direct role in elevating the relative HCVR in hibernation. The addition of hypercapnia increased \dot{V}_E in bilateral LC lesioned animals and sham animals identically. Hypercapnia induced increases in f_R without changes in V_T in both sham and bilaterally lesioned animals as reported previously in intact animals of this species (Sprenger and Milsom 2021(submitted)(chapter 4)). Thus, lesion of the LC only appears to have a noticeable effect on the HCVR in euthermic or sleeping animals (Guyenet *et al.*, 1993; Li & Nattie, 2006; Biancardi *et al.*, 2010).

6.6 Conclusions

Our data suggest that the LC significantly contributes to the HCVR in euthermic 13-lined ground squirrels via increase V_T as has been shown in rats (Biancardi *et al.* 2008). Aside from

this however, the LC appears to play no significant role in establishing basal ventilation in normocapnia (euthermia and hibernation) nor the HCVR in hibernation. Placement of a re-entrant cannula into the LC in euthermic 13-lined ground squirrels caused no change in total \dot{V}_E but did change the pattern by which they breathe. Normocapnic sham squirrels with a re-entrance cannula breathed with a slower frequency. It is likely that our re-entrant cannula disrupted normal function of the PbC and that this hindered the animal's ability to reach the same depth of hibernation as control animals as indicated by a higher \dot{V}_E and \dot{V}_{O_2} when in steady state hibernation (Heller, 1979; Fuller *et al.*, 2011; Martelli *et al.*, 2013). LC lesion slightly (but insignificantly) mitigated the increased basal \dot{V}_E and \dot{V}_{O_2} seen in the hibernating ground squirrels with sham injection suggesting the lighter plane of hibernation brought on by the re-entrant cannula was partly due to disruption of the LC as well. It is clear however, that the elevated HCVR in hibernation is not due to direct modification of LC input but is derived from other sources. Data from the present study do indicate that the PRG and the reticular activating system contribute to arousal state, which does alter the HCVR in hibernation, warranting further investigation.

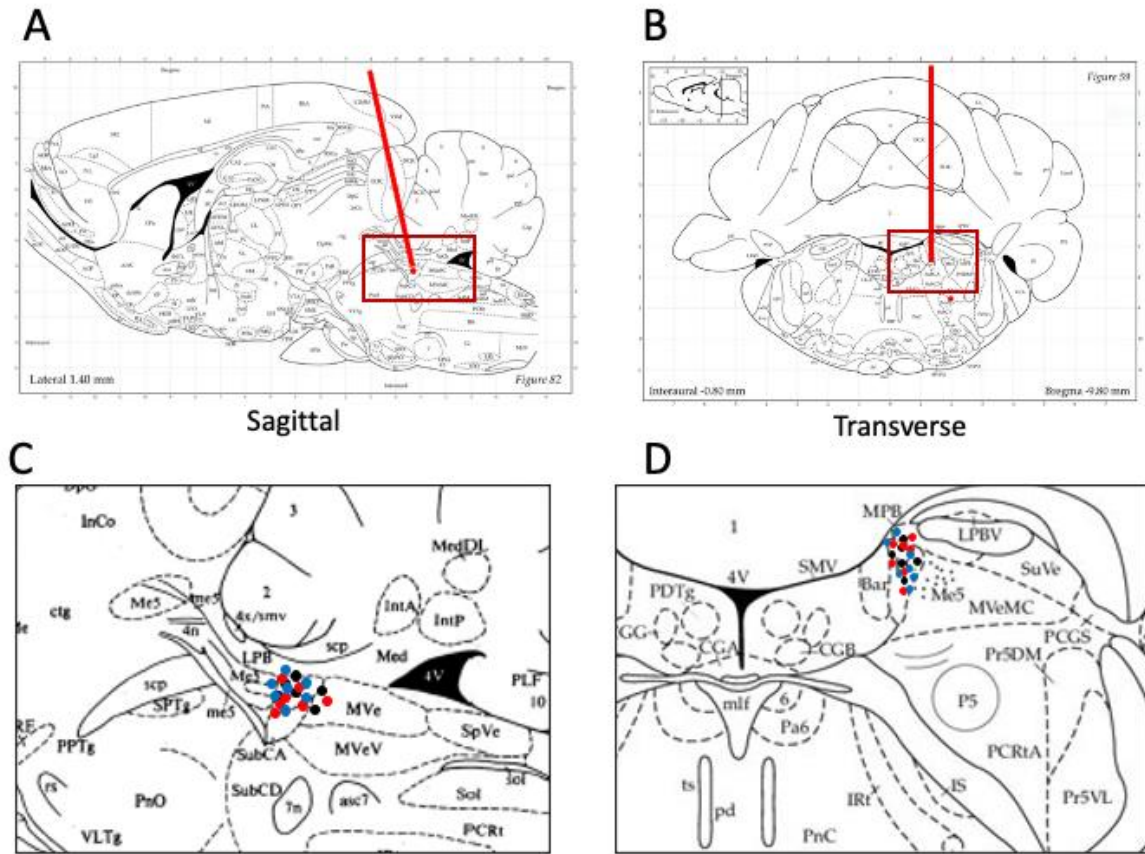


Figure 6.1 Representative diagrams from the rat atlas (for complete list of structures see; Paxinos, George, and Charles Watson. *The rat brain in stereotaxic coordinates: hard cover edition*. Access Online via Elsevier, 2006) of the cannula tract used for injections into the locus coeruleus in sagittal (A) and transverse (B) sections. Red line represents the cannula tract. The locus coeruleus was located ± 1.2 mm from midline, -7.2 mm ventral to the skull surface, and -0.8 to -1.0 mm from the interaural line (IA). Transverse section reveals sites that the cannula passed through including: dorsal cortex of the inferior colliculus (DCIC), exterior cortex of the inferior colliculus (ECIC), waist subnuclei (PBW), and ventral part of the lateral parabrachial nucleus (LPBV). Sagittal section reveals other sites the cannula passed through: lateral parabrachial nucleus (LPB), mesencephalic trigeminal nucleus (Me5) and small sections of the cerebellum. Red boxes indicate the approximate area focused in on in the sagittal (C) and transverse (D) planes. Both focused areas indicate cannula tip location for LC sham (black dots), unilateral LC (blue dots), and bilateral LC (red dots) injections.

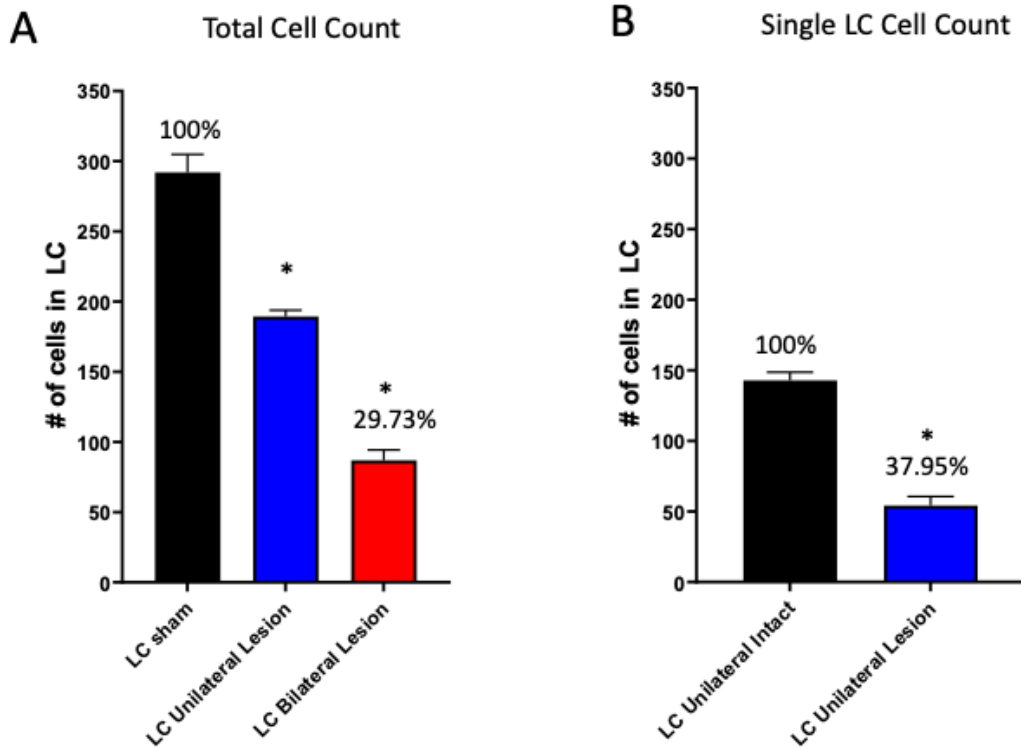


Figure 6.2 Number of live cells in the derived outline of the tyrosine hydroxylase positive locus coeruleus (LC) region determined by cresyl violet stains in LC sham (black bars), LC unilateral lesioned (blue bars), and LC bilateral lesioned animals (red bars) (A). Number of live cells in unilaterally lesioned animals comparing the intact side (black bars) and the lesioned side (blue bars) (B). Error bars indicate S.E.M. * indicate significant difference from sham (A) and the intact side (B) (one-way ANOVA; dunnet's post-hoc test ($p < 0.05$)).

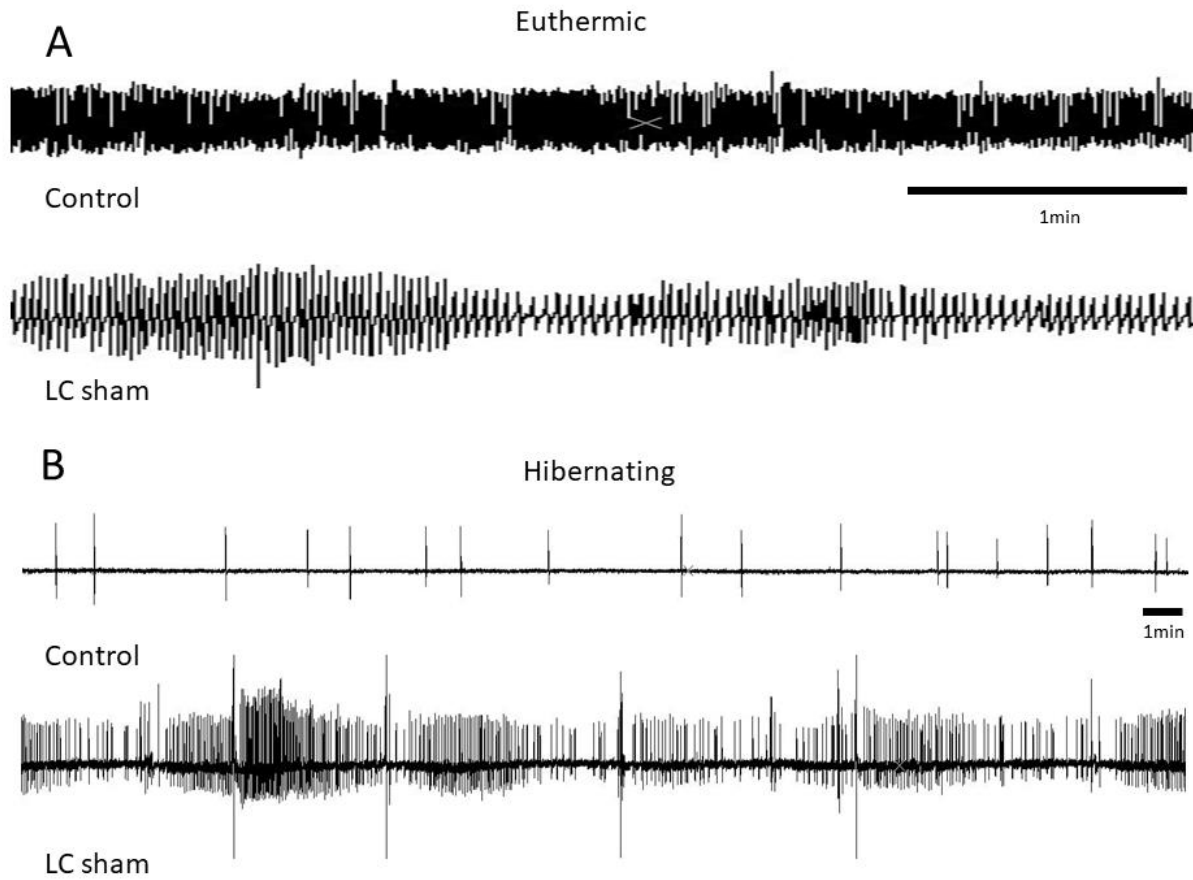


Figure 6.3 Representative breathing traces from euthermic squirrels (A) and hibernating squirrels (B) that had either no surgery (Control, top), or sham injection (bottom) in normocapnia (0% CO₂).

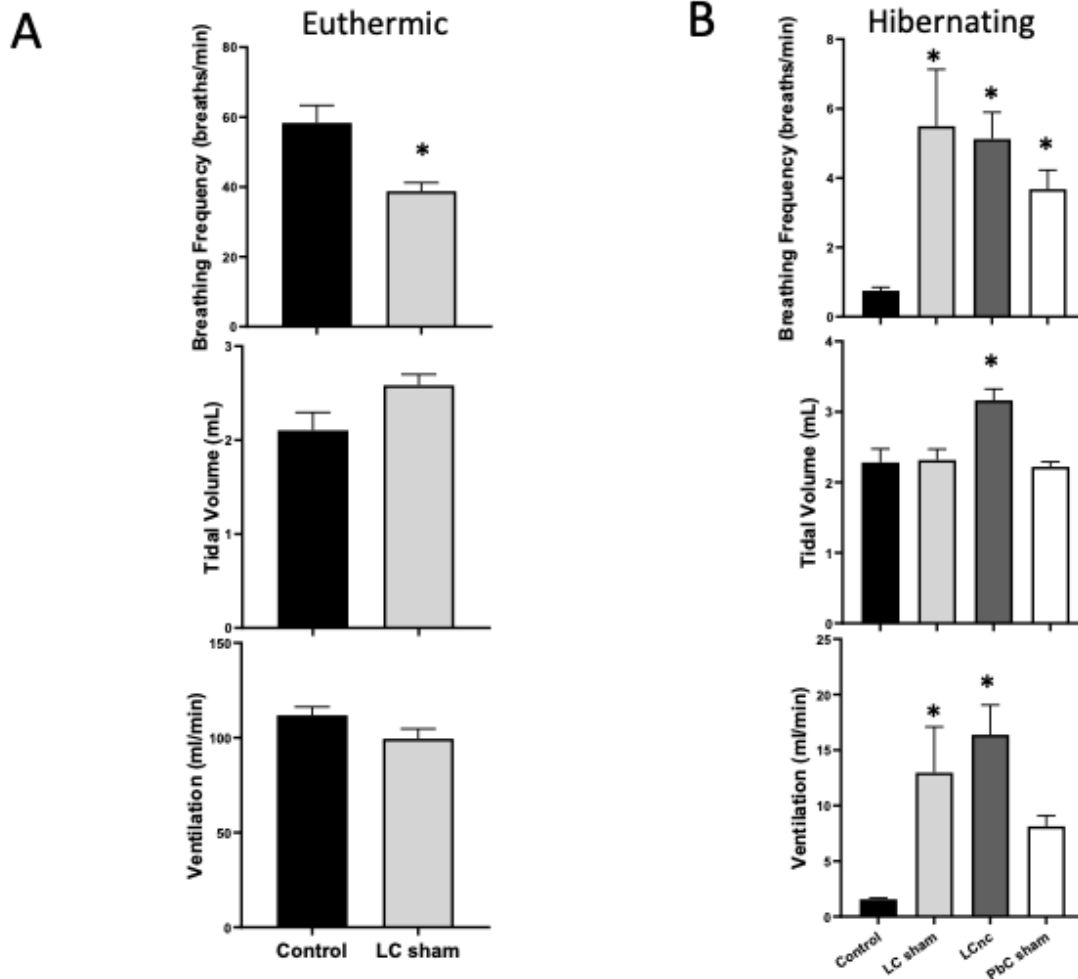


Figure 6.4 Ventilation (mL/min), tidal volume (mL/min), and breathing frequency (breaths/min) in euthermic (A) and hibernating (B) squirrels breathing normocapnia (0% CO₂) in Control (black bars), locus coeruleus (LC) sham (grey bars), locus coeruleus cannula withdrawn (LCnc) (dark grey bars), or parabrachial complex (PbC) sham animals (white bars). Error bars indicate S.E.M. * indicate significant differences from control animals (two-way ANOVA; tukeys post-hoc test (p<0.05)).

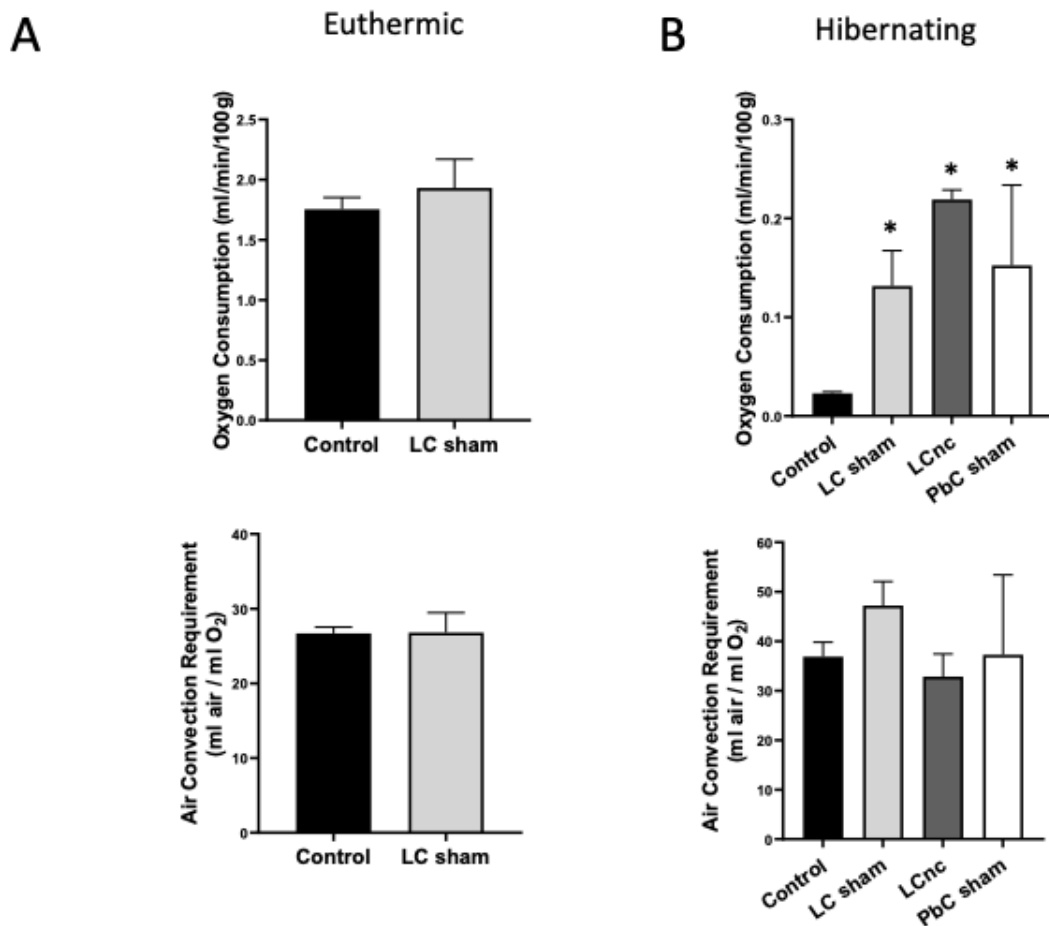


Figure 6.5 Oxygen consumption rate (mL/min/100g) and the air convection requirement (mL(air)/mL O₂) in Control (black), locus coeruleus (LC) sham (grey), locus coeruleus cannula withdrawn (LCnc) (dark grey), and parabrachial complex (PbC) sham animals (white) while in euthermia (A) and hibernation (B). Error bars indicate S.E.M. * indicate significant differences compared to no-surgery (control) animals (two-way ANOVA; tukeys post-hoc test (p<0.05)).

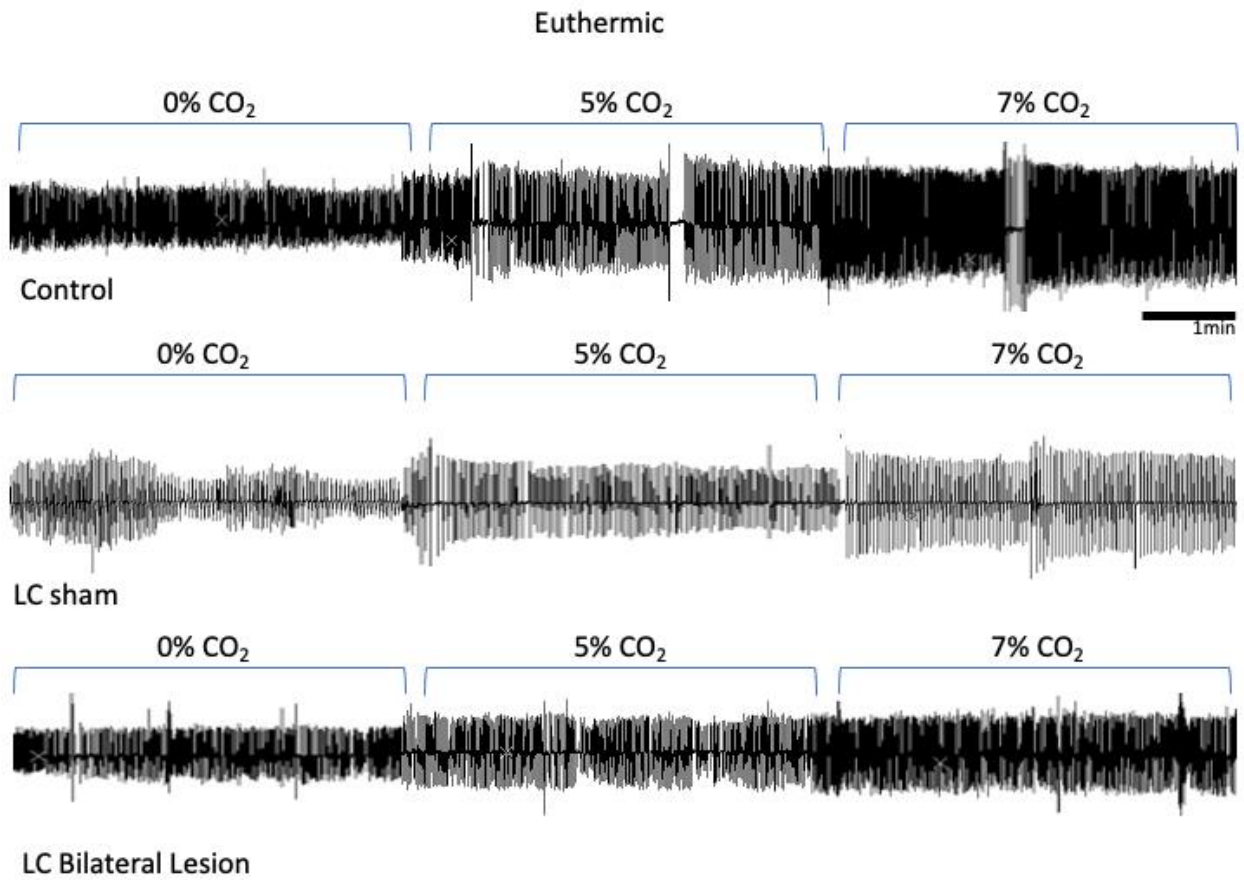


Figure 6.6 Representative breathing traces from euthermic Control squirrels (top), LC sham injection (middle), or locus coeruleus (LC) bilateral lesion squirrels (bottom) in normocapnia (0% CO₂) and 5% and 7% hypercapnia.

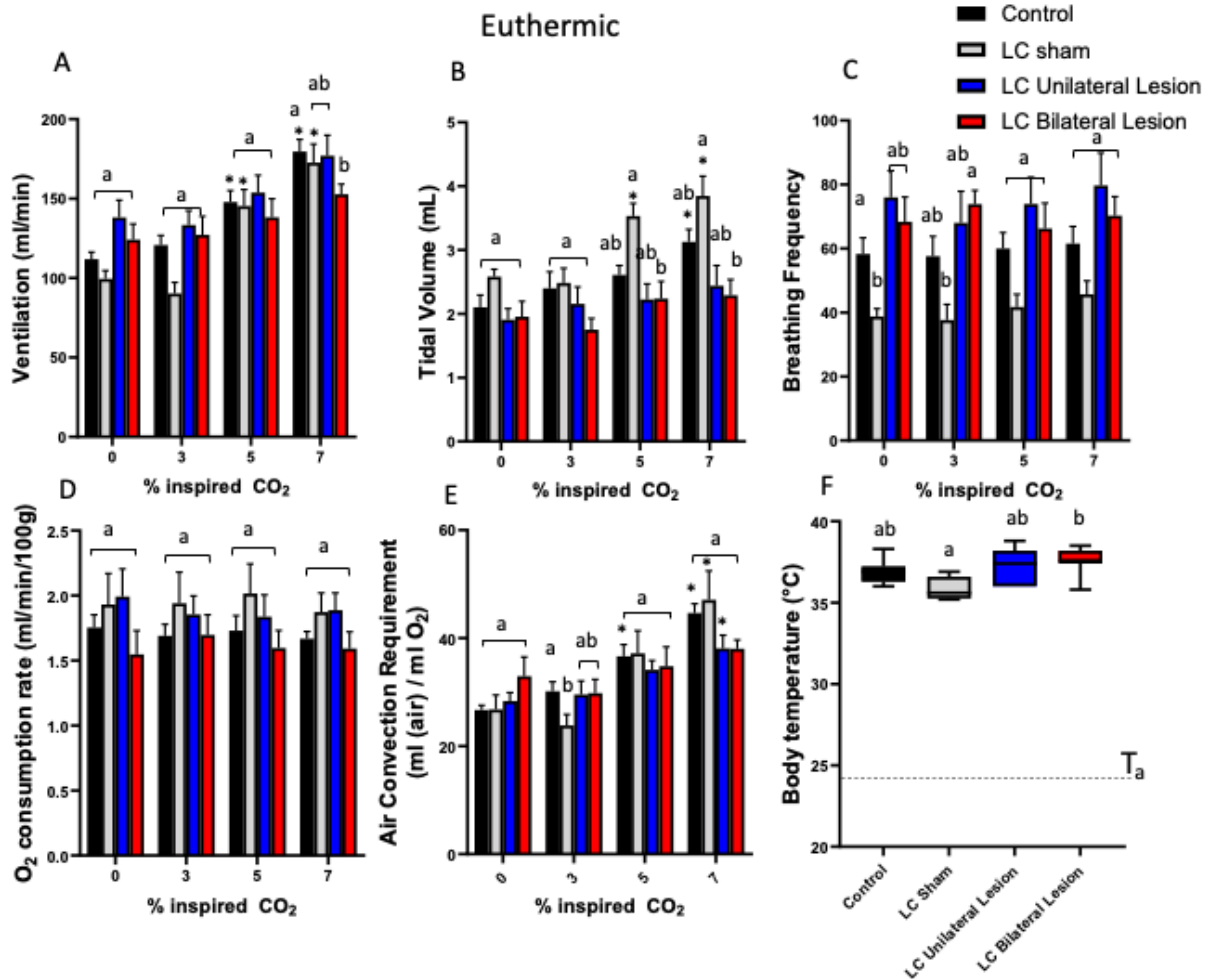


Figure 6.7 Ventilation (mL/min)(A), tidal volume (mL/min)(B), breathing frequency (breaths/min)(C), oxygen consumption rate (mL/min/100g)(D), and the air convection requirement (mLair/mL O₂)(E) in Control (black), locus coeruleus (LC) sham (grey), LC unilateral lesion (blue), and LC bilateral lesion (red) euthermic animals breathing normocapnia, and 3%, 5% and 7% hypercapnia. Body temperature (C°) in animals breathing normocapnia (F). Error bars indicate S.E.M. Letters indicate significant differences between injection group within a gas group, and * indicate significant difference from the normocapnia treatment within injection groups (two-way ANOVA; tukeys post-hoc test (p<0.05)).

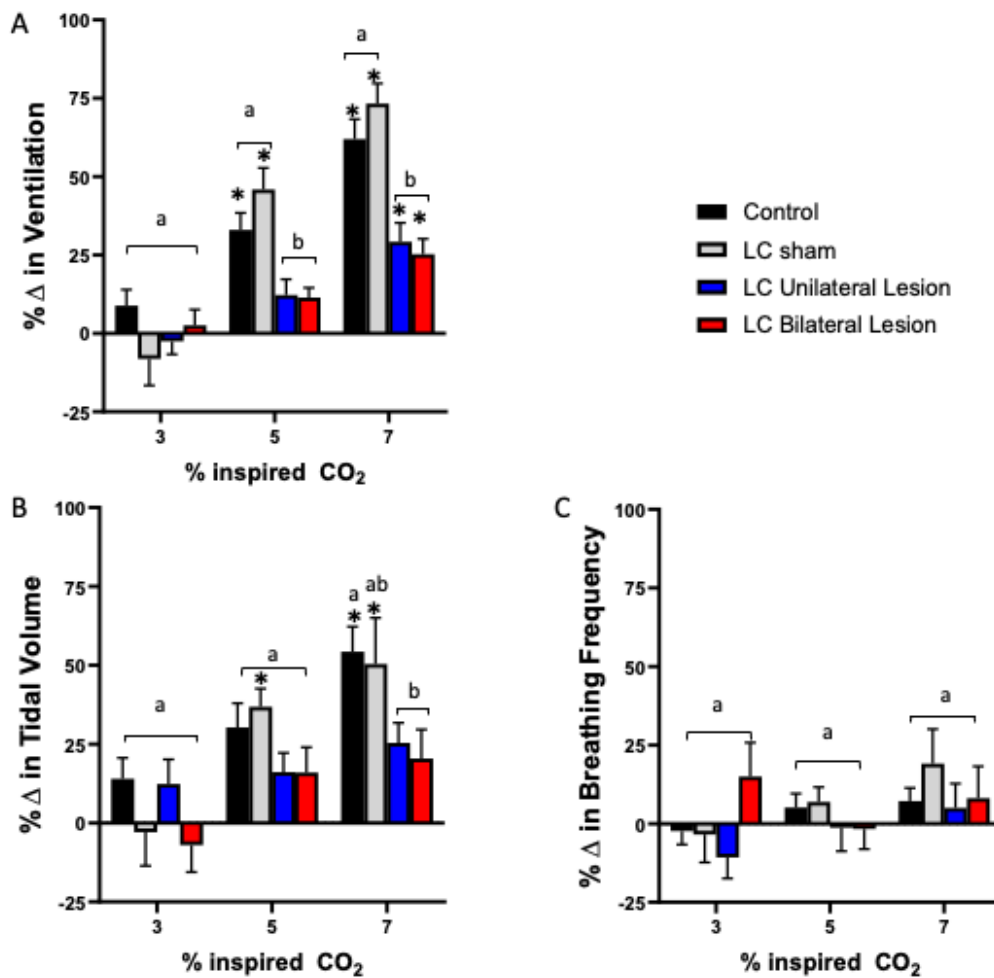


Figure 6.8 Relative increases in ventilation (A), tidal volume (B), and breathing frequency (C) from normocapnia in Control (black), locus coeruleus (LC) sham (grey), LC unilateral lesion (blue), and LC bilateral lesion (red) euthermic animals breathing 3%, 5% and 7% hypercapnia. Error bars indicate S.E.M. Letters indicate significant differences between injection group within a gas group, and * indicate significant difference from the 3% hypercapnia treatment within injection groups (two-way ANOVA; tukeys post-hoc test ($p < 0.05$)).

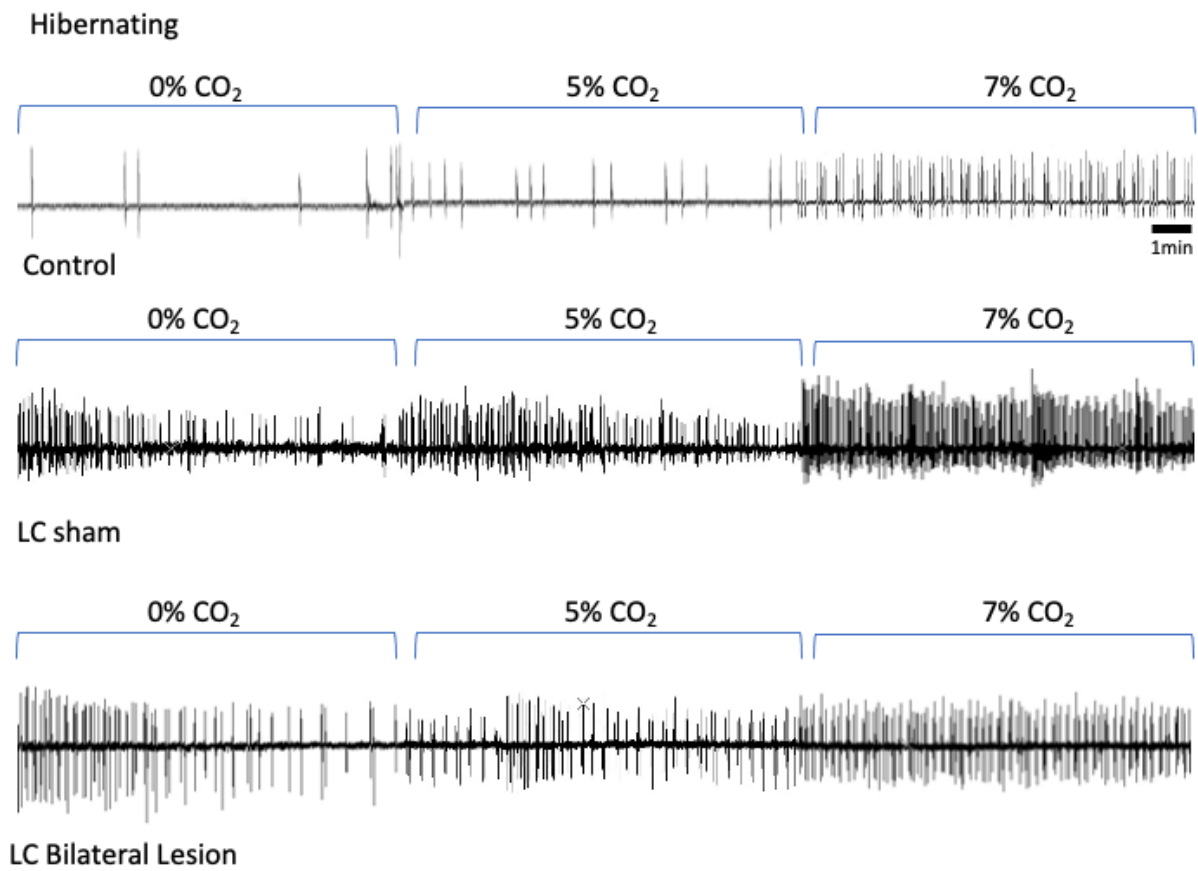


Figure 6.9 Representative breathing traces from hibernating squirrels with no surgery (control (top trace), locus coeruleus (LC) sham (middle trace), and LC bilateral lesion squirrels (bottom) in normocapnia (0% CO₂) and 5% and 7% hypercapnia.

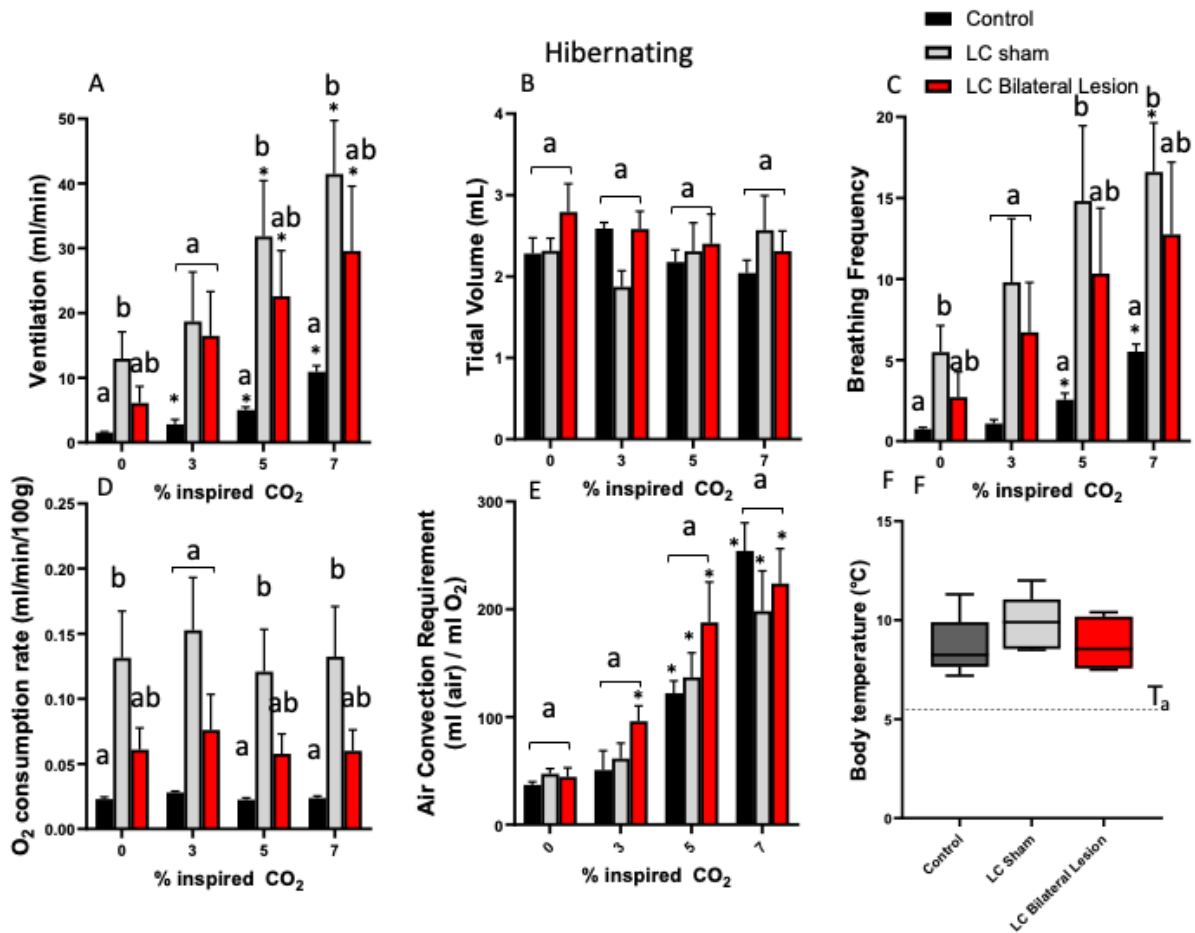


Figure 6.10 Ventilation (mL/min)(A), tidal volume (mL/min)(B), breathing frequency (breaths/min)(C), oxygen consumption rate (mL/min/100g)(D), and the air convection requirement (mL(air)/mL O₂)(E) in Control (black), locus coeruleus (LC) sham (grey), and bilateral LC lesion (red) hibernating animals breathing normocapnia, and 3%, 5% and 7% hypercapnia. Body temperature (C°) in animals breathing normocapnia (F). Error bars indicate S.E.M. Letters indicate significant differences between injection group within a gas group, and * indicate significant difference from the normocapnia treatment within injection groups (two-way ANOVA; tukeys post-hoc test (p<0.05)).

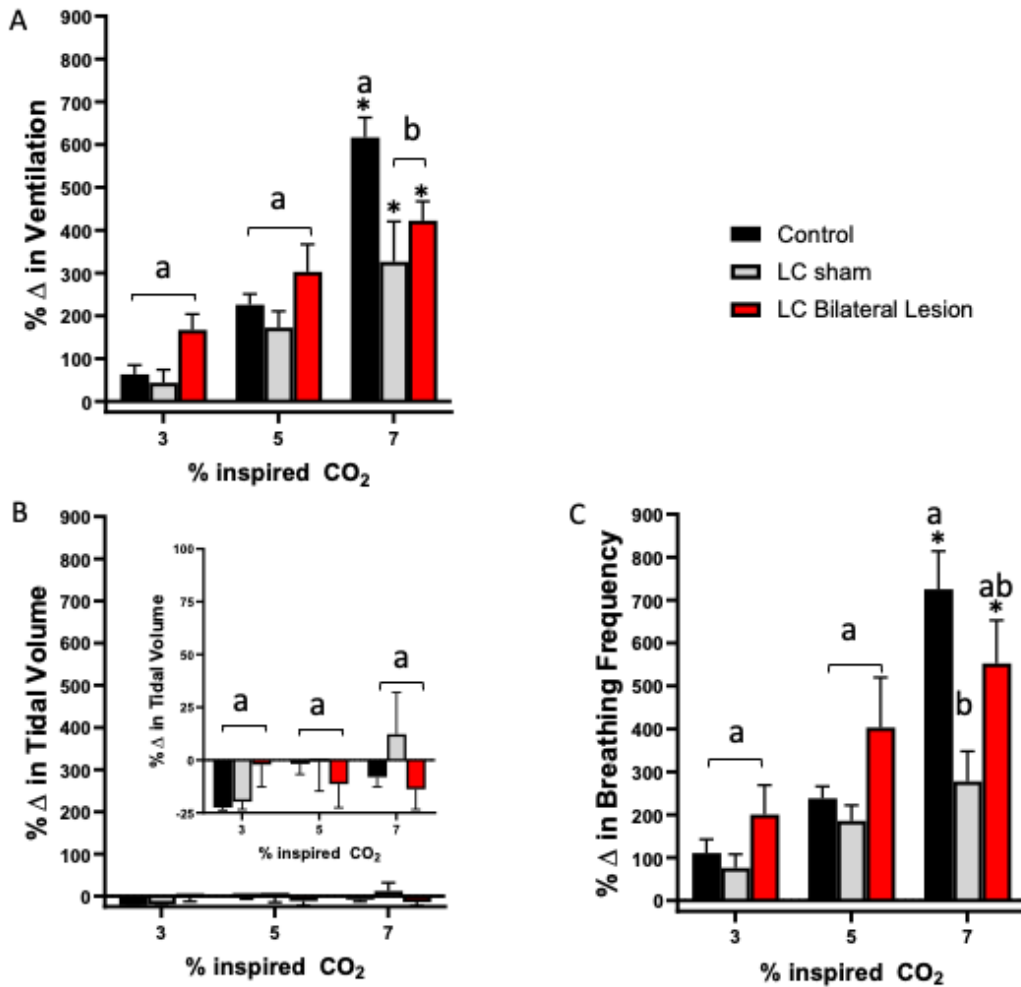


Figure 6.11 Relative increases in ventilation (A), tidal volume (B), and breathing frequency (C) from normocapnia in Control (black), locus coeruleus (LC) sham (grey), and LC bilateral lesion (red) hibernating animals breathing 3%, 5% and 7% hypercapnia. Error bars indicate S.E.M. Letters indicate significant differences between injection group within a gas group, and * indicate significant difference from the normocapnia treatment within injection groups (two-way ANOVA; tukeys post-hoc test ($p < 0.05$)).

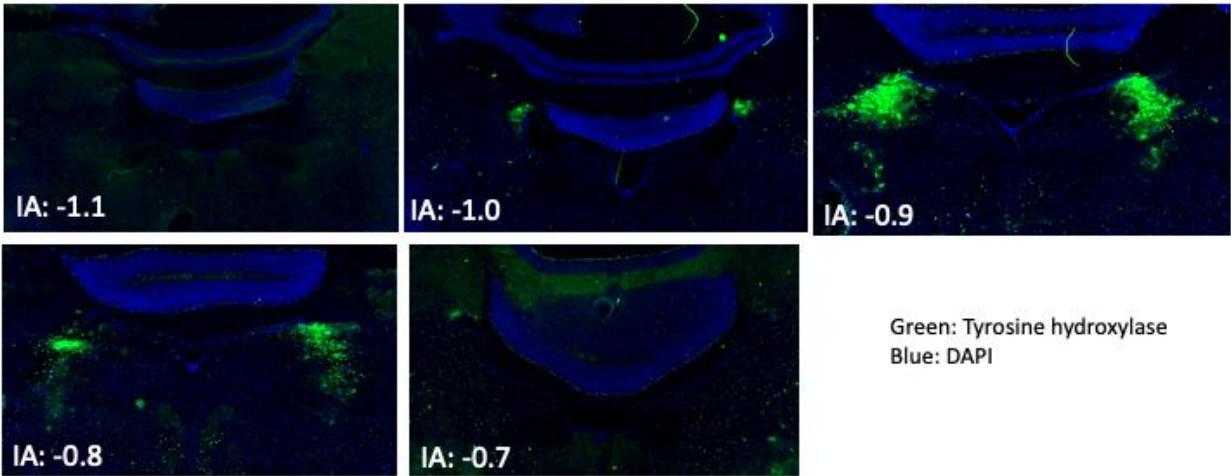


Figure 6.12 Tyrosine hydroxylase (TH; green) and DAPI (blue) staining over the range of the locus coeruleus (-1.1 to -0.7mm from the interaural line (IA)) showing positive TH at its most concentrated from -1.0 to -0.8mm from interaural line.

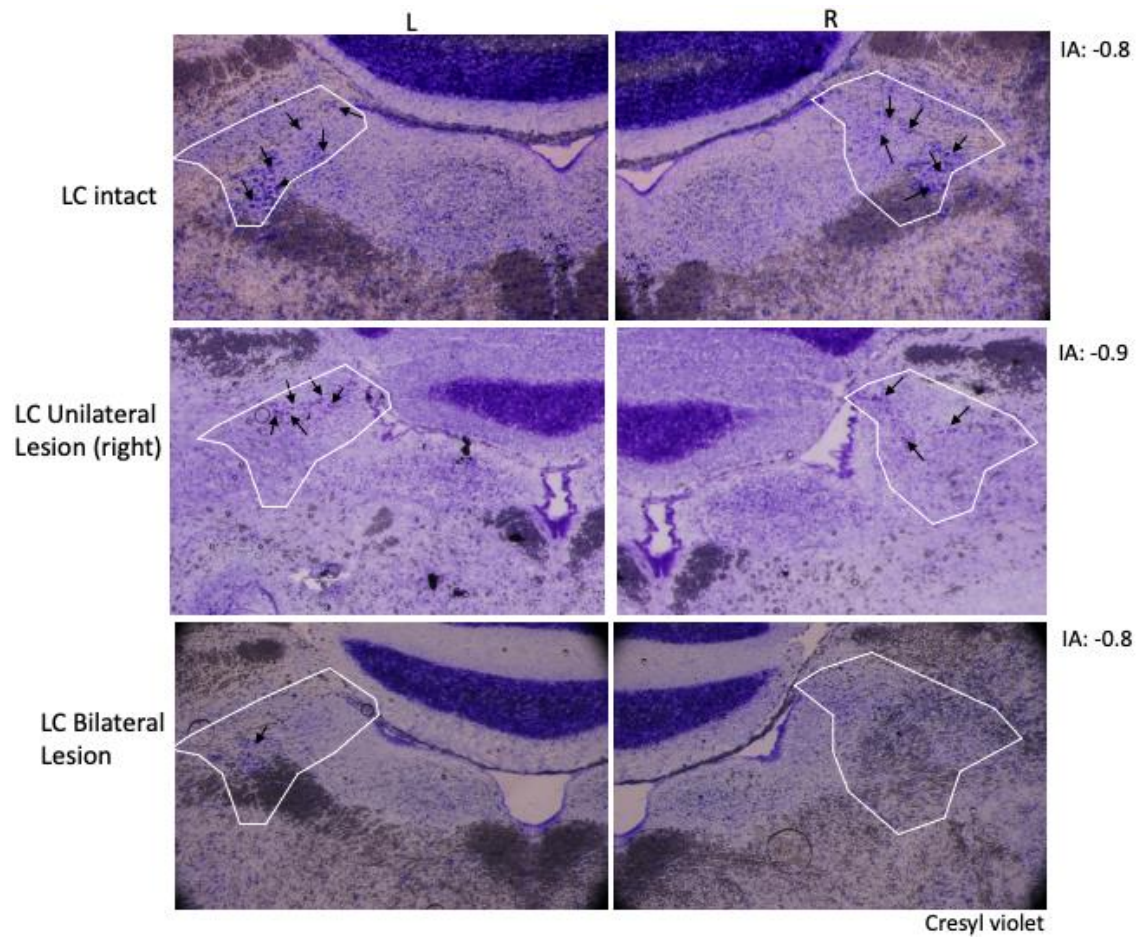


Figure 6.13 Representative cresyl violet stains from sham injected animals (top row; -0.8mm from interaural line), unilaterally lesioned animals (middle row; -0.9mm from interaural line) and bilaterally lesioned animals (bottom row; -0.8mm from interaural line). Representative cells indicated with black arrows, and derived tyrosine hydroxylase positive region of the LC indicated by white outlines.

Chapter 7: General Discussion and Conclusions

In my thesis I show that the ventilatory response to hypercapnia (HCVR) is influenced by developmental stage, fossoriality (chapters 2 and 3), as well as temperature and arousal state (chapters 4, 5, and 6). In both non-fossorial and fossorial mammals, adult sensitivity to hypercapnia is not innate at birth, but rather developed over the first 30 days of postnatal development (chapter 2). Further, I demonstrate that in two fossorial species (13-lined ground squirrel and golden-Syrian hamster), the HCVR on the day of birth is actually greater than that of a non-fossorial rodent (Sprague-Dawley rat) before developing to a more blunted response during adulthood. In all species examined in this thesis, development in a burrow environment produced only transient changes to the HCVR that did not persist upon removal from the burrow conditions (chapter 3). The chapters investigating the development of the HCVR suggest 1) a strong genetic component in the developmental trajectory of the adult HCVR in mammals and 2) that the postnatal change in the HCVR is a consequence of neurochemical development. My thesis also demonstrates a condition in which the HCVR is altered after development. In 13-lined ground squirrels, the HCVR is greatly enhanced in hibernation, and this enhanced response is plastic depending on state and temperature (chapter 4). Indeed, hibernation likely presents a period in which there is a greater reliance on CO₂ regulation in the HCVR given evidence of CO₂ retention contributing to metabolic suppression during entrance, as well as the loss of the hypoxic ventilatory response during steady state hibernation. I show a period of CO₂ retention at the onset of arousal just prior to metabolic rate falling, during which the sensitivity to hypercapnia fell leading to transient hypoventilation (chapter 5). Further, the change in the HCVR in hibernation is correlated with metabolic rate during entrance and arousal from hibernation rather than body temperature. The regulation of hypercapnic sensitivity then must be derived from a change in chemoreceptor input, or the central integration of that input. One main central chemoreceptor (the locus coeruleus), appears to contribute to the HCVR only in euthermia (chapter 6) and thus the modification of CO₂ sensitivity through a hibernation bout must occur due to changes elsewhere. Chapters investigating the HCVR through a hibernation bout do suggest that the changes to CO₂ sensitivity are tightly regulated. Thus, the nature of the changes in CO₂ sensitivity in development and hibernation are different, but where those changes are derived from may be similar. Here I will briefly integrate my findings with the relevant

literature to comment on the conditional nature of the HCVR and examine unanswered questions.

7.1 CO₂ and development

It is well known that fossorial mammals (and several fossorial avian species) have an attenuated ventilatory response to hypercapnia compared to species that do not burrow (Boggs *et al.*, 1984a; Tenney & Boggs, 1986; Boggs & Birchard, 1989). Non-fossorial rodents are not born with their adult response, but rather they develop it (Stunden *et al.*, 2001; Putnam *et al.*, 2005; Bavis *et al.*, 2006; Davis *et al.*, 2006). One well studied species, the Sprague-Dawley rat, develops a HCVR in a distinct way, progressing through three phases over postnatal development. At birth (phase-I) the HCVR is elevated, but this strong response quickly dissipates over the next 2 days after birth ushering in a period of CO₂ insensitivity (phase-II). Around postnatal days 10-14, the HCVR begins to return and reaches adult levels at ~P18-20 (Stunden *et al.*, 2001; Putnam *et al.*, 2005). Postnatal development of the HCVR in other non-fossorial species consists of a modest newborn response that rises to the adult response much like the second two phases of the Sprague-Dawley rat response. Prior to my investigation, it was not known how the hypercapnic response arose in the fossorial adult, but given that it was known to be smaller than non-fossorial rodents (Boggs *et al.*, 1984a), it begged the question of whether the adult fossorial response was a retention of the blunted period seen in Sprague-Dawley rats (Stunden *et al.*, 2001), and thus the result of similar postnatal neurochemical development, or if they are simply born with it.

Data from my thesis clearly show a pronounced HCVR in at least two newborn fossorial species, but the magnitude and postnatal developmental pattern of the HCVR differs between them. In golden-Syrian hamsters, the newborn HCVR is strikingly high (~250% increase to 7% hypercapnia) compared to both 13-lined ground squirrels (~175%) and Sprague-Dawley rats (~100%). Further, the adult response in hamsters develops late (P18, like Sprague-Dawley rats) while ground squirrels reach their adult response much sooner (P7-10). Thus, while ground squirrels do appear to retain the second phase of the Sprague-Dawley triphasic pattern, golden-Syrian hamsters slowly develop their attenuated response over time. Given my data however, it seems likely that 1) fossorial rodents are not born with the blunted adult response but develop it

and 2) that the developmental time course differs among fossorial species. The mechanistic basis of these differences remains unclear. But, owing to the observation that the adult response is not present at birth, postnatal neurochemical development of the HCVR in fossorial mammals is likely.

The mechanisms behind the development of the HCVR in mammals is most thoroughly studied in Sprague-Dawley rats. Extensive work has been done in this species examining the development of both central and peripheral chemoreceptors, and the pattern by which the HCVR develops appears to be a combination of changes in both groups (Bamford *et al.*, 1999; Liu & Wong-Riley, 2005, 2008; Wang & Bisgard, 2005; Wong-Riley & Liu, 2005; Gao *et al.*, 2011; Wong-Riley *et al.*, 2013, 2019). There exists a transient preeminence of inhibitory neural pathways over excitatory pathways during the blunting (phase-II) in several key central pattern generators and chemoreceptors of Sprague-Dawley rats (Wong-Riley *et al.*, 2019). After this, the imbalance reverses during phase-III and, at about the same time, carotid body sensitivity to hypercapnia also rises (Bamford *et al.*, 1999; Wang & Bisgard, 2005; Wong-Riley *et al.*, 2019). Thus, the changes in the HCVR during development in this species appear to be a consequence of neural development which presents a period of insensitivity to hypercapnia that is innately determined (Wong-Riley *et al.*, 2019). The necessity of this period of neurochemical development appears to be strong as perinatal hyperoxia or carotid body denervation (after P10) merely delays and sometimes prolongs it but does not eliminate it (Liu & Wong-Riley, 2003; Wong-Riley *et al.*, 2019). Yet, interestingly, this critical period renders the animal vulnerable to external stressors and is described as one of three stressors associated with sudden infant death syndrome (SIDS) in humans (Wong-Riley *et al.*, 2019). Whether neurochemical development is similar among mammalian species and the extent to which this critical period exists in other species remains an intriguing question. Fossorial mammals present an interesting model where they develop in conditions that normally would be described as external stressors (hypercapnia and hypoxia). Data from this thesis describes a patterned development of the HCVR in at least two species of fossorial mammals suggesting that these species also go through periods of postnatal neurochemical development modified to suit the fossorial lifestyle.

Raising non-fossorial rodents in hypercapnia and hypoxic hypercapnia (simulated burrow conditions) has shed light on the intrinsic neurochemical development of the HCVR.

Development in these conditions allows insight into the developmental plasticity of the HCVR as well as how fossorial mammals develop their attenuated adult HCVR (Birchard *et al.*, 1984; Bavis & Kilgore Jr, 2001; Bavis *et al.*, 2006, 2018; Bavis & MacFarlane, 2017). The HCVR is known to be plastic in developing Sprague-Dawley rats in that chronic hypercapnia during postnatal development does attenuate the response while the pattern of development (triphasic response) remains (Bavis *et al.* 2006; Sprenger and Milsom 2021a(chapter 4)). Further, this attenuation is removed when the animals are removed from the chronic hypercapnia revealing that 1) the HCVR in Sprague-Dawley rats is primarily genetically determined, and 2) the fossorial response cannot be produced in a non-fossorial species by simulated burrow conditions. The extent to which the development of the fossorial HCVR is affected by the burrow conditions is clearly demonstrated in this thesis. Hypercapnia merely reduces the time it took for both 13-lined ground squirrels and golden-Syrian hamsters to reach their adult response. However, this should be confirmed by removing chronic hypercapnia in the middle of postnatal development (~P10-15), which was not done in my study. But, by adulthood, it is clear that the burrow conditions do not alter the HCVR permanently. Further, hypercapnia as an external stressor (at ~3% inspired CO₂) is not enough to produce mortality during the period of vulnerability in any rodent species exposed to it (Birchard *et al.*, 1984; Bavis *et al.*, 2006). This must be the case in fossorial mammals given the conditions they continually are raised in (Boggs *et al.*, 1984a). The severity of external stressors on the respiratory system that do produce mortality during the critical period likely vary.

Conclusion

Given data from my thesis I propose that 1) neurochemical development of the HCVR is common among species with differing lifestyles, but how that neurochemical development progresses may not be, and because of this 2) the pattern by which the HCVR develops is different among species. I also propose that 3) the HCVR is plastic in developing mammals depending on the environment, and 4) the HCVR has a strong genetic component driving the development of the adult response. I propose based on my thesis and previous data that the temporal alteration of the HCVR in development is not a regulated process, but rather a consequence of intrinsic neurochemical development. It remains to be seen if this also is the case for fossorial mammals, but it is likely.

Future directions

Common to many research endeavors, my examination into the development of the HCVR in fossorial rodents has raised more questions. Here I list two important future directions.

1. Determining the neurochemical development of the HCVR in fossorial species is key to understanding the nature of the pattern by which the adult fossorial HCVR arises. Extensive work on Sprague-Dawley rats has highlighted distinct changes in chemosensory networks of the brainstem which likely shape the development of the HCVR in this species. A similar examination in fossorial species would shed light on similarities or differences in the root of these developmental patterns.
2. Unexamined in my thesis, as well as many other studies on developing rodents, are blood gases. Key to understanding the development of the HCVR is knowing the magnitude by which the stimulus (pH/P_{CO2}) changes that elicits the ventilatory response. It is likely that the threshold at which a ventilatory response is elicited varies among the species I examined, thus knowing these characteristics would shed light on my observations.

7.2 CO₂ and Hibernation

CO₂ appears to play an integral role in hibernation (Snapp & Heller, 1981; Bickler, 1984; Malan, 1988; Nestler, 1990). A period of CO₂ retention at the onset of entrance into hibernation has been observed numerous times in several species (Snapp & Heller, 1981; Bickler, 1984; Nestler, 1990) where the respiratory exchange ratio (RER) drops precipitously just prior to metabolic rate falling suggesting this retention contributes, in part, to the drop in metabolic rate associated with entrance into hibernation. Body temperature begins to fall after these events suggesting a temperature independent drop in metabolic rate, or metabolic suppression with CO₂ retention as a contributing factor (Snapp & Heller, 1981; Geiser, 1988). It is unclear if the contribution of CO₂ retention at the onset of hibernation has global effects on metabolic rate, on central integrative processes regulating metabolic rate, or is merely a coincidental event, but it is most likely one of the first two possibilities (Snapp & Heller, 1981). However, this period of retention is not observed in dormice (Elvert & Heldmaier, 2000), thus there exists the possibility that different species rely more heavily on other mechanisms to lower metabolic rate. Further, in some species (Hammel *et al.*, 1968; Geiser, 1988; Szewczak & Jackson, 1992; Wilz &

Heldmaier, 2000; Zimmer & Milsom, 2001), at about the mid-point of entrance, Q_{10} values are between 2-3 suggesting that after the initial suppression, temperature effects on metabolic rate take on a larger role. In other species, metabolic rate reaches its minimum long before temperature does, and it remains low and temperature independent through the hibernation bout (Buck & Barnes, 2000; Ortmann & Heldmaier, 2000). It appears then, that the degree to which active metabolic suppression occurs, and the time course over which it occurs, varies among hibernating species. Thus, the ventilatory sensitivity to CO_2 also likely varies at the onset of entrance into hibernation depending on the overall contribution of CO_2 retention to temperature-independent metabolic suppression. On arousal, a transient spike in the RER (up to 1.2) is commonly observed as well (Bickler, 1984; Nestler, 1990), which signals a CO_2 “dump” that would effectively remove the brakes on metabolic rate (Nestler, 1990; Milsom & Jackson, 2011). Indeed, shortly after the expulsion of CO_2 , metabolic rate rises, and the arousal progresses.

I show both a transient decrease (on entrance) and increase (on arousal) in the RER in 13-lined ground squirrels as described in several other species. Further, these perturbations in the RER precede changes in metabolic rate. My thesis provides new evidence that hypoventilation likely contributes to the retention of CO_2 on entrance, and hyperventilation that contributes to the expulsion CO_2 on arousal. I also observed that lung oxygen extraction increases allowing oxygen consumption to remain steady while CO_2 production falls on entrance, with the reverse happening on arousal. The mechanism of increased lung oxygen extraction during entrance into hibernation is unknown, but one possible explanation is an increase in blood O_2 carrying capacity such as via a splenic discharge of red blood cells. In this species, temperature-independent metabolic suppression dominates the first half on entrance but when nearing minimum metabolic rate during hibernation, there is strong evidence of temperature-dependent metabolic changes. There appears to be a continuum in the level of temperature-dependent metabolic suppression observed across hibernating species during entrance into hibernation, and 13-lined ground squirrels fall in the middle using a combination of both temperature-independent and dependent metabolic suppression. Like other hibernating species (Snapp & Heller, 1981; Bickler, 1984; Nestler, 1990), the 13-lined ground squirrel uses CO_2 retention to aid temperature-independent metabolic suppression early in entrance, but the mechanism by which hypercapnia suppresses metabolic rate is unknown. However, it is clear that the sensitivity to CO_2 must shift

when the need to retain CO₂ supersedes the need to maintain CO₂/pH homeostasis (Milsom & Jackson, 2011).

Hypercapnia consistently produces a strong ventilatory response in hibernation (Endres & Taylor, 1930; Lyman, 1951; Tähti, 1975; McArthur & Milsom, 1991*a*; Harris & Milsom, 1993; Webb & Milsom, 2017). Indeed, evidence of the involvement of CO₂ in temperature-independent metabolic suppression as well as the loss of the hypoxic ventilatory response in deep hibernation presents a basis for a greater importance of CO₂. Novel to my thesis is evidence of hypercapnia insensitivity during the period when CO₂ is being retained (on entrance) and hypersensitivity during the period of CO₂ expulsion (on arousal) providing support for an altered regulation of CO₂/pH setpoint and sensitivity. During sleep, the HCVR is reduced in rodents (Burke *et al.*, 2015; Guyenet & Bayliss, 2015), thus the insensitivity seen at the onset of hibernation may be caused by a shift in state. There still exists a component of increased difficulty expelling CO₂ considering CO₂ is more soluble at colder temperatures, but at least for entrance, these events occur before body temperature changes. Interestingly, PCO₂ in hibernation is generally reported to be lower (~35 compared to ~42 Torr) yet the animals are relatively acidotic given the change in body temperature and temperature-dependent shift in neutral pH (Malan *et al.*, 1973; Malan, 1977; Bharna & Milsom, 1993). How this relates to the sensitivity to hypercapnia in hibernation is unclear.

Following the initial onset of entrance and arousal, the HCVR rises as the entrance into hibernation progresses and falls when moving to euthermia in 13-lined ground squirrels. Previous data provided compelling evidence that simply reducing temperature was not enough to increase the HCVR, suggesting the change in the HCVR was due to other physiological factors associated with hibernation (Zimmer & Milsom, 2004). However, a more recent study showed that cooling hibernating golden-mantled ground squirrels from 7°C to 5°C reduces the HCVR (Webb & Milsom, 2017). Data from my thesis (chapter 4) show that cooling hibernating 13-lined ground squirrels over a larger range also influences the HCVR. But when tracking the HCVR during entrance and arousal, it is clear that it changed with metabolic rate (state) and not temperature (chapter 5). Interestingly, the change to the elevated HCVR during entrance occurs around the time that temperature-dependent suppression is seen late in entrance, and similarly, the HCVR falls shortly after the CO₂ “dump” finishes during arousal. In relation to this,

metabolic rate does change in steady-state hibernation when body temperature changes in 13-lined ground squirrels suggesting that metabolic rate and state drive the change in the HCVR. Additionally, changing temperature in all cases (entrance, steady-state hibernation, and arousal) alters breathing pattern (Webb & Milsom, 2017). Thus, the exact effector (temperature, state, or breathing pattern) that changes the HCVR remains unclear, but the data suggest that temperature is not playing a direct role in modulating the HCVR but rather an indirect role (Zimmer & Milsom, 2002a; Webb & Milsom, 2017). In support of this is the shift in the HCVR on entrance that comes before any noticeable change in body temperature (chapter 5), the animals may be sleeping (Heller, 1979), but EEG examination is needed to confirm this. The mechanism of HCVR modulation (by temperature, state, or some other effector) remains intriguing and largely unstudied. However, it is likely that the change in CO₂ sensitivity during entrance into hibernation is the result of a regulated change in either chemosensory input, or central integration of these inputs to fit the current need to regulate CO₂.

Several central sites may contribute to the changes in the HCVR observed in hibernating mammals. It is unlikely that the peripheral chemoreceptors (carotid bodies) contribute to the change as denervation of them does little to the overall HCVR in golden-mantled ground squirrels (Webb & Milsom, 2017). One key site of interest to me is the pontine locus coeruleus (LC). This site is a known central chemoreceptor that is also part of the reticular activating system (RAS) (Feldman, 1986; Drew *et al.*, 2007; Gargaglioni *et al.*, 2010). Thus, when examining effect of state on the CO₂ response, the LC provides a prime target given its role in state determination. Data from my thesis however reveal that the LC only contributes to the HCVR in euthermia and not hibernation, and so the change in the regulation of CO₂ sensitivity in hibernation is likely derived elsewhere (discussed below), but disruption to basal ventilation in hibernation makes this conclusion difficult to make.

Unexpectedly, I show large changes in basal ventilation in hibernating animals with sham cannulas implanted into the brainstem, which may serve to shed light on the role of state on the HCVR in hibernation. It is possible that disruption of the parabrachial complex (PBC; part of the midbrain reticular formation (MRF)) contributes to this as the cannula tract I use goes through it. Basal ventilation and metabolic rate are both substantially higher in sham animals (and animals with the cannula specifically placed in the PBC) suggesting that disruption of the MRF alters the

depth of hibernation in which the animals are able to attain. Sham animals in my study are likely still in a hibernating state, considering that the overall reduction in metabolic rate (~93%) and ventilation (86%) from euthermia is still very large. But this also highlights the shift in the depth of hibernation considering the reduction of metabolic rate (99%) and ventilation (98.5%) are greater in control animals. Indeed, the PBC is known to contribute substantially to arousal state (Fuller *et al.*, 2011), and previous data in golden-mantled ground squirrels showed that MK-801 injection (NMDA type glutamate receptor antagonism) into the MBF caused arousal from hibernation (Harris & Milsom, 2003). This fits the explanation that the increased basal ventilation in my study was in response to an increased metabolic rate due to the animals being in a lighter depth of hibernation brought on by PBC disturbance. Interestingly, the HCVR is also lower in sham animals compared to animals with no surgery in hibernation corroborating a role of state in the HCVR during hibernation. Specifically, arousing animals (chapter 5) lose their elevated HCVR within minutes of the onset of arousal. Thus, it is possible that animals with disruption to the MBF (or more specifically the PBC) (chapter 6) were not in deep hibernation contributing to the lower HCVR observed. This is further corroborated by the reduction in the HCVR I show in hibernating animals cooled from 7°C to 5°C (minimum defended body temperature) in chapter 4 and in golden-mantled ground squirrels (Webb & Milsom, 2017) where state likely is shifting out of deep hibernation in preparation for arousal.

Because of the disruption to either the MBF or RAS, the contribution of the LC to the HCVR in hibernation is not totally clear. However, one key piece of evidence suggests that it does not contribute in hibernation. If it is true that MBF disruption results in the animals not entering as deep of hibernation, then the role of the LC should become more apparent. However, this is not the case as LC lesion does not reduce the HCVR compared to sham animals. Thus, it is likely that even if an approach to lesion the LC without disrupting the MBF is taken, it still will not contribute to the elevated HCVR in hibernation. What is more likely the case, is that the LC remains a contributor to the tidal volume response during hypercapnia (Biancardi *et al.*, 2010) even in hibernation and its contribution wouldn't show until late in arousal when the HCVR returned to normal (chapter 5). To confirm this, LC lesion in golden-mantled ground squirrels may be more applicable as they show an increase in tidal volume to 6% CO₂ or higher in hibernation. There still exists the possibility of a change in state with elevated hypercapnia,

but data from my thesis suggest that in the preparative state (prior to arousal) where ventilation and metabolic rate elevate, the LC does not contribute to the HCVR. Investigation into the loss of the LC contribution would be interesting, as there is a period of insensitivity to hypercapnia at the onset of arousal, thus stimulation of the LC during that period may indicate if this site is being silenced to allow for CO₂ retention. What makes this more attractive, is that BK currents and L-type Ca⁺ channels in the LC serve to “brake” the HCVR (see discussion from chapters 2 and 3), thus silencing the LC may give way to an elevated HCVR (which is seen in hibernation) if these channels become more heavily relied on in hibernation. Chemical lesion wouldn’t shed light on this, but electrical stimulation would. It is clear that several brainstem locations involved in basal pattern generation and CO₂ chemoreception require closer examination with regard to their role in the HCVR as well as arousal state, particularly the PBC and the LC during the transitional states.

I also show in my thesis a shift in the relationship between ventilation and metabolic rate throughout a hibernation bout. During the transitional states, ventilation appears to regulate oxygen consumption. Specifically, 13-lined ground squirrels in chapter 5 hypoventilate at the onset of entrance. As discussed earlier this hypoventilation appears drive CO₂ retention that contributes to temperature-independent metabolic suppression. The RER returns to normal values as the hibernation bout progresses, suggesting that the retained CO₂ remains retained. Similarly, on arousal, ventilation rises before oxygen consumption likely resulting in the expulsion of the retained CO₂ from entrance. This is supported by the observed spike in RER just prior to oxygen consumption rising. Differentially, during steady state hibernation, the opposite appears true where oxygen consumption now dictates ventilation. An elevated air convection requirement was found in golden-mantled ground squirrels (Webb & Milsom, 2017), Columbian ground squirrels (McArthur & Milsom, 1991a), and in the present thesis I show 13-lined ground squirrels also hyperventilate under normocapnic conditions. Thus, while metabolic rate is determining the level of ventilation, hibernating animals consistently hyperventilate. Despite a relative hyperventilation, metabolically produced CO₂ drives ventilation and further elevation of CO₂ (via environmental perturbation) elevates it even further, unlike at the onset of hibernation.

Conclusion

Hibernation presents a condition in which the HCVR is altered from a basal state. Based on data from the present thesis, as well as previous data I propose that in 13-lined ground squirrels a tightly regulated change in CO₂ sensitivity contributes to entrance and arousal preceding as follows: First, respiratory sensitivity to CO₂ is lowered, either by changes to central chemoreceptor input or integration of those inputs. This allows for, second, a period of hypoventilation that serves to retain CO₂ while total metabolic rate is unchanged. During this, oxygen extraction is elevated to compensate for the reduction in ventilation. Third, the retention of CO₂ (marked by a dramatic fall in RER) aids in the suppression of metabolism independent of temperature either by global metabolic suppression, or suppression of central integrative networks. Fourth, total metabolic rate falls independent of temperature (and the RER returns to normal values) until late in entrance where, fifth, temperature-dependent changes in metabolic rate take over and respiratory sensitivity to CO₂ returns and becomes elevated. Sixth, in steady state hibernation, CO₂ sensitivity is elevated but plastic depending on arousal state. Seventh, on arousal, the retained CO₂ is excreted (RER spikes). During this period, sensitivity to CO₂ is elevated until the retained CO₂ is eliminated (and RER returns to normal), after which eighth, CO₂ sensitivity falls to euthermic levels.

Future directions

My examination of the HCVR through a hibernation bout has raised more questions than answers. Here I will list four major questions derived from my thesis.

1. It is clear that a retention of CO₂ just prior to entrance into hibernation contributes to the first reductions in oxygen consumption in 13-lined ground squirrels, as well as several other species in which this phenomenon has been recorded (see chapter 5). Yet, some species show no such retention suggesting other contributing factors facilitate the reduction in metabolic rate. Common among several species as well, is temperature dependent changes in oxygen consumption particularly late in entrance when the animals are nearing a steady hibernating state. Yet, again, some species show no temperature dependent changes to metabolic rate throughout the hibernation bout. Begging to be explored more thoroughly then, is the degree to which CO₂ retention and temperature dependence contribute to the reduction in metabolic rate in hibernation.

2. The initiation into hibernation has long been coveted, yet no clear picture has been accepted. My thesis highlights one of the contributing factors (CO₂ retention), which occurs in 13-lined ground squirrels. Understanding the extent to which CO₂ retention contributes to the initiation into hibernation would shed light on the process as a whole. Vital to this, one would need to measure blood gases before and during the entrance period, as well as be able to manipulate pH/Pco₂. Evidence from my thesis supports the notion that added environmental CO₂ facilitates the drop in metabolic rate, but this is not the case for all species. The extent to which increasing or decreasing hypercapnia (measured directly from blood) affects the animal's ability to enter hibernation (either delaying or hastening the reduction in metabolic rate) would be useful.
3. It is abundantly clear in my thesis that the PbC (part of the MBF) and the RAS contribute greatly to state during hibernation. This notion is not novel, but it is in desperate need of further examination. Data from my thesis point to the PbC playing a larger role in state determination, thus selective lesion of this site would be the obvious next step. Both lesion prior to attempting entrance into hibernation, as well as during steady state hibernation would clarify the role the PbC has in determining state.
4. The LC appears to contribute very little to the HCVR in hibernation. However, the HCVR is plastic throughout the hibernation bout, thus it remains likely that chemosensitivity, the integration of signals from chemosensitive sites, or motor output from this integration is altered. Where these changes are rooted is unresolved and require further investigation. Either chemical lesion of other chemosensitive sites or simulation of these sites at different points in hibernation would be a good starting point for this endeavor.

Final remarks

In this thesis I examine two different conditions in which CO₂/pH set point and sensitivity are altered. During development, the HCVR is dramatically changed signaling a shift in CO₂/pH set point and sensitivity, and this shift is driven by neurochemical development of central chemoreceptors and respiratory pattern generators. However, the change in the HCVR is

not regulated but rather a consequence of neurochemical development that ultimately renders the postnatal respiratory system vulnerable which could otherwise be seen as a dysregulation of CO₂ status derived from these areas. Hibernation, however, presents a condition where Pco₂/pH setpoint and sensitivity is specifically altered for two main reasons: first, the contribution of changes in Pco₂/pH to temperature-independent metabolic suppression and second, the acquisition of oxygen becoming easier. Thus, CO₂/pH regulation via ventilation appears to carry more weight. Under normal resting conditions in mammals, CO₂/pH regulation predominantly drive ventilation, and numerous chemoreceptors function to maintain homeostatic Pco₂/pH levels. However, the regulation of CO₂ quickly becomes secondary should the need for oxygen rise making it evident that regulating oxygen remains the more vital process. So, while CO₂/pH status in hibernation appears to hold even more predominance, it is clear that it is being used to aid in the regulation metabolism thus altering oxygen demand. Nevertheless, CO₂/pH setpoint and sensitivity can be, and are, dramatically shifted throughout life.

Bibliography

- Adams JM & Severns ML (1982). Interaction of chemoreceptor effects and its dependence on the intensity of stimuli. *J Appl Physiol* **52**, 602–606.
- Arieli R & Ar A (1979). Ventilation of a fossorial mammal (*Spalax ehrenbergi*) in hypoxic and hypercapnic conditions. *J Appl Physiol* **47**, 1011–1017.
- Arnold W, Heldmaier G, Ortmann S, Pohl H, Ruf T & Steinlechner S (1991). Ambient temperatures in hibernacula and their energetic consequences for alpine marmots *Marmota marmota*. *J Therm Biol* **16**, 223–226.
- Bairam A & Carroll JL (2005). Neurotransmitters in carotid body development. *Respir Physiol Neurobiol* **149**, 217–232.
- Bairam A, Niane LM & Joseph V (2013). Role of ATP and adenosine on carotid body function during development. *Respir Physiol Neurobiol* **185**, 57–66.
- Ballantyne D & Scheid P (2001). Central respiratory chemosensitivity: Cellular and network mechanisms. In *Frontiers in Modeling and Control of Breathing*, pp. 17–26.
- Bamford OS, Sterni LM, Wasicko MJ, Montrose MH & Carroll JL (1999). Postnatal maturation of carotid body and type I cell chemoreception in the rat. *Am J Physiol* **276**, L875-84.
- Barnes B (1989). Freeze avoidance in a mammal : body temperatures below 0 ° c in an arctic hibernator. *Science (80-)* **244**, 1593–1595.
- Barnes BM & Buck CL (2000). Hibernation in the extreme: burrow and body temperatures, metabolism and limits to torpor bout length in Arctic ground squirrels. *Life cold 11th Int Hibernation Symp* 65–72.
- Barros RCH, Zimmer ME, Branco LGS & Milsom WK (2001). Hypoxic metabolic response of the golden-mantled ground squirrel. *J Appl Physiol* **91**, 603–612.
- Baudinette R V (1974). Physiological correlates of burrow gas conditions in the california ground squirrel. *Comp Biochem Physiol* **48**, 733–743.
- Bavis RW, Johnson RA, Ording KM, Otis JP & Mitchell GS (2006). Respiratory plasticity after perinatal hypercapnia in rats. *Respir Physiol Neurobiol* **153**, 78–91.
- Bavis RW & Kilgore Jr DL (2001). Effects of embryonic CO₂ exposure on the adult ventilatory response in quail : does gender matter ? *Respir Physiol* **126**, 183–199.
- Bavis RW & MacFarlane PM (2017). Developmental plasticity in the neural control of

- breathing. *Exp Neurol* **287**, 176–191.
- Bavis RW, Millström AH, Kim SM, MacDonald CA, O’Toole CA, Asklof K & McDonough AB (2018). Combined effects of intermittent hyperoxia and intermittent hypercapnic hypoxia on respiratory control in neonatal rats. *Respir Physiol Neurobiol* 0–1.
- Bebout DE & Hempleman SC (1999). Chronic hypercapnia resets CO₂ sensitivity of avian intrapulmonary chemoreceptors. *Am J Physiol - Regul Integr Comp Physiol* **276**, 317–322.
- Bharma S & Milsom WK (1993). Acidosis and metabolic rate in golden mantled ground squirrels (*Spermophilus lateralis*). *Respir Physiol* **94**, 337–351.
- Biancardi V, Bicego KC, Almeida MC & Gargaglioni LH (2008). Locus coeruleus noradrenergic neurons and CO₂ drive to breathing. *Pflugers Arch Eur J Physiol* **455**, 1119–1128.
- Biancardi V, da Silva LT, Bicego KC & Gargaglioni LH (2010). Role of locus coeruleus noradrenergic neurons in cardiorespiratory and thermal control during hypoxia. *Respir Physiol Neurobiol* **170**, 150–156.
- Bickler PE (1984). CO₂ balance of a heterothermic rodent: comparison of sleep, torpor, and awake states. *Am J Physiol*; DOI: 10.1152/ajpregu.1984.246.1.R49.
- Birchard GF, Boggs DF & Tenney SM (1984). Effect of perinatal hypercapnia on the adult ventilatory response to carbon dioxide. 341–347.
- Bissonnette JM & Knopp SJ (2004). Hypercapnic ventilatory response in mice lacking the 65 kDa isoform of Glutamic Acid Decarboxylase (GAD65). *Respir Res* **7**, 1–7.
- Boggs DF & Birchard GF (1989). Cardiorespiratory responses of the woodchuck and porcupine to CO₂ and hypoxia. *J Comp Physiol B* 641–648.
- Boggs DF, Kilgore DL & Birchard GF (1984a). Respiratory physiology of burrowing mammals and birds. *Comp Biochem Physiol -- Part A Physiol* **77**, 1–7.
- Boggs DF, Kilgore Jr DL & Birchard GF (1984b). Respiratory physiology and of burrowing mammals and birds. *Comp Biochem Physiol* **77A**, 1–7.
- Boon JA, Garnett NBL, Bentley JM & Milsom WK (2004). Respiratory chemoreflexes and effects of cortical activation state in urethane anesthetized rats. *Respir Physiol Neurobiol* **140**, 243–256.
- Boon JA & Milsom WK (2008). NMDA receptor-mediated processes in the Parabrachial/Kölliker fuse complex influence respiratory responses directly and indirectly

- via changes in cortical activation state. *Respir Physiol Neurobiol* **162**, 63–72.
- van Breukelen F & Martin SL (2015). The hibernation continuum: physiological and molecular aspects of metabolic plasticity in mammals. *Physiology* **30**, 273–281.
- Buck CL & Barnes BM (2000). Effects of ambient temperature on metabolic rate, respiratory quotient, and torpor in an arctic hibernator. *Am J Physiol Regul Integr Comp Physiol* **255**–262.
- Buckler KJ, Vaughan-Jones RD, Peers C, Lagadic-Gossmann D & Nye PCG (1991). Effects of extracellular pH, pCO₂, and HCO₃⁻ on intracellular pH in isolated type-I cells of the neonatal rat carotid body. 703–721.
- Burda H, Sumner R & Begall S (2007). Microclimate in burrows of subterranean rodents – revisited. In *Subterranean Rodents*, pp. 21–33.
- Burke PGR, Kanbar R, Basting TM, Hodges WM, Viar KE, Stornetta RL & Guyenet PG (2015). State-dependent control of breathing by the retrotrapezoid nucleus. *J Physiol* **593**, 2909–2926.
- Carey H V., Andrews MT & Martin SL (2003). Mammalian hibernation: cellular and molecular responses to depressed metabolism and low temperature. *Physiol Rev* **83**, 1153–1181.
- de Carvalho D, Bicego KC, de Castro OW, da Silva GSF, Garcia-Cairasco N & Gargaglioni LH (2010). Role of neurokinin-1 expressing neurons in the locus coeruleus on ventilatory and cardiovascular responses to hypercapnia. *Respir Physiol Neurobiol* **172**, 24–31.
- Clarke JA & de Burgh Daly M (1985). The volume of the carotid body and periadventitial type 1 and type 2 cells in the carotid bifurcation regions of the pregnant and lactating cat. *Anat Anz* **165**, 35–44.
- Comroe JH & Schmidt CF (1937). The part played by reflexes from the carotid body in the chemical regulation of respiration in the dog.
- Cragg BYP & Drysdale DB (1983). Interaction of hypoxia and hypercapnia on ventilation, tidal volume and respiratory frequency in the anaesthetized rat. *J Physiol* **477**–493.
- Cunningham JC, Robbins PA & Wolff CB (1986). Integration of respiratory responses to changes in alveolar partial pressures of CO₂ and O₂ and in arterial pH. In *Handbook of Physiology, Sect. 3: The respiratory system, Vol. II: Control of breathing, Part 2.*, pp. 475–528.

- Davis SE, Solhied G, Castillo M, Dwinell M, Brozoski D & Forster H V. (2006). Postnatal developmental changes in CO₂ sensitivity in rats . *J Appl Physiol* **101**, 1097–1103.
- Day T a & Wilson RJ a (2009). A negative interaction between brainstem and peripheral respiratory chemoreceptors modulates peripheral chemoreflex magnitude. *J Physiol* **587**, 883–896.
- Dempsey JA & Forster H V. (1982). Mediation of ventilatory adaptations. *Physiol Rev* **62**, 262–331.
- Donnelly DF (2005). Development of carotid body/petrosal ganglion response to hypoxia. *Respir Physiol Neurobiol* **149**, 191–199.
- Drew KL, Buck CL, Barnes BM, Christian SL, Rasley BT & Harris MB (2007). Central nervous system regulation of mammalian hibernation: Implications for metabolic suppression and ischemia tolerance. *J Neurochem* **102**, 1713–1726.
- Drorbaugh JE & Fenn WO (1955a). A barometric method for measuring ventilation in newborn infants. *Pediatrics* 81–87.
- Drorbaugh JE & Fenn WO (1955b). A barometric method for measuring ventilation in newborn infants. *Pediatrics* **16**, 81–87.
- Dzal YA, Sprenger RJ & Milsom WK (2020). Postnatal changes in O₂ and CO₂ sensitivity in rodents. *Respir Physiol Neurobiol* **272**, 103313.
- Elam M, Thorén P & Svensson TH (1981). Hypercapnia and hypoxia: Chemoreceptor-mediated control of locus coeruleus neurons and splanchnic sympathetic nerves. *Brain Res* **222**, 373–381.
- Elvert R & Heldmaier G (2000). Retention of Carbon Dioxide during Entrance into Torpor in Dormice. In *Life in the Cold*, ed. Heldmaier G & Klingenspor M, pp. 183–190. Springer Berlin Heidelberg.
- Elvert R & Heldmaier G (2005). Cardiorespiratory and metabolic reactions during entrance into torpor in dormice, *Glis glis*. *J Exp Biol* **208**, 1373–1383.
- Endres G & Taylor H (1930). Observations on certain physiological processes of the marmot. II—the respiration. *Proc R Soc B Biol Sci* **107B**, 231–240.
- Feldman JL (1986). Neurophysiology of breathing in mammals. *Compr Physiol* 463–524.
- Filosa J a, Dean JB & Putnam RW (2002). Role of intracellular and extracellular pH in the

- chemosensitive response of rat locus coeruleus neurones. *J Physiol* **541**, 493–509.
- Forster H V., Pan LG, Lowry TF, Serra A, Wenninger J & Martino P (2000). Important role of carotid chemoreceptor afferents in control of breathing of adult and neonatal mammals. *Respir Physiol* **119**, 199–208.
- Fuller P, Sherman D, Pedersen NP, Saper CB & Lu J (2011). Reassessment of the structural basis of the ascending arousal system. *J Comp Neurol* **519**, 933–956.
- Fulwiler CE & Saper CB (1984). Subnuclear organization of the efferent connections of the parabrachial nucleus in the rat. *Brain Res Rev* **7**, 229–259.
- Gao X ping, Liu Q song, Liu Q & Wong-Riley MTT (2011). Excitatory-inhibitory imbalance in hypoglossal neurons during the critical period of postnatal development in the rat. *J Physiol* **589**, 1991–2006.
- Gargaglioni LH, Hartzler LK & Putnam RW (2010). The locus coeruleus and central chemosensitivity. *Respir Physiol Neurobiol* **173**, 264–273.
- Geiser F (1987). Hibernation and daily torpor in two pygmy possums (cercartetus spp., marsupialia). *Physiol Zool* **60**, 93–102.
- Geiser F (1988). Reduction of metabolism during hibernation and daily torpor in mammals and birds: temperature effect or physiological inhibition? *J Comp Physiol B* **158**, 25–37.
- González C, Almaraz L, Obeso A & Rigual R (1992). Oxygen and acid chemoreception in the carotid body chemoreceptors. *Trends Neurosci* **15**, 146–153.
- Guyenet PG & Bayliss DA (2015). Neural Control of Breathing and CO₂ Homeostasis. *Neuron* **87**, 946–961.
- Guyenet PG, Koshiya N, Huangfu D, Verberne AJM & Riley TA (1993). Central respiratory control of A5 and A6 pontine noradrenergic neurons. *Am J Physiol - Regul Integr Comp Physiol*; DOI: 10.1152/ajpregu.1993.264.6.r1035.
- Guyenet PG, Stornetta RL & Bayliss DA (2008). The retrotrapezoid nucleus and central chemoreception. *J Physiol* **20**, 239–242.
- Hammel HT, Dawson TJ, Abrams RM & Andersen HT (1968). Total calorimetric measurements on citellus lateralis in hibernation. **39**, 341–356.
- Harper RM & Sieck GC (1980). Discharge correlations between neurons in the nucleus parabrachialis medialis during sleep-waking states. *Brain Res* **199**, 343–358.

- Harris MB & Milsom WK (1993). The ventilatory response to hypercapnia in hibernating golden-mantled ground squirrel.
- Harris MB & Milsom WK (1995). Parasympathetic influence on heart-rate in euthermic and hibernating ground-squirrels. *J Exp Biol* **198**, 931–937.
- Harris MB & Milsom WK (2003). Apneusis follows disruption of NMDA-type glutamate receptors in vagotomized ground squirrels. *Respir Physiol Neurobiol* **134**, 191–207.
- Heldmaier G & Elvert R (2004). How to enter Torpor: thermodynamic and physiological mechanisms of metabolic depression. *Life Cold Evol Mech Adapt Appl* 185–198.
- Heldmaier G, Klingenspor M, Werneyer M, Lampi BJ, Brooks SPJ & Storey KB (1999). Metabolic adjustments during daily torpor in the Djungarian hamster. *Am J Physiol - Endocrinol Metab*; DOI: 10.1152/ajpendo.1999.276.5.e896.
- Heldmaier G, Ortmann S & Elvert R (2004). Natural hypometabolism during hibernation and daily torpor in mammals. *Respir Physiol Neurobiol* **141**, 317–329.
- Heldmaier GR Steiger, T Ruf. (1993) Suppression of metabolic rate in hibernation. Pp. 545–548 in C. Carey, GL Florant, BA Wunder, and B. Horowitz, eds. *Life in the Cold: Ecological, Physiological, and Molecular Mechanisms*. West- view, Boulder, Colo.
- Heller HC (1979). Hibernation: neural aspects. *Annu Rev Physiol* **41**, 305–321.
- Hertzberg T, Hellstrom S, Lagercrantz H & Pequignot JM (1990). Development of the arterial chemoreflex and turnover of carotid body catecholamines in the newborn rat. *J Physiol* 211–225.
- Heymans, C. and JJB (1930). Sinus caroticus and respiratory reflexes. *J Physiol* **69.2**, 254–266.
- Hilaire G, Viemari JC, Coulon P, Simonneau M & Bévençut M (2004). Modulation of the respiratory rhythm generator by the pontine noradrenergic A5 and A6 groups in rodents. *Respir Physiol Neurobiol* **143**, 187–197.
- Huxtable AG, Zwicker JD, Poon BY, Pagliardini S, Vrouwe SQ, Greer JJ & Funk GD (2009). Tripartite purinergic modulation of central respiratory networks during perinatal development: The influence of ATP, ectonucleotidases, and ATP metabolites. *J Neurosci* **29**, 14713–14725.
- Ibuka N & Fukumura K (1997). Unpredictable Deprivation of Water Increases the Probability of Torpor in the Syrian Hamster. *Physiol Behav* **62**, 551–556.

- Imber AN, Patrone LGA, Li KY, Gargaglioni LH & Putnam RW (2018). The role of ca²⁺ and bk channels of locus coeruleus (lc) neurons as a brake to the CO₂ chemosensitivity response of rats. *Neuroscience* **381**, 59–78.
- Ivy CM & Scott GR (2017). Ventilatory acclimatization to hypoxia in mice: Methodological considerations. *Respir Physiol Neurobiol* **235**, 95–103.
- Jacky JP (1978). A plethysmograph for long-term measurements of ventilation in unrestrained animals. *J Appl Physiol* **45**, 644–647.
- Jacky JP (1980). Barometric measurement of tidal volume: effects of pattern and nasal temperature. *J Appl Physiol* **49**, 319–325.
- Jennings DB & Laupacis A (1982). The effect of body warming on the ventilatory response to CO₂ in the awake dog. 355–369.
- Krukoff TL, Harris KH & Jhamandas JH (1993). Efferent projections from the parabrachial nucleus demonstrated with the anterograde tracer Phaseolus vulgaris leucoagglutinin. *Brain Res Bull* **30**, 163–172.
- Kuhnen G, Petersen P & Wünnenberg W (1983). Hibernation in golden hamsters (*Mesocricetus auratus*, W.) exposed to 5% CO₂. *Experientia* **39**, 1346–1347.
- Kumar P & Prabhakar NR (2012). Peripheral chemoreceptors: function and plasticity of the carotid body. *Compr Physiol* **2**, 141–219.
- Kuwaki T, Cao WH, Kurihara Y, Kurihara H, Ling GY, Onodera M, Ju KH, Yazaki Y & Kumada M (1996). Impaired ventilatory responses to hypoxia and hypercapnia in mutant mice deficient in endothelin-1. *Am J Physiol* **270**, R1279-86.
- Leirão I.P., C.A. Silva, L.H. Gargaglioni, and G.S.F. da Silva. 2018. Hypercapnia-induced active expiration increases in sleep and enhances ventilation in unanaesthetized rats. *J Physiol* **596**:3271–3283.
- Li A & Nattie E (2006). Catecholamine neurones in rats modulate sleep, breathing, central chemoreception and breathing variability. *J Physiol* **570**, 385–396.
- Li A, Zhou S & Nattie E (2006). Simultaneous inhibition of caudal medullary raphe and retrotrapezoid nucleus decreases breathing and the CO₂ response in conscious rats. *J Physiol* **577**, 307–318.
- Lighton JRB (2008). *Measuring Metabolic Rates : A Manual for Scientists*, 1st edn. Oxford

University Press.

- Ling L, Olson Jr. EB, Vidruk EH & Mitchell GS (1997). Developmental plasticity of the hypoxic ventilatory response. *Respir Physiol* **110**, 261–268.
- Liu Q & Wong-Riley MTT (2003). Postnatal changes in cytochrome oxidase expressions in brain stem nuclei of rats: Implications for sensitive periods. *J Appl Physiol* **95**, 2285–2291.
- Liu Q & Wong-Riley MTT (2005). Postnatal developmental expressions of neurotransmitters and receptors in various brain stem nuclei of rats. *J Appl Physiol* **98**, 1442–1457.
- Liu Q & Wong-Riley MTT (2008). Postnatal changes in the expression of serotonin 2A receptors in various brain stem nuclei of the rat. *J Appl Physiol* **104**, 1801–1808.
- Loeschcke HH, De Lattre J, Schlafke ME & Trough CO (1969). Effects on respiration and circulation of electrically stimulating the ventral surface of the medulla oblongata. *Respir Physiol* **10**, 184–197.
- Loeschcke HH, Mitchell RA, Katsaros B, Perkins JF & Konig A (1963). Interaction of intracranial chemosensitivity with peripheral afferents to the respiratory centers. *Ann N Y Acad Sci* **493**–497.
- Lyman CP (1951). Effect of increased CO₂ on respiration and heart rate of hibernating hamsters and ground squirrels. *Am J Physiol* **167**, 638–643.
- Lyman CP (1958). Oxygen consumption, body temperature and heart rate of woodchucks entering hibernation. *Am J Physiol* **194**, 83–91.
- Lyman CP & Chatfield P (1950). Mechanisms of Arousal in the Hibernating Hamster. *J Exp Zool* **114**, 491–516.
- Malan A (1973). Ventilation measured by body plethysmography in hibernating mammals and in poikilotherms. *Respir Physiol* **17**, 32–44.
- Malan A (1977). Blood acid-base state at a variable temperature. A graphical representation. *Respir Physiol* **259**, 259–275.
- Malan A (1982) Respiration and acid-base state in hibernation. In Lyman CP, Willis JS, Malan A, Wang LCH, editors. *Hibernation and Torpor in Mammals and Birds*. New York: Academic Press.
- Malan A (1986) pH as a control factor in hibernation. Pages 61-70 in HC Heller, XJ Musacchia, and LCH Wang, eds. *Living in the cold*. Elsevier, New York.

- Malan A (1988). pH and hypometabolism in mammalian hibernation. *Can J Zool* **66**, 95–98.
- Malan A, Arens H & Waechter A (1973). Pulmonary respiration and acid-base state in hibernating marmots and hamsters. *Respir Physiol* **17**, 45–61.
- Malan A, Rodeau JL & Daull F (1985). Intracellular pH in hibernation and respiratory acidosis in the European hamster. *J Comp Physiol B* **156**, 251–258.
- Marina N, Abdala A, Trapp S, Li A, Nattie E, Hewinson J, Smith J, Paton J & Gourine A (2009). Essential role of phox2b-expressing ventrolateral brainstem neurons in the chemosensory control of inspiration and expiration. *Cancer* **19**, 975–980.
- Martelli D, Stanić D & Dutschmann M (2013). The emerging role of the parabrachial complex in the generation of wakefulness drive and its implication for respiratory control. *Respir Physiol Neurobiol* **188**, 318–323.
- McArthur MD, Hanstock CC, Malan A, Wang LCH & Allen PS (1990). Skeletal muscle pH dynamics during arousal from hibernation measured by ³¹P NMR spectroscopy. *J Comp Physiol B* **160**, 339–347.
- McArthur MD & Milsom WK (1991a). Changes in ventilation and respiratory sensitivity associated with hibernation in columbian (*spermophilus columbianus*) and golden-mantled (*spermophilus lateralis*) ground squirrels. *Physiol Zool* **64**, 940–959.
- McArthur MD & Milsom WK (1991b). Ventilation and Respiratory Sensitivity of Euthermic Columbian and Golden-mantled Ground Squirrels (*Spermophilus columbianus* and *Spermophilus lateralis*) during the Summer and Winter. *Physiol Zool* **64**, 921–939.
- McArthur MD & Milsom WK (1991c). Sensitivity of euthermic columbian and golden-mantled ground squirrels (*spermophilus columbianus* and *spermophilus lateralis*). *Physiol Zool* **64**, 921–939.
- Milsom WK & Burlison ML (2007). Peripheral arterial chemoreceptors and the evolution of the carotid body. *Respir Physiol Neurobiol* **157**, 4–11.
- Milsom WK & Jackson DC (2011). Hibernation and gas exchange. *Compr Physiol* **1**, 397–420.
- Milsom WK, Zimmer MB & Harris MB (1999). Regulation of cardiac rhythm in hibernating mammals. *Comp Biochem Physiol A Mol Integr Physiol* **124**, 383–391.
- Mitchell, R.A., Loeschcke, H.H., Massion, W.H., Severinghaus JW (1963). Respiratory responses mediated through superficial chemosensitive areas on the medulla. *J Appl Physiol*

18, 523–533.

- Mitchell RA, Loeschcke HH, Severinghaus JW, Richardson BW & Massion WH (1963). Regions of respiratory chemosensitivity. *Ann N Y Acad Sci* **109**, 661–681.
- Mitchell RA & Singer MM (1965). Respiration and cerebrospinal fluid pH in metabolic acidosis and alkalosis. *J Appl Physiol* **20**, 905–911.
- de Moreno VS, Bicego KC, Szawka RE, Anselmo-Franci JA & Gargaglioni LH (2010). Serotonergic mechanisms on breathing modulation in the rat locus coeruleus. *Pflugers Arch Eur J Physiol* **459**, 357–368.
- Mortola JP (1991). Hamsters versus rats: ventilatory responses in adults and newborns. *Respir Physiol* **85**, 305–317.
- Mortola JP (2001a). Respiratory physiology of newborn mammals changes in temperature and respiratory gases. In *Respiratory Physiology of Newborn Mammals*.
- Mortola JP (2001b). Respiratory physiology of newborn mammals: a comparative perspective. Johns Hopkins University Press.
- Mortola JP & Lanthier C (1996). The ventilatory and metabolic response to hypercapnia in newborn mammalian species. *Respir Physiol* **103**, 263–270.
- Musacchia XJ & Volkert WA (1971). Blood gases in hibernating and active ground squirrels: HbO₂ affinity at 6 and 38 C. *Am J Physiol* **221**, 128–130.
- Nattie E & Li A (2009). Central chemoreception is a complex system function that involves multiple brain stem sites. *J Appl Physiol* **106**, 1464–1466.
- Nattie EE & Edwards WH (1981). CSF acid-base regulation and ventilation during acute hypercapnia in the newborn dog. *J Appl Physiol* **50**, 566–574.
- Nestler JR (1990). Relationships between respiratory quotient and metabolic rate during entry to and arousal from daily torpor in deer mice (*Peromyscus maniculatus*). *Physiol Zool* **63**, 504–515.
- Nicol S., N.A. Andersen, and U. Mesch. 1992. Metabolic rate and ventilatory pattern in the echidna during hibernation and arousal. Pp. 150–159 in M.L. Augée, ed. *Platypus and Echidnas*. Royal Zoological Society of New South Wales, Sydney.
- Nottingham S, Leiter JC, Wages P, Buhay S & Erlichman JS (2001). Developmental changes in intracellular pH regulation in medullary neurons of the rat. *Am J Physiol - Regul Integr*

- Comp Physiol* **281**, 1940–1951.
- Nurse CA (2014). Synaptic and paracrine mechanisms at carotid body arterial chemoreceptors. *J Physiol* **592**, 3419–3426.
- O'Regan RG & Majcherczyk S (1982). Role of peripheral chemoreceptors and central chemosensitivity in the regulation of respiration and circulation. *J Exp Biol* **100**, 23–40.
- Ortmann S & Heldmaier G (2000). Regulation of body temperature and energy requirements of hibernating Alpine marmots (*Marmota marmota*). *Am J Physiol - Regul Integr Comp Physiol* **278**, 698–704.
- Osborne S & Milsom WK (1993). Ventilation is coupled to metabolic demands during progressive hypothermia in rodents. *Respir Physiol* **92**, 305–318.
- Oyamada Y, Ballantyne D, Mückenhoff K & Scheid P (1998). Respiration-modulated membrane potential and chemosensitivity of locus coeruleus neurones in the in vitro brainstem-spinal cord of the neonatal rat. *J Physiol* **513** (Pt 2, 381–398.
- Parer JT & Hudson WA (1974). Respiratory studies of monotremes. IV. Normal respiratory functions of echidnas and ventilatory response to inspired oxygen and carbon dioxide. *Respir Physiol* **21**, 307–316.
- Parisian K, Wages P, Smith A, Jarosz J, Hewitt A, Leiter JC & Erlichman JS (2004). Ventilatory effects of gap junction blockade in the NTS in awake rats. *Respir Physiol Neurobiol* **142**, 127–143.
- Peers C, Wyatt CN & Evans AM (2010). Mechanisms for acute oxygen sensing in the carotid body. *Respir Physiol Neurobiol* **174**, 292–298.
- Pepper DR, Landauer RC & Kumar P (1995). Postnatal development of CO₂-O₂ interaction in the rat carotid body in vitro. *J Physiol* **485**, 531–541.
- Pineda J & Aghajanian GK (1997). Carbon dioxide regulates the tonic activity of locus coeruleus neurons by modulating a proton- and polyamine-sensitive inward rectifier potassium current. *Neuroscience* **77**, 723–743.
- Putnam RW, Conrad SC, Gdovin MJ, Erlichman JS & Leiter JC (2005). Neonatal maturation of the hypercapnic ventilatory response and central neural CO₂ chemosensitivity. *Respir Physiol Neurobiol* **149**, 165–179.
- Putnam RW, Filosa JA & Ritucci NA (2004). Cellular mechanisms involved in CO₂ and acid

- signaling in chemosensitive neurons. *Am J Physiol Cell Physiol* **287**, C1493–C1526.
- Rezzonico R & Mortola JP (1989). Respiratory adaptation to chronic hypercapnia in newborn rats. *J Appl Physiol* **67**, 311–315.
- Roper TJ, Bennett NC, Conrath L & Molteno AJ (2001). Environmental conditions in burrows of two species of African mole-rat, *Georchys capensis* and *Cryptomys damarensis*. *J Zool* **254**, 101–107.
- Saiki C & Mortola JP (1996). Effect of CO₂ on the metabolic and ventilatory responses to ambient temperature in conscious adult and newborn rats. *J Physiol* **491** (Pt 1, 261–269.
- Samuels E & Szabadi E (2008). Functional neuroanatomy of the noradrenergic locus coeruleus: its roles in the regulation of arousal and autonomic function part I: principles of functional organisation. *Curr Neuropharmacol* **6**, 235–253.
- Saper CB & Loewy AD (1980). Efferent connections of the parabrachial nucleus in the rat. *Brain Res* **197**, 291–317.
- Schaefer KE & Wünnenberg W (1976). Threshold temperatures for shivering in acute and chronic hypercapnia. *J Appl Physiol* **41**, 67–70.
- Schneider JE & Wade GN (1990). Effects of ambient temperature and body fat content on maternal litter reduction in syrian hamsters. *Physiol Behav* **49**, 135–139.
- Serra A, Brozoski D, Hedin N, Franciosi R & Forster H V. (2001). Mortality after carotid body denervation in rats. *J Appl Physiol* **91**, 1298–1306.
- Shams I, Avivi A & Nevo E (2005). Oxygen and carbon dioxide fluctuations in burrows of subterranean blind mole rats indicate tolerance to hypoxic – hypercapnic stresses. **142**, 376–382.
- Shibao C, Gamboa A, Diedrich A, Ertl AC, Chen KY, Byrne DW, Farley G, Paranjape SY, Davis SN & Biaggioni I (2007). Autonomic contribution to blood pressure and metabolism in obesity. *Hypertension* **49**, 27–33.
- Silva CA, Vicente MC, Tenorio-Lopes L, Soliz J & Gargaglioni LH (2017). Erythropoietin in the locus coeruleus attenuates the ventilatory response to CO₂ in rats. *Respir Physiol Neurobiol* **236**, 11–18.
- Smith CA, Forster H V., Blain GM & Dempsey JA (2010). An interdependent model of central/peripheral chemoreception: Evidence and implications for ventilatory control.

- Respir Physiol Neurobiol* **173**, 288–297.
- Snapp B & Heller HC (1981). Suppression of metabolism during hibernation in ground squirrels (*Citellus lateralis*). *Physiol Zool* **54**, 297–307.
- Song X, Körtner G & Geiser F (1997). Thermal relations of metabolic rate reduction in a hibernating marsupial. *Am J Physiol - Regul Integr Comp Physiol* **273**, 2097–2104.
- Søvik S & Lossius K (2004). Development of ventilatory response to transient hypercapnia and hypercapnic hypoxia in term infants. *Pediatr Res* **55**, 302–309.
- Sprenger RJ, Kim AB, Dzal YA & Milsom WK (2019). Comparison of the CO₂ ventilatory response through development in three rodent species: Effect of fossoriality. *Respir Physiol Neurobiol* **264**, 19–27.
- Sprenger RJ & Milsom WK (2021). Respiratory development in burrowing rodents: Effect of perinatal hypercapnia. *Respir Physiol Neurobiol* **288**, 1–11.
- Studier EH & Baca TP (1968). Atmospheric conditions in artificial rodent burrows. *Southwest Assoc Nat* **13**, 401–410.
- Stunden CE, Filosa JA, Garcia AJ, Dean JB & Putnam RW (2001). Development of in vivo ventilatory and single chemosensitive neuron responses to hypercapnia in rats. *Respir Physiol* **127**, 135–155.
- Šumbera R, Chitaukali WN, Elichová M, Kubová J & Burda H (2004). Microclimatic stability in burrows of an Afrotropical solitary bathyergid rodent, the silvery mole-rat (*Heliophobius argenteocinereus*). *J Zool* **263**, 409–416.
- Szewczak JM & Jackson DC (1992). Apneic oxygen uptake in the torpid bat, *Eptesicus fuscus*. *J Exp Biol* **173**, 217–227.
- Tähti H (1975). Effects of changes in CO₂ and O₂ concentrations in the inspired gas on respiration in the hibernating hedgehog (*Erinaceus europaeus* L.) Author (s): Hanna Tähti
Published by : Finnish Zoological and B. *Ann Zool Fennici* **12**, 183–187.
- Tattersall GJ (2016). Infrared thermography: A non-invasive window into thermal physiology. *Comp Biochem Physiol -Part A Mol Integr Physiol* **202**, 78–98.
- Tenney SM & Boggs DF (1986). Comparative mammalian respiratory control. *Handb Physiol Sect 3 Respir Syst Vol II Control breathing, Part* 2833-855.
- Thurlbeck W (1975). Postnatal growth and development of the lung. *Am Rev Respir Dis* **111**,

803–844.

- Twente J & Twente J (1968). Effects of epinephrine upon progressive irritability of hibernating *citellus lateralis*. *Comp Biochem Physiol* **25**, 475–483.
- Vaughan DK, Gruber AR, Michalski ML & Seidling J (2006). Capture , care , and captive breeding of 13-lined ground squirrels , *Spermophilus tridecemlineatus*. *Lab Anim (NY)* **35**, 33–40.
- Vincent A, Kessler JP, Baude A, Dipasquale E & Tell F (2004). N-methyl-D-aspartate receptor activation exerts a dual control on postnatal development of nucleus tractus solitarii neurons in vivo. *Neuroscience* **126**, 185–194.
- Walker BR, Adams EM & Voelkel NF (1985). Ventilatory responses of hamsters and rats to hypoxia and hypercapnia. *J Appl Physiol* **59**, 1955–1960.
- Wang W, Pizzonia JH & Richerson GB (1998). Chemosensitivity of rat medullary raphe neurones in primary tissue culture. *J Physiol* **511**, 433–450.
- Wang W & Richerson GB (1999). Development of chemosensitivity of rat medullary raphe neurons. *Neuroscience* **90**, 1001–1011.
- Wang W, Tiwari JK, Bradley SR, Zaykin R V & Richerson GB (2001). Acidosis-stimulated neurons of the medullary raphe are serotonergic. *J Neurophysiol* **85**, 2224–2235.
- Wang Z & Bisgard GE (2005). Postnatal growth of the carotid body. *Respir Physiol Neurobiol* **149**, 181–190.
- Webb CL & Milsom WK (1990). Carotid Body Contribution to Hypoxic Ventilatory Responses in Euthermic and Hibernating Ground Squirrels.
- Webb CL & Milsom WK (1994). Ventilatory Responses to Acute and Chronic Hypoxic Hypercapnia in the Ground-Squirrel. *Respir Physiol* **98**, 137–152.
- Webb CL & Milsom WK (2017). Effects of low temperature on breathing pattern and ventilatory responses during hibernation in the golden-mantled ground squirrel. *J Comp Physiol B Biochem Syst Environ Physiol* **187**, 793–802.
- Wickström R, Hökfelt T & Lagercrantz H (2002). Development of CO₂-response in the early newborn period in rat. *Respir Physiol Neurobiol* **132**, 145–158.
- Williams DD & Rausch RL (1973). Seasonal carbon dioxide and oxygen concentrations in the dens of hibernating mammals (Sciuridae). *Comp Biochem Physiol -- Part A Physiol*; DOI:

10.1016/0300-9629(73)90261-2.

- Wilson KJ & Kilgore DL (1978). The effects of location and design on the diffusion of respiratory gases in mammal burrows. *J Theor Biol* **71**, 73–101.
- Wilz M & Heldmaier G (2000). Comparison of hibernation, estivation and daily torpor in the edible dormouse, *Glis glis*. *J Comp Physiol - B Biochem Syst Environ Physiol* **170**, 511–521.
- Withers PC (1977). Metabolic, respiratory and haematological adjustments of the little pocket mouse to circadian torpor cycles. *Respir Physiol* **31**, 295–307.
- Wolsink JG, Berkenbosch A, DeGoede J & Olievier CN (1992). The effects of hypoxia on the ventilatory response to sudden changes in CO₂ in newborn piglets. *J Physiol* 39–48.
- Wong-Riley MTT & Liu Q (2005). Neurochemical development of brain stem nuclei involved in the control of respiration. *Respir Physiol Neurobiol* **149**, 83–98.
- Wong-Riley MTT, Liu Q & Gao X (2013). Peripheral–central chemoreceptor interaction and the significance of a critical period in the development of respiratory control. *Respir Physiol Neurobiol* **185**, 156–169.
- Wong-Riley MTT, Liu Q & Gao X (2019). Mechanisms underlying a critical period of respiratory development in the rat. *Respir Physiol Neurobiol* **264**, 40–50.
- Zimmer MB & Milsom WK (2001). Effects of changing ambient temperature on metabolic, heart, and ventilation rates during steady state hibernation in golden-mantled ground squirrels (*Spermophilus lateralis*). *Physiol Biochem Zool* **74**, 714–723.
- Zimmer MB & Milsom WK (2002a). Ventilatory pattern and chemosensitivity in unanesthetized, hypothermic ground squirrels (*Spermophilus lateralis*). *Respir Physiol Neurobiol* **133**, 49–63.
- Zimmer MB & Milsom WK (2002b). Effects of changing ambient temperature on metabolic, heart, and ventilation rates during steady state hibernation in golden-mantled ground squirrels (*Spermophilus lateralis*). *Physiol Biochem Zool* **74**, 714–723.
- Zimmer MB & Milsom WK (2004). Effect of hypothermia on respiratory rhythm generation in hamster brainstem-spinal cord preparations. *Respir Physiol Neurobiol* **142**, 237–249.